

**B-ZONE PIT:  
LIMNOLOGY 1993-1996  
AND  
THE FATE OF ARSENIC AND NICKEL**

**FINAL REPORT**

**For**

**CAMECO Corporation**

**May, 1997**

## TABLE OF CONTENTS

|       |  |     |
|-------|--|-----|
| 1.0   | INTRODUCTION .....   | 1   |
| 2.0   | B-ZONE FLOODED PIT OBSERVATIONS .....  | 8   |
| 2.1   | Physical/Chemical Parameters of the Pit .....                                  | 8   |
| 2.2   | Nutrient Concentrations .....  | 24  |
| 2.3   | Sedimenting Material .....   | 45  |
| 3.0   | BIOLOGY OF THE FLOODED PIT .....   | 59  |
| 3.1   | Species Diversity .....  | 60  |
| 3.2   | Phytoplankton Cell Density .....   | 65  |
| 3.3   | The Biology of the Dominant Species in the B-Zone Pit .....                    | 69  |
| 3.4   | Assessing Pit Bio-Productivity .....   | 73  |
| 4.0   | ARSENIC AND NICKEL REMOVAL: BIOLOGICAL AND PHYSICAL<br>APPROACHES .....        | 81  |
| 4.1   | Biologically-Mediated Contaminant Removal .....                                | 81  |
| 4.1.1 | Biology and Growth Control of <i>Dictyosphaerium pulchellum</i> ....           | 81  |
| 4.1.2 | Environmental Stress and Mucilage Production .....                             | 82  |
| 4.1.3 | Nutrient Conditions in the B-Zone Pit .....                                    | 85  |
| 4.1.4 | Effect of Light and Temperature on Growth of <i>Dictyosphaerium</i> ..         | 86  |
| 4.1.5 | Nutrient Ratios and Mucilage Production .....                                  | 89  |
| 4.1.6 | Nickel and Arsenic Adsorption on <i>Dictyosphaerium pulchellum</i> .           | 98  |
| 4.1.7 | B-Zone Flooded Pit Limnology: Summary of 1995 Productivity<br>Conditions ..... | 103 |
| 4.1.8 | Nickel and Arsenic Pathways in the Flooded Pit .....                           | 106 |

|       |   |     |
|-------|---|-----|
| 4.2   | Physically-Mediated Contaminant Removal .....                                     | 111 |
| 4.2.1 | Bentonite and Algal Biomass Additions to pit water .....                          | 115 |
| 4.2.2 | iron salts Additions to pit water .....   | 115 |
| 4.2.3 | Treatment Costs for Arsenic Removal By Iron Salt Additions<br>to B-Zone Pit ..... | 125 |
| 5.0   | CONCLUSIONS .....   |     |
| 5.1   | Contaminant Behaviour and Removal Mechanisms .....                                |     |
| 5.2   | B-Zone Flooded Pit Limnology: Summary of 1995 Productivity<br>Conditions .....    |     |
| 6.0   | REFERENCES .....  |     |

## LIST OF TABLES

|            |  |    |
|------------|--|----|
| Table 1a:  | Nutrient Concentration in the Flooded Pit, 1995 .....  | 26 |
| Table 1b:  | Nutrient Concentration in the Flooded Pit, 1996 .....  | 27 |
| Table 2:   | B-Zone Pit Particle Size Distribution .....  | 45 |
| Table 3:   | Sedimentation rates from sediment traps .....  | 49 |
| Table 4:   | Sequential extractions on sediment trap material,<br>September 16, 1995 .....  | 56 |
| Table 5:   | B-Zone Pit, Picoplankton and Phytoplankton, 1996 .....   | 62 |
| Table 6:   | Seasonal distribution of <i>Dictyosphaerium</i> in the water column<br>of the pit during April to September, 1995 .....                  | 69 |
| Table 7:   | Estimated primary productivity in the pit using changes in water<br>chemistry and literature production numbers for Northern Lakes ..... | 77 |
| Table 8:   | Areas and depth contours of the flooded pit used in productivity<br>calculations .....   | 79 |
| Table 9:   | B-Zone Pit, N:P Molar Ratios for 1995 .....  | 86 |
| Table 10a: | The effect of various light intensities on the growth of <i>Dictyosphaerium<br/>pulchellum</i> at an N:P ratio of 10:1 .....             | 87 |



|            |  |     |
|------------|--|-----|
| Table 10b: | The effect of various temperatures on the growth of <i>Dictyosphaerium pulchellum</i> at an N:P ratio of 10:1 .....        | 87  |
| Table 10c: | Changes in Carbohydrate Concentration for <i>Dictyosphaerium pulchellum</i> at an N:P ratio of 10:1 .....                  | 87  |
| Table 11:  | Growth rates (as divisions/day) of <i>Dictyosphaerium</i> at various temperatures based on cell densities .....            | 88  |
| Table 12:  | Growth rates (as divisions@day <sup>-1</sup> of the lab strain of <i>Dictyosphaerium</i> grown under nutrient stress ..... | 90  |
| Table 13:  | B-Zone Pit arsenic field experiment results, September 19, 1995 .....  | 123 |
| Table 14:  | Interconversion of mM/L, M/L and mg/L for various compounds .....  | 126 |
| Table 15:  | Approximate chemical cost of iron salt treatment of B-Zone Flooded Pit for arsenic removal .....                           | 127 |

## LIST OF FIGURES

|            |  |    |
|------------|--|----|
| Figure 1a: | Flooded Pit, Temperature vs Depth, March-May, 1993-1996      | 11 |
| Figure 1b: | Flooded Pit, Temperature vs Depth, June, 1993-1995           | 11 |
| Figure 1c: | Flooded Pit, Temperature vs Depth, August, 1993-1996         | 11 |
| Figure 1d: | Flooded Pit, Temperature vs Depth, October, 1993-1996        | 11 |
| Figure 2a: | Flooded Pit, Dissolved Oxygen vs Depth, March-May, 1993-1996 | 12 |
| Figure 2b: | Flooded Pit, Dissolved Oxygen vs Depth, June, 1993-1995      | 12 |
| Figure 2c: | Flooded Pit, Dissolved Oxygen vs Depth, August, 1993-1996    | 12 |
| Figure 2d: | Flooded Pit, Dissolved Oxygen vs Depth, October, 1993-1996   | 12 |
| Figure 3a: | Flooded Pit, Eh vs Depth, March-May, 1993-1996               | 14 |
| Figure 3b: | Flooded Pit, Eh vs Depth, June, 1993-1995                    | 14 |
| Figure 3c: | Flooded Pit, Eh vs Depth, August, 1993-1996                  | 14 |
| Figure 3d: | Flooded Pit, Eh vs Depth, October, 1993-1996                 | 14 |
| Figure 4a: | Flooded Pit, pH vs Depth, March-May, 1993-1996               | 15 |
| Figure 4b: | Flooded Pit, pH vs Depth, June, 1993-1995                    | 15 |

|            |  |    |
|------------|--|----|
| Figure 4c: | Flooded Pit, pH vs Depth, August, 1993-1996 .....                            | 15 |
| Figure 4d: | Flooded Pit, pH vs Depth, October, 1993-1996 .....                           | 15 |
| Figure 5a: | Flooded Pit, Conductivity vs Depth, March-May, 1993-1996 .....               | 16 |
| Figure 5b: | Flooded Pit, Conductivity vs Depth, June, 1993-1995 .....                    | 16 |
| Figure 5c: | Flooded Pit, Conductivity vs Depth, August, 1993-1996 .....                  | 16 |
| Figure 5d: | Flooded Pit, Conductivity vs Depth, October, 1993-1996 .....                 | 16 |
| Figure 6a: | Flooded Pit, Sodium Concentration vs Depth,<br>March-May, 1993-1996 .....    | 18 |
| Figure 6b: | Flooded Pit, Sodium Concentration vs Depth, June, 1993-1995 .....            | 18 |
| Figure 6c: | Flooded Pit, Sodium Concentration vs Depth, August, 1993-1996 .....          | 18 |
| Figure 6d: | Flooded Pit, Sodium Concentration vs Depth, October, 1993-1996 .....         | 18 |
| Figure 7a: | Flooded Pit, Potassium Concentration vs Depth,<br>March-May, 1993-1996 ..... | 19 |
| Figure 7b: | Flooded Pit, Potassium Concentration vs Depth, June, 1993-1995 .....         | 19 |
| Figure 7c: | Flooded Pit, Potassium Concentration vs Depth, August, 1993-1996 ...         | 19 |
| Figure 7d: | Flooded Pit, Potassium Concentration vs Depth, October, 1993-1996 ..         | 19 |

|             |  |    |
|-------------|--|----|
| Figure 8a:  | Flooded Pit, Magnesium Concentration vs Depth,<br>March-May, 1993-1996 ..... | 20 |
| Figure 8b:  | Flooded Pit, Magnesium Concentration vs Depth, June, 1993-1995 .....         | 20 |
| Figure 8c:  | Flooded Pit, Magnesium Concentration vs Depth, August,<br>1993-1996 .....    | 20 |
| Figure 8d:  | Flooded Pit, Magnesium Concentration vs Depth, October,<br>1993-1996 .....   | 20 |
| Figure 9a:  | Flooded Pit, Calcium Concentration vs Depth, March-May,<br>1993-1996 .....   | 21 |
| Figure 9b:  | Flooded Pit, Calcium Concentration vs Depth, June, 1993-1995 .....           | 21 |
| Figure 9c:  | Flooded Pit, Calcium Concentration vs Depth, August, 1993-1996 .....         | 21 |
| Figure 9d:  | Flooded Pit, Calcium Concentration vs Depth, October, 1993-1996 .....        | 21 |
| Figure 10a: | Flooded Pit, Sulphate Concentration vs Depth,<br>March-May, 1993-1996 .....  | 22 |
| Figure 10b: | Flooded Pit, Sulphate Concentration vs Depth, June, 1993-1995 .....          | 22 |
| Figure 10c: | Flooded Pit, Sulphate Concentration vs Depth, August, 1993-1996 .....        | 22 |
| Figure 10d: | Flooded Pit, Sulphate Concentration vs Depth, October, 1993-1996 .....       | 22 |

|  |    |
|--|----|
| Figure 11a: Flooded Pit, Bicarbonate Concentration vs Depth,<br>March-May, 1993-1996 ..... | 23 |
| Figure 11b: Flooded Pit, Bicarbonate Concentration vs Depth, June, 1993-1995 ....          | 23 |
| Figure 11c: Flooded Pit, Bicarbonate Concentration vs Depth,<br>August, 1993-1996 .....    | 23 |
| Figure 11d: Flooded Pit, Bicarbonate Concentration vs Depth, October,<br>1993-1996 .....   | 23 |
| Figure 12: Flooded Pit, Phosphate Concentration vs Depth, 1993-1996 .....                  | 29 |
| Figure 13: Flooded Pit, Nitrate Concentration vs Depth, 1993-1996 .....                    | 30 |
| Figure 14: Flooded Pit, Ammonia Concentration vs Depth, 1993-1996 .....                    | 32 |
| Figure 15: Flooded Pit, Total Organic Carbon vs Depth, 1993-1996 .....                     | 34 |
| Figure 16: Flooded Pit, Total Suspended Solids vs Depth, 1993-1996 .....                   | 34 |
| Figure 17a: Flooded Pit, Arsenic, Nickel, Temperature vs Depth, April 12, 1995 ....        | 36 |
| Figure 17b: Flooded Pit, Arsenic, Nickel, Temperature vs Depth, June 14, 1995 ....         | 36 |
| Figure 17c: Flooded Pit, Arsenic, Nickel, Temperature vs Depth,<br>August 17, 1995 .....   | 36 |

|   |    |
|---|----|
| Figure 17d: Flooded Pit, Arsenic, Nickel, Temperature vs Depth,<br>October 14, 1995 ..... | 36 |
| Figure 18a: Flooded Pit, Arsenic, Nickel, Temperature vs Depth, May 9, 1996 .....         | 37 |
| Figure 18b: Flooded Pit, Arsenic, Nickel, Temperature vs Depth,<br>August 26, 1996 .....  | 37 |
| Figure 18c: Flooded Pit, Arsenic, Nickel, Temperature vs Depth,<br>October 28, 1996 ..... | 37 |
| Figure 19a: Flooded Pit, Aluminum, Iron, Temperature vs Depth, April 12, 1995 .....       | 43 |
| Figure 19b: Flooded Pit, Aluminum, Iron, Temperature vs Depth, June 14, 1995 .....        | 43 |
| Figure 19c: Flooded Pit, Aluminum, Iron, Temperature vs Depth,<br>August 17, 1995 .....   | 43 |
| Figure 19d: Flooded Pit, Aluminum, Iron, Temperature vs Depth,<br>October 14, 1995 .....  | 43 |
| Figure 20a: Flooded Pit, Aluminum, Iron, Temperature vs Depth, May 9, 1996 .....          | 44 |
| Figure 20b: Flooded Pit, Aluminum, Iron, Temperature vs Depth,<br>August 26, 1996 .....   | 44 |
| Figure 20c: Flooded Pit, Aluminum, Iron, Temperature vs Depth,<br>October 28, 1996 .....  | 44 |

|   |    |
|---|----|
| Figure 21a: Flooded Pit, Arsenic Concentration in Sedimentation Traps,<br>1992-1996 ..... | 55 |
| Figure 21b: Flooded Pit, Nickel Concentration in Sedimentation Traps,<br>1992-1996 .....  | 55 |
| Figure 21c: Flooded Pit, Iron Concentration in Sedimentation Traps, 1992-1996 ....        | 55 |
| Figure 22a: B-Zone Pit, Qualitative Data: Species Diversity .....                         | 61 |
| Figure 22b: B-Zone Pit, Enumeration Data: Species Diversity .....                         | 61 |
| Figure 23: B-Zone Pit, Phytoplankton Density .....  | 67 |
| Figure 24: B-Zone Pit, Semi-Quantitative Phytoplankton Data .....                         | 68 |
| Figure 25a: Primary Productivity, Cell density vs depth, April, 1996 .....                | 72 |
| Figure 25b: Primary Productivity, Cell density vs depth, August, 1996 .....               | 72 |
| Figure 26a: Growth responses of a lab strain of <i>Dictyosphaerium</i> .....              | 91 |
| Figure 26b: Changes in total carbohydrate during growth .....                             | 91 |
| Figure 26c: Changes in carbohydrate level .....   | 93 |
| Figure 26d: Changes in nitrate concentration .....  | 93 |
| Figure 26e: Changes in phosphate concentration .....                                      | 97 |

|             |  |     |
|-------------|--|-----|
| Figure 26f: | Changes in N:P ratio .....                                   | 97  |
| Figure 27:  | Summary of Nickel Adsorption experiments (Round 1) .....     | 99  |
| Figure 28:  | Nickel Adsorption .....                                      | 101 |
| Figure 29:  | Arsenic Adsorption .....                                     | 101 |
| Figure 30a: | Arsenic experiment: 40 m water+algal biomass+Bentonite ..... | 116 |
| Figure 30b: | Arsenic experiment: 40 m water+Bentonite .....               | 116 |
| Figure 30c: | Arsenic experiment: 15 m water+Bentonite .....               | 116 |
| Figure 30d: | Arsenic experiment: 2 m water+Bentonite .....                | 116 |
| Figure 31a: | Nickel experiment: 40 m water+algal biomass+Bentonite .....  | 117 |
| Figure 31b: | Nickel experiment: 40 m water+Bentonite .....                | 117 |
| Figure 31c: | Nickel experiment: 15 m water+Bentonite .....                | 117 |
| Figure 31d: | Nickel experiment: 2 m water+Bentonite .....                 | 117 |
| Figure 32a: | Percentage of dissolved arsenic removed .....                | 120 |
| Figure 32b: | Total arsenic adsorption .....                               | 120 |
| Figure 32a: | Percentage of dissolved nickel removed .....                 | 121 |
| Figure 32b: | Total nickel adsorption .....                                | 121 |



## LIST OF SCHEMATICS

|  |     |
|--|-----|
| Schematic 1: Components of Primary Productivity and Physical/Chemical Aspects of Water Bodies .....          | 25  |
| Schematic 2: Nature and Size Domain of the Important Particles of Aquatic System .....                       | 41  |
| Schematic 3: Schematic diagram of a <i>Dictyosphaerium</i> colony with surrounding mucilaginous sheath ..... | 83  |
| Schematic 4: Nickel and arsenic paths in 1995 .....  | 107 |

## LIST OF MAPS

|                              |   |
|------------------------------|---|
| Map 1: B-Zone Open Pit ..... | 9 |
|------------------------------|---|

## LIST OF PLATES

|   |    |
|---|----|
| Plate 1: Sedimentation traps August 1994 2, 12, 22, 32 m with weight recovered after 37 days suspension in the B-Zone Pit .....                                 | 47 |
| Plate 2: Algal material from sedimentation traps of the pit collected in September 1995 from different depths after 6 months of settling in the cold room ..... | 47 |
| Plate 3: Micrograph of <i>Dictyosphaerium</i> colonies collected from the B-Zone Pit and used in laboratory experiments .....                                   | 83 |

## INDEX OF APPENDICES

### **APPENDIX A:**

PART 1: IRON SALT TREATMENT FOR REMOVAL OF ARSENIC AND NICKEL

PART 2: BENTONITE ADDITION FOR REMOVAL OF ARSENIC AND NICKEL

PART 3: B-ZONE PIT WATER CHEMISTRY AND SEDIMENTATION TRAP SOLIDS ANALYSES

PART 4: BIOGEOCHEMICAL PATHWAYS OF ARSENIC IN LAKES  
ADSORPTION REACTIONS OF NICKEL SPECIES AT OXIDE SURFACES

### **APPENDIX B:** REPORT ON ANALYSIS OF B-ZONE SAMPLES

### **APPENDIX C:** NICKEL AND ARSENIC ADSORPTION ONTO MUCILAGE PRODUCING ALGAL COLONIES. ADDENDUM. 1997 CANMET REPORT

## 1.0 INTRODUCTION

In the winter of 1991, the B-Zone Pit was force-flooded with Collins Bay water. During the summer in 1992, collection of limnological information on the flooded pit started. Profiles of pH, Eh, O<sub>2</sub>, electrical conductivity and temperature are obtained 4 to 5 times during the year. Water samples are collected every 5 m to the bottom of the pit to a maximum depth of 52 m. Generally, 47 analytical parameters are determined in each water sample including metals, nutrients and radionuclides.

The first interpretation of the limnology of the pit was presented in July 1993, forming Appendix 4A of the CAMECO report entitled: “**Collins Bay B-Zone Decommissioning Year 1-Proposed Target Levels**”. The man-made lake stratifies and turns over after the breakdown of the thermocline in fall and during the ice covered season. Erosion of the pit walls produced TSS, which served as surficial adsorption sites for As and Ni. The capacity of clay particles to adsorb metals has been well documented. The use of TSS was considered as a potential avenue to reduce the already relatively low concentrations (0.3 mg@L<sup>-1</sup>) of both contaminants of concern, As and Ni, in the pit water in order to reach SSWQ objectives for protection of aquatic life. These objectives are an order of magnitude lower than current concentrations for both contaminants.

Sedimentation traps were set up at various depth to quantify the amount of TSS settling to the bottom of the pit. In the first year, the data suggested that 26 t@d<sup>-1</sup> settled just after ice breakup, decreasing to 0.7 t@d<sup>-1</sup> by the fall. In addition to inorganic adsorption sites for the contaminants on clay, iron oxides and silicates, it was postulated that primary biological productivity formed part of the TSS and would also contribute to metal removal. Although in the first years after flooding the species diversity of phytoplankton in the pit was low, algal growth and diversity was expected to increase due to the relatively high concentrations of nitrogen and phosphate in the water.

An extensive data set had been generated by fall 1994 facilitating a good description of the overall limnology of the flooded pit, forming Appendix E in the CAMECO report entitled: **“Collins Bay, A-Zone, D-Zone and Eagle Point Waste Management Plan”** submitted in January 1995.

After three growing seasons, it was evident that arsenic and nickel loads (total and suspended) in the pit had decreased by 35% to 22%, along with iron by 39%. One mucilage forming algae, *Dictyosphaerium pulchellum*, dominated the pit. Based on the biomass collected in the sedimentation traps, it was estimated that 31 tonnes of dry weight biomass were generated during the growing season. A mass balance, considering both dissolved and suspended As and Ni, suggested that the majority of both elements were in the dissolved form, generally defined as that portion passing through a 0.45  $\mu$ m filter prior to analysis. These findings, together with the literature review on the function of algae as flocculating agents (Appendix 4A, Year 1 Collins Bay decommission report) suggested that the use of algae should be investigated for reduction of contaminants in the flooded pit.

The algal biomass, collected together with the TSS in the 2 m sedimentation traps, could account reasonably well for the noted decrease in the concentration of Ni and Fe in the surface water in the first two growing seasons. However the estimates for the reduction of As concentrations in surface water could account only for one tenth of the total arsenic load removed from the surface water. These findings suggested that the adsorption behaviour of As and Ni must be different. Adsorption onto surfaces is a complex process which is affected by many factors, such as the chemical form in which the metal is present, the characteristics of the adsorption site and the surface charge of the adsorbent.

Adsorption characteristics will differ between dead and living cells, be modified by the presence of mucilage and be altered by changes in water characteristics such as redox and pH which take place either at the thermocline or at the bottom of the pit. Considering the

conditions of the pit, with its thermocline, all these factors have to be taken into account if biomass is to be increased or utilized as a flocculating agent. As the biomass reaches the thermocline, some decomposition would be expected, possibly resulting in release of the contaminants. However the material in the sedimentation traps at 32 m depth, well below the thermocline, contained moderate contaminant enrichment (up to 0.3% As and 0.1% Ni). These findings indicated that some metals reached the bottom of the pit. The mechanism by which contaminants reached the bottom was however lacking a verifiable explanation.

A series of investigations were initiated with the main objective of addressing the fate of As and Ni in the pit and improving our understanding of pit limnology. The current report summarizes the investigations carried out in 1995 and 1996. The findings will eventually form the foundation to a waste management plan, which would facilitate decommissioning the steel-cell containment which remains separated from Collins Bay. The ability to model long term behaviour of the pit is greatly improved if pit limnology is well understood.

The growth characteristics of the dominant algae in the B-Zone Pit were studied in the laboratory along with the factors which govern the production of extracellular polysaccharides, or mucilage. The investigation also addressed the adsorption capacity of these algae for As and Ni. The role of the algal-produced mucilage in As and Ni removal was tested using pure cultures in the laboratory. Factors leading to mucilage production, a sheath which binds together the *Dictyosphaerium* colonies, were also investigated. The growth response of these extremely hardy algae to low temperatures and light conditions was considered important, as these harsh conditions would be typical for the lower depths of the pit. From this work, jointly funded by CAMECO and CANMET, Department of Natural Resources Canada, under the National Biotechnology Strategy Program, two reports were published:

**Kalin, M. and Olaveson, M. 1996: Controlling factors in the production of extracellular polysaccharides in phytoplankton, pp 109, CANMET contract # 23440-5-1136/01 SQ.**

**Kalin, M. 1997 Nickel and Arsenic adsorption onto Mucilage producing algal colonies, CANMET Biotechnology, pp 28, CANMET Contract# 23440-6-1011/001/SQ.**

The second report (Kalin 1997) expanded upon the findings of the initial laboratory investigations, using a culture derived from B-Zone Pit algae. The first round of experiments on adsorptions of As and Ni onto algal biomass and on mucilage produced different results for the two elements. Ni adsorption reached a maximum at  $2.5 \text{ mg} \cdot \text{L}^{-1}$  and decreased with higher concentrations, whereas As adsorption was very low and essentially not detectable with colorimetric methods used in the initial investigation. As and Ni behaviour in the pit, based on the monitoring data, also indicated different adsorption behaviour for the two elements with respect to transport to the bottom. It appeared, therefore, that the experiments may reflect the ongoing processes in the pit very well. The adsorption experiments were repeated to define clearly the adsorption isotherms at concentrations of As and Ni prevailing in the pit. Through these experiments, the role of algae and mucilage produced by them can be defined in the transport mechanism of these elements in the pit. Summaries of the data generated in these two studies will be used in this report to elucidate the fate of As and Ni in the pit, along with the physical/chemical monitoring data collected since the flooding of the pit in 1991/1992.

With these studies, many important aspects of the potential role of algae as adsorbents for As and Ni in the B-Zone Pit were addressed. However, the dimictic nature of the pit leading to annual turn over of the water column required further questions to be answered. It is all very well to define the adsorption characteristics of As and Ni onto the biomass, but for practical application, the biomass has to reach the bottom of the pit, preferably without releasing the

metals. During qualitative identifications of phytoplankton samples in 1994 collected at different depth in the pit, it was noted that the morphology of the algal cells disintegrated with depth. This lead to the question of the transport mechanisms which prevailed in the lower portion of the pit for As and Ni. It would be expected that the decomposing biomass would release its contaminants.

From the literature, it was suggested that primary productivity of that portion of photosynthetic algae which are smaller than 2 : m might form up to 80% of the primary productivity in a water body such as the flooded B-Zone Pit. The optical microscope used for conventional algal identifications does not recognize particles which are smaller than 2 : m. It was deemed possible that in stressed ecosystems, such as the B-Zone Pit, picoplankton (plankton smaller than 2 : m) could be playing a significant role both in contaminant transport and pit primary productivity. Picoplankton has generally a low light requirement and growth prevails at low temperatures, both of which are conditions which prevail in the lower parts of the pit. With the optical microscope it was observed that the algal colonies disintegrate with depth, despite their growth tolerance to low light and temperature. The disintegration still noticeable with the light microscope, could have resulted in smaller algal cells, no longer visible with the optical microscope.

In 1996, water samples were collected at different depths in the B-Zone Pit and analysed for the presence of picoplankton, using Flow Cytometry methods developed in Germany. Details of this work, jointly funded by the same sponsor as the previous studies, are given in:

**Kalin, M. Wheeler, W and Smith M.P.; 1997: The role of Picoplankton as primary producers in mining waste water effluents. CANMET Contract # 23440-5-1302/001/SQ.**

Significant quantities of picoplankton were found at depth in the pit. Quantitative enumerations are presented, forming part of the description of biological processes which

take place in the lower portion of the pit. These results elucidate the origin of the organic portion of the material in the lower sedimentation traps, but the question remains whether these small particles carry As and Ni. This question was elucidated by evaluating the particle size and the nature of the material collected in the sedimentation traps. The contents of sedimentation traps from the B-Zone Pit formed part of a study of particle formation in mine waste water. Details of this work can be found in an MSc. thesis, also in part supported by the National Biotechnology Strategy Program through CANMET, entitled:

**Chemical, Physical and Biological Characteristics of Particulates Formed in Mine Drainage Environment, University of Toronto MSc thesis, E.A.Lowson, Department of Geology University of Toronto, Supervisor G. Ferris**

Sequential extractions on sedimentation trap material and granulometric determinations are presented in this thesis and references will be made to investigations of the characteristics of the surfaces of the particles using SEM/EDX and SIMS electron microscopy. The reader is referred to the individual reports for detail, as only portions of the data are relevant to the current report. Very early in the investigations of the particles in mine waste water, it became apparent that the contaminants in the pit associate with very small particles which may remain suspended in the water column for a long time. It was also suggested that the contaminants are not necessarily present as ions but present in a colloidal form. The traditional distinction between dissolved and suspended matter, which is made by filtration through a 0.45  $\mu$ m filter, may therefore not be representative of the actual chemical form of the "dissolved" contaminants in the pit. The chemical form of "dissolved" As and Ni will not only determine the adsorption behaviour of these metals and thereby treatability, but also affect their toxicity. Generally, adsorbed or colloidal metals are less toxic than those in an ionic form. Since water quality is being judged against that quality which is required to avoid impacting aquatic life, these considerations are potentially significant for the decommissioning plans.



Experiments were therefore carried out in 1996, to determine the form and the likely surface charges of particles which are associated with As and Ni in the pit. This was examined indirectly through a series of experiments carried out in 1996 on site. Pit water was charged with various iron salts, used in conventional treatment processes for As, as well as mixtures of algae and bentonite. The particle formation and settling characteristics are described. Fractionation of both As and Ni, converting dissolved (defined by  $0.45 \mu\text{m}$ ) fractions to a flocculant which settles, and the fractions which remains suspended in solution as a result of additions of adsorbents to the pit water, were carried out. The results from these experiments lead to our understanding of the fate of Ni and As in the pit. The report ends with a discussion comparing the expected behaviour of the contaminants from the literature to the behaviour of these elements in the pit, focussing on colloid formation and adsorption.

## 2.0 B-ZONE FLOODED PIT OBSERVATIONS

### 2.1 Physical/Chemical Parameters of the Pit

The flooded pit contains approximately  $5 \times 10^6 \text{ m}^3$  of water and has a surface area of  $282,600 \text{ m}^2$ . During the spring and summer, the pit develops a stratified temperature distribution, with a warmer layer (the epilimnion) lying on top of a colder layer (the hypolimnion). The formation of the thermocline is a very important physical factor which affects many chemical and physical aspects of the pit. Along with the changes in temperature, it can be expected that changes in oxygen concentrations, Eh, and electrical conductivity will take place with depth. In order to better understand the fate of the contaminants of concern (As and Ni), these field measured parameters have been monitored since the flooding of the pit. Measurements of these parameters are generally taken 4 times during the year at 1 m intervals, and water samples are collected every 5 m (Map 1). To assess any relevant changes in the pit, the monitoring data are presented for each monitoring period for successive years. Only the profiles which reach the bottom of the pit are considered in this analysis. Data for the 1992 season are ignored, since this first year was dominated by excessive load of suspended solids and erosion from the pit wall. As the light penetration in the pit in the first year was essentially nil, very little to no biological activity was taking place. The monitoring data are discussed starting from the measurements under the ice in the spring of 1993 to October 1996.

The pit water is separated from Collins Bay by a steel dyke structure, and therefore represents a water body which is isolated from the surrounding ground water regime. The pit reached a stable water level in 1996, and the amount of water leaving the pit is small in comparison to the pit volume. The limnology of the flooded pit is therefore best viewed as a closed water body. It is thus reasonable, given these conditions of the pit, to conclude that changes in chemical or physical parameters in the pit are the result of processes taking place within this closed water body.

**LEGEND**

- Limnological profile station
- ▲ Limnological profile and sedtrap station
- A—A' Cross-section (shown in Fig. 8)
- 43 Depth (metres)
- ▨ Dyke
- - - Road

**Collins Bay**  
398.7m ASL.

*Grenier's Pond*

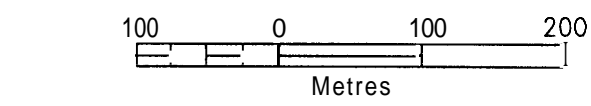
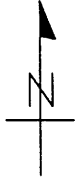
Stn. 6.71  
43

Stn. 6.72

BP-1  
▲ 53

Stn. 6.73

**B Zone  
Open Pit**  
W/L 398m ASL. (full)



|                                     |        |
|-------------------------------------|--------|
| Boojum Research Ltd.                |        |
| <b>CAMECO: B ZONE</b>               |        |
| Rabbit Lake Operation. Saskatchewan |        |
| <b>B ZONE OPEN PIT</b>              |        |
| Date: Dec./94                       | Map: 1 |

The temperature profiles of the flooded pit are divided into the ice-covered period (March-May, 1993 to 1996) in Figure 1a, after ice breakup (June, 1993 to 1995) in Figure 1b, for late summer (August, 1993 to 1996) in Figure 1c and for late fall (October, 1993 to 1996) in Figure 1d. Sampling stations for the pit are given in Map 1; for discussion the deepest station (6.72) is selected. During the ice covered season, the thermal inversion has not changed over the monitored years. After ice breakup, the depth of the thermocline varies with air temperature. The late summer stratification (Figure 1c) has remained the same over the years. Thermal stratification is well developed, with the warmer upper layer of water extending down to 9 m. By late fall, in October, the difference in temperature between the waters above and below the thermocline is reduced and the pit is close to the point of developing an inverted profile once again, resembling the conditions under the ice, thereby completing the yearly cycle.

In Figures 2a to 2d the profiles for dissolved oxygen are presented in the same sequence as the temperature data. During the ice cover, in 1993, very little oxygen was consumed at the bottom of the pit. Since then, oxygen consumption has increased from year to year. This is expected, as increased algal growth in the surface water has generated organic matter which in turn decomposes and moves through the water column to the bottom of pit. Over the years up to 1996, additional organic matter is produced, resulting in a bottom accumulation of material which allows growth of heterotrophic bacteria which consume  $O_2$  and release  $CO_2$  by respiration. Therefore the progressive increase in oxygen consumption over the three monitored years indirectly reflects the accumulation of organics in the lower reaches of the pit (Figure 2a). After breakup, the pit water re-oxygenates completely to the bottom of the pit, up to 1995. By late summer, oxygen concentration has decreased in the last two years to about  $8 \text{ mg} \cdot \text{L}^{-1}$ , whereas in previous years, this was not the case (Figure 2c). This suggests that decomposition proceeds up to late summer but by late fall, the entire pit water column is oxygenated again.

**Fig. 1a: Flooded Pit, March-May  
Temperature vs Depth, 1993-96**

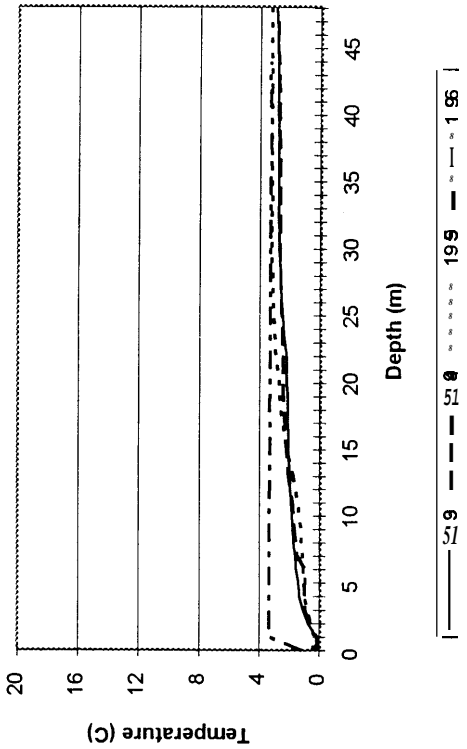


**Fig. 1b: Flooded Pit, June  
Temperature vs Depth, 1993-95**

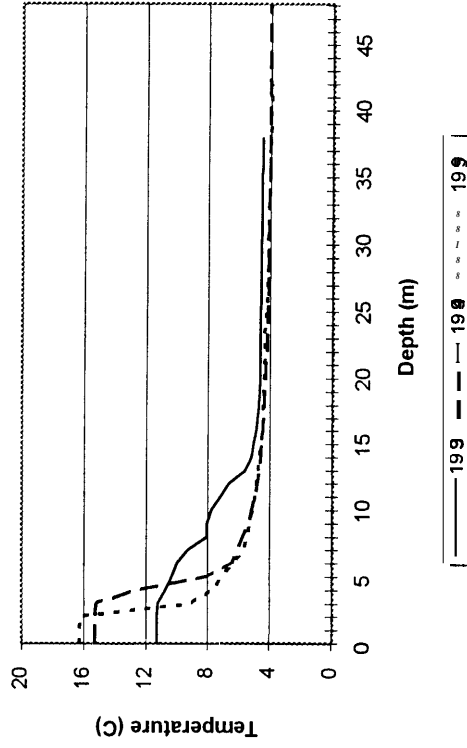


**Fig. 1c: Flooded Pit, August  
Temperature vs Depth, 1993-96**

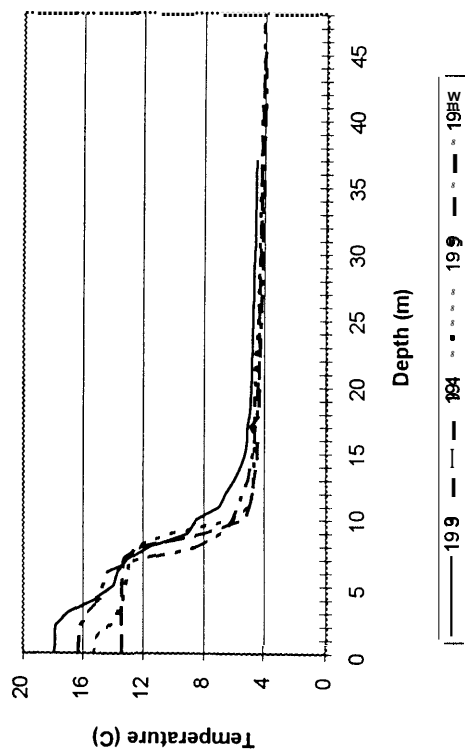


**Fig. 1d: Flooded Pit, October  
Temperature vs Depth, 1993-96**

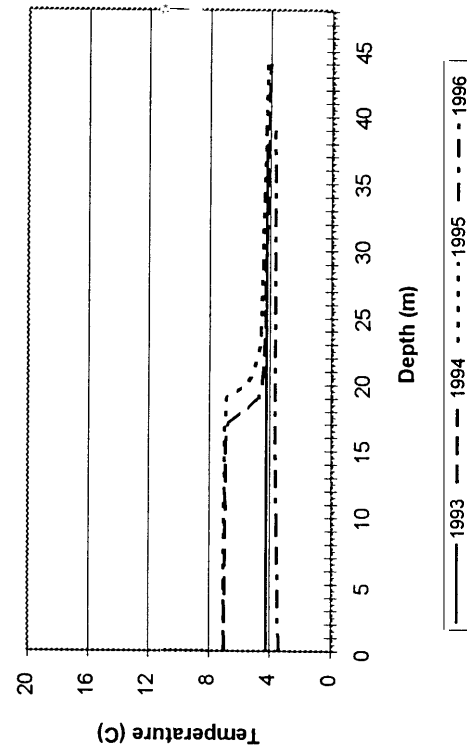


**Fig. 2a: Flooded Pit, March-May  
 Dissolved Oxygen vs Depth, 1993-96**

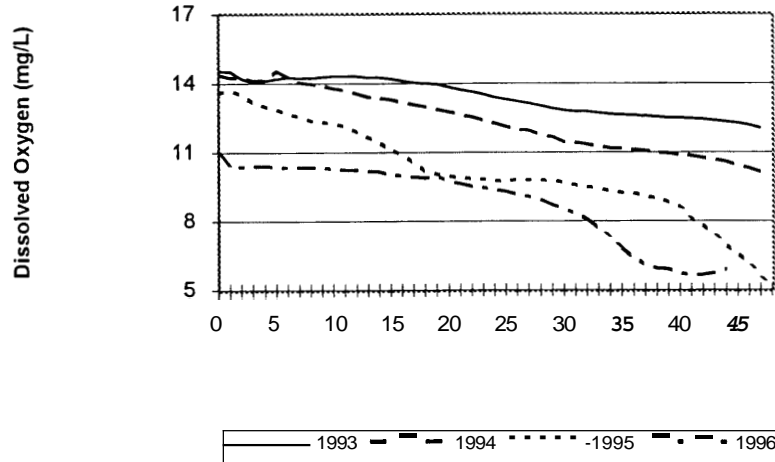


**Fig. 2b: Flooded Pit, June  
 Dissolved Oxygen vs Depth, 1993-95**

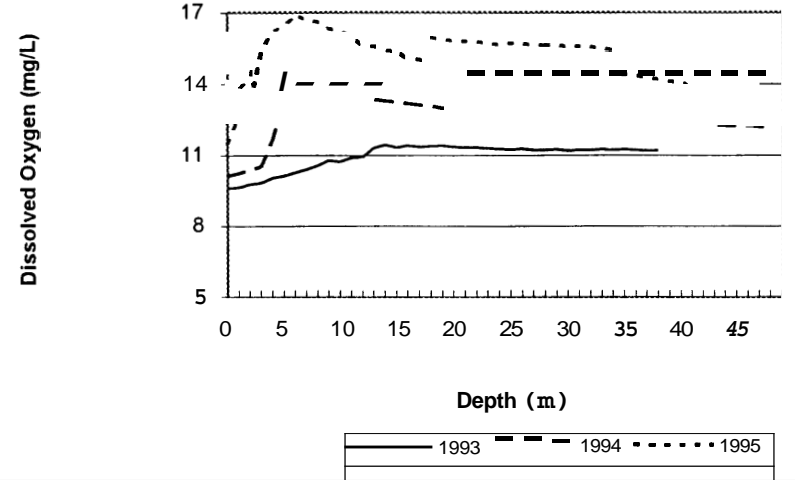


**Fig. 2c: Flooded Pit, August  
 Dissolved Oxygen vs Depth, 1993-96**

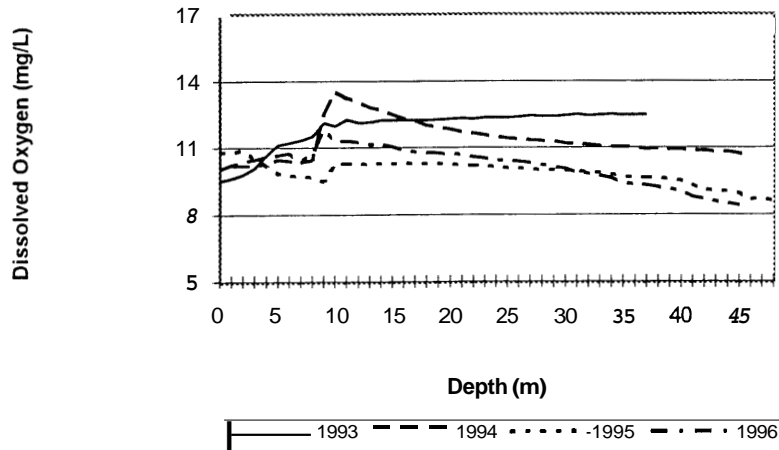
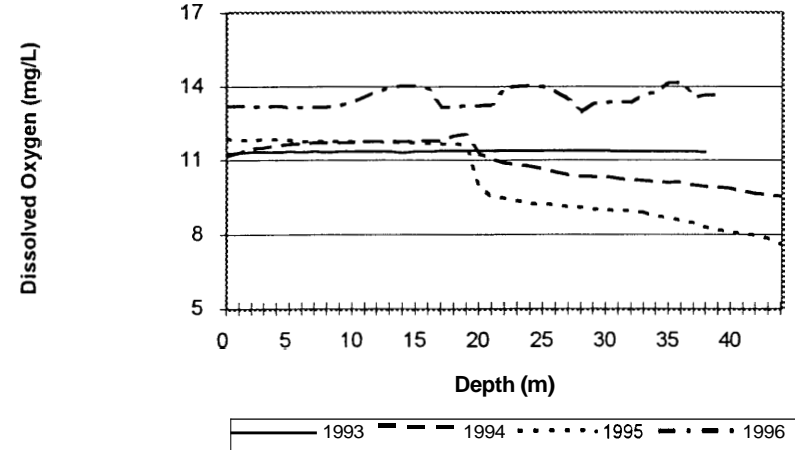


**Fig. 2d: Flooded Pit, October  
 Dissolved Oxygen vs Depth, 1993-96**



In Figures 3a to 3d, the Eh profiles are presented. Over the years, the Eh under the ice has increased from year to year (Figure 3a). However by the end of the season in late fall, the values are in the same range, around 350 mV (Figure 3d). At present, the process which would lead to the changes in Eh over the season is not clear as the profiles are relatively uniform for the periods when the thermocline is well established during the summer months (Figures 3b and 3c). The seasonality of the Eh response does, however, suggest that the oxidation products which lead to the increase in Eh during the ice covered season have reacted by the end of the season.

The pH of the pit with depth under the ice is very uniform with values ranging between 6.5 and 6.9. The depression noted in 1994 where the pH decreased to a value of 5.2 on the surface may have been generated by a measurement error, as this trend did not prevail prior to or after 1994 (Figure 4a). As the ice breaks up, the pH increases due to photosynthesis, which peaked in 1995, raising the pit to a pH value above 8 by mid summer (Figure 4c). The lower reaches of the pit, however, remain at the pH value similar to the conditions underneath the ice, i.e. 6.5 to 6.8 (Figure 4d).

The electrical conductivity is generally very low, but displays some interesting changes with time. Underneath the ice (Figure 5a) at the bottom of the pit, a pronounced increase is evident in the years 1993 and 1994, somewhat subsiding in 1995 to 1996. Below 40 m depth, the conductivity increased from 60 to 90 :  $S\text{cm}^{-1}$  in 1995 and from 70 to 92 :  $S\text{cm}^{-1}$  in 1996. In the previous years, 1993 to 1994, the increase in bottom conductivity was larger, increasing from about 40 :  $S\text{cm}^{-1}$  to about 110 :  $S\text{cm}^{-1}$  below 40 m. As the pit stratifies in the summer months (Figures 5b and 5c), the entire pit reaches the conductivity values which were generated in the bottom during the ice-covered season. Thus, a year-to-year annual increase is evident for conductivity.

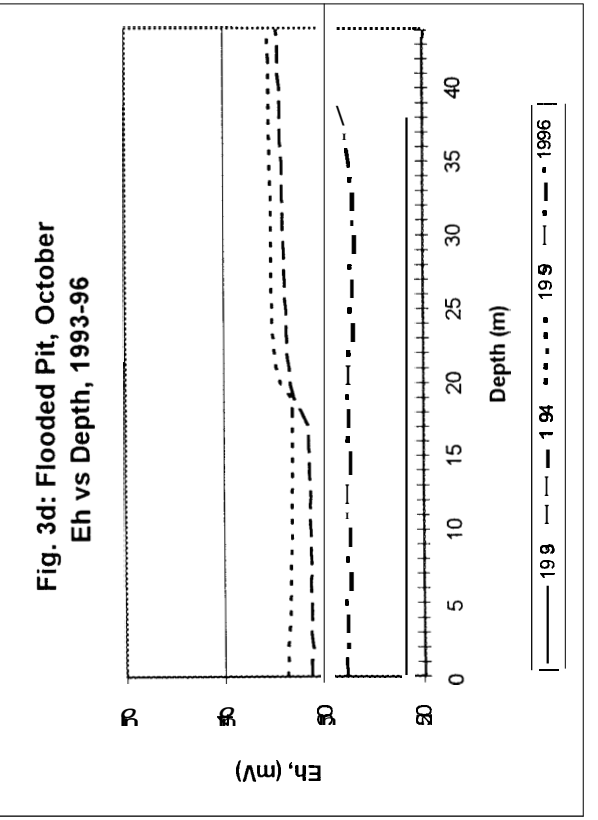
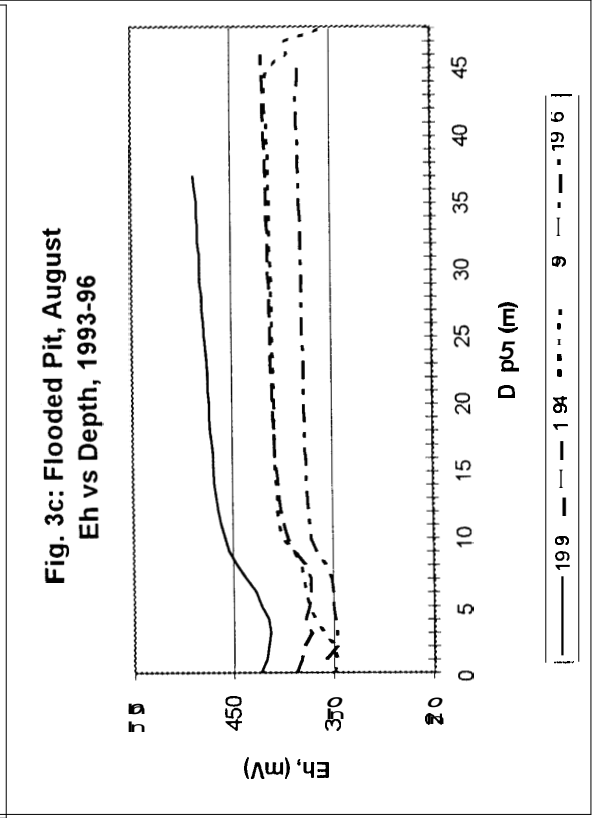
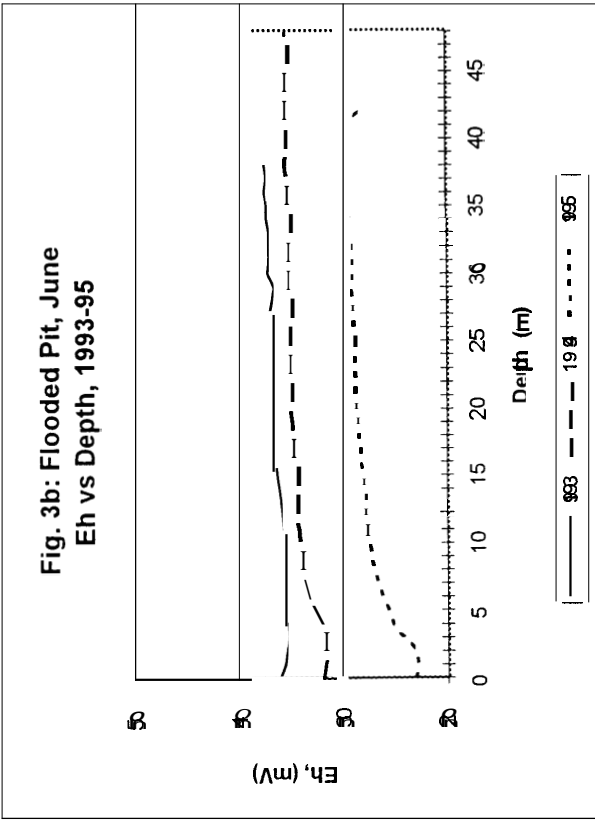
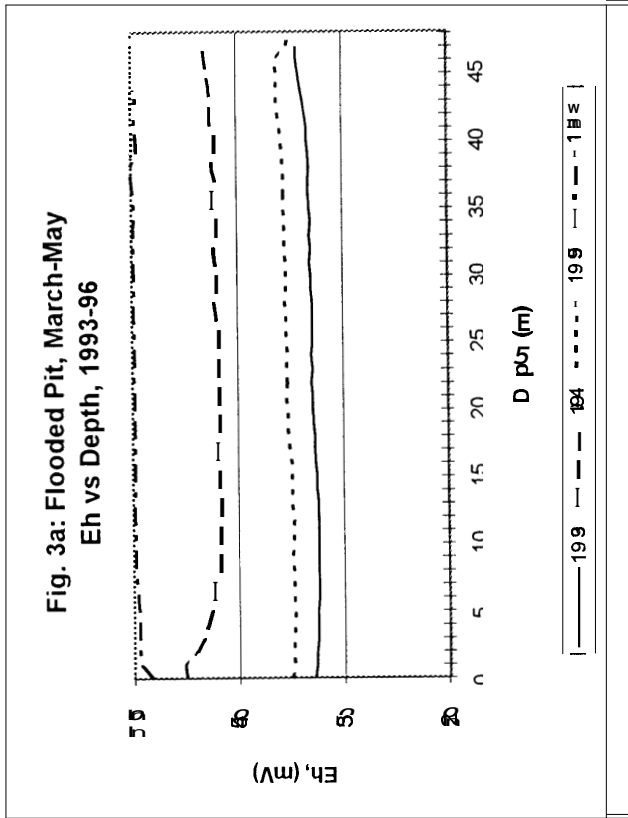




**Fig. 4b: Flooded Pit, June  
pH vs Depth, 1993-95**

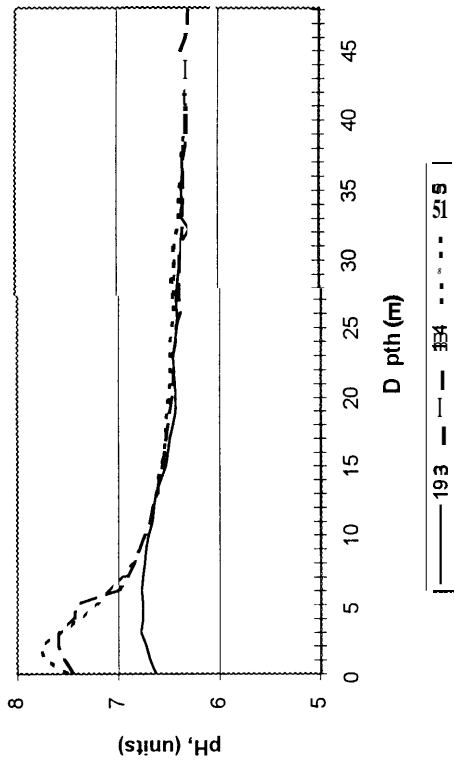


**Fig. 4d: Flooded Pit, October  
pH vs Depth, 1993-96**

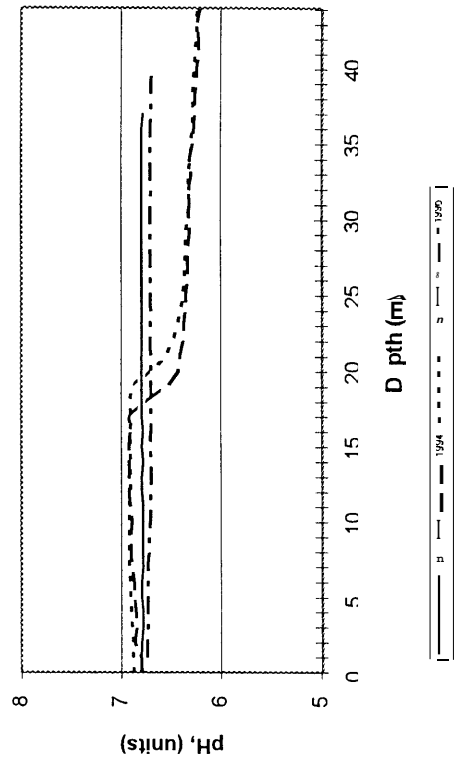


**Fig. 4a: Flooded Pit, March-May  
pH vs Depth, 1993-96**

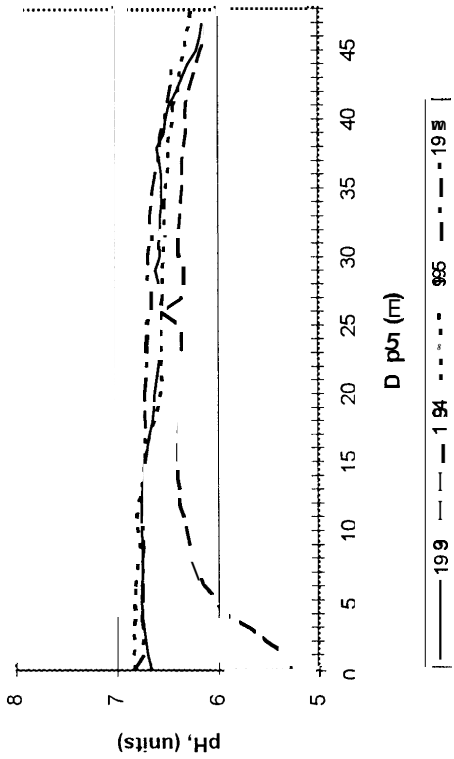


**Fig. 4c: Flooded Pit, August  
pH vs Depth, 1993-96**

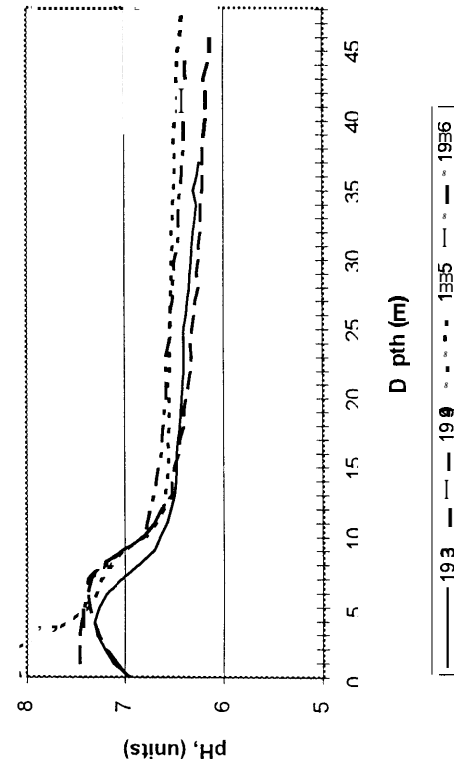


**Fig. 5a: Flooded Pit, March-May  
Conductivity vs Depth, 1993-96**

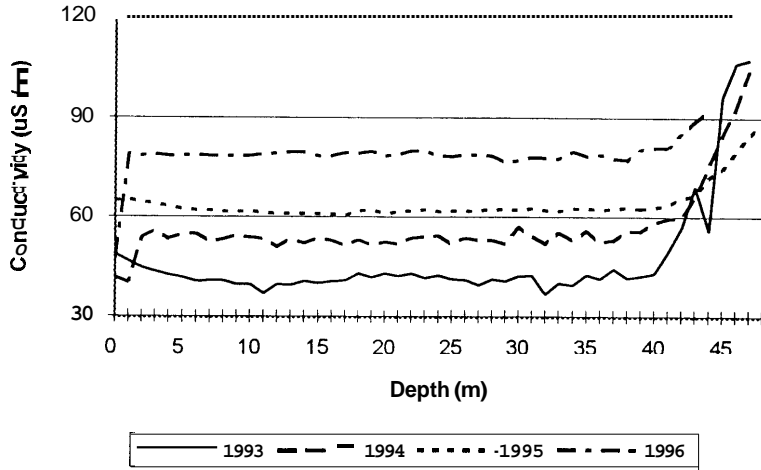


**Fig. 5b: Flooded Pit, June  
Conductivity vs Depth, 1993-95**

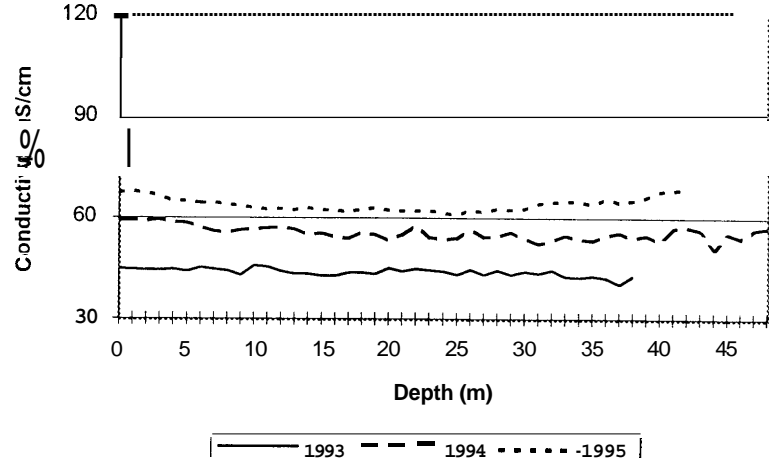


**Fig. 5c: Flooded Pit, August  
Conductivity vs Depth, 1993-96**

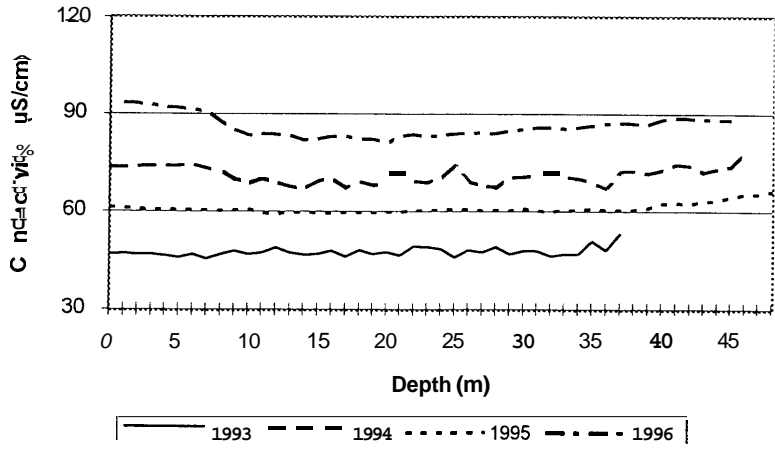
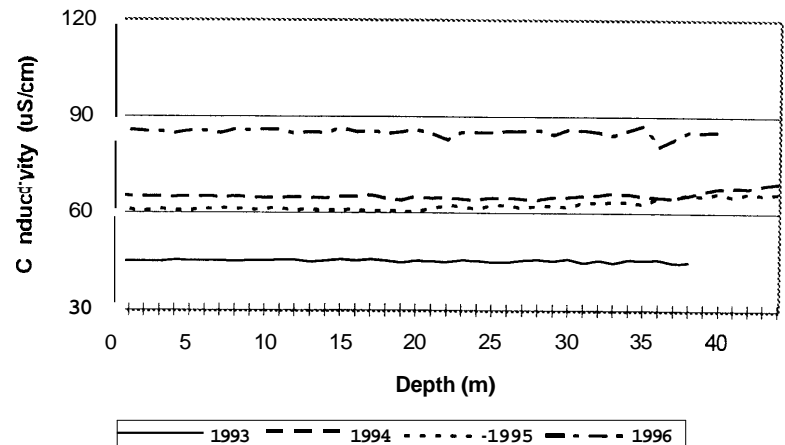


**Fig. 5d: Flooded Pit, October  
Conductivity vs Depth, 1993-96**

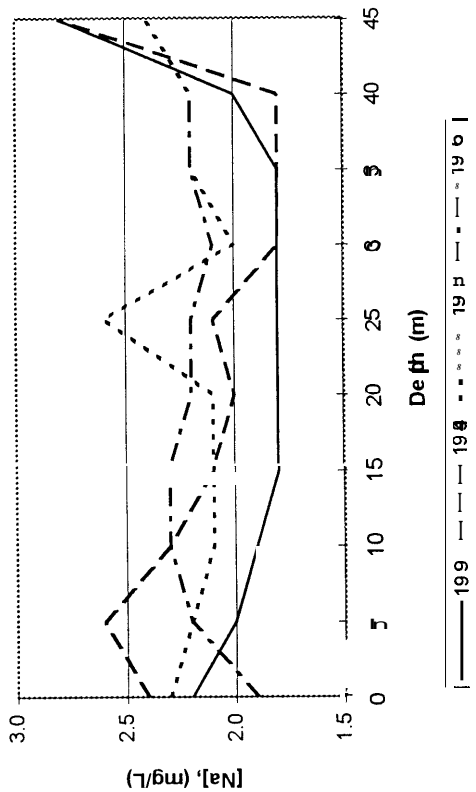


In order to determine which elements are contributing to the increase in conductivity, the monitoring data were examined and those elements which showed variations throughout the years with depth are presented. In Appendix A, the data are tabulated for all years and all elements which were present in concentrations above the detection limit for the years 1992 to 1996.

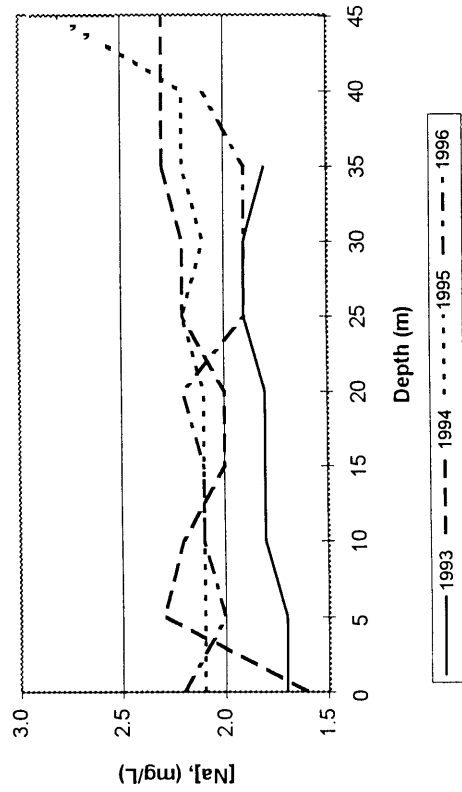
Increases in concentrations at the very bottom of the pit, when the pit is ice covered, are evident for the elements sodium (Figures 6a to 6d), potassium (Figures 7a to 7d), magnesium (Figures 8a to 8d), and calcium (Figures 9a to 9d). For these elements, the increase in concentration below 40 m is generally of the range of 1 to 3 mg@L<sup>-1</sup> for each element. The concentrations of sulphate increase in the ice-covered season below 40 m by about 5 mg@L<sup>-1</sup> to 20 mg@L<sup>-1</sup> (Figures 10a to 10d). The largest increase was noted in 1993 with relatively lower increases in the years 1994 and 1995. Unfortunately, in 1996 the measurements ceased at 40 m. Throughout the ice-free portion of the year, all the parameters tend to drop back to more stable concentration levels which range between 1.5 mg@L<sup>-1</sup> and 6 mg@L<sup>-1</sup>. In other words, the apparent formation of a deep chemocline disappears. This is also the case for sulphate, which displays average concentrations since 1993 in the ice-free season ranging between 10 mg@L<sup>-1</sup> and 14 mg@L<sup>-1</sup>.

This data set reflects the changes which take place due to oxidation-reduction reactions. These reactions affect adsorption and desorption reactions along with dissolution and precipitation. The major factor in the pit which leads to these changes is believed to be the biology of the pit, as no other factor, such as continued dissolution of elements from pit walls or significant contributions from the ground water are evident. Assuming that biological activity is the main component, the increases in bicarbonate over the years should be apparent and reflect the year-to-year trends seen in the conductivity measurements. In Figures 11a to 11d, bicarbonate concentrations are plotted which confirm a steady increase from 1993 to 1996. In 1993 the pit water contained about 14 mg@L<sup>-1</sup> bicarbonate, which increased slightly to about 16 mg@L<sup>-1</sup> in 1994. After light

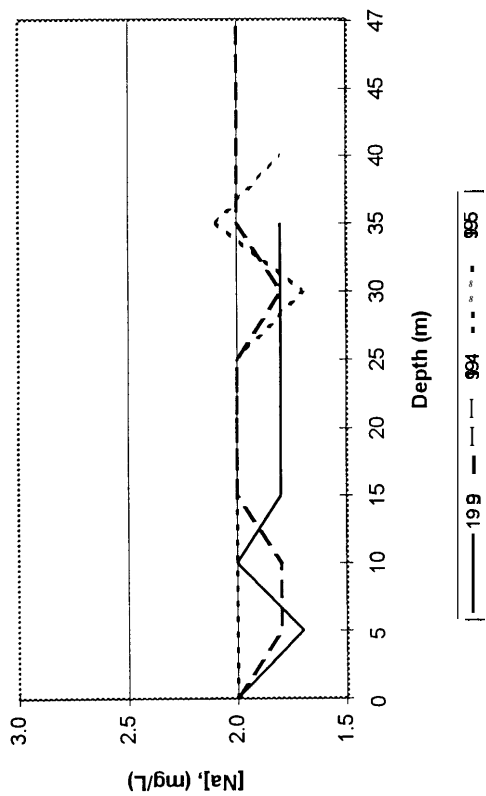
**Fig. 6a: Flooded Pit, March-May  
Sodium Concentration, 1993-96**



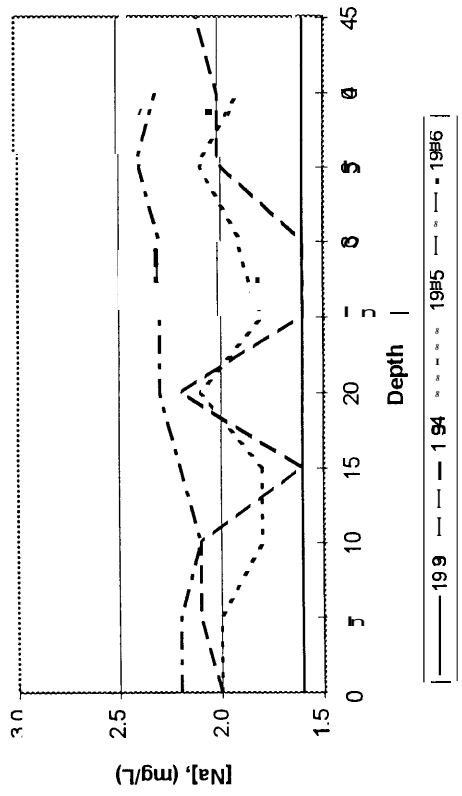
**Fig. 6c: Flooded Pit, August  
Sodium Concentration, 1993-96**



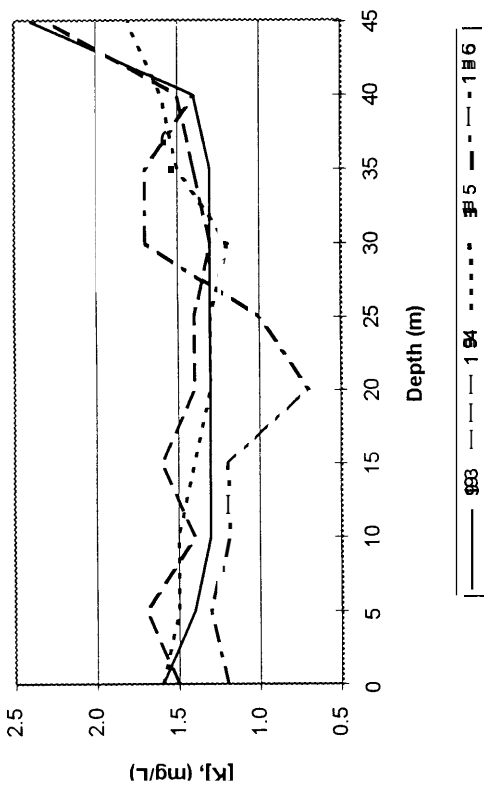
**Fig. 6b: Flooded Pit, June  
Sodium Concentration, 1993-95**



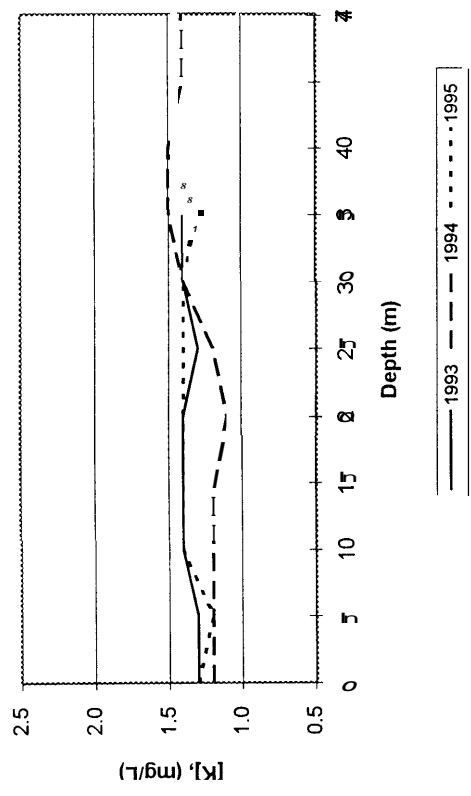
**Fig. 6d: Flooded Pit, October  
Sodium Concentration, 1993-96**



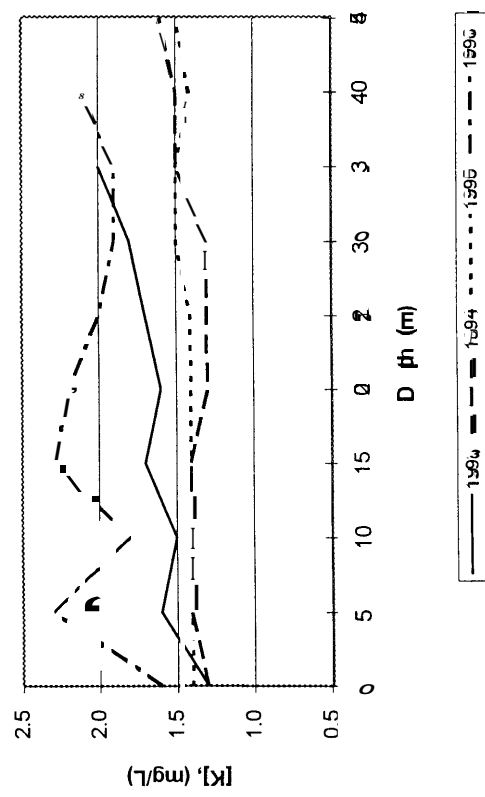
**Fig. 7a: Flooded Pit, March-May  
Potassium Concentration, 1993-1996**



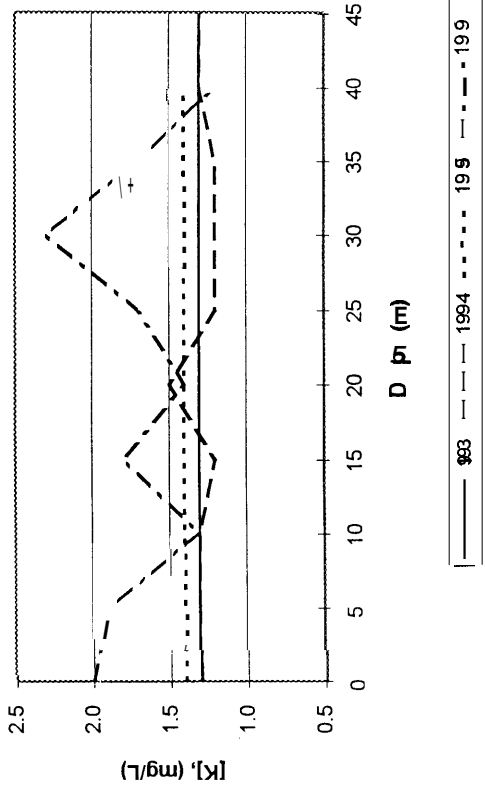
**Fig. 7b: Flooded Pit, June  
Potassium Concentration, 1993-1995**



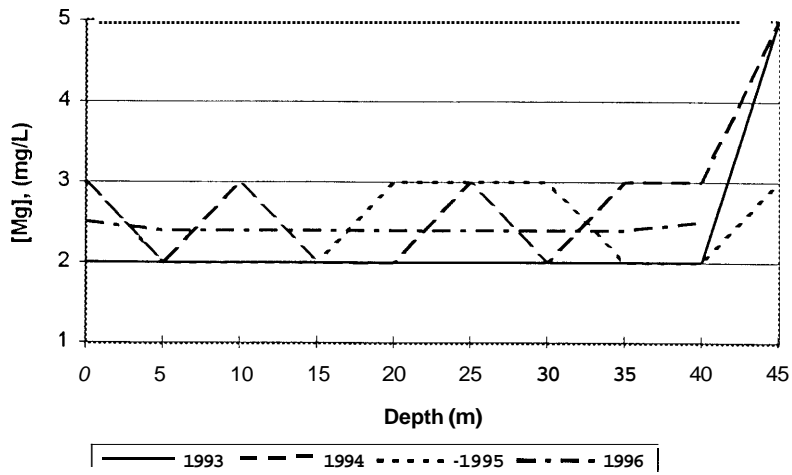
**Fig. 7c: Flooded Pit, August  
Potassium Concentration, 1993-1996**



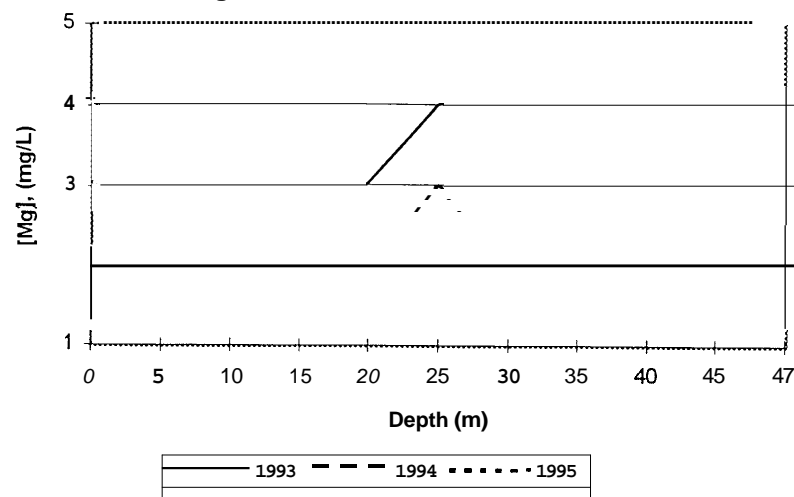
**Fig. 7d: Flooded Pit, October  
Potassium Concentration, 1993-1996**



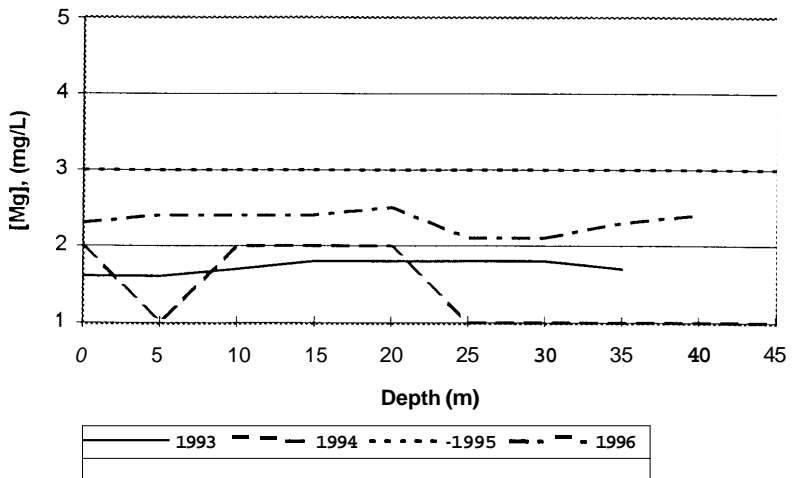
**Fig. 8a: Flooded Pit, March-May  
 Magnesium Concentration, 1993-96**



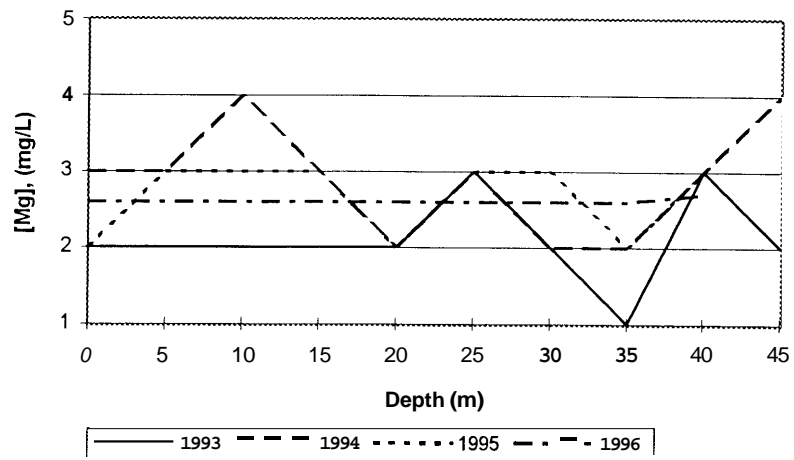
**Fig. 8b: Flooded Pit, June  
 Magnesium Concentration, 1993-95**



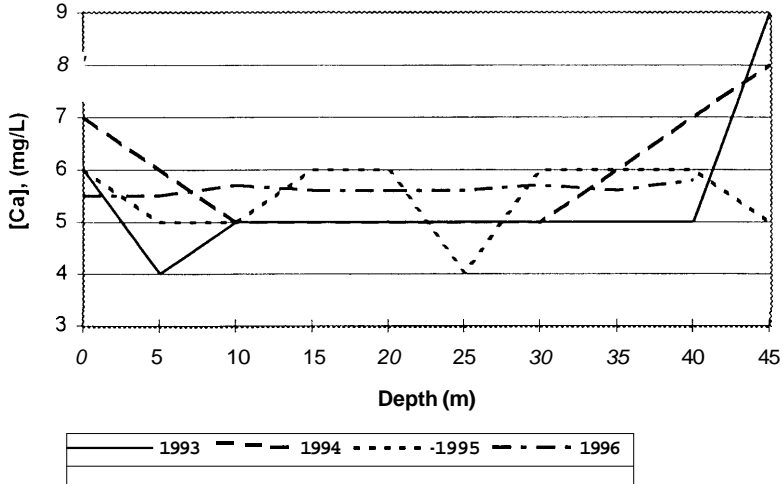
**Fig. 8c: Flooded Pit, August  
 Magnesium Concentration, 1993-96**



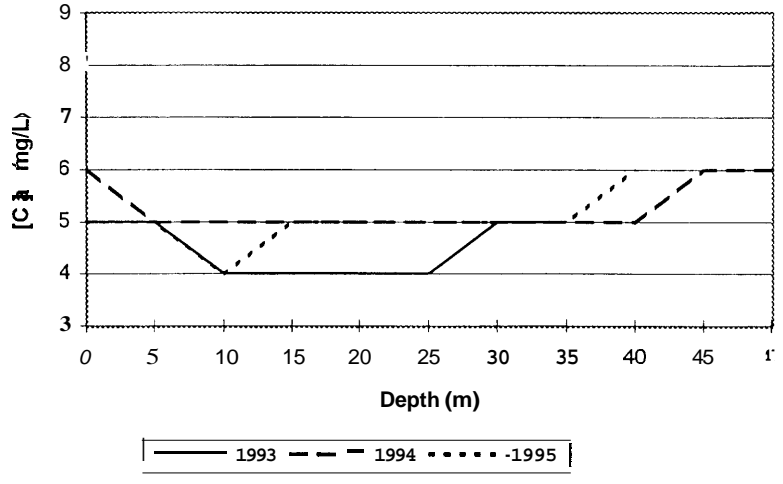
**Fig. 8d: Flooded Pit, October  
 Magnesium Concentration, 1993-96**



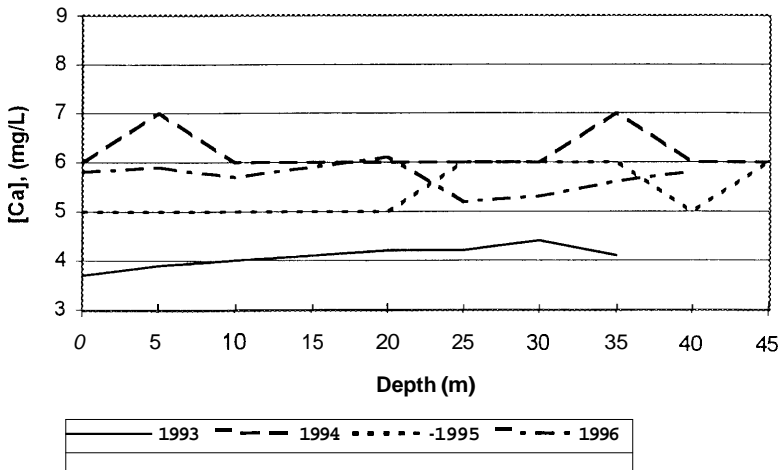
**Fig. 9a: Flooded Pit, March-May  
 Calcium Concentration, 1993-96**



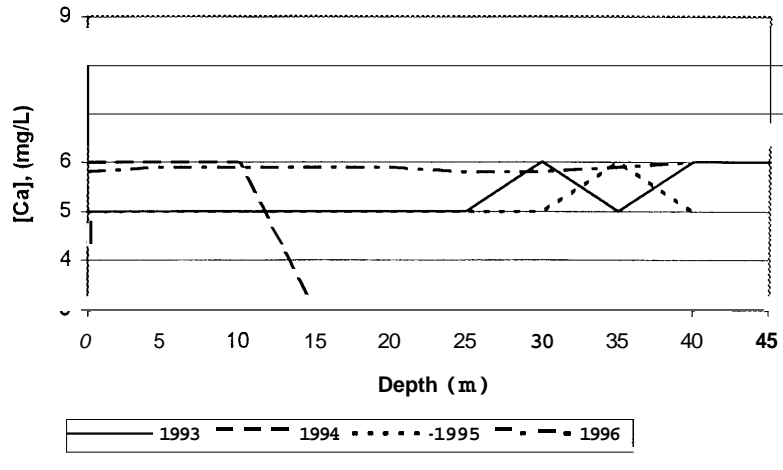
**Fig. 9b: Flooded Pit, June  
 Calcium Concentration, 1993-95**



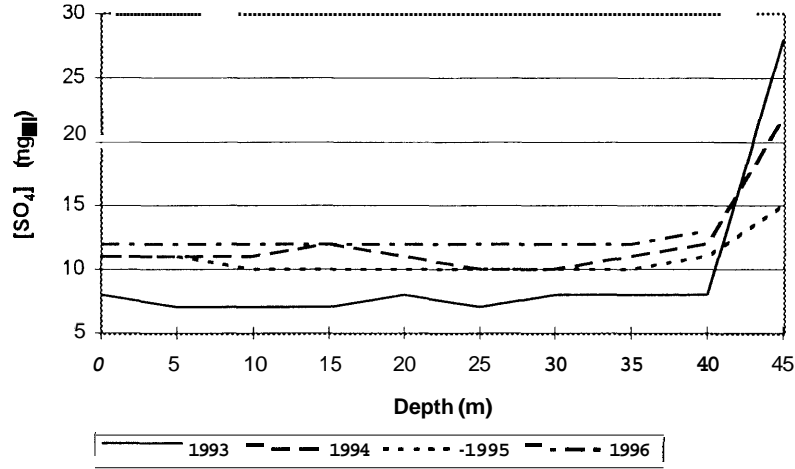
**Fig. 9c: Flooded Pit, August  
 Calcium Concentration, 1993-96**



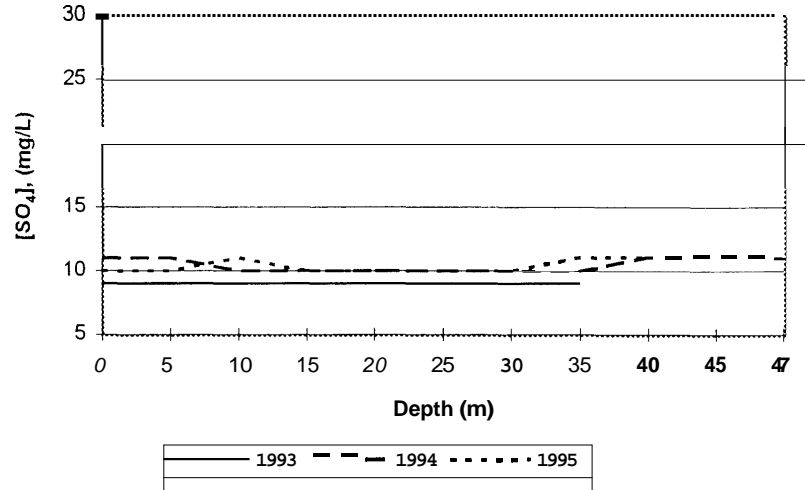
**Fig. 9d: Flooded Pit, October  
 Calcium Concentration, 1993-96**



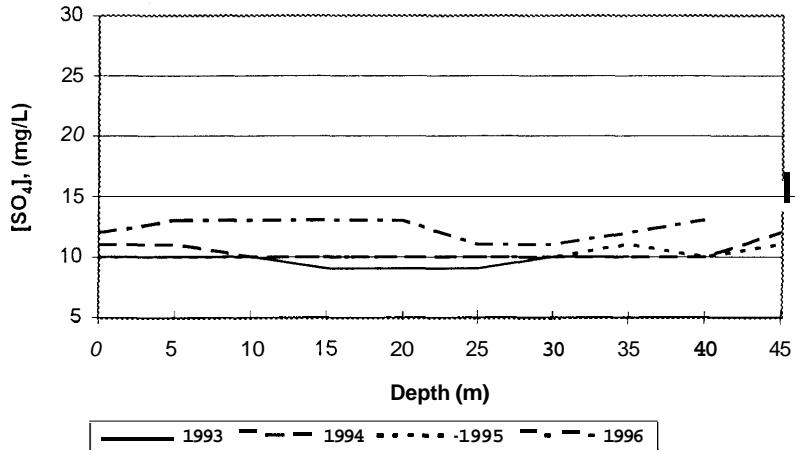
**Fig. 10a: Flooded Pit, March-May Sulphate Concentration, 1993-96**



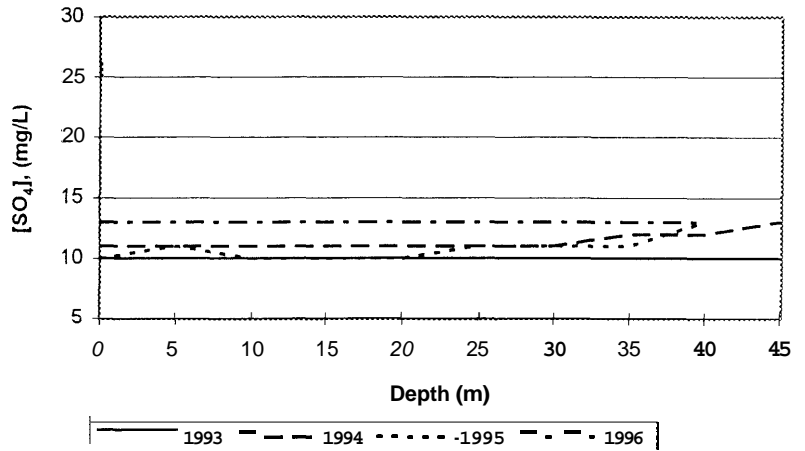
**Fig. 10b: Flooded Pit, June Sulphate Concentration, 1993-95**



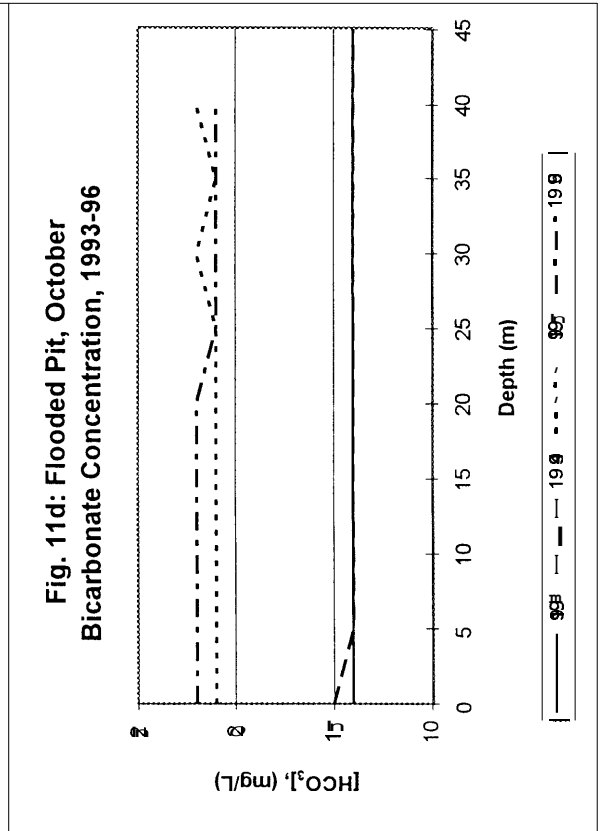
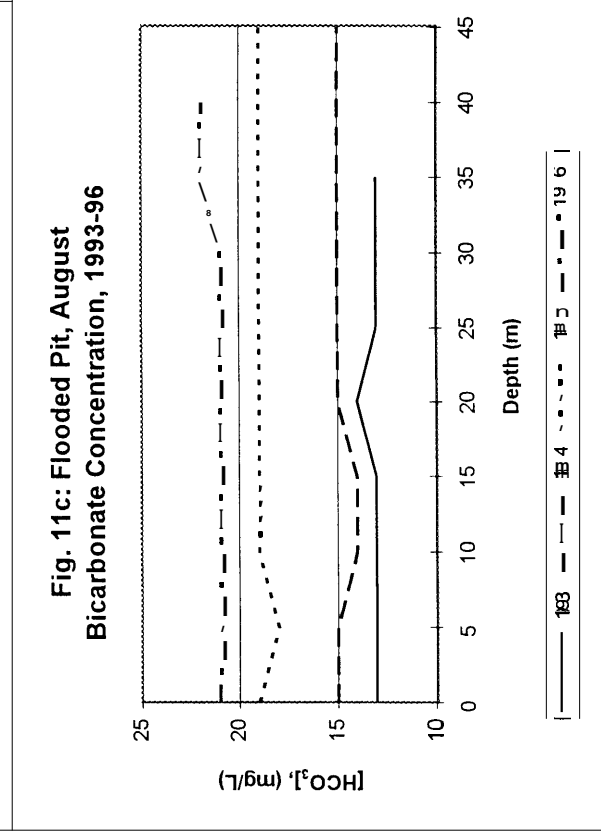
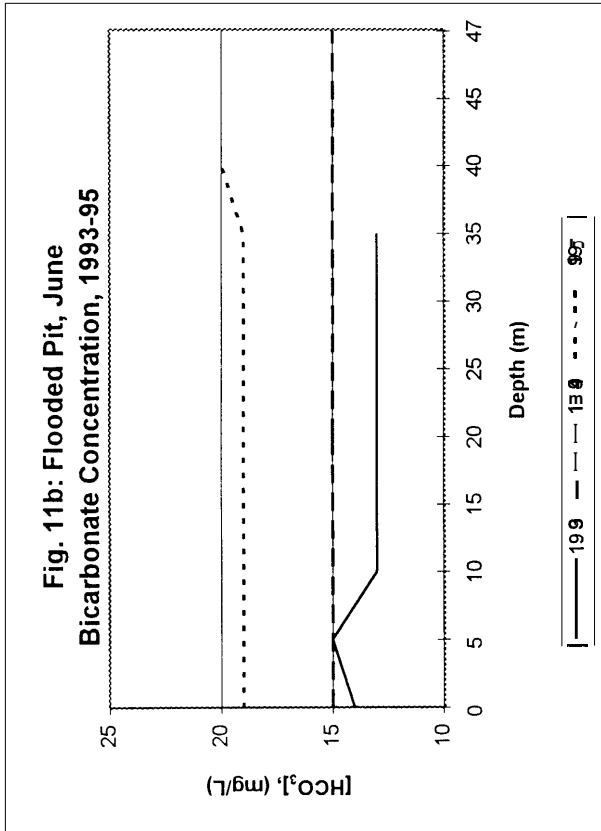
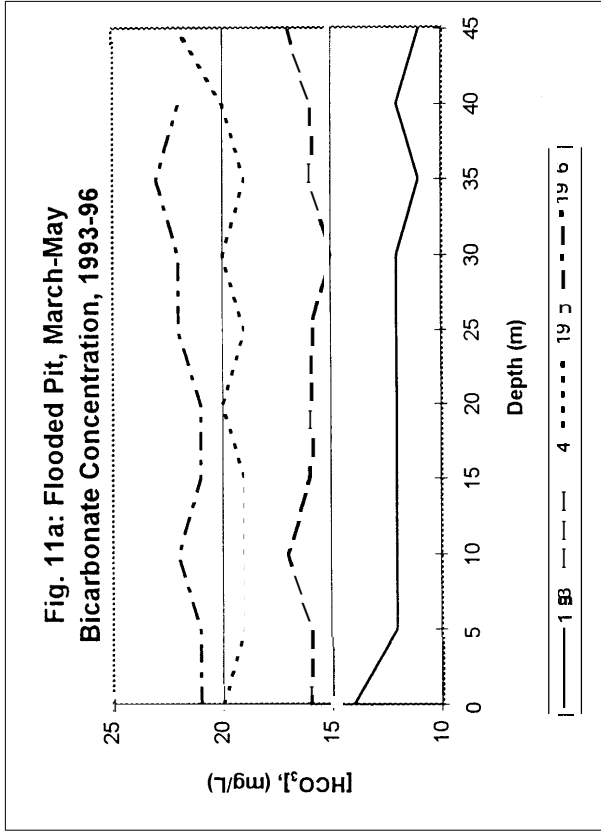
**Fig. 10c: Flooded Pit, August Sulphate Concentration, 1993-96**



**Fig. 10d: Flooded Pit, October Sulphate Concentration, 1993-96**







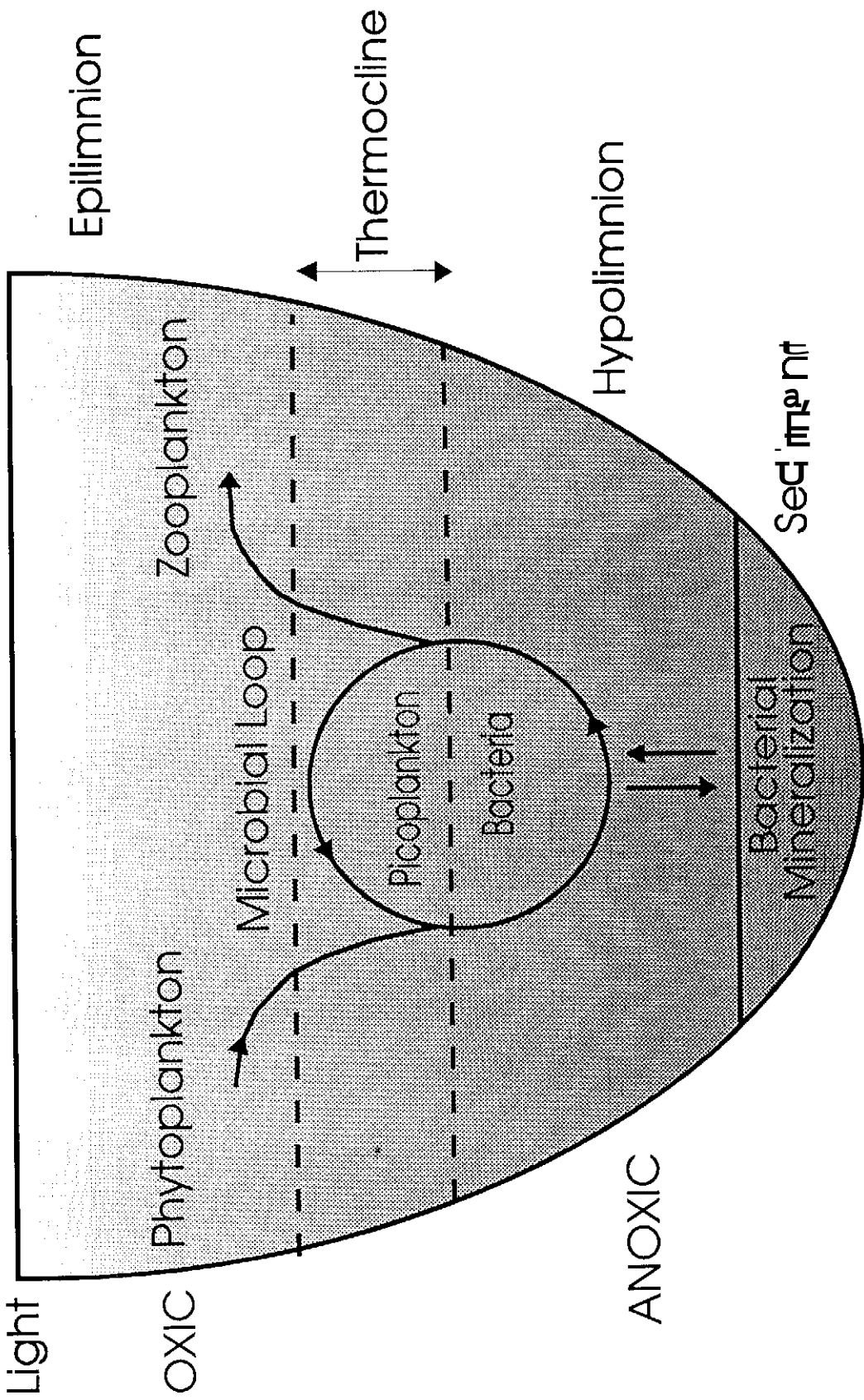
penetration had improved in the pit and the algal productivity increased, the bicarbonate concentration had reached  $21 \text{ mg@L}^{-1}$  by 1996.

From an ecological viewpoint, the pit limnology is very interesting. The major force controlling the flooded pit water chemistry is its biological component, supported by the observed chemical changes. It follows that toxicological considerations, which lead to the environmental concern regarding the elevated concentrations of As and Ni are not suppressing aquatic life with respect to primary productivity and microbial decomposition. The forms of As and Ni present in the pit or their concentrations are such that toxicological concentrations established for the protection of higher forms of aquatic life do not apply. Given that the biology of the pit is a dominant factor, the organisms inhabiting the pit must be tolerant to the conditions in the pit and are capable of affecting the nutrient balance in the surface waters.

## **2.2 Nutrient Concentrations**

Nutrient concentrations can be expected to change in relation to uppermost layer of water, where light penetrates. This must be considered when evaluating the primary productivity in the pit. Schematic 1 shows the likely spatial distribution of phytoplankton, which is the primary force in pit chemistry, and its relation to the microbial loop. This loop is likely present in the pit and active below the thermocline, leading to the previously noted oxygen depletion and production of bicarbonate.

The summary of the 1995 nutrient concentrations is given in Table 1a. In Table 1b, the same information is given for 1996. The water samples were collected every 5 m, however the thermocline extends below 5 m throughout the growing season or may be located at a depth somewhere between the 5 m intervals where water samples are taken. The average concentrations of nutrients above the thermocline are calculated by including the



Schematic 1: Components of primary productivity and physical/chemical aspects of water bodies

| 1995           | Depth            | Nutrients,      |                 | g/L             |             |             |
|----------------|------------------|-----------------|-----------------|-----------------|-------------|-------------|
|                |                  | PO <sub>4</sub> | NO <sub>3</sub> | NH <sub>4</sub> | N,TKN       |             |
| April 12       | 0                | 0.46            | 0.44            | 0.01            |             |             |
|                | 5                | 0.43            | 0.44            | 0.03            |             |             |
|                | 10               | 0.40            | 0.40            | 0.01            |             |             |
|                | 15               | 0.40            | 0.35            | 0.03            |             |             |
|                | 20               | 0.40            | 0.44            | 0.03            |             |             |
|                | 25               | 0.40            | 0.57            | 0.03            |             |             |
|                | 30               | 0.37            | 0.44            | 0.01            |             |             |
|                | 35               | 0.37            | 0.53            | 0.03            |             |             |
|                | 40               | 0.49            | 0.70            | 0.01            |             |             |
|                | 45               |                 |                 | 0.04            |             |             |
| <b>Average</b> |                  | <b>0.41</b>     | <b>0.48</b>     | <b>0.02</b>     |             |             |
| June 14        | Above            | 0               | 0.40            | 0.13            | 0.05        |             |
|                | Below            | 5               |                 | 0.53            |             |             |
|                | Thermocline      | 10              | 1.38            | 0.35            | 0.05        | 0.14        |
|                |                  | 15              | 0.28            | 0.40            | 0.08        | 0.31        |
|                |                  | 20              | 0.21            | 0.35            | 0.03        | 0.16        |
|                |                  | 25              | 0.28            | 0.40            | 0.12        | 0.24        |
|                | Thermocline 3 m  | 30              | 0.40            | 0.40            | 0.10        | 0.63        |
|                |                  | 35              | 0.46            | 0.35            | 0.03        | 0.8         |
|                |                  | 40              | 0.49            | 0.44            | 0.07        | 0.27        |
|                | <b>Average</b>   |                 | <b>Above</b>    | <b>0.40</b>     | <b>0.33</b> | <b>0.05</b> |
|                |                  | <b>Below</b>    | <b>0.50</b>     | <b>0.40</b>     | <b>0.01</b> |             |
|                |                  |                 |                 |                 | <b>0.24</b> |             |
|                |                  |                 |                 |                 | <b>0.36</b> |             |
| Aug 17         | 0                | 0.37            | 0.04            | 0.10            |             |             |
|                | 5                | 0.46            | 0.04            | 0.05            |             |             |
|                | Above            | 10              | 0.77            | 0.35            | 0.05        |             |
|                | Below            | 15              | 0.37            | 0.31            | 0.04        |             |
|                | Thermocline      | 20              | 0.40            | 0.35            | 0.05        |             |
|                |                  | 25              | 0.52            | 0.44            | 0.18        |             |
|                |                  | 30              | 0.52            | 0.48            | 0.09        |             |
|                |                  | 35              | 0.61            | 0.40            | 0.13        |             |
|                | Thermocline 10 m | 40              | 0.64            | 0.62            | 0.22        |             |
|                |                  | 45              | 0.77            | 0.40            | 0.04        |             |
| <b>Above</b>   |                  | <b>0.53</b>     | <b>0.14</b>     | <b>0.07</b>     |             |             |
|                |                  | <b>Below</b>    | <b>0.57</b>     | <b>0.42</b>     | <b>0.10</b> |             |
| Oct 14         | 5                | 0.43            | 0.09            | 0.05            |             |             |
|                | 10               | 0.31            | 0.09            | 0.03            |             |             |
|                | 15               | 0.28            | 0.18            | 0.05            |             |             |
|                | Above            | 20              | 0.43            | 0.09            | 0.03        |             |
|                | Below            | 25              | 0.18            | 0.31            | 0.08        |             |
|                | Thermocline      | 30              | 0.31            | 0.48            | 0.03        |             |
|                |                  | 35              | 0.43            | 0.48            | 0.03        |             |
|                |                  | 40              | 0.49            | 0.44            | 0.03        |             |
|                | Thermocline 20 m | <b>Average</b>  |                 | <b>Above</b>    | <b>0.36</b> | <b>0.11</b> |
|                |                  |                 |                 | <b>Below</b>    | <b>0.37</b> | <b>0.36</b> |
|                |                  |                 |                 | <b>0.04</b>     |             |             |
|                |                  |                 |                 | <b>0.04</b>     |             |             |

Table 1b: Nutrient concentration in the flooded pit, 1996.

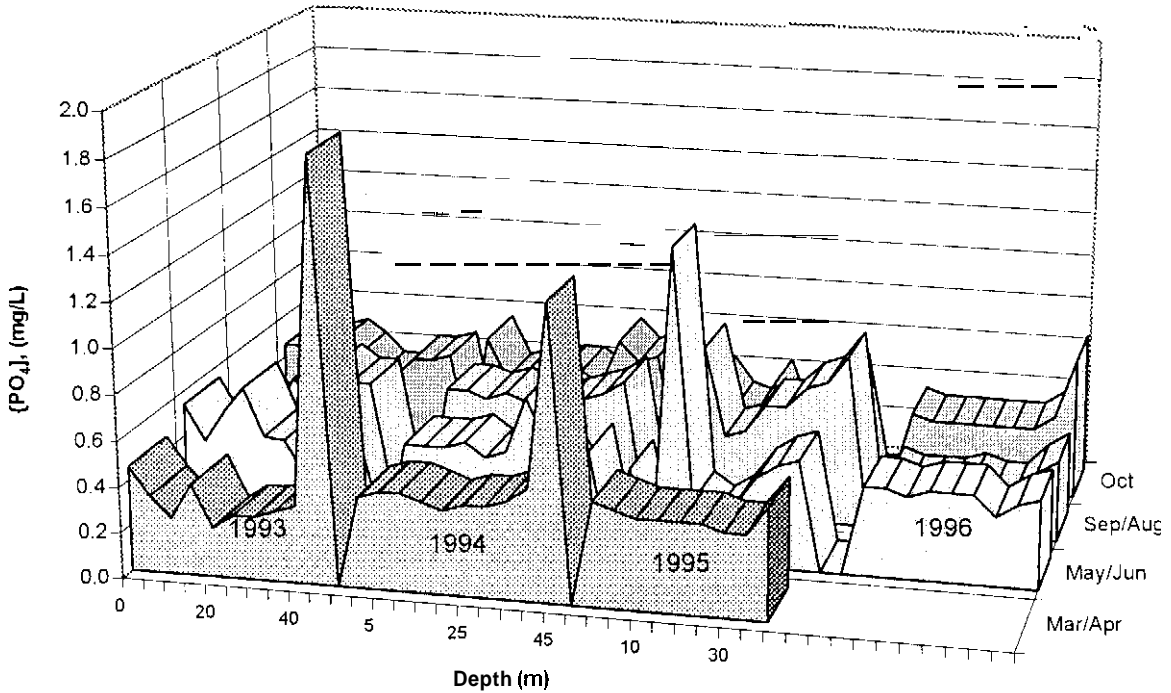
| 1996   |                        | Depth        | Nutrients, mg/L |                 |                 |       |
|--------|------------------------|--------------|-----------------|-----------------|-----------------|-------|
|        |                        |              | PO <sub>4</sub> | NO <sub>3</sub> | NH <sub>4</sub> | N,TKN |
| May 9  |                        | 0            | 0.40            | 0.66            | 0.03            |       |
|        |                        | 5            | 0.40            | 0.75            | 0.01            |       |
|        |                        | 10           | 0.37            | 0.75            | 0.03            |       |
|        |                        | 15           | 0.40            | 0.48            | 0.03            |       |
|        |                        | 20           | 0.40            | 0.48            | 0.03            |       |
|        |                        | 25           | 0.40            | 0.53            | 0.03            |       |
|        | <b>No Thermocline</b>  | 30           | 0.31            | 0.57            | 0.04            |       |
|        |                        | 35           | 0.37            | 0.35            | 0.04            |       |
|        |                        | 40           | 0.40            | 0.18            | 0.04            |       |
|        | <b>Average</b>         |              | <b>0.38</b>     | <b>0.53</b>     | <b>0.03</b>     |       |
| Aug 26 | Above                  | 0            | 0.24            | 0.04            | 0.05            |       |
|        |                        | 5            | 0.21            | 0.04            | 0.03            |       |
|        | Below                  | 10           | 0.21            | 0.04            | 0.02            |       |
|        | Thermo-<br>cline       | 15           | 0.21            | 0.04            | 0.01            |       |
|        |                        | 20           | 0.24            | 0.04            | 0.05            |       |
|        |                        | 25           | 0.21            | 0.04            | 0.10            |       |
|        | <b>Thermocline 9 m</b> | 30           | 0.21            | 0.04            | 0.04            |       |
|        |                        | 35           | 0.31            | 0.09            | 0.03            |       |
|        |                        | 40           | 0.37            | 0.13            | 0.04            |       |
|        | <b>Average</b>         | <b>Above</b> | <b>0.22</b>     | <b>0.04</b>     | <b>0.03</b>     |       |
|        |                        | <b>Below</b> | <b>0.25</b>     | <b>0.06</b>     | <b>0.04</b>     |       |
| Oct 28 |                        | 0            | 0.34            | 0.13            | 0.01            |       |
|        |                        | 5            | 0.31            | 0.18            | 0.04            |       |
|        |                        | 10           | 0.31            | 0.13            | 0.01            |       |
|        |                        | 15           | 0.31            | 0.09            | 0.05            |       |
|        |                        | 20           | 0.31            | 0.22            | 0.03            |       |
|        |                        | 25           | 0.31            | 0.13            | 0.01            |       |
|        | <b>No Thermocline</b>  | 30           | 0.31            | 0.18            | 0.01            |       |
|        |                        | 35           | 0.37            | 0.13            | 0.01            |       |
|        |                        | 40           | 0.64            | 0.04            | 0.05            |       |
|        | <b>Average</b>         |              | <b>0.35</b>     | <b>0.14</b>     | <b>0.03</b>     |       |

value reported just below the thermocline into the average, depending on the depth of the thermocline. For example, the representative phosphate concentration above the thermocline for August in 1996, would be the values at 0, 5 and 10 m divided by 3, as the thermocline was at 9 m at that time. If the thermocline coincides with measurement point such as in August 1995, the value at 10 m is taken for above and below averages.

**Phosphate:** The phosphate concentrations in the epilimnion (the water above the thermocline, Schematic 1) possibly decreased slightly over the phytoplankton growing season, with epilimnion averages of 0.36 to 0.53 mg@L<sup>-1</sup> for 1995, given as PO<sub>4</sub>, not P. In 1996 the concentrations in August were slightly lower than in the previous year, but were very similar by October in both years. The fact that the concentrations never dropped more than 20% in the epilimnion indicates that phosphate is not limiting to the existing biomass and is likely present in a biologically available form, being recycled frequently. The highest phosphate concentrations were found in water near the bottom of the pit in both years, at 0.77 mg@L<sup>-1</sup> and 0.64 mg@L<sup>-1</sup>. Part of this phosphate may be inorganic particulate phosphate and only through microbial degradation would this phosphate be liberated and become biologically available.

The phosphate concentrations in the pit show interesting patterns which are likely to influence the phytoplankton community over the growing season. Waters of oligotrophic lakes often contain less than 0.001 mg@L<sup>-1</sup> inorganic phosphate. The total phosphate reported for Collins Bay is 0.15 mg@L<sup>-1</sup> (CAMECO 1994, Pit report). The pit has a total concentration between 0.22 and 0.57 mg@L<sup>-1</sup>, which is considered high. According to Wetzel (1983), such concentrations indicate extremely eutrophic, bordering on hypereutrophic, waters. At such levels, phosphate should support very large biomass standing crops. The phosphate concentrations have not changed since the flooding of the pit and do not change markedly with the season (Figure 12). The unusual high value reported in June 1995 at 10 m is considered an analytical error, or originating from contributions by organic phosphate.

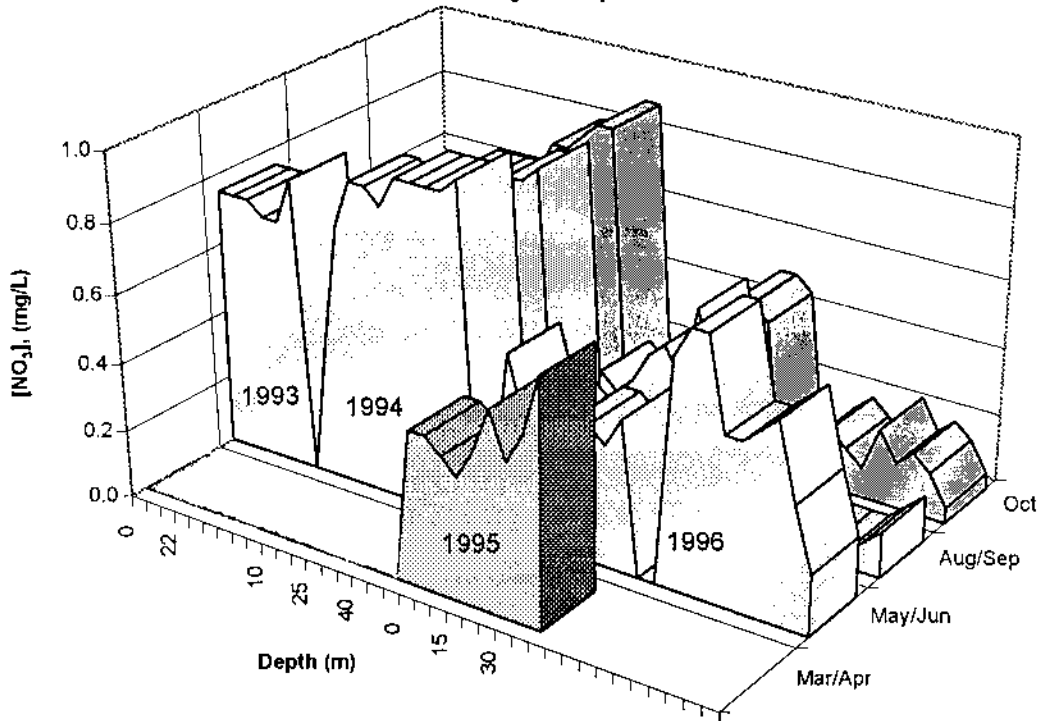
Fig. 12: Flooded Pit, 1993-1996 Data  
PO<sub>4</sub> vs Depth



**Nitrate:** Nitrate levels in the pit are also high compared to natural lake waters (Table 1a and 1b). For example, Wisconsin Lakes on average contain only  $0.06 \text{ mg}\cdot\text{L}^{-1}$  nitrate (Ruttner, 1953) and Collins Bay reports a concentration of  $0.04 \text{ mg}\cdot\text{L}^{-1}$  (CAMECO 1994, Pit report). The average concentration in the flooded pit in April 1995 was  $0.48 \text{ mg}\cdot\text{L}^{-1}$  nitrate as  $\text{NO}_3^-$ , and  $0.53 \text{ mg}\cdot\text{L}^{-1}$  in May 1996.

The development of the nitrate concentrations since flooding of the pit are given in Figure 13. 1995 is the first year when the effect of biological activity is evident, as seen in the notable reductions in nitrate concentrations. The decrease in nitrate continued to be present in 1996; in August,  $0.04 \text{ mg}\cdot\text{L}^{-1}$  prevailed throughout the entire water column. At the time the pit was flooded, the physical aspects related to the suspended solids prevented any noticeable primary productivity. In 1993, nitrate concentrations

Fig. 13: Flooded Pit, 1993-1996 Data  
NO<sub>3</sub> vs Depth



(determined for June 11 only: Figure 13) were high and showed no depth-related pattern. Only after the spring turn-over in 1993 could one expect improved light penetration. Secchi depth started to increase from 0.3 m in 1992, to 0.5 m in 1994 and to about 1.0 m in 1995, reaching a depth of 1.75 m by 1996. In 1993 and 1994, two years following flooding of the pit in 1992, there was no depletion of nitrate from surface waters. During the same time period (1993-1994) phytoplankton growth was starting to become apparent.

With the increase in the photic zone in the pit in 1995, the nitrate reduction in the epilimnion over the growing season can be more closely examined. Nitrate decreases from 0.48 mg·L<sup>-1</sup> in April, to an overall average of 0.33 mg·L<sup>-1</sup> in June, to 0.14 mg·L<sup>-1</sup> in August. In fact, in August, the nitrate concentration at the surface and at 5 m depth was only 0.04 mg·L<sup>-1</sup>. This drop in nitrate has to be due to the assimilation by phytoplankton, as no other vegetation is present in significant quantities.



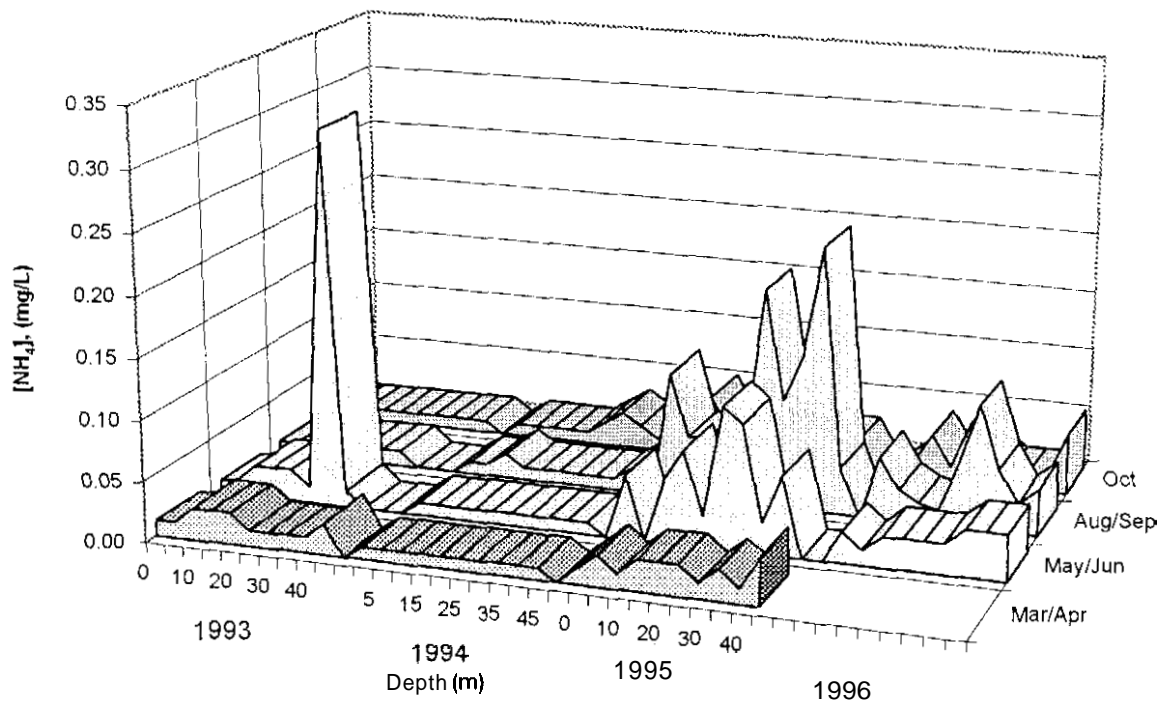
Given that phosphate concentrations remain generally high, while nitrate depletion is evident from the data, the nitrate concentration is likely a major factor limiting algal primary productivity. The reduction in concentrations of nitrate in 1995 also suggests that some of the nitrate used to produce biomass is not returned to the water column but accumulates as organic matter on the bottom of the pit. In this case, nitrate would have been assimilated into the biomass as proteins. It is of more than passing interest to note that, during the data assembly for the 1996 report by Kalin and Olaveson, it was anticipated that growth limitation would be encountered. Fertilization was contemplated in order to retain the primary productivity which had established. However, possible side effects of fertilisation could not be fully evaluated, as it would be accompanied by extensive mucilage production typical for the dominant algae in the pit. These organic molecules were found to exert control over the ability to remove or treat both As and Ni, as discussed later. If in-situ removal of these contaminants could not be achieved, fertilisation could potentially produce problems for alternative chemical treatment methods, since biological material would be detrimental to treatment efficiency (i.e. fouling).

In 1996 the nitrate concentrations decreased further and affected primary productivity, as discussed later. In these waste management situations, the ecological conditions are generally less complex than in healthy ecosystems and therefore easier to predict.

**Ammonium:** Ammonium levels in 1995 in the pit water varied from a low of  $0.02 \text{ mg@L}^{-1}$  in the epilimnion in April, to an average high of  $0.10 \text{ mg@L}^{-1}$  in the hypolimnion in August (Table 1a and Table 1b). In the previous year, 1994, the concentrations were at the detection limit of  $0.01 \text{ mg@L}^{-1}$ . The concentrations in 1996 varied very little ( $0.03\text{-}0.04 \text{ mg@L}^{-1}$ ) throughout the season above and below the thermocline. Ammonium levels in natural lakes are around  $0.19 \text{ mg@L}^{-1}$  (average ammonium level in Wisconsin Lakes; Ruttner, 1953). The concentrations reported for Collins Bay are  $0.07 \text{ mg@L}^{-1}$ , slightly higher than in the pit (CAMECO 1994, Pit report).

The long term development of the ammonium concentrations in the pit is given in Figure 14. In 1995, for the first time, the ammonium concentration increased slightly in mid-growing season. This supports the proposed origin of ammonium as being due to the decomposition of biomass generated in the pit. Ammonium production due to biomass decomposition takes place by dissimilatory nitrate reduction or by ammonification. Both of these processes occur generally under low oxygen or anaerobic conditions

**Fig. 14: Flooded Pit, 1993-1996 Data  
NH<sub>4</sub> vs Depth**



Ammonium concentrations in natural water are maintained at a relatively constant level, depending on the trophic status of the water body. The rate of assimilation of ammonium by organisms is at least twice as fast as that of nitrate (Klapper, 1992).

The absence of changes in ammonium concentrations in the pit with respect to depth over the growing season and the very low concentrations in 1994, prior to significant development of primary productivity, would be compatible with the theory that the pit might be colonized by picoplankton and bacterial population, as indicated in Schematic 1. These populations do not respond to the thermocline, as light is not a key controlling factor to their growth. These considerations prompted the investigation of the presence or absence of picoplankton in the pit, discussed later.

**Organic Carbon and TSS:** If biology is driving the pit chemistry, then organic carbon concentrations should reflect the biological activity. The standard measurement is Total Organic Carbon (TOC). In Figure 15 the concentrations of total organic carbon in the pit are given for the years since the flooding of the pit in 1992. It is evident that, by the end of 1994, the first extensive growing season for the algae, an increase in TOC was starting to develop. This became more prominent by 1995. The concentration of TOC at the thermocline depth had essentially doubled from a value of  $3.5 \text{ mg}\cdot\text{L}^{-1}$  to values as high as  $8.5 \text{ mg}\cdot\text{L}^{-1}$  by October 1995. In 1996, this trend was not observed.

Assuming that the biomass forms part of the pit's total suspended solids (TSS), a corresponding increase in TSS should be evident at the end of the growing season. Concentration of TSS are presented in Figure 16 for 1993 to 1996. The data from 1992 are not relevant as, of course, the TSS loading after force flooding was very high, consisting mainly of inorganic mineral particles and erosion from the pit walls. Two years after flooding, in 1994, the TSS values can be considered stabilized with respect to initial erosion. The increase in TSS in 1995 (Figure 16) suggests that more particulates reach the pit bottom at the end of the season. The TSS changes cannot be attributed only to biological activity. It could also be due to late summer storms and the resulting run-off. However, the corresponding increase in dissolved organic carbon measured in the pit corroborates the suggestion that biological activity contributes to both increases in TSS, and TOC.

**Fig. 15: Flooded Pit, 1993-1996 Data  
Total Organic Carbon vs Depth**

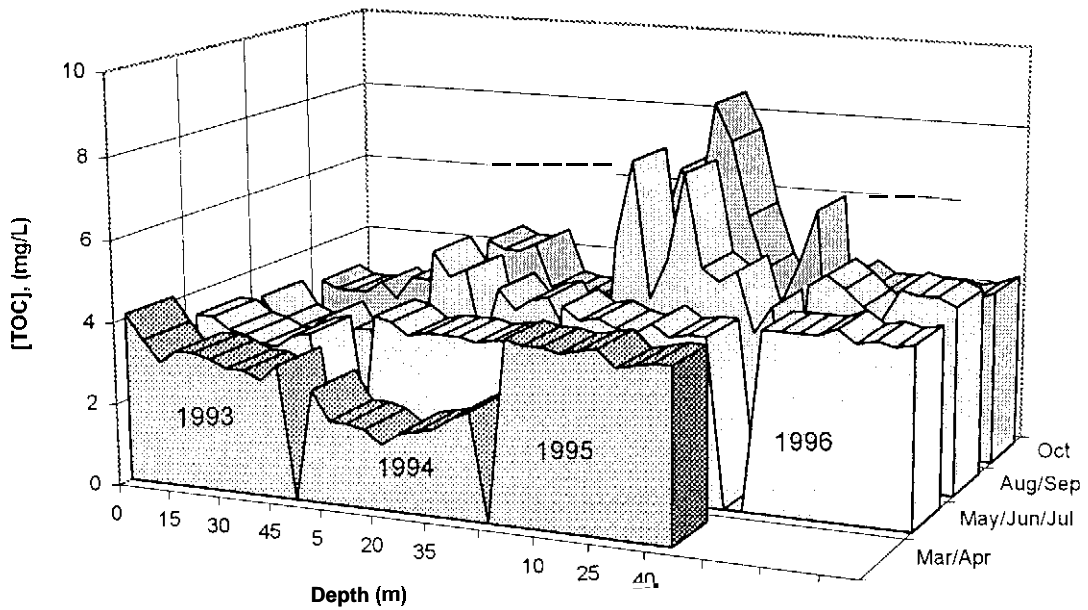
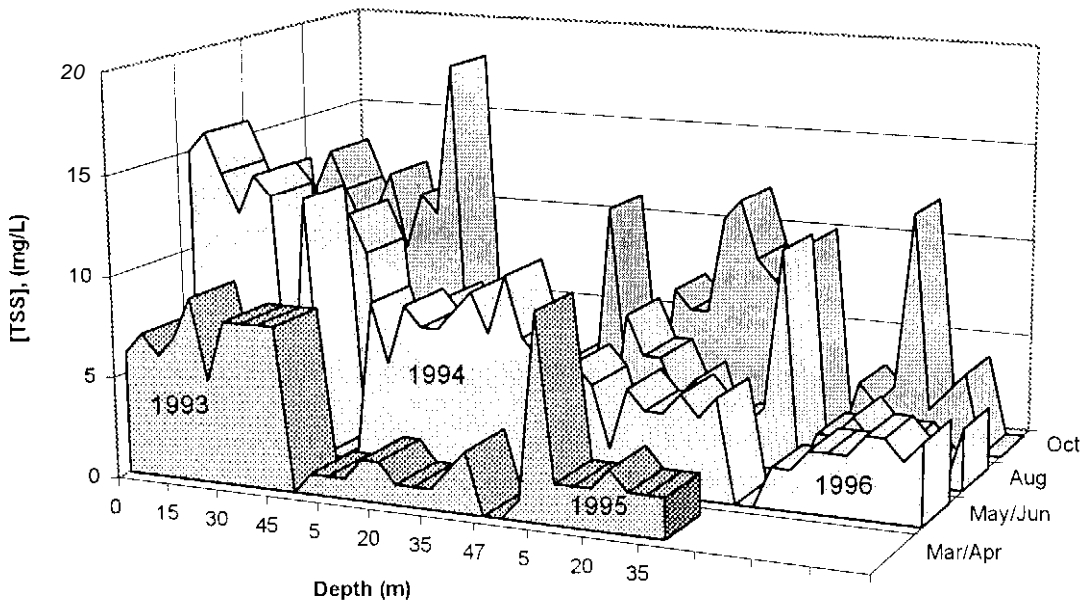


**Fig. 16: Flooded Pit, 1993-1996 Data  
Total Suspended Solids vs Depth**



As previously stated, Total Organic Carbon (TOC) is an indicator of biological productivity. The phytoplankton populations were less prominent during the ice-free season, 1996, resulting in the observed reduction in TOC. Phytoplankton populations fix carbon through photosynthesis and some of the resultant fixed carbon is released back into the water in the form of extracellular polysaccharides, i.e., the mucilage and its degradation products. Dissolved Organic Carbon (DOC) could probably be approximated as a carbohydrate concentration, as was used in the experiments to quantify mucilage production, discussed later in the report. The cells and the characteristics of the mucilage sheath have been observed to undergo changes with the depth in the pit. The peaks and valleys in the distribution of TOC concentrations (Figure 15) and in the distribution of TSS in relation to the thermocline are also indicative of intense thermocline biological activity. Some of the TOC is used to build biomass (particulate organic carbon, POC) towards the end of the growing season, as evidenced by the increase in TOC and TSS at and below the thermocline. Although the data interpretation of TSS values are prone to influence by rain and storm events, a reduction in TSS is expected in 1996, due to nitrate depletion.

**The contaminants:** The main objective of this work is to understand the transport mechanisms which take place in the B-Zone Pit with respect to the contaminants. In-situ treatment methods can be suggested if this mechanism is understood. The contaminant data are presented in a slightly different manner than the parameters discussed previously, which were evaluated with respect to potential changes since flooding. It was concluded that, although seasonal fluctuations in the parameters were evident, the only parameters which increased over the years were conductivity and bicarbonate concentrations. Those changes are attributed to the biological processes which are taking place in the pit.

The As and Ni concentrations with depth in the pit are presented for 1995 for the four measurement periods in Figure 17a to 17d, and for 1996 for three measuring periods in Figure 18a to 18c. These two years are selected as only those would reflect differences

**Fig 17a: Flooded Pit, April 12, 1995  
 As, Ni, Temp. vs Depth**

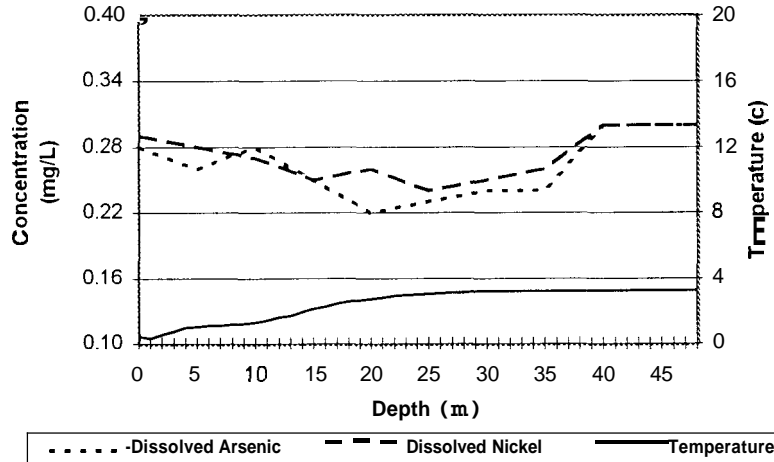


**Fig 17b: Flooded Pit, June 14, 1995  
 As, Ni, Temp. vs Depth**

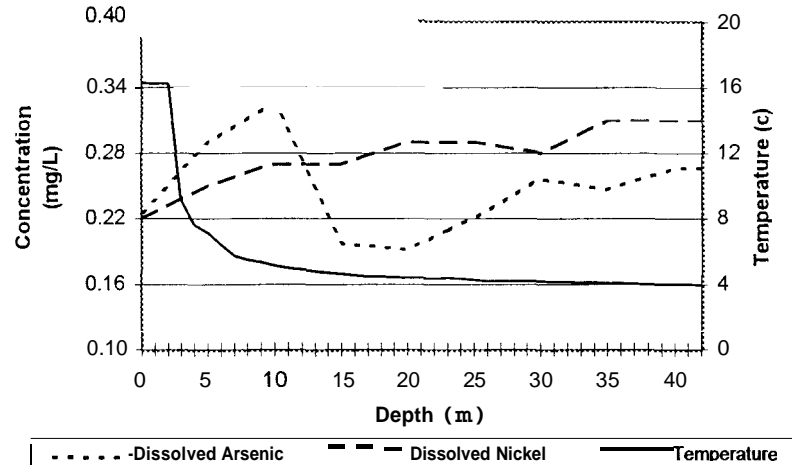


**Fig 17c: Flooded Pit, August 17, 1995  
 As, Ni, Temp. vs Depth**

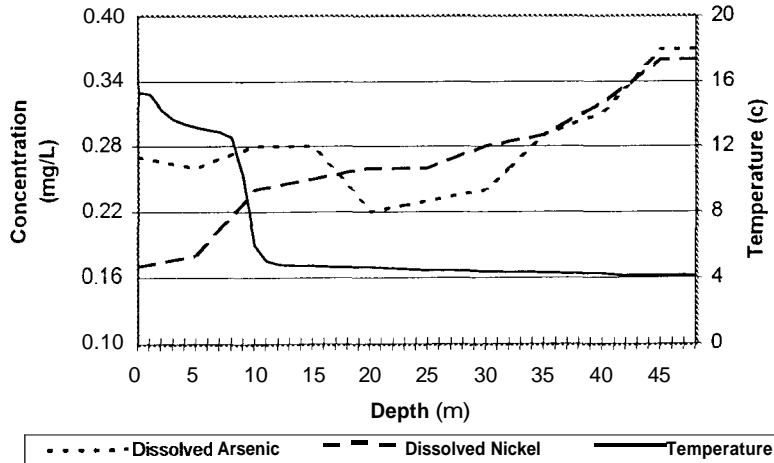


**Fig 17d: Flooded Pit, October 14, 1995  
 As, Ni, Temp. vs Depth**

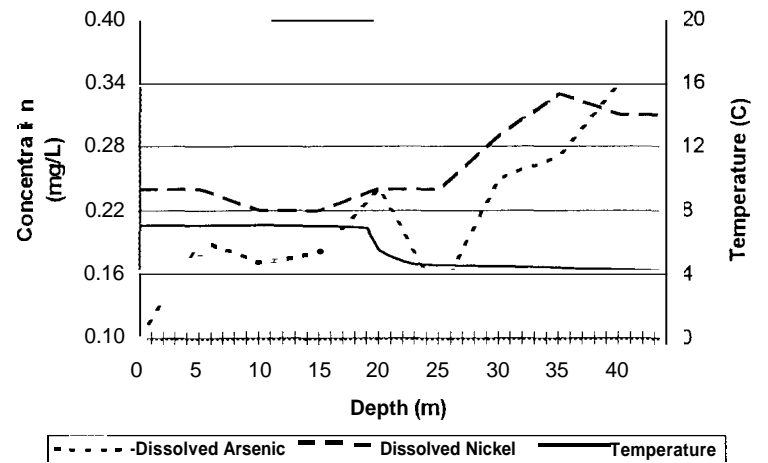


**Fig 18a: Flooded Pit, May 9, 1996  
As, Ni, Temp. vs Depth**

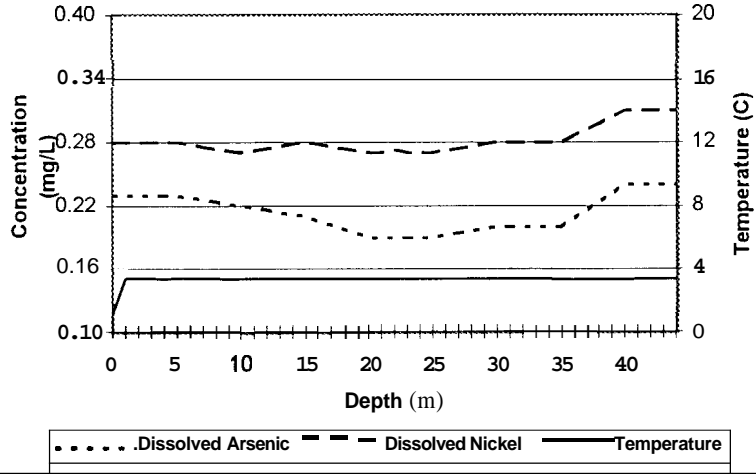


**Fig 18b: Flooded Pit, August 26, 1996  
As, Ni, Temp. vs Depth**

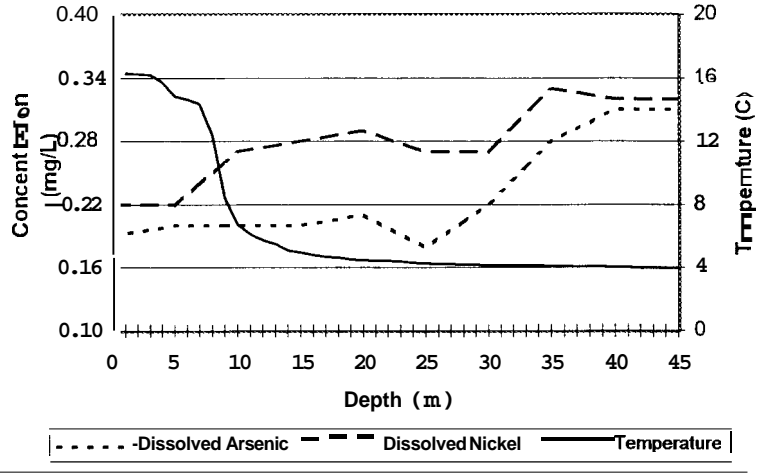
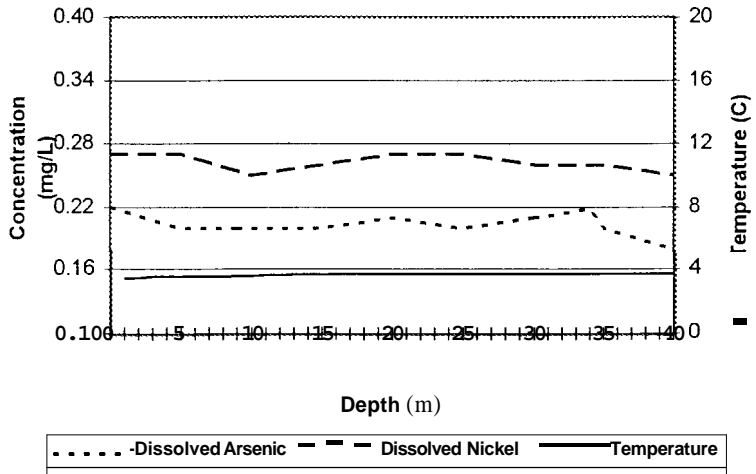


**Fig 18c: Flooded Pit, October 28, 1996  
As, Ni, Temp. vs Depth**



in transport mechanism due to the changes brought about by algal growth, if the transport mechanism is controlled by primary productivity. The first major growth period for algae occurred in 1994. By 1995, the 1994 biomass would have been decomposed. Thus the effects noted on the distribution of the contaminants in 1995 would reflect the first year of the full cycle of growth and decomposition on the distribution of these elements with depth. The data are presented together with the temperature profiles, as the thermocline is believed to be a key physical factor which affects primary productivity and hence distribution of both As and Ni. The detailed data are provided in the summary tables in Appendix A. It should be noted that the graphs are based on 5 m sampling intervals, not 1 m intervals as might be suggested by the graphs where the data points are joined into a continuous curve.

In 1995, over the winter, there was a small change in concentrations gradient from  $0.28 \text{ mg}\cdot\text{L}^{-1}$  on the surface to about  $0.22 \text{ mg}\cdot\text{L}^{-1}$  at a depth of 20 m for both As and Ni, somewhat coinciding with temperature stabilization at  $4^\circ\text{C}$ , above which the pit water was colder with slightly higher As and Ni concentrations (Figure 17a). During this period, the pit is thermally characterized as inversely stratified. As the growing season begins (June 14, Figure 17b), the Ni and As concentration at the surface had declined to  $0.22 \text{ mg}\cdot\text{L}^{-1}$ . Below the thermocline, which at that time was around 3 m depth, the concentrations of As increase slightly but rapidly decrease after 10 m to levels of about  $0.20 \text{ mg}\cdot\text{L}^{-1}$ . Nickel concentrations remain the same below the thermocline as they were under the ice.

Towards the end of the growing season (August 17, Figure 17c), two distinct trends are noted. First, there is a significant reduction in nickel concentration at the surface ( $0.17 \text{ mg}\cdot\text{L}^{-1}$ ), with the depth of the reduced nickel concentrations coinciding with the depth of the thermocline. Second, there is an increase in nickel concentration at the bottom of the flooded pit ( $0.36 \text{ mg}\cdot\text{L}^{-1}$ ). For As, the reduction in concentrations at the surface is not apparent. A slight depression in arsenic levels at the 15 to 20 m level is evident in April, June and August profiles. This suggests that some factor is operating at around 20 m, to result in an As



decrease. This factor is not the same for Ni, as its profile with depth is different.

By October (Figure 17d), the surface Ni concentrations increases again compared to August, from  $0.17 \text{ mg}\cdot\text{L}^{-1}$  to  $0.24 \text{ mg}\cdot\text{L}^{-1}$ . These higher concentrations prevail to depth where a remnant of the summer thermocline is still noticeable. Below 20 m, Ni levels continue to increase towards the bottom of the pit. A reduction is noted in the bottom water by October ( $0.31 \text{ mg}\cdot\text{L}^{-1}$ ) compared to August concentrations ( $0.36 \text{ mg}\cdot\text{L}^{-1}$ ). These concentrations are significantly above those at the surface (Figures 17c and 17d). The same seasonal gradient occurred in 1994. On August 16, 1994, the nickel concentration in the epilimnion was  $0.12 \text{ mg}\cdot\text{L}^{-1}$ , and the concentration near the bottom of the flooded pit was  $0.40 \text{ mg}\cdot\text{L}^{-1}$  (Appendix A).

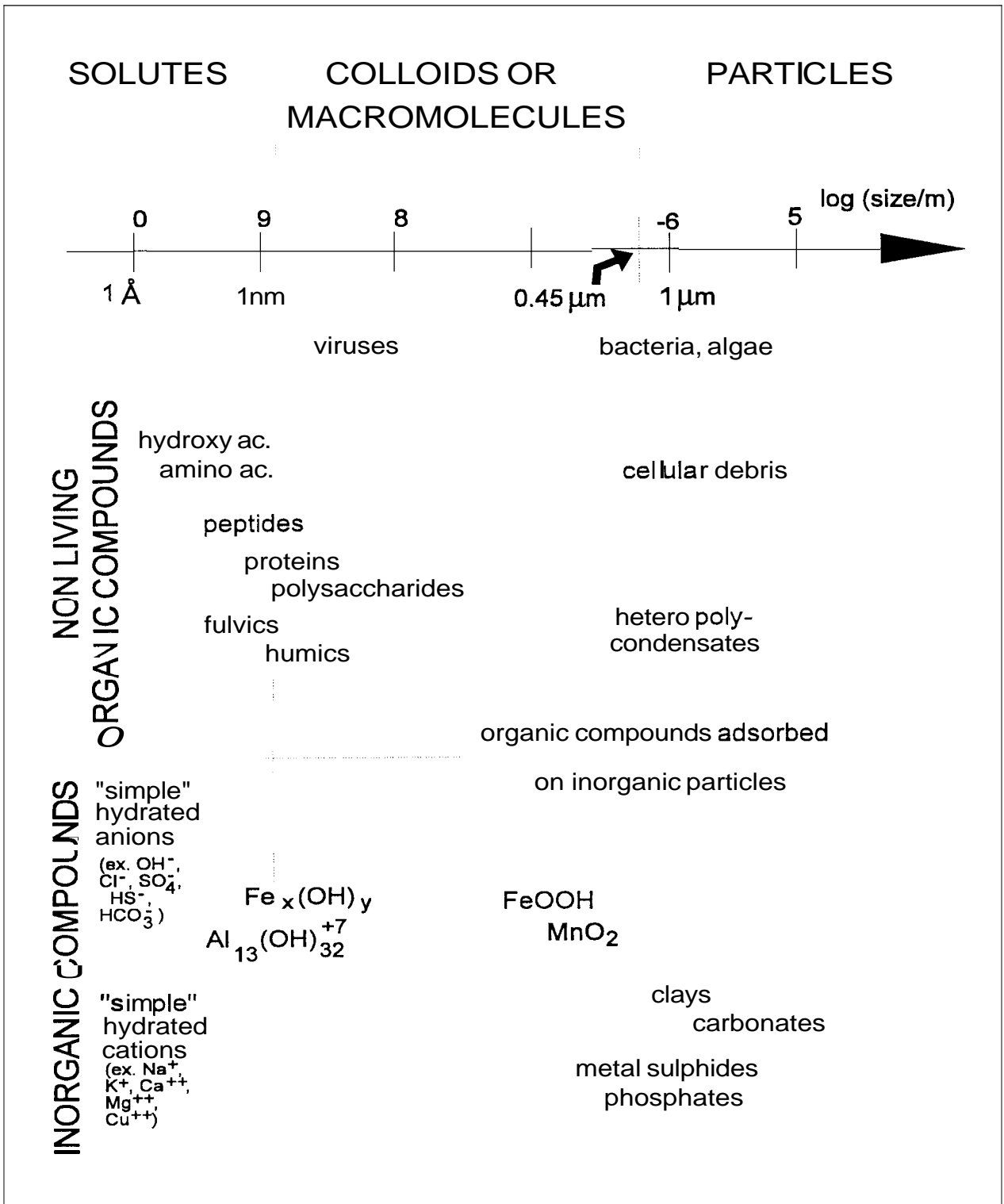
The behaviour of As in October 1995 mirrors that of Ni in August. The As concentrations at the surface now reach lowest concentrations ever recorded ( $0.1 \text{ mg}\cdot\text{L}^{-1}$ ), which was the case for Ni in August. These low As concentrations gradually climb toward the bottom of the pit, showing the same mid-depth depression noted previously, but at 25 m rather than at 15-20 m. These observations suggest that Ni is adsorbed by the algae in the surface water, possibly followed later in the season by As. Some of the material sinks to the bottom of the pit, but only a small fraction is actually removed.

Reflecting on these patterns, one could summarize that these contaminants are associated with particles of different sizes which have different adsorption capacities and settle and aggregate at different rates. Algal productivity was predicted to be lower in 1996 due to the nitrogen limitation in the pit. If the basic premise is correct, one would expect less pronounced effects on the distribution of As and Ni with depth. The data from the three monitoring periods in 1996 reflect a less pronounced gradation for both As and Ni (Figures 18a to 18c). This is, at best, a tentative observation since the apparent reduced primary productivity still generated shifts in conductivity and bicarbonate concentrations.

Comparing the conditions under the ice in 1996, the Ni and As concentrations were slightly lower than in the previous year (Figure 18a), but they did not reach the same record low mid-year concentrations as in the previous year. Some nickel suppression above the thermocline, as seen in 1994 and 1995, was however evident again in 1996. The increases in concentrations at the bottom of the pit were less than in the previous year, when comparing the same measurement period (Figure 17c and Figure 18b). By October 1996, the concentrations of both As and Ni had dropped slightly, likely by only that fraction which had reached the bottom by August (Figure 18b). The apparent year-end drop in surface arsenic levels, and the mid-depth depression noted for 1995 were not evident in 1996. However, on October 28, 1996 there was also no evidence of a residual thermocline.

The overall assessment that the patterns of movement of contaminants and their removal from the water column is associated with the creation of organic particles in the epilimnion, i.e. the algal growth, has to be examined with respect to the particle size. Contaminant transport to the bottom of the pit is likely related to the size of the particles, i.e. large enough to settle. Particles form aggregations which lead to surface charges and changes in adsorption characteristics. In addition, the organic particles undergo decay during transit to the bottom of the pit.

In Schematic 2, the particle sizes of various constituents in water are given (Buffle 1995). It is apparent that standard filtration at 0.45  $\mu$ m differentiates between particle sizes which may be relevant in the transport process in the pit. Clearly, Al and Fe oxy-hydroxides, which are well known to serve as adsorbents of metals, are typically small enough to pass through the filter. This also is the case for the polysaccharides, which are the main constituent of the mucilage produced by the algae in the pit. It is assumed, that indeed organic matter is part of the transport mechanism of the contaminants in the pit, then the lower concentrations in both Ni and As in 1996 is suggesting a clear role of primary productivity, i.e. lower growth in 1996, less pronounced changes in the contaminant transport. For contaminant transport, particularly for the lower portion of the pit, the



Schematic 2: Nature and size domain of the important particles of aquatic systems.

distribution with depth for Al and Fe will be important. It can be assumed that, as organic decay takes place in the lower portion of the pit, the contaminants become available for adsorption of Al and Fe oxides.

In Figure 19a to 19d the distribution of iron and aluminum is presented for 1995, and in Figure 20a to 20c for 1996. Occasionally, abnormally high iron and aluminum concentrations are reported, such as indicated by the blank in Figure 20b, where Fe was reported at  $5.1 \text{ mg}\cdot\text{L}^{-1}$  and Al  $3.6 \text{ mg}\cdot\text{L}^{-1}$ . Those instances of anomalous results occur very rarely, and are likely due to either sampling errors or due to material being disturbed from the pit wall benches during sampling. The high values have been ignored.

Aluminum and iron concentrations are generally very low. Essentially, the increases in concentrations are evident in the late summer profiles. Furthermore, these increases only take place in the bottom of the pit, and may be related to particle aggregation, carrying both As and Ni to the lower parts of the pit, which result in the slight decrease in concentrations at end of the growing season. The fact that inorganic adsorbents do increase in concentration at the bottom of the pit, may in fact present the key to the slight reductions in arsenic and nickel, noted already. Through an assessment of the sedimenting material, i.e. the particles which settle out in the sedimentation traps, further light is shed on the sorption processes which prevail in the pit.

**Fig. 19a: Flooded Pit, April 12, 1995**  
Al, Fe, Temp. vs Depth

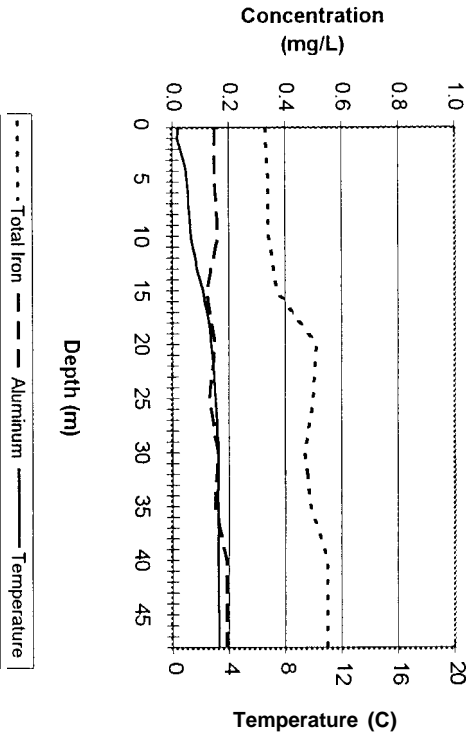


**Fig. 19c: Flooded Pit, August 17, 1995**  
Al, Fe, Temp. vs Depth

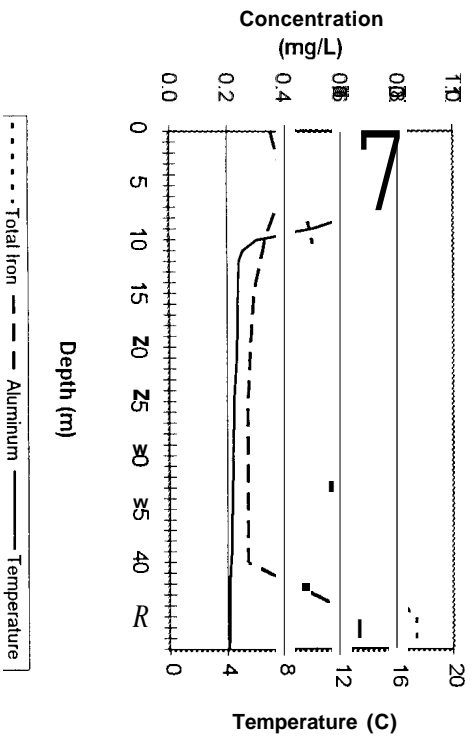


**Fig. 19b: Flooded Pit, June 14, 1995**  
Al, Fe, Temp. vs Depth

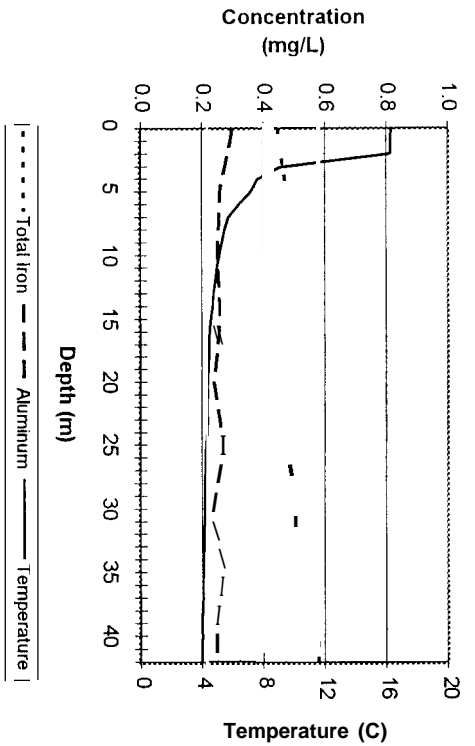


**Fig. 19d: Flooded Pit, October 14, 1995**  
Al, Fe, Temp. vs Depth

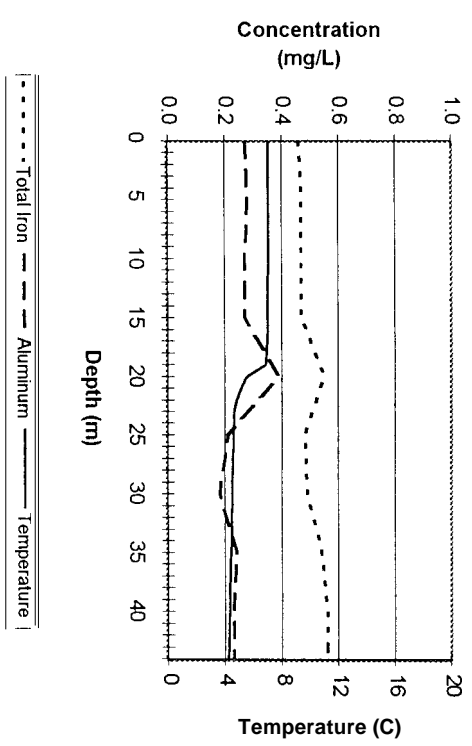


**Fig. 20a: Flooded Pit, May 9, 1996**  
Al, Fe, Temp. vs Depth

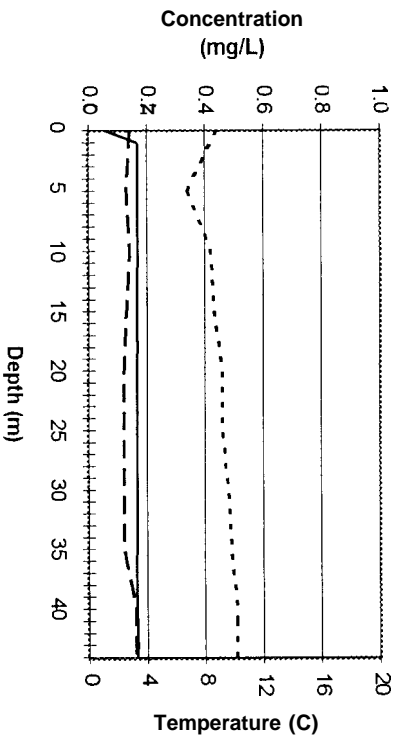


**Fig. 20b: Flooded Pit, August 26, 1996**  
Al, Fe, Temp. vs Depth

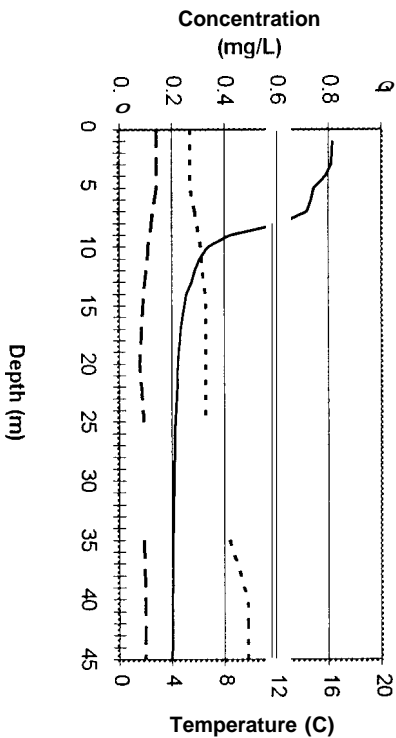
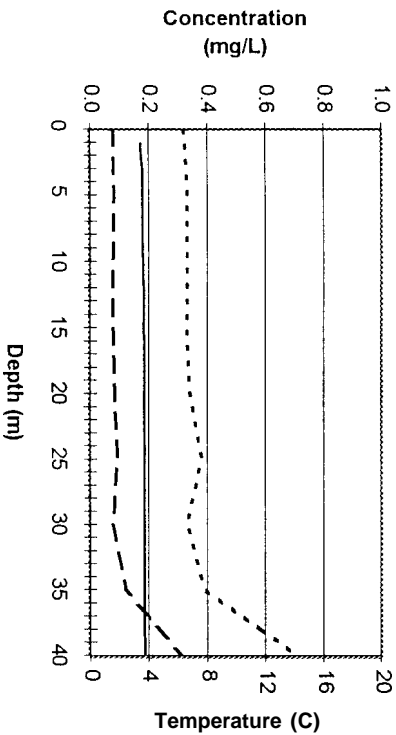


**Fig. 20c: Flooded Pit, October 28, 1996**  
Al, Fe, Temp. vs Depth



## 2.3 Sedimenting Material

The sedimentation traps suspended at 2 m, 12 m, 22 m and 32 m have been used for a number of years to determine the amount of settling material. By August 1994, the traps revealed a clear gradient of clay-like material in the surface trap and in the lower parts considerably less clay like sediment was present (Plate 1). In the bottom of the traps, a band of dark green material is noted just above the blue caps of the tubes, which reflects the large amount of algal material.

The particulate flux in the years 1992 to 1994 was described in CAMECO, 1994, Pit Report, where it was concluded that the particle size was decreasing over the years, and most particles, based on particle settling rates, fell into a range above 2 : m. In 1995, the material collected in the sedimentation traps in September was subjected to granulometric analysis, investigated by E.A. Lowson (1997). Granulometric analysis is carried out by using a light microscope to view the particles and measure their diameter.

The granulometric determinations resulted in the finding that the majority of particle are of a size < 1 : m in diameter. About 20% to 30% of the particles fall into a size range of 1 : m to 5 : m and larger particles are essentially absent. It is noteworthy to recognize that the fraction of larger particles increases with depth, with little difference in size distribution after a depth of 22 m, where 63% are < 1 : m and 30% are in the size range of 1 to 5 : m. This indicates that, with depth, particles aggregate (Table 2).

Table 2: B-Zone Pit Particle Size Distribution.

| Depth | Total Particle Count | Particle Size Distribution as % of Total |         |          |           |           |         |
|-------|----------------------|--|---------|----------|-----------|-----------|---------|
|       |                      | # 1 : m                                  | 1-5 : m | 5-10 : m | 10-15 : m | 15-25 : m | >25 : m |
| 12 m  | 7,554                | 80.7                                     | 17.7    | 1.2      | 0.1       | 0.1       | 0.2     |
| 22 m  | 1,776                | 62.8                                     | 30.4    | 4.8      | 0.6       | 0.6       | 0.8     |
| 32 m  | 2,693                | 64.5                                     | 28.6    | 4.5      | 0.8       | 0.8       | 0.8     |

Examination of the algal material collected from the pit suggests that the amount and density of the mucilage layers surrounding the colonies show visible changes, related to the depth of sampling in the pit. Disintegration of the cells and the mucilage could be occurring during the sinking of large quantities of *Dictyosphaerium* out of the water column of the pit in late summer and early fall. These observations suggested that this algal species may be involved in the transport of As and Ni in the pit. Material from the sedimentation traps were depicted in Plate 2, from the traps suspended at various depths collected in September 1995, and photographed 6 months later during storage in the coldroom.

Given the large fraction of particles smaller than 1 : m, their settling behaviour will be affected by organic molecules from the mucilage. If these particles are the carriers of As and Ni, they also may pass through the 0.45 : m filter and report as "dissolved" concentration in the monitoring data. From the granulometry it is suggested that significant fraction of the particulates are likely smaller than 0.45 : m.

The vials depicted in Plate 2 certainly support the contention that mucilage is affecting settling. The 2 m sample characteristics suggest that settling essentially does not take place, in comparison to the material collected from deeper portions of the pit. The 2 m algae with mucilage had still not settled in comparison to the algae from the deeper portion of the pit. This observation prompted a settling experiment with the nutrient stressed algal cultures and the nutrient ratio 1:1, simulating the field conditions. Algal cultures (100 mL) were pipetted into pit water and left to settle. After 6 weeks, cells in the culture with a N:P nutrient ratio 1:1 (nitrogen stressed) had not settled, confirming the observations of the effect of mucilage on settling.

The characteristics of the mucilage may change over the season and will certainly change with depth due to decomposition by heterotrophic bacteria. The diffuse, low density mucilaginous layers present in the spring and early summer, keep the colonies



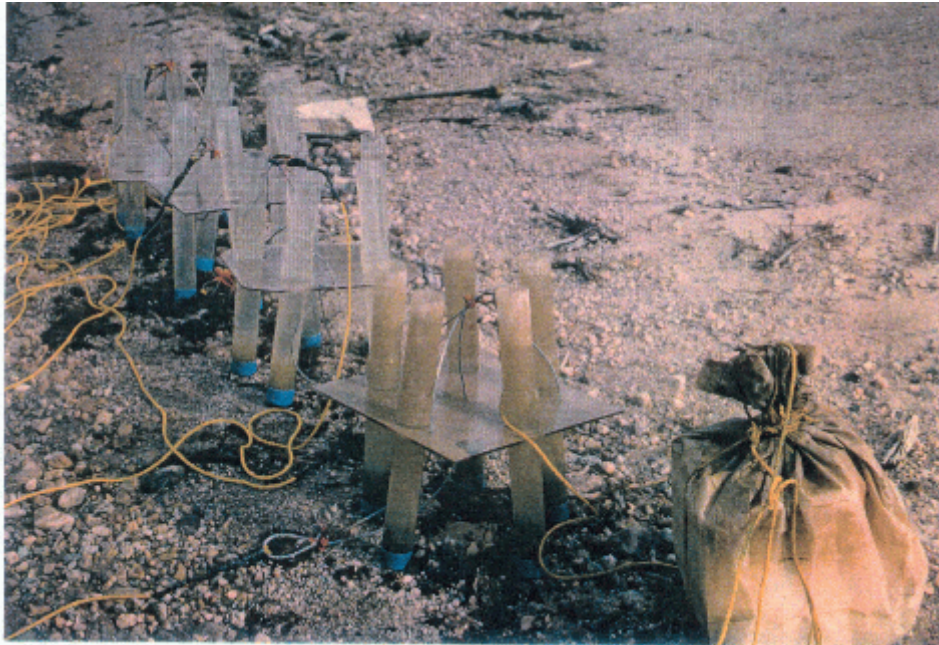


Plate 1: Sedimentation traps August 1994 2, 12, 22, 32 m with weight recovered after 37 days suspension in the B-Zone Pit.

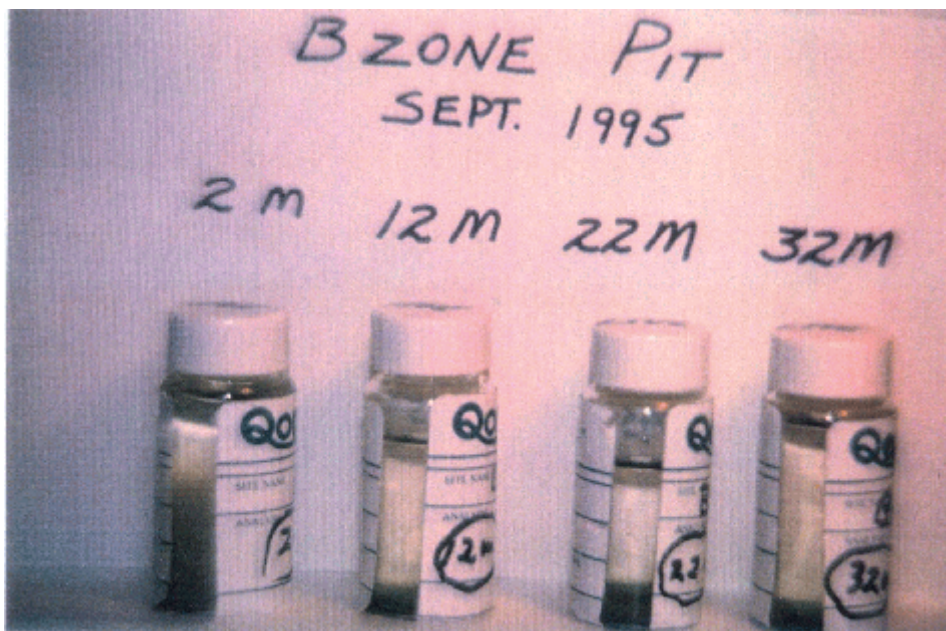


Plate 2: Algal material from sedimentation traps of the pit collected in September 1995 from different depths after 6 months of settling in the cold room.

suspended in the water column. As growth decreases mucilage production increases and particles are less likely to settle.

If it is assumed that the affinity for As and Ni is somewhat related to the conditions of the mucilage-forming colonies, then the different times, i.e. different growth stages, when either As or Ni are removed from the surface water, could be explained (Figures 17a-17d, 18a-18c). This would also hold for the different distribution of As and Ni with depth, as the settling behaviour changes with depth.

The microscopic observations of the September 1995 samples further suggest that the cells/colony and mucilage patterns change, with more colonies having fewer cells and more mucilage at that time, even in the surface water samples. As well, other microbial species, especially Cyanobacteria who fix atmospheric nitrogen, become abundant by the end of the growing season, along with the *Dictyosphaerium*. This supports the notion that the *Dictyosphaerium* bloom peaked due to nutrient limitation. Examples of the variation in mucilage quality and quantity with depth in the August samples are shown in the plates presented in Appendix B. Considering these observations, it is not difficult to relate the slow decay of the organics with depth to the movement of As and Ni. If the main agents of removal in the surface water are indeed the algae, then the observations on the mucilage should also be reflected in the settling rates of the particles.

In Table 3, the sedimentation rates derived from the sampling intervals for which the sedimentation traps were installed are presented. The sedimentation traps installed in the pit capture material settling at different depths. Over one growing season, therefore, the sedimentation traps represent that fraction of the suspended material which has reached the depth where the sedimentation trap is located.

The sedimentation rates are presented as dry weight of the material collected in the sedimentation traps at various depths. The amount of material present at that depth in the

Table 3: Sedimentation rates from sediment traps

| Depth  | Sample           |           | Sedimentation rate    |            |             |
|--|------------------|-----------|-----------------------|------------|-------------|
| m  | g                |           | g/m <sup>2</sup> /day |            |             |
| <b>From</b>  | <b>11-Jun-93</b> | <b>to</b> | <b>13-Aug-93</b>      | <b>63</b>  | <b>days</b> |
| 2  | 14.71            |           | 23.8                  |            |             |
| 12   | 16.64            |           | 26.9                  |            |             |
| 22   | 14.24            |           | 23.0                  |            |             |
| 32   | 17.74            |           | 28.7                  |            |             |
| <b>From</b>  | <b>26-Jun-94</b> | <b>to</b> | <b>08-Sep-94</b>      | <b>74</b>  | <b>days</b> |
| 2  | 4.49 (1.08)      |           | 6.2 (1.5)             |            |             |
| 12   | 10.58 (0.55)     |           | 14.6 (0.8)            |            |             |
| 22   | 12.61            |           | 17.4                  |            |             |
| 32   | 8.41             |           | 11.6                  |            |             |
| <b>From</b>  | <b>26-Jun-95</b> | <b>to</b> | <b>10-Aug-95</b>      | <b>45</b>  | <b>days</b> |
| 2  | 6.37             |           | 14.4                  |            |             |
| 12   | 3.83             |           | 8.7                   |            |             |
| 22   | 5.30             |           | 12.0                  |            |             |
| 32   | 4.49             |           | 10.2                  |            |             |
| <b>From</b>  | <b>10-Aug-95</b> | <b>to</b> | <b>16-Sep-95</b>      | <b>37</b>  | <b>days</b> |
| 2  | 6.12 (0.26)      |           | 21.0 (0.9)            | <b>(*)</b> |             |
| 12   | 4.69             |           | 12.9                  |            |             |
| 22   | 5.52             |           | 15.2                  |            |             |
| 32   | 5.78             |           | 15.9                  |            |             |
| <b>From</b>  | <b>05-Jul-96</b> | <b>to</b> | <b>30-Aug-96</b>      | <b>56</b>  | <b>days</b> |
| 2  | 0.90             |           | 1.6                   |            |             |
| 12   | 2.91             |           | 5.3                   |            |             |
| 22   | 1.94             |           | 3.5                   |            |             |
| 32   | no sample        |           |                       |            |             |
| Sed. Trap Area= 98.17 cm <sup>2</sup>                          |                  |           |                       |            |             |
| (*) - Sed.Trap Area = 78.54 cm <sup>2</sup> (4 out of 5 tubes) |                  |           |                       |            |             |
| () - number in brackets, based on biomass weight               |                  |           |                       |            |             |

pit could be derived from the area of the pit at the appropriate depth. The number of days which represent the sampling period can be used to derive the load of material which would sediment for that period. The surface area for 2 m depth has been derived from the pit contour map. For the surface trap, a value of 24 ha would be applicable.

Sedimentation rates are reported since 1993, when the rates were considerably higher than in the following years (Table 3). In 1995, the sedimentation rates in the first and second halves of the ice-free season are generally similar, with possibly a lower sedimentation rates noted in the beginning of the growing season and an increase in rates towards the end of the year, when the thermocline starts to break down.

The end of the growing season would represent that portion of the growth period of the algae when most mucilage is produced, since it's production takes place in response to growth stress. Mucilage would be expected to reduce the sedimentation rates and more material would remain suspended in the water column. Calculations of the sedimentation rates for algal material alone (numbers given in brackets in Table 3) suggest that the rate at which algal material is settling in the sedimentation traps is effectively 10 times lower than the rate which includes the inorganic material. Biomass settling rates could only be calculated for those periods where the amount of organic material was sufficient to be separated from the inorganic fraction to obtain meaningful values.

Using the sedimentation trap data, a tonnage of sedimenting material leaving from the surface water can be estimated. Assuming an average rate for 1995 of  $12 \text{ g@m}^{-2}\text{day}^{-1}$  for a 185 day growing period, this would result in  $2.2 \text{ kg@m}^{-2}$  and for the entire pit with the surface area of about 24 ha results in a total of 533 tonnes. Considering the sedimentation of the algal material alone, at rates of about  $1 \text{ g@m}^{-2}\text{day}^{-1}$ , then over the growing period this would represent about 44 tonnes of algal material for the 185 days of growing season. The sedimentation rates for 1996 were significantly lower than 1995, being  $1.6 \text{ g@m}^{-2}\text{day}^{-1}$  on the surface. This is the lowest rate ever reported since sampling started. These results strongly

support the fact that algal growth being limited by N in 1996 is a key factor in the particle formation and settling in the pit.

The concentrations of major elements in the material collected in the sedimentation traps are presented in Table A-3-2 in Appendix A. The concentrations of As, Ni and Fe are plotted in Figures 21a to 21c, comparing the year of collection and the depth of sampling.

The concentration of As in the sedimentation trap at 32 m is generally higher than the material collecting at 2 m. Nickel concentrations in material collected at 2 m depth are generally higher than in the material collected at 32 m. It is also interesting to note that, since 1992, the As concentration in the sediment trap material at depth has increased, whereas for Ni the concentrations remained the same. It is unfortunate that, in 1996, no material was recovered from the 32 m depth, as logistics problems occurred. All other elements determined showed no trends, with depth, similar to the concentration of Fe (Figure 21c).

From the sedimentation rates and the As and Ni concentrations in the sedimentation trap material, an evaluation can be performed of whether the material collected in the sedimentation traps could account for the removal in the first metre of the surface water, since the trap was situated at 2 m depth. The loading of Ni and As for 1995 which could be removed from this surface layer could theoretically be estimated. Extensive efforts have been spent tackling the estimates using sedimentation rates, relative growth rates and the concentrations for both elements reported in the sedimenting material. If particle formation is affected by algal growth, the question of As and Ni association with the particles follows.

The distribution of As and Ni in the material in the sedimentation traps reflects the chemical nature of these elements and their sorption behaviour. In Appendix A-4 two papers are included, which were found to be the best description of the sorption behaviour of these two elements, relevant to the conditions of the pit. Rodie et al. (1995) give an excellent detailed

review of As biogeochemistry and Theis and Richter (1980) give a thorough review of Ni adsorption on oxides.

The concentrations of As and Ni in material collected in the sedimentation traps are the result of the sorption processes. Sorption processes are a function of the surface charge of the species to be sorbed, and this in turn is related to pH. The differences in pH in the pit between the surface and the bottom are generally only 0.5 of a pH unit. In the range between pH 7 and 8, however, the fractions of the predominant forms of arsenic change from  $\text{HAsO}_4^{2-}$ , at the higher pH, and to  $\text{H}_2\text{AsO}_4^-$  at lower pH prevailing in the bottom of the pit. With these changes in pH, the sorption behaviour changes (Figure 1, Rodie et al., Appendix A-4). In oxic waters, As is present as arsenate and reported to have a 50% stronger affinity of being sorbed, than arsenite. These differences are due to changes in the surface charges resulting in the differences between the material at the surface and at the bottom.

Nickel only exists in one valence state,  $\text{Ni}^{2+}$ , therefore changes in pH between the bottom and the surface of the pit, will not affect the surface charge, as was reported for As. The extremely detailed studies of factors controlling Ni adsorption, reported by Theis and Richter, 1980 (Figure 4, Appendix A-4), confirm that adsorption changes in relation to pH are not expected. The material in the sedimentation traps contains more Ni on the surface than at the bottom, as a result of the affinity of Ni to the organics. The algae decay in the deeper portions of the pit and the Ni is released, i.e., the concentration of Ni in the sedimentation material is reduced.

The other interesting observation which can be derived from the sedimentation trap material, is that with time, As concentrations increase in the material in the bottom (Figure 21a) but not for Ni. Iron concentrations in the bottom material are relatively the same between 1992 - 1996. From the literature it is suggested, that with time iron oxides change their surface sorption characteristics thus possibly explaining the time trend. For the As removal in the pit, this may be the essential process accounting for the overall slight downward trend in As concentrations.

Using sedimentation rates it was previously estimated that about 533 tonnes of settled material was produced in 1995. Assuming that As is about 0.2% of the solids material and Ni about 0.1%, it is expected that 1000 kg of As and 530 kg of Ni would be removed from the surface water. Over the growing season, the As reduction in the surface water can be considered to be  $0.12 \text{ mg}\text{L}^{-1}$  (Figure 17b to 17d). Nickel reduction, taking a shorter time span (Figure 17b to 17c), results in a smaller reduction,  $0.06 \text{ mg}\text{L}^{-1}$ . The first two metres of the pit contain about  $480,000 \text{ m}^3$  of water, therefore a reduction of about 58 kg of As and 29 kg of Ni could be expected.

The estimation of reductions using this approach, is flawed fundamentally by two key aspects. Firstly, the measurements of both sedimentation material and concentrations in the pit, are snapshots in time, which related to the growth dynamics discussed earlier, are not reflecting the transport processes which take place much faster (sorption, sinking, particle aggregation and decay of sorbed material). Thus, a static reflection of the transport process is created, which should be quantified dynamically.

Secondly, the low concentrations of contaminants in the large volume of water in the pit, result in a loading error of at least 0.5 t of contaminants (by a change in the first decimal,  $\text{m}^3$  and  $0.1 \text{ mg}\text{L}^{-1}$ ). With the interval of sampling being 5 m, any attempt at a mass balance of contaminants (fractionated between solids and the “dissolved  $0.45 \mu\text{m}$ ” or total concentrations, for instance, the difference between total and dissolved As is  $0.04 \text{ mg}\text{L}^{-1}$  and for Ni it is  $0.03 \text{ mg}\text{L}^{-1}$ , for 1996) is futile. However, the data do clearly indicate, that particles transport contaminants from the surface water to the deeper portions of the pit. The quantity which is transported, however, is somewhat elusive. The differences in the concentrations of As and Ni in the solids at the surface and the bottom, are very interesting. They reflect the changes which take place on the solids as they travel through the water column and are examined in more details, below.

The chemical composition of the material in the sedimentation traps were further analysed

with sequential extractions, revealing more specific characteristics of the material. The sequential extractions are of interest in the transport mechanism of the contaminants in the pit, because the distribution of As and Ni based on the total chemical composition (Table A-2 and Figures 21a and 21b) revealed differences in concentrations with respect to depth and age of the material.

Sequential extractions were carried out on material collected in the sedimentation traps to elucidate in what form the particulate matter is adsorbing the contaminants. The same material was exposed to sequential extractions, identifying water soluble fractions, ion exchangeable fractions, fractions associated with organics, fractions associated with oxides, and finally the residual portion which is inert. The details of the sequential extraction methodology are presented in Lowson (1997).

In Table 4, the amount (as a percentage) of selected elements present in the particulate matter associated with the different fractions is presented. The fractionation for arsenic shows the strongest affinity for oxides (100 % of the arsenic), and is associated with the oxide fraction in the particulates. The fractionation for nickel also confirms the expected physical/chemical process of adsorption, in that nickel is associated with both organic and the oxide fractions, and is also associated with the soluble fractions. It is interesting to note that, as the particulate material moves deeper to 32 m, the nickel fractionation changes. As the particulates travel down through the pit, nickel is also associated with the oxide fraction. The oxides which can generally serve as adsorbents are predominantly iron, magnesium and aluminum. Phosphate, not unexpectedly, is present as the organic form as well as in the inorganic oxide.



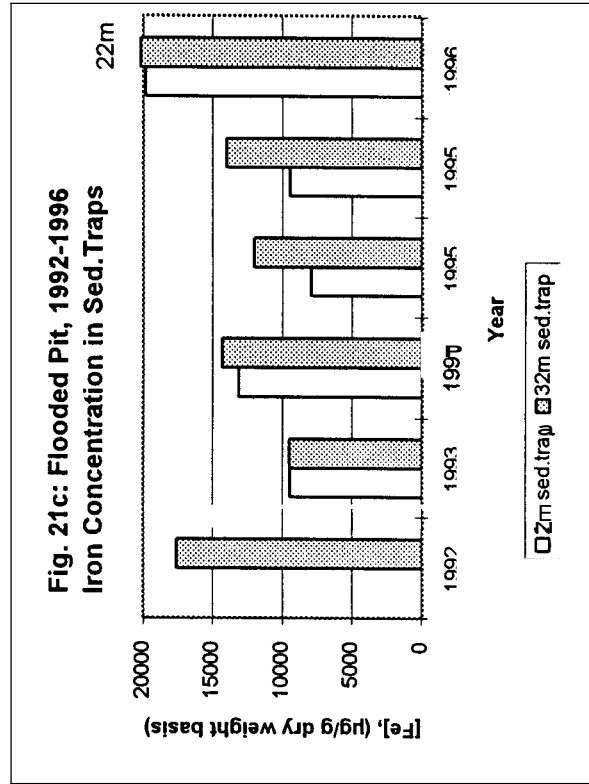
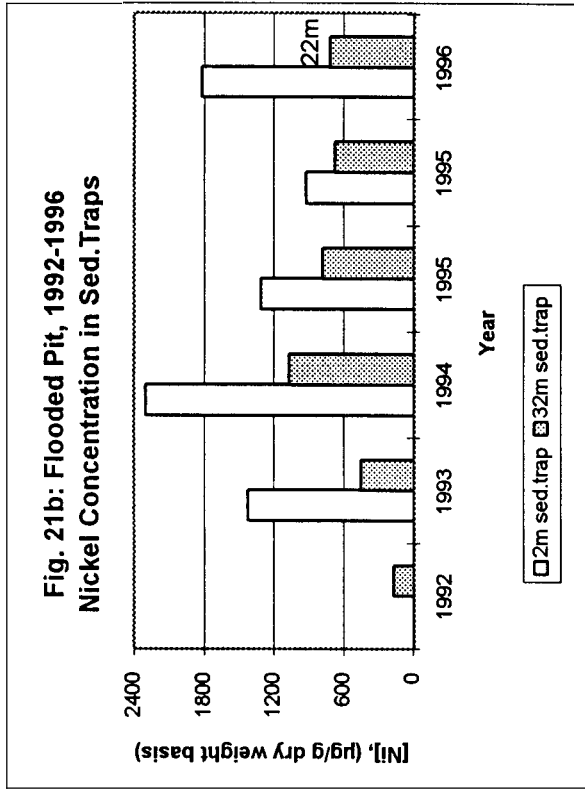
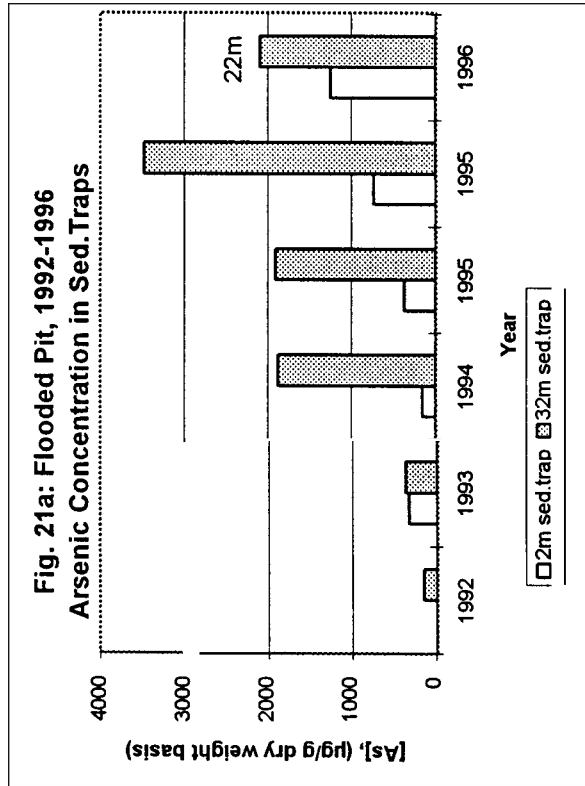


Table 4: Sequential Extractions on Sediment Trap Material, September 16, 1995.

|                       | ELEMENTS |       |      |      |        |        |        |       |       |       |       |       |
|-----------------------|----------|-------|------|------|--------|--------|--------|-------|-------|-------|-------|-------|
|                       | As       |       | Ni   |      | Fe     |        | Al     |       | P     |       | Mg    |       |
|                       | 22 m     | 32 m  | 22 m | 32 m | 22 m   | 32 m   | 22 m   | 32 m  | 22 m  | 32 m  | 22 m  | 32 m  |
| Concentration (: g/g) | 2,117    | 1,740 | 727  | 468  | 21,115 | 17,493 | 10,385 | 8,222 | 1,996 | 2,248 | 4,362 | 3,293 |
| Residual (%)          | 0        | 0     | 0    | 0    | 34     | 33     | 60     | 72    | 0     | 0     | 100   | 100   |
| Organic (%)           | 0        | 0     | 27   | 0    | 21     | 21     | 20     | 17    | 53    | 35    | 0     | 0     |
| Oxide (%)             | 100      | 100   | 42   | 100  | 39     | 46     | 11     | 11    | 47    | 65    | 0     | 0     |
| Exchange (%)          | 0        | 0     | 0    | 0    | 0      | 0      | 0      | 0     | 0     | 0     | 0     | 0     |
| Soluble (%)           | 0        | 0     | 31   | 0    | 6      | 0      | 9      | 0     | 0     | 0     | 0     | 0     |

The change in fractionation of the adsorbed nickel with depth suggests that the processes involved in the transport of nickel are not the same as for arsenic in the water column. The fractionation of the adsorbed contaminants indicates that oxides are serving an important role in the transfer of dissolved nickel and arsenic to the particulates. The role of the organic fraction or the biomass appears to be limited to nickel to a depth of 27 m down from surface of the flooded pit. None of the As and Ni, or any of the other elements analysed from the depth of 22 and 32 m, are sorbed to the surface in a soluble or exchangeable form. It would have been interesting to obtain data from material at 2 m depth, where the organically-bound fraction might have been higher.

A brief summary of the findings on the electron microscopic investigations is given below. Scanning electron microscopy (SEM) coupled with Energy Dispersive X-ray microanalysis (EDX) report atomic abundances of elements on the particle surface. Details of these investigations can be found in Lawson (1997) and in Kalin and Olaveson (1996). The SEM/EDX analysis indicated that there is a wide distribution of grain sizes with particles ranging from < 1 : m to >10 : m. The associated atomic abundance of elements in the SEM/EDX analysis indicates that particles in both 2 m and 32 m samples have surfaces

with a significant fraction of silica up to about 50%. Silica is most likely present as an oxide, and thus would also play a role in sorption and transport of As and Ni.

Secondary Ion Mass Spectroscopy (SIMS) was used to determine the depth of the layer on the outside of the particles where both As and Ni is located. Details of the SIMS analysis are presented in Appendix B. The SIMS analysis of particles reveals the depth at which the metals attach to the particulates and to which grain size it attaches. Examining the elemental distribution, where the diameter of the imaged area is about 150 : m, both As and Ni are present in the material at both depths, 2 m and 32 m. The image also reveals that As and Ni are generally associated with very fine grained material smaller than 1 : m in size. From these images, locations are selected where the thickness of the layer is examined.

Both elements are present as a surface layer which is about 1 : m thick in the 2 m surface sample and becomes a thinner layer, with an estimated thickness of 0.5 : m, at deeper sample collection points. These observations indicate as the particles move to the deeper portion of the pit the surfaces of the particles change. The change in thickness can be due to the decay of the organics.

As the particles move through the deeper portions, organics decay and sorption sites become available which were previously occupied by organic material. The adsorption mechanism in the deeper part is therefore no longer mainly onto organics, but forms a combination of organically complexed contaminants or contaminants adsorbed onto oxides, which are probably predominant iron oxides. As was found through the study of As and Ni adsorption onto algal biomass (Kalin, 1997), the sorption sites for As or Ni are different between the contaminants, as different isotherms described the behaviour. The literature suggests that the sorption behaviour will also differ for the oxides (Appendix A-4).

Using the material from the pit in order to elucidate the ongoing sorption processes, the repertoire of available methodologies commonly used to address this type of speciation work, has been exhausted. No other feasible approach is known for working in the low

concentration ranges of these elements and the small size of the particles, applicable to the conditions in the B-Zone pit.

The postulated transport mechanism has been confirmed as much as possible with the literature. Although the literature reports the behaviour of ionic species in a pure system, for the pit the transport and adsorption mechanism is a mixture of organic bound contaminants with inorganic adsorption onto oxides, particularly for As in the bottom of the pit. Nickel is most likely present in organic complexed form and travels with small particles in the pit. Particle aggregation and adsorption to specific oxides depends on their surface charge, i.e. for As positive sites and for Ni negative sites, the difference in behaviour is noted with depth.

### 3.0 BIOLOGY OF THE FLOODED PIT

In the previous sections, the chemistry and the transport mechanisms of As and Ni have been addressed through analysis of particles collected in sedimentation traps. All the evidence suggested that primary productivity in the pit is playing a key role in the transport of the contaminants and the settling of the particles. It therefore follows that the biology of the pit should be elucidated.

The biology of the B-Zone Pit has been monitored with collecting three types of different data; semi-quantitative phytoplankton evaluations, phytoplankton enumeration and biovolume determination, and picoplankton (<2 : m) enumeration. During semi-quantitative phytoplankton evaluations, the species present are identified and their relative abundance is ranked. This information is useful when addressing species diversity, and data are available for the flooded pit since 1992. These observations indicate that the pit is dominated by very few species, but those present are quite abundant.

As the biological activity was implicated as the dominant factor in the transport of contaminants, the phytoplankton samples were enumerated in 1995 and 1996 to determine cell density and biomass volumes. In addition, given the majority of the particles were generally < 1 : m and their potential association with As and Ni transport, picoplankton were enumerated in 1996. Optical microscope enumerations are limited to size fractions around 2 : m. Picoplankton are identified using flow cytometry which facilitates particle size determinations along with taxonomic identifications. This methodology is based on extractions of proteins and pigments. This would provide information on the role of biology in the transport of Ni and As with the particle sizes smaller than 1 : m to 2 : m. The data have been reported previously in the work by Kalin et. al (1997) on the role of picoplankton in mine waste waters.

### 3.1 Species Diversity

Species diversity in the B-Zone Pit is of ecological significance in that the variety and density of species is related to the nutrient status of the pit, and ecological succession in the pit can be assessed. It would be expected that the pit, after flooding, does not display a similar species diversity than the surrounding water body or the wetlands in the vicinity. Although the pit was flooded with Collins Bay water, in the initial phase following flooding sedimentation would be high, and most living biomass would have been carried to the bottom on the clay particles. In Figure 22a, the low species diversity present in the pit since flooding is displayed. In comparison to Collins Bay where, about 48 species are present, or in the small lakes surrounding the pit where about 20 species were identified (Lake 1), the pit supports less than 10 taxa (Figure 22a). The species diversity has neither increased or decreased by 1996 and does not change appreciably with depth (Figure 22b). Seasonal differences in diversity would be expected, as the samples in April are collected under the ice.

Clearly, most taxa introduced to the pit in Collins Bay water are not tolerant of the existing limnological conditions in the pit, as the nutrient status is hypoeutrophic, while most of the introduced species were those which thrive in oligotrophic or nutrient poor conditions. However, it is interesting to note that diversity increases towards the end of the growing season. The few species present are likely those which are considered as 'weedy' species, or those which can prevail in the physical/chemical conditions prevailing in the pit. These include, for example, mucilage-producing algae which, through the production of the sheath, are protected against possible toxic effects of As and Ni.

The abundance of phytoplankton species, grouped by algal family, is summarized in Table 5. The data presented in this manner helps identify which groups are tolerant to the conditions in the B-Zone Pit. Algal groups present in size classes smaller than 2 : m can be identified by flow cytometry and are given in the column labeled FC, and those

**Figure 22a: B-Zone Pit  
Qualitative Data: Species Diversity**

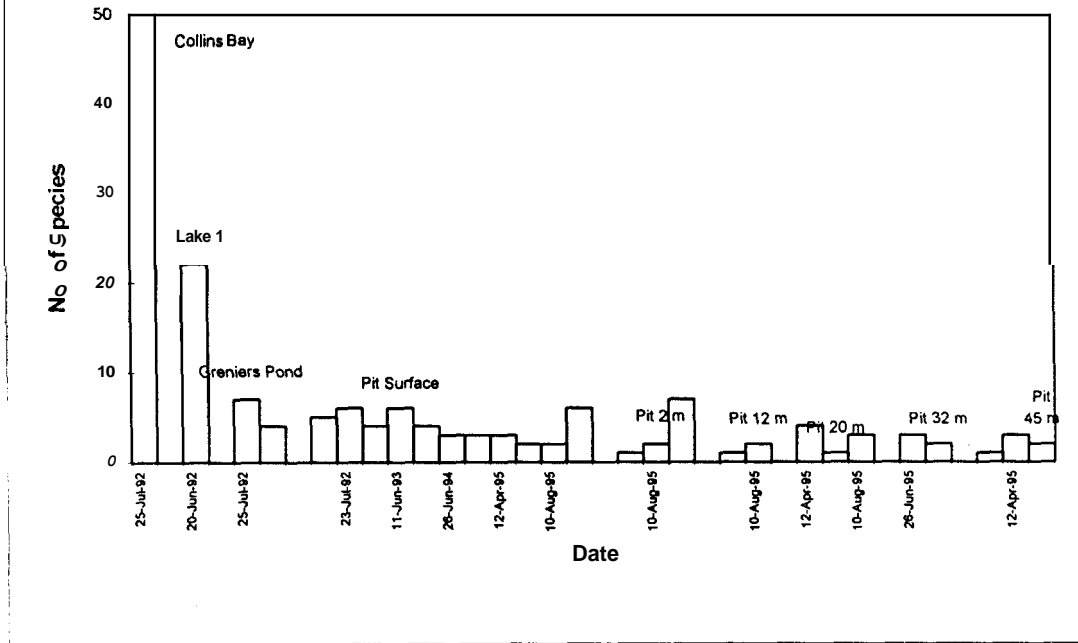


**Figure 22b: B-Zone Pit  
Enumeration Data: Species Diversity**

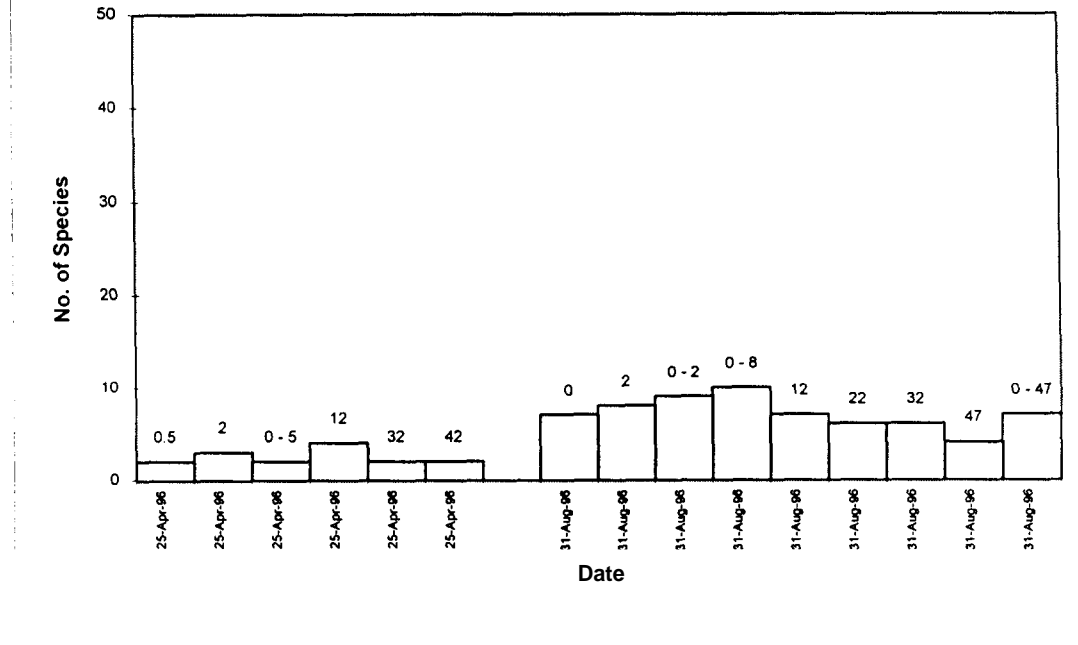


Table 5: B-Zone Pit, Picoplankton and Phytoplankton, 1996

| Station          | Cyanobacteria        |         |        | Chlorophyta          |         |         | Euglenophyta         |         | Chrysophyta          |         |         | Bacillariophyta      |        | Cryptophyta          | Pyrrophyta           |
|------------------|----------------------|---------|--------|----------------------|---------|---------|----------------------|---------|----------------------|---------|---------|----------------------|--------|----------------------|----------------------|
|                  | EN                   | FC      | FC     | EN                   | FC      | FC      | EN                   | FC      | EN                   | FC      | FC      | EN                   | FC     | EN                   | EN                   |
|                  | cell.L <sup>-1</sup> |         |        | cell.L <sup>-1</sup> |         |         | cell.L <sup>-1</sup> |         | cell.L <sup>-1</sup> |         |         | cell.L <sup>-1</sup> |        | cell.L <sup>-1</sup> | cell.L <sup>-1</sup> |
|                  | > 2 um               | pico    | > 2 um | > 2 um               | pico    | > 2 um  | > 2 um               | > 2 um  | > 2 um               | pico    | > 2 um  | > 2 um               | > 2 um | > 2 um               | > 2 um               |
| 0-5rn int        | 0                    | -       | -      | 1.9E+07              | -       | -       | 0                    | -       | 0                    |         |         | 0                    |        | 9.0E+02              | 0                    |
| 0.5 m            | 0                    | 2.6E+05 | 0      | 7.1E+06              | 0       | 7.1E+06 | 0                    | 0       | 0                    | 0       | 0       | 0                    |        | 1.1E+03              | 0                    |
| 2 m              | 0                    | 4.1E+05 | 0      | 9.8E+06              | 0       | 1.0E+07 | 0                    | 0       | 0                    | 0       | 0       | 2.3E+02              |        | 2.3E+02              | 0                    |
| 12 m             | 0                    | 3.2E+05 | 0      | 2.0E+07              | 0       | 2.0E+07 | 0                    | 0       | 0                    | 0       | 0       | 5.6E+01              |        | 8.5E+02              | 0                    |
| 32 m             | 0                    | 8.7E+05 | 0      | 4.3E+07              | 0       | 4.0E+07 | 0                    | 0       | 0                    | 0       | 0       | 0                    |        | 1.7E+03              | 0                    |
| 42 m             | 0                    | 1.5E+06 | 0      | 3.9E+07              | 0       | 3.7E+07 | 0                    | 0       | 0                    | 0       | 0       | 0                    |        | 3.4E+02              | 0                    |
| <b>AUGUST 31</b> |                      |         |        |                      |         |         |                      |         |                      |         |         |                      |        |                      |                      |
| 2 m              | 0                    | 0       | 0      | 1.9E+07              | 2.3E+05 | 0       | 0                    | 2.5E+05 | 6.5E+04              | 0       | 1.6E+04 | 8.5E+02              |        | 8.5E+02              | 9.0E+03              |
| 15 m             | 0                    | 0       | 0      | 6.4E+06              | 1.6E+05 | 0       | 0                    | 1.2E+06 | 5.9E+04              | 0       | 0       | 1.1E+03              |        | 0                    | 2.8E+03              |
| 47 m             | 0                    | 0       | 0      | 2.3E+06              | 9.3E+05 | 1.2E+06 | 0                    | 0       | 0                    | 5.3E+05 | 0       | 4.5E+03              |        | 2.8E+03              | 4.5E+03              |



determined by light microscopy are presented under the column labeled EN. Note that flow cytometry reports enumerations in two size classes, larger than, and less than, 2 : m.

Flow cytometry is essentially a method originally developed for medicine, for blood cell counts. It was eventually adapted and developed for algae. A dual laser is used to count particles, recorded in changes in light penetration in the water. The algae are identified by their pigment groups based on absorption in different wavelengths. Details of this method are given in Kalin et al. 1997.

Discussion of data presented in Table 5 will use the following ranges of cell densities to comment on the population size of either picoplankton or phytoplankton. If the phytoplankton family's cell density ranges between 0 -  $10^4$  cells  $\text{L}^{-1}$ , this is considered low density,  $10^4$  -  $10^6$  cells  $\text{L}^{-1}$  are referred to as moderate density, and finally  $10^6$  cells  $\text{L}^{-1}$  or greater is considered high density. A brief summary is provided for each algal group present in the B-Zone Pit.

The first group, picoplankton Cyanophytes or Cyanobacteria (< 2 : m; determined by flow cytometry [FC]) were present at moderate densities in April, 1996 underneath the ice but were not found in August. During optical and FC examinations of samples for the larger cyanophytes, this group was not identified in April or August. In fact, the optical phytoplankton enumeration technique never identified Cyanobacteria, that group of phytoplankton which can fix atmospheric nitrogen. This suggests that, beneath the ice cover, picoplankton Cyanophytes remain in the water column and their density may increase measurably by spring.

The second group are the Chlorophytes, which were present as phytoplankton (> 2 : m) at moderate to high densities in April at all depth sampled (0.5, 2.0, 12, 15, 32, and 42 m) beneath the ice, according to both the optical (EN) and flow cytometry (FC) techniques. In August, however, Chlorophyte picoplankton (< 2 : m) were not detected in any samples

in April. High densities of Chlorophyte phytoplankton were detected in the water column according to the optical enumeration technique (EN). The flow cytometry (FC) results suggests that most of these cells were in the picoplankton size range, with the exception of the 47 m sample, where a high density of larger Chlorophyte cells ( $> 2 : m$ ) were counted. As will be discussed in detail later, the nutrient status at the end of the growing season changes to a severe form of nitrogen starvation. These small greens indicate that generally the cells comprising the Chlorophyte populations are smaller late in summer, and/or the colonies of *Dictyosphaerium*, the dominant Chlorophyte species, are breaking up.

No Euglenophyte cells were detected in the April samples by either the optical enumeration or flow cytometry techniques. The flow cytometry data for August samples indicate that larger cells ( $> 2 : m$ ) of this group were present at moderate densities in the 2 m and 15 m samples, while optical enumeration technique did not detect any Euglenophytes. The optical enumeration technique is based on a 1 L sample, while the flow cytometry technique is based on only a 0.25 L sample. Either the Euglenophyte cells were too small to identify optically, or the flow cytometry technique is erroneously detecting this group of phytoplankton.

No Chrysophyte phytoplankton or picoplankton cells were detected in April, 1996 samples by either the optical enumeration or the flow cytometry methods. However, by August, 1996 both picoplankton and phytoplankton cells of Chrysophytes were present in the pit. Larger celled phytoplankton ( $> 2 : m$ ) were detected by both methods in surface water, while picoplankton were only detected in the 47 m sample.

Bacillariophytes, or diatoms, were identified only by the optical method, and at low densities in middle depths of the water column in April, and at somewhat higher densities in August throughout the water column. Flow cytometry did not detect any diatoms at any time at any depth in either size category ( $<, > 2 : m$ ).

According to the optical enumeration method, Cryptophytes were found throughout the water column both in April and August, but in low numbers. The flow cytometry technique cannot detect cryptophytes.

The last group, the Pyrrophyta (or dinoflagellates) were detected in the pit in low numbers only in the August, 1996 samples by optical enumeration. Flow cytometry cannot detect Pyrrophytes.

In summary, picoplankton-sized Cyanophytes may be present early in spring, but not later in summer. In contrast, Chlorophytes start out as large cells (> 2 : m), and their cells diminish in size, colonies break-up, and/or smaller species succeed larger ones over the growing season. Euglenophytes, Chrysophytes and Pyrrophytes were reported only in August, and in low numbers. Bacillariophytes and Cryptophytes were found in the pit water column both in later winter and late summer, but at low densities.

The presence of phytoplankton cells in samples collected from beneath the ice in April is an overall important observation, in that these cells are somehow remaining in the water column despite the six-month settling period over the winter months. Some species' cells may be sufficiently small such that settling is extremely slow. Other species may be motile maintain their position in the water column. Finally, there may be adequate light beneath the ice cover over winter such that phytoplankton and picoplankton cells grown at the pit surface are continuously settling through the water column.

### **3.2 Phytoplankton Cell Density**

According to the optical enumeration data, the B-Zone Pit water column is dominated by taxa of the Chlorophyceae (Figure 23), specifically *Dictyosphaerium* species. Most other algal groups are represented, with the exception of Desmids and the Euglenophyceae.

Cyanobacteria were rarely enumerated in pit samples. In April, 1996 (under ice cover), the cell density of the Chlorophycean taxa increased with depth, indicating these cells had settled and were accumulating in the lower strata of the pit (Figure 23). However, the accumulation of cell biomass towards the bottom of the pit indicates that this biomass's density had decreased during transit, and settling decelerated as the particles approached the pit bottom. The high Chlorophycean cell densities present at the bottom of the pit in April, 1996 were not present later during the August sampling campaign (Figure 23). This indicates that either the cells still had the opportunity to completely settle prior to break-up of the ice cover in June, 1996, or that the dense algal population at the bottom of the pit was mixed with the entire pit volume during spring turn-over.

In August, 1996, Chlorophycean taxa densities were higher in the upper strata of the pit, compared to lower strata. This indicates that growth of new algal cells was occurring over the ice free season. The densities of the different algal groups were only discussed for the year 1996, since this was the only year when such data are available.

To determine whether the Chlorophyceae have been dominant over the years since flooding, the semi-quantitative phytoplankton data, collected between 1992 and 1995, are presented in Figure 24. From this data set, covering a longer period, it suggests that the Chlorophytes have always dominated the phytoplankton community, commencing very soon after flooding of the pit. The species diversity contributed by other algal groups has diminished since 1992, especially that of the Chrysophytes, Cryptophytes and Desmids.

**Figure 23: B-Zone Pit  
Phytoplankton Density**

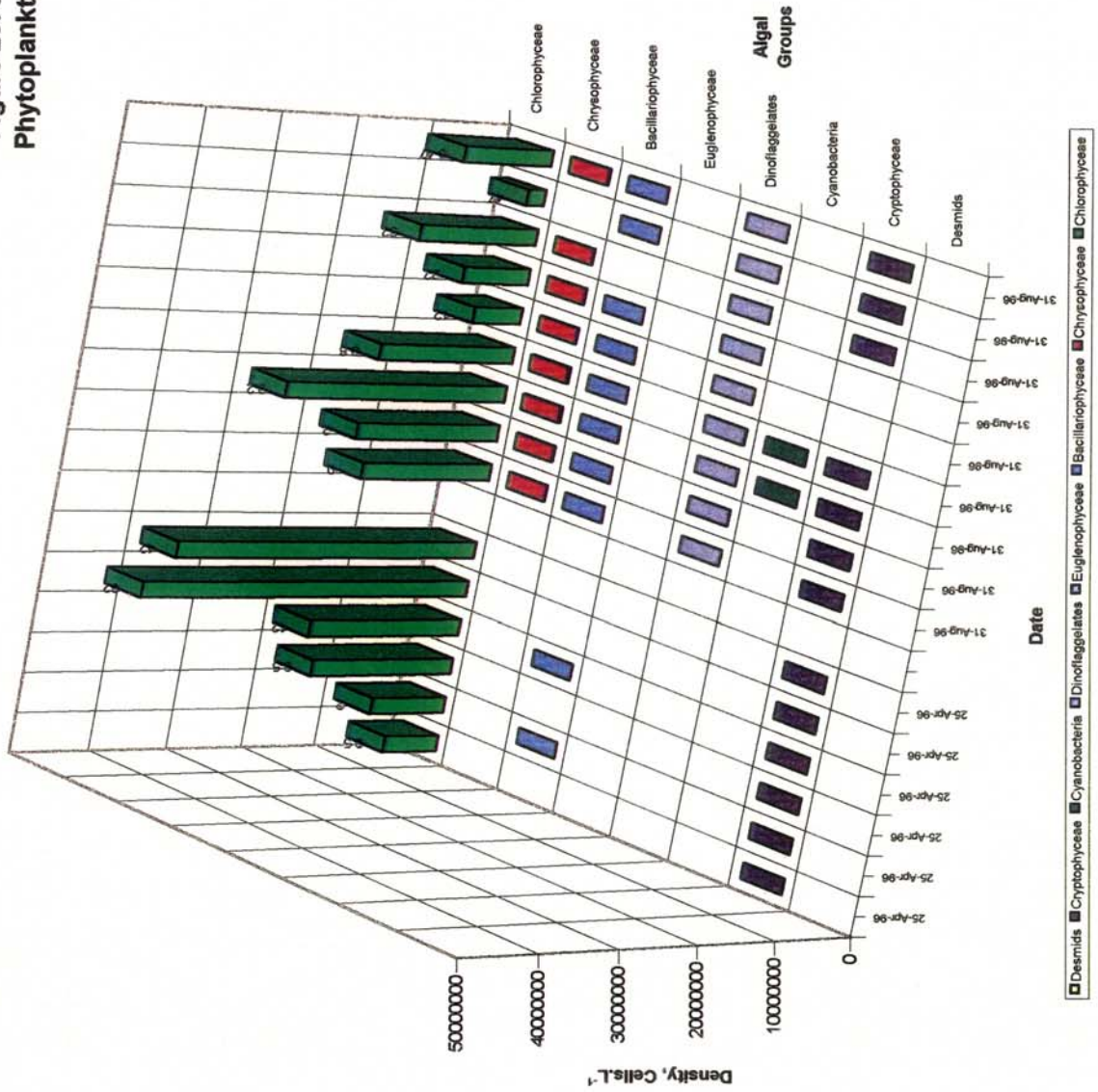
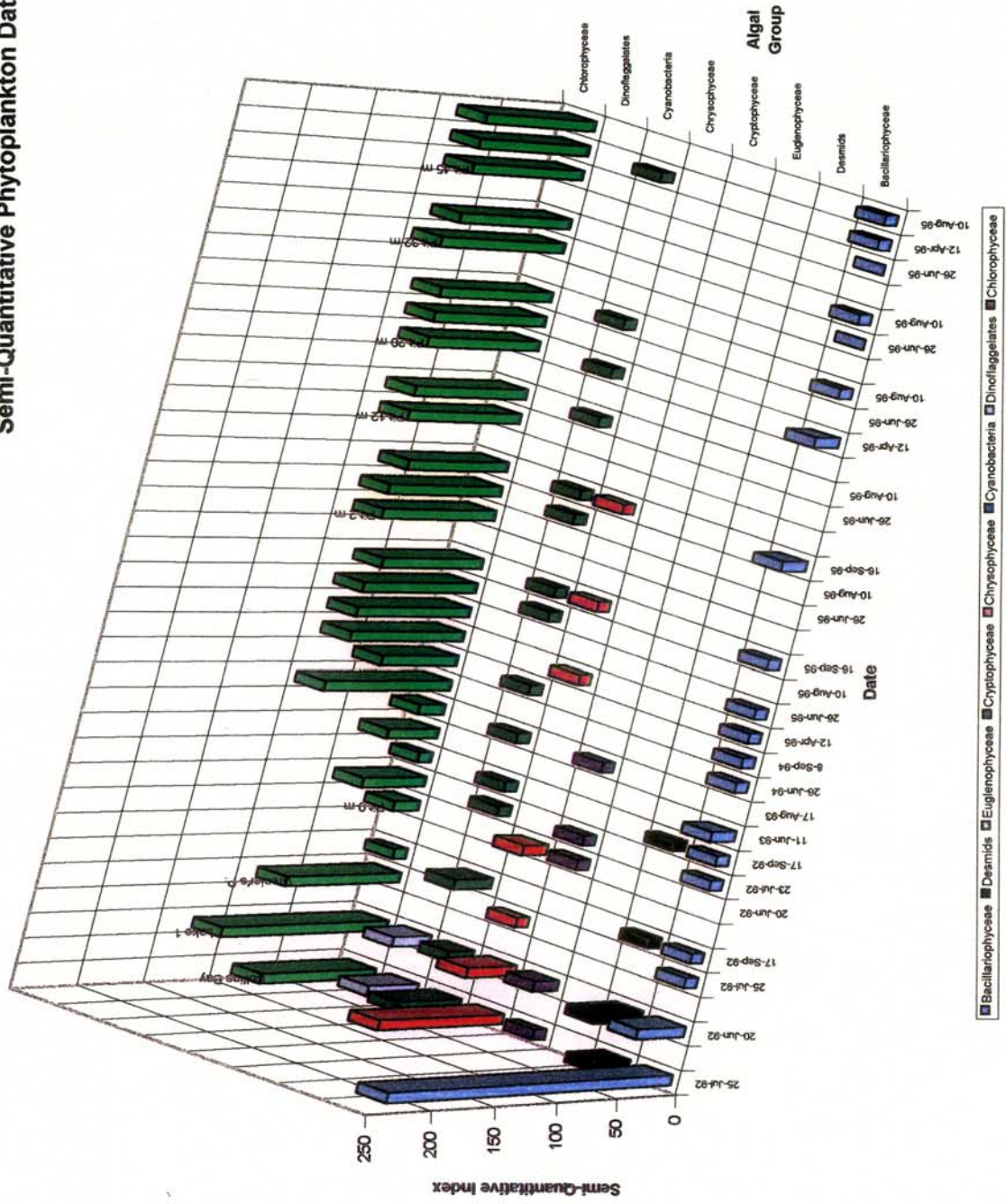


**Figure 24: B-Zone Pit  
Semi-Quantitative Phytoplankton Data**



### 3.3 The Biology of the Dominant Species in the B-Zone Pit

The phytoplankton community is dominated by the mucilaginous colonial Chlorophyte, *Dictyosphaerium*, which grows throughout the year. Cell densities and biomass of this species alone are presented over the sampling period in Table 6 for 1995, the year where the majority of the biological investigations were carried out.

Table 6: Seasonal distribution of *Dictyosphaerium* in the water column of the pit during April to September, 1995. Cells densities are given as  $10^8$  cells  $L^{-1}$ ; the biomass estimates are given as  $mg L^{-1}$  of "fresh weight".

| Depth<br>(m) | Cell Density<br>(as $10^8$ cells $L^{-1}$ ) |      |       |      | Biomass<br>(as $mg L^{-1}$ ) |       |       |       |
|--------------|---|------|-------|------|------------------------------|-------|-------|-------|
|              | Apr   | Jun  | Aug   | Sep  | Apr                          | Jun   | Aug   | Sep   |
| 0            | 0.96  | 4.33 | 12.95 | 3.03 | 3.26                         | 9.79  | 41.30 | 10.98 |
| 2            | ns  | 6.52 | 10.13 | 2.09 | ns                           | 16.71 | 32.40 | 7.04  |
| 12           | ns  | 1.88 | 5.98  | ns   | ns                           | 5.72  | 19.15 | ns    |
| 22           | 1.13  | 1.27 | 0.87  | ns   | 3.66                         | 3.66  | 2.23  | ns    |
| 32           | ns  | ns   | 0.50  | ns   | ns                           | ns    | 1.70  | ns    |
| 42           | 2.71  | 2.88 | ns    | ns   | 7.42                         | 8.57  | ns    | ns    |

ns - not sampled

Biomass is derived based on measurements of the diameter of the colonies, assuming that the colonies are spherical.

Microscopically-visible changes in the form of the *Dictyosphaerium* are discussed later based on the 1994 observations, in this section, and the presence of cells of this species was evident throughout the water column, as was evident from the April 1995 data, and the picoplankton results (Table 5). The colonies in the surface waters were typical in form and suggested that the species involved was *D. pulchellum*, as it appeared very similar to

the lab strain (UTEX 70) used for the experiments. In the surface waters, which are nutrient-rich after spring turn-over, most of the *Dictyosphaerium* was present as colonies consisting of 4-8 cells. The cells were small (~5 : m in diameter) and the mucilage was diffuse and only visible with India ink staining.

In the June, 1995 and August, 1995 samples, *Dictyosphaerium* densities were appreciably higher in the top 2 m of the water column, compared to samples collected from greater depths. These density differences can also be expressed as the differences in biomass at different depths in the pit (Table 6). The cell densities are averaged, based on integrated counts and size measurements, for above and below the thermocline. The changes in colony shape with depth can now be quantified through biomass;  $4.33 \times 10^8$  cells  $\text{L}^{-1}$  in the June, 1995 surface sample is equivalent to  $9.8 \text{ mg} \cdot \text{L}^{-1}$  fresh weight. The June, 1995 12 m sample contained  $1.88 \times 10^8$  cells  $\text{L}^{-1}$ , equivalent to a biomass of  $5.7 \text{ mg} \cdot \text{L}^{-1}$ .

In the deeper water sample (from 45 m), the colonies usually had only 1 or 2 cells and the cells were usually larger in size; the mucilage surrounding these colonies appeared more dense and could be seen without staining, suggesting that the denser mucilage protects the cells. Furthermore, the presence of algal cells in April samples (from under the ice) suggests that the mucilage has served to protect the cells. When the ice cover melts in spring, the colonies are re-suspended from lower strata of the pit's water column. As the colonies reach more favourable conditions (i.e., higher light intensity and temperature conditions) in the surface waters, the colonies begin to reproduce, leading to the *Dictyosphaerium* bloom later in the summer. This pattern of variation in cells/colony and in quality/quantity of mucilage with depth in the water column was also seen in the June, 1995 samples, as expected.

Phytoplankton plays a key role in primary productivity, particularly in large, deep lakes. The role of very small phytoplankton cells, or picoplankton (0.2 to 2 : m) in connection to the microbial loop (consisting of bacterial biomass) has been under investigation by several

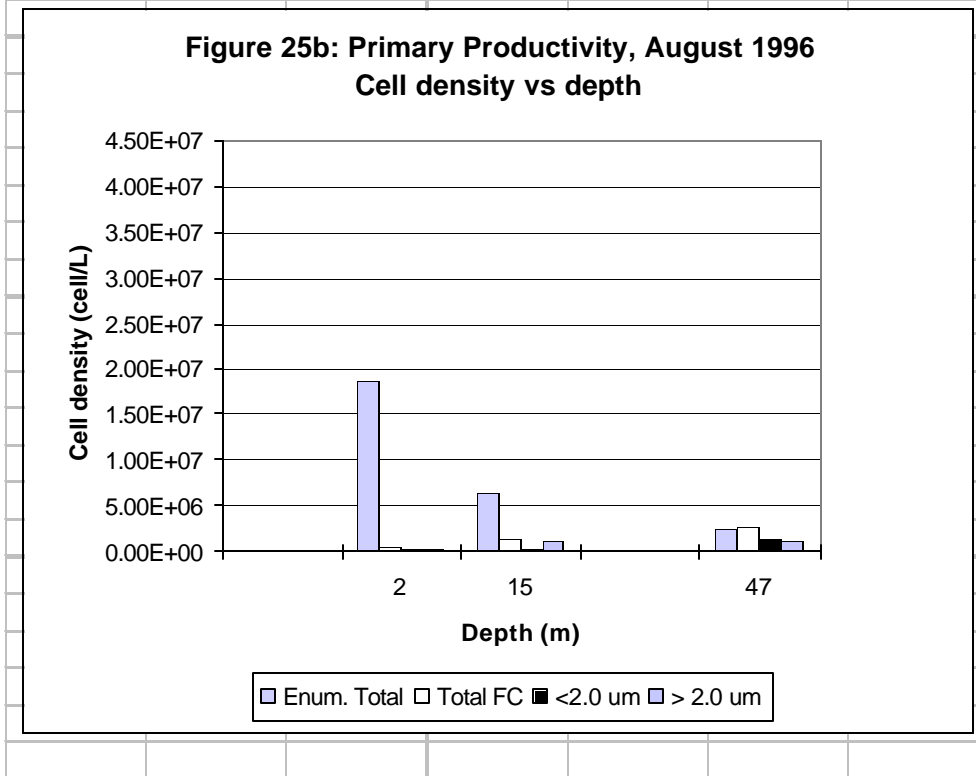
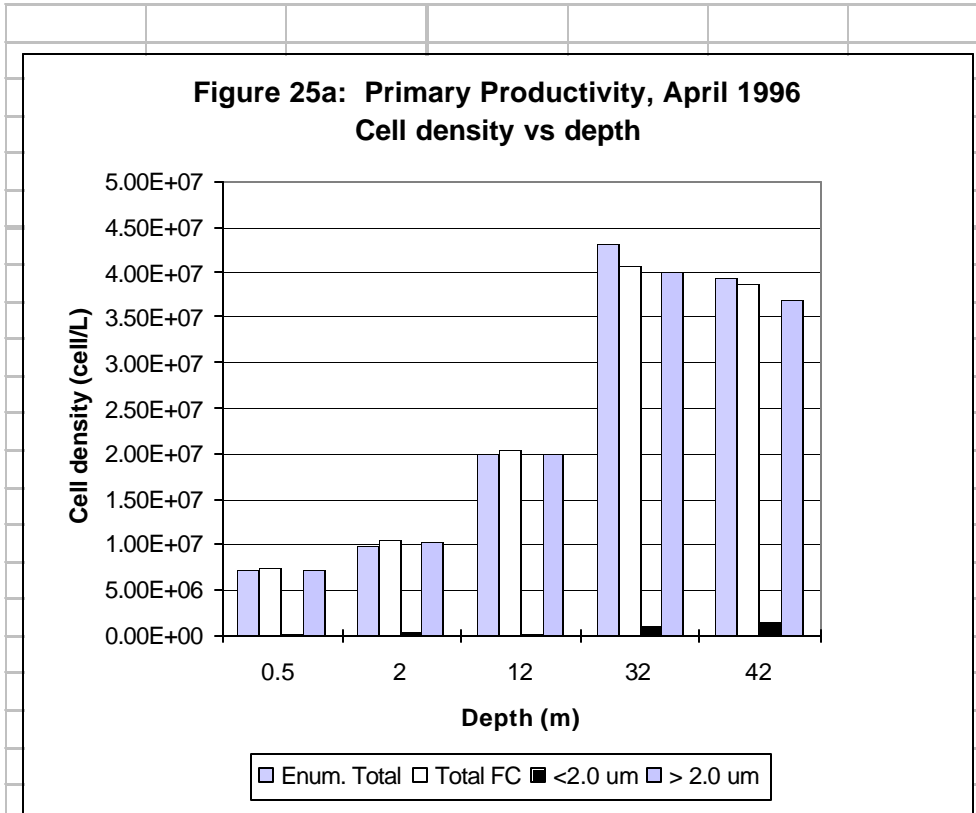


researchers. Stockner (1988) reports that, based on several limnological studies on primary productivity, between 70% and 90% of primary production could be due to picoplankton production. Phytoplankton and the microbial loop, at the base of the food chain, are responsible for most of the primary production (or carbon fixation through photosynthesis) taking place in lakes and ponds (Ruttner, 1963; Wetzel, 1983).

Picoplankton abundance as a function of depth is shown in Figure 25a for April, 1996. High cell densities are found at depths of 32 m and 42 m, with noticeably lower densities at the surface. It is also of interest to note that, at the end of the season in August, 1996 (Figure 25b) the trend is reversed, supporting the contention that these particles are moving downward in the pit underneath the ice. As biomass is carrying As and Ni to the pit bottom, the quantity of which is difficult to define, the biology of the pit is certainly important in the contaminant transport and removal from the water column.

As this report summarizes the cumulative investigations covering at least 2.5 years, from the growth studies starting in 1994/1995 leading to the prediction of lower growth rates in 1996 the 1996 summer reduction on the surface water to confirm the relevance of the biology. A brief examination of the surface water in 1996 (Figures 18b and 18c) reveals, that indeed no reduction is evident, in fact it remained the same.

Comparing the cell densities for 1996 (Figure 25 a and Fig 25 b) to those densities for 1995 (Table 6) the differences are striking. The densities underneath the ice in 1995 were 2 times higher at the surface, 4 times higher at 22 m and 7 times higher at 42 metres than in 1996. For the end of the growing season, comparing 1996 to 1995, the cell densities which are reported, remaining after one season stressed by the nitrogen depletion, a reduction in density is 50 times on lower on the surface in August and 200 times at 12 m and 10 to 20 times lower at 32 m in 1996. These observations clearly support the postulated transport mechanism along with giving the biology of the pit its appropriate role in relation to movement of As and Ni. Without the algal growth, As and Ni would likely not reach the bottom of the pit .



### 3.4 Assessing Pit Bio-Productivity

With the identification and quantification of the dominant algal group, the next step is to estimate of the productivity of the phytoplankton in the pit. Since the algae are involved in the transport of As and Ni in the water column, the key question to be addressed is: Can they be used to relegate the contaminants to the bottom of the pit? To answer this question, an assessment has to be made of the current phytoplankton growth in the pit.

Primary production is most frequently expressed in water bodies as carbon fixation, in **mg C@m<sup>-2</sup>@day<sup>-1</sup>**. Carbon fixation can then be compared to natural freshwater lakes at a similar latitude which are assumed to have similar light and temperature regimes. If productivity is higher in lakes at similar latitudes, then a nutrient limitation can be identified for the pit and measures can be taken to improve the productivity.

Productivity estimates in mg C@m<sup>-2</sup>@day<sup>-1</sup> can be derived from measured **changes in nutrient concentrations** in the pit water and measurements of **bio-products**, such as TOC (Total Organic Carbon) concentrations. Finally, the biological material collected in **sedimentation traps** can be quantified using well-established C:P ratios in biomass.

To determine the fraction contributed to primary productivity by the dominant species, extrapolations can be made by using *Dictyosphaerium* cell counts from the pit water samples and deriving **Relative Growth Rates (RGR)**. The biomass expected in the pit, based on the relative growth rates, will facilitate an assessment of the fraction of primary productivity contributed by the dominant species alone.

To arrive at comparative estimates, primary productivity in the flooded pit was considered over the period from April to August for 1995. This represents an estimate of the production for the summer season, starting with spring conditions. Most of the biological activity takes place in the epilimnion, determined by the thermocline and light penetration. Integrations are

made between measuring intervals with respect to depth of the thermocline and the euphotic zone (the zone in which photosynthesis takes place).

### Productivity Estimate Based on Nutrient Changes

Changes in nitrate concentrations can be used to predict the level of primary production in the pit. The accepted nutrient ratios present in the phytoplankton are represented as a C:N molar ratio of 4:1. This ratio of C:N is representative of actively growing phytoplankton in large bag experiments (Antia et al. 1963). C:N ratios vary from 3:1 for well-fed plants, to 6:1 for stressed populations. A key assumption in the analysis is that there is no significant input of  $\text{NO}_3$  (e.g. from decay processes, acid rain, ground water etc.).

The reduction in productivity, expressed as lower cell density in 1996, seem to confirm this key assumption.

In April, 1995, the average nitrate concentration throughout the pit was  $0.48 \text{ mg}\text{L}^{-1}$ . By August, the thermocline depth was 10 m. The volume of water above the thermocline was  $1,824,000 \text{ m}^3$ , and below the thermocline,  $3,400,000 \text{ m}^3$ . The average nitrate concentrations in August were  $0.14$  and  $0.42 \text{ mg}\text{L}^{-1}$  above and below the thermocline, respectively. This amounts to a total of  $824,000 \text{ g}$  of nitrate ( $620,000 \text{ g}$  above and  $204,000 \text{ g}$  below) removed from the pit by August. This is first converted to moles of N (by dividing by the molecular weight of  $\text{NO}_3 = 62 \text{ g}\text{M}^{-1}$ ), then converted to moles of C by multiplying by 4 (C:N ratio is 4), followed by converting to grams of carbon by multiplying by 12. This gives  $637,935 \text{ g}$  C produced in the pit from April to August. Dividing by the number of days (127) and the surface area of the flooded pit ( $282,600 \text{ m}^2$ ) results in a productivity estimate of  **$18 \text{ mg}\text{m}^{-2}\text{d}^{-1}$  of C.**

If we take the same approach for 1996, the average concentrations throughout the pit was  $0.53 \text{ mg}\text{L}^{-1}$  in May and  $0.04 \text{ mg}\text{L}^{-1}$  above the thermocline and  $0.06 \text{ mg}\text{L}^{-1}$  below the thermocline in August. This results in a nitrate removal of  $894,000 \text{ g}$  above and  $1,598,000 \text{ g}$

below. The effective productivity for 1996 converting nitrogen to g C produced results in 1,929,290 g of C which converts into a productivity estimate for the time period of 109 days for 1996, using the same surface area to **62 mg@m<sup>-2</sup>@d<sup>-1</sup> of C**. The higher productivity is a direct reflection of the greater Secchi depth in 1996, which was 2 m by August, 1996 compared to a depth of 0.7 m in June, 1995. Thus higher productivity since a bigger part of the water body was supporting growth.

This estimate is probably on the low side, since it was assumed that only the nitrate was removed, and that there was no net input or nitrogen turnover operating in the flooded pit during the growing season.

#### Productivity Estimate Based On Measured Bio-Products

Average TOC concentrations throughout the pit in April, June, August and October were 4.3, 4.2, 5.7 and 6.0 mg@L<sup>-1</sup>, respectively. These values are based on the top 75% (of the depth) of water column. Only the April and August values are used in the calculation. The increase in TOC over that period was 1.4 mg@L<sup>-1</sup>. Multiplying this increase by the total volume of the flooded pit, dividing by the surface area of the flooded pit, and dividing by the number of days between readings (127) gives an estimate of carbon productivity of **204 mg@m<sup>-2</sup>@d<sup>-1</sup> of C**. These values for the equivalent period in 1996 were lower, where the change in TOC was 0.3 mg@L<sup>-1</sup>, reflecting the lower cell densities for 1996. The same calculation for 1996 gives an estimate of carbon productivity of **51 mg@m<sup>-2</sup>@d<sup>-1</sup> of C**.

#### Productivity Estimate Based on Sedimenting Organic Matter

A third approach to arriving at estimates of primary productivity can be based on data collected from the sedimentation traps in the pit. An upper and lower estimate is made based on: (a) assuming that the amount of sedimenting algae measured is 100% algae with no particulates included, and (b) for this organic matter, the generally accepted C:P ratio of

33:1 is valid.

In September, 1995, the sediment collected over the previous 37 days was separated into sediment and "algal" content. The dry weight contribution of the algae was  $0.9 \text{ g dw m}^{-2} \text{ d}^{-1}$ . If this weight represents algal biomass consisting normally of about 40% carbon, then the carbon fixation rate would have been approximately  $360 \text{ mg C m}^{-2} \text{ d}^{-1}$ . This primary productivity is high, as it assumes that the material separated was indeed all "algal", which is unlikely. For 1996, the estimate using the sedimentation data (Table 3) would result in lower productivity, as the sedimentation rates were very much lower at the surface and 3 to 5 times lower at a depth of 12 m and 22 m respectively. Given that in 1996 the amount collected was lower, no separation of algal in inorganic material was possible, and thus no value is given.

In 1994, algal material collected from the sedimentation traps was analyzed for elemental composition. The phosphate concentration in the material can be used to estimate the percent of carbon in the "algal material". The concentration of phosphate in the dried algae was  $1000 \text{ : g@gdw}^{-1}$ . Using this value to estimate primary productivity a lower value is obtained of about  $20 \text{ mg C m}^{-2} \text{ d}^{-1}$ , which suggests that not all the phosphate is present in organic form. This is likely due to phosphate mineralisation in the B-Zone Pit.

In Table 7, all estimates are summarized and compared to productivity reported for the natural lakes at latitudes similar to the pit. Primary productivity estimates could not be found for Collins Bay, although an extensive environmental data set has been accumulated over the years.

The lakes cited are considered mesotrophic. While the definitions of oligotrophic, mesotrophic and eutrophic are related to nutrient inputs, lake dimensions and retention times, one can also classify lakes by their carbon productivity per square metre per day or year. From the data in Schanz and Wälti (1982), carbon productivity is related to lake

Table 7: Estimated primary production in the pit using changes in water chemistry and literature production numbers from Northern Lakes.

| Estimator                           | mg C@m <sup>-2</sup> @d <sup>-1</sup> | Production numbers form Northern Lakes* |                 |                                       |
|-------------------------------------|---------------------------------------|---|-----------------|---------------------------------------|
|                                     |                                       | Lake                                    | Location        | mg C@m <sup>-2</sup> @d <sup>-1</sup> |
| NO <sub>3</sub>                     | 18                                    | Wabumun                                 | 53°N<br>Canada  | 880                                   |
| TOC                                 | 217                                   | Trummen                                 | 58°N; Sweden    | 616                                   |
| Algae from<br>Sedimentation<br>Trap | 20-<br>360                            | Erken                                   | 58°N;<br>Sweden | 285                                   |

(\* data from Schanz and Wälti, 1982)

productivity as follows: Lakes which support less than 250 mg C@m<sup>-2</sup>@d<sup>-1</sup> are considered oligotrophic; those with primary production in the range of 250-850 mg C@m<sup>-2</sup>@d<sup>-1</sup> are mesotrophic; and those with production between 900-2000 mg C@m<sup>-2</sup>@d<sup>-1</sup> are eutrophic.

Those lakes with primary production in excess of 2000 mg C@m<sup>-2</sup>@d<sup>-1</sup> are hypereutrophic. All of the pit productivities suggest an oligotrophic to mesotrophic water body in terms of primary production, and yet eutrophic to hypereutrophic when based on nutrient concentrations. Given that the pit is not a natural lake system at the present time, the difficulty incurred when classifying the ecosystem is not unexpected. Generally, in healthy lakes primary production is limited by the lack of phosphorus (Ryther and Dunstan, 1971) and the classifications are based on the phosphorus availability. This is not the case in the pit, where no changes in the concentrations of phosphate in pit waters were noted throughout the season or with depth (Table 1a and 1b).

The primary productivity estimates for the pit suggests that an improvement could be achieved when pit productivities are compared to natural lakes in similar climate regimes. Only the sedimentation trap estimates are in the range which suggest an mesotrophic system, if the weights are not adjusted to the expected nutrient ratio.

### Productivity Estimates Based on the RGR of the Dominant Species

If we assume that the major component of the primary productivity is contributed by the dominant species in the pit, *Dictyosphaerium* cell counts or cell volumes over the summer of 1995 can be used (Table 6). Growth rates in the pit for the period from April to August can be calculated according to the general standard formula  $RGR = \text{relative growth rate} = \ln(W2/W1)/t$  where  $W2$  is biovolume in August  $(41.3+32.4)/2 = 36.85$  and  $W1$  is biovolume in spring (3.26). The time between the measurements is 127 days. The RGR can be estimated for *Dictyosphaerium* based on biomass, thus,  $RGR = \ln(36.85/3.26)/127 = \mathbf{0.019\ d^{-1}}$ . This relative growth rate in the pit is, therefore, about **2%** per day. The same calculations carried out for 1996 (using cell densities), result in a  $RGR = \ln(1.87/0.5)/128 = \mathbf{0.008\ d^{-1}}$  or **0.8%** per day, effectively reduction by half due to the nitrogen depletion.

These RGRs, calculated for the pit using the cell counts, can be compared to the laboratory growth experiments (described later in this report) to determine if they are within the range one would expect in the pit. In the laboratory, a ten-fold increase in growth rate is expected, due to the improved temperature and light conditions. The growth rates, in divisions per day, are converted to RGR by multiplying by  $\ln(2)$ , resulting in RGR of  $0.233\ d^{-1}$  for light-saturated cultures under similar nutrient regimes. Flooded pit *Dictyosphaerium* growth rates are therefore in the expected range. These evaluations suggest the growth rate can be improved through nutrient additions, since the experiment showed a reduction in the RGR in N-limited conditions. It also suggests that the pit conditions are indeed successfully simulated by the laboratory experiments.



Estimates of the primary productivity of the *Dictyosphaerium pulchellum* throughout the flooded pit between April and August of 1995 are made from measured cell densities at various depths from Table 6. These were first converted to biomass, based on cell diameter and assuming a density of 1. From these values, an average between each depth measurement was taken for both August and April, and their difference recorded (it was assumed that, at depths of 2 m and 12 m in April, the biomass was the same as at the surface, i.e. 3.3 mg@L<sup>-1</sup>). These estimates are presented in Table 8.

Table 8: Areas and depth contours of the flooded pit used in productivity calculations.

| Depth Interval<br>m | Area of Interval<br>m <sup>2</sup> | Volume of Interval<br>m <sup>3</sup> | Biomass<br>mg@L <sup>-1</sup> | Total Mass in<br>Interval<br>(tonnes) |
|---------------------|------------------------------------|--------------------------------------|-------------------------------|---------------------------------------|
| 0-2                 | 240,000                            | 480,000                              | 33.6                          | 16.1                                  |
| 2-12                | 168,000                            | 1,680,000                            | 22.5                          | 37.8                                  |
| 12-22               | 131,000                            | 1,310,000                            | 8.0                           | 10.4                                  |
| 22-32               | 100,000                            | 1,000,000                            | 0                             | 0                                     |
| 32-42               | 43,000                             | 430,000                              | 0                             | 0                                     |
| 42-50               | 43,000                             | 344,000                              | 0                             | 0                                     |

The biomass estimates were then multiplied by the volume of that water for the depth interval. The total biomass of the *Dictyosphaerium pulchellum* produced in the flooded pit between April and August 1995 is 64 tonnes (fresh weight). This amount is converted to the amount of carbon produced by taking 5% (80% of the algae is water) and then 40% (40% of the dry weight of algae is carbon), giving a total amount of carbon produced by the algae of 5.2 tonnes.

The amount of extra TOC produced between April and August was determined to be 1.5 mg@L<sup>-1</sup>. Multiplying this by the volume of the pit gives a total production for carbon in the pit of 7.8 tonnes. Thus, the amount that the algae is contributing to primary production is

$5.2/7.8 \times 100\% = 67\%$ . If the productivity decreases in the pit due to the nitrogen limitation become more severe with time, it would be expected that the TOC would decrease, as was observed in 1996. In comparison to 1995, when the difference for the growing season was  $1.4 \text{ mg@L}^{-1}$  TOC, in 1996 the difference between May and August is only  $0.3 \text{ mg@L}^{-1}$  TOC.

Phytoplankton plays an important role in primary productivity, particularly in large, deep lakes. The productivity estimate derived from the dominant algae would suggest that picoplankton and microbial activities possible represent a large fraction of the remainder of the primary productivity. Although picoplankton is present in the pit, its contribution to primary productivity is less significant than that of the dominant species *Dictyosphaerium*, which alone can account for 70% of the primary productivity based on carbon fixation.

## 4.0 ARSENIC AND NICKEL REMOVAL: BIOLOGICAL AND PHYSICAL APPROACHES

The evaluation of the biology in the pit together with the growth dynamics and the characterization of the particulate matter in the pit, indicated relatively conclusively, that pit biology and contaminant transport are related. The key question, which was addressed through laboratory experiments, is: Can the contaminant transport be quantified? It was proposed, that should quantification be possible, through controlling the algal growth, it would be possible to effect contaminant movement, and ultimately removal and relegation to the bottom of the pit in a controlled manner. Although it was clear, that conditions in the laboratory were ideal and would not likely reflect those in the pit, the laboratory work related surprisingly well to the pit. In this section, the laboratory results are summarized from Kalin et al. 1997, with the main emphasis to relate the results to the pit limnology.

### 4.1 Biologically-Mediated Contaminant Removal

#### 4.1.1 Biology and Growth Control of *Dictyosphaerium pulchellum*

The evaluation of the biological aspects of the pit indicated clearly that *Dictyosphaerium pulchellum* was the dominant algae. It will therefore be the main biological agent which might be utilized in any in-situ treatment approaches. If this species is to be utilized, a detailed knowledge of the growth-controlling factors of this species is required.

#### *Taxonomy*

*Dictyosphaerium* spp. are common members of the phytoplankton community in many lakes. This genus reportedly contains 12 species, of which 4 are commonly found: *D. pulchellum*, *D. simplex*, *D. planctonicum* and *D. ehrenbergianum*. Due to their size, their contribution to the overall biomass of phytoplankton in pristine waters is small. The species are distinguished on the basis of cell shape (e.g., spherical, ovoid, reniform). Colonies are

formed when the 4 (or rarely 8) autospores remain attached through fragments of the mother-cell wall. The colonies are characteristically surrounded by a copious gelatinous matrix. This species is suspended in the water column for much of the year due to the very small cells (usually < 10 : m in diameter) in combination with the mucilaginous layer. In Plate 3, healthy algal colonies are depicted from a culture medium. Schematic 3 is a representation of the algal colonies of the species.

While the taxonomy of this genus is well known, very little is known about its physiological requirements. As the gelatinous matrix is part of the taxonomic characteristics of this genus, it may be possible that mucilage production is genetically controlled and thus can not be influenced through environmental conditions in all species of the genus. Generally mucilage production is considered a response to environmental stress, but in this algal group, this may not be the case.

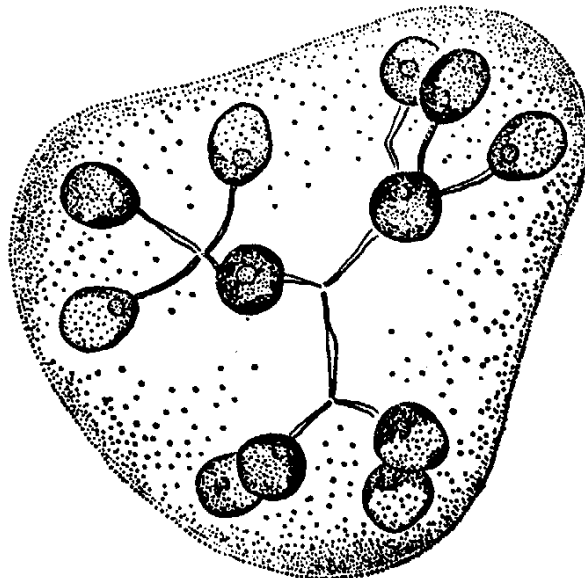
#### 4.1.2 Environmental Stress and Mucilage Production

Given the dominance of this species in the pit, the stress factors which lead to mucilage production (if not genetically controlled) should be understood. This is also of importance in relation to treatment options, as organically complexed metals at these low concentrations would be more difficult to remove than when they are present as free ions. A brief review of the factors which are generally believed to contribute to mucilage production is necessary.

Phytoplankton blooms and mucilage production are frequently connected and represent the end of the healthy growth phase for a species. Increase in cell density occurs during growth resulting in a peak cell density, referred to as a bloom. At that time nutrients frequently become limited and mucilage production takes place. Therefore, in natural unpolluted waters, blooms are usually the result of normal changes in environmental conditions such as alterations in the relative proportions of nutrients, as well as light and temperature conditions during the growing season (Wetzel, 1983).



Plate 3: Micrograph of *Dictyosphaerium* colonies collected from the B-Zone Pit and used in laboratory experiments. Specimen stained with India ink in order to display mucilaginous sheath surrounding cells. Bar = 40 : m.



Schematic 3: Schematic diagram of a *Dictyosphaerium* colony with surrounding mucilaginous sheath.

Phytoplankton blooms can be viewed as a stress response if they take place during the life cycle of phytoplankton populations (weeks) and not at the end of the cycle. The stress would be associated with the production of large quantities of extracellular polysaccharides (Hellebust, 1974). This response can be species-specific and can occur during various changes in nutrient ratios.

As seasonal environmental conditions change and induce stress on phytoplankton, each species has developed physiological and, possibly, genetic adaptations to that stress in order to survive. In phytoplankton species, one of the most commonly reported adaptations to environmental stresses, such as nutrient depletion or contaminant elevation, is a physiological adjustment involving the excess production of carbohydrates, variously referred to as exopolymers, extracellular polysaccharides, mucilage, mucus, slime, etc. (Hellebust, 1974). According to Shuter (1979), algal populations produce excess carbohydrates under two kinds of growth situations: (1) nutrient stress (usually phosphorus and/or nitrogen) limitation; and, (2) light stress (either high light or low light). When light conditions are adequate, excess carbohydrates will be produced under nutrient stresses (e.g. nitrogen or phosphorus limitation).

Unlike phosphorus, which can be stored internally as polyphosphates for later use, algae are unable to store reserves of nitrogen. Therefore, the depletion of nitrogen in particular has serious consequences for the continued growth of algal species. Nitrogen starvation is known to cause the cessation of growth and a shift from the production of proteins to the production of carbohydrates (Arad et al., 1988). When nutrients are adequate and balanced, high light (at inhibitory levels) or low light (at limiting levels) may also shift the cells' metabolism in favour of carbohydrate production, but this is not common.

This excretion of carbohydrates is a normal consequence of nutrient stress in small algal species. At first glance, such losses of photosynthetic material appear to be negative. However, there is evidence that the excreted carbohydrates provide cells with protection from

contaminants in the ecosystem (Mangi and Schumacher, 1979). The mechanism(s) of such protection are not well understood but probably involve chelation, co-precipitation, adsorption and adhesion for contaminants such as metals. The accumulation of these complexes can lead to increases in colloidal and particulate material in the water column which, depending on the contaminant, can cause subsequent problems. However, the binding properties of this excreted material can provide a unique opportunity to remove contaminants (Koren, 1992). Therefore, a better understanding of these properties is essential in order to capitalize on the bioremediation potential of planktonic microorganisms.

#### 4.1.3 Nutrient Conditions in the B-Zone Pit

To evaluate the nutrient status which prevails in the pit, the nutrient ratio of N:P is determined. The ratios of the major nutrients, N and P, are expressed as molar (=atomic) ratios. These are calculated by dividing the sum of : moles of nitrate and ammonium per litre by : moles of phosphate per litre.

In Table 9, the N:P molar ratios are presented for 1995, since this is the year for which all productivity values were generated. It can be concluded that a nitrogen limitation can occur during the end of the growing season, or the pit will be colonized by algae which have the ability to fix atmospheric nitrogen. This, however, will only take place if the conditions in the pit are tolerated by Cyanobacteria. The fact that they are present, but only as picoplankton and have not shown great abundance in the pit since flooding (Figures 23, 24, 25a and 25b) suggest that the conditions are less than favourable for their growth. It is not unreasonable to anticipate that the pit will become severely nitrogen limited. The effects of nutrients limitation on growth of the algae requires that growth conditions under healthy nutrient ratios are defined as well as other key factors on growth, such as light and temperature. Growth experiments have been carried out and are described in detail in Kalin and Olaveson (1996). The data from this report are briefly summarized below.

| Table 9: B-Zone Pit, N : P Molar Ratios for 1995. |      |      |      |      |      |      |      |      |      |      |
|---|------|------|------|------|------|------|------|------|------|------|
| Depth (m)   | 0    | 5    | 10   | 15   | 20   | 25   | 30   | 35   | 40   | 45   |
| April 12, 1995                                    |      |      |      |      |      |      |      |      |      |      |
| N : P   | 1.58 | 1.94 | 1.67 | 2.53 | 2.08 | 2.58 | 1.97 | 2.62 | 2.30 |      |
| June 14, 1995                                     |      |      |      |      |      |      |      |      |      |      |
| N : P   | 1.16 |      | 0.58 | 3.70 | 3.31 | 4.45 | 2.85 | 1.45 | 2.13 |      |
| August 17, 1995                                   |      |      |      |      |      |      |      |      |      |      |
| N : P   | 1.60 | 0.71 | 1.04 | 1.85 | 2.00 | 3.12 | 2.33 | 2.13 | 3.30 | 1.07 |
| October 14, 1995                                  |      |      |      |      |      |      |      |      |      |      |
| N : P   | 1.25 | 0.69 | 1.30 | 1.55 | 0.69 | 4.98 | 2.88 | 2.08 | 1.70 |      |

#### 4.1.4 Effect of Light and Temperature on Growth of *Dictyosphaerium*

The experiments where light intensity were tested used the lab strain (UTEX 70) of *Dictyosphaerium*. Growth rates of the population were slowest at the lowest light intensity, as expected. Over a 2-week period, however, the cell densities achieved were similar to those in the ambient and high light treatments (Table 10a). The high, medium, and low light conditions represent 1.35-1.50, 0.88-0.96, and 0.20-0.29 x 10<sup>16</sup> quanta@cm<sup>-2</sup>@sec<sup>-1</sup>, respectively. It appears, based on the cell densities, that the light conditions provided in the experiment in the presence of sufficient nutrients did not affect growth. These light intensities, converted to ft-candles, are similar to the light regime in the pit in the strata above and below the Secchi depth between the years 1993 and 1996.

The effect of temperature on cell growth was evaluated for 8, 16 and 24 °C. Two nutrient treatments were used; a Control Treatment (N:P = 10:1) using Chu-10 solution and a Field Simulation Treatment (N:P = 1:1) simulating the N:P ratio found in the flooded pit. At 10 days of growth and after, the cell densities at temperatures of 24 and 16 °C were very similar (Table 10 b). Over the first 10 days, the growth rate at 24 °C is somewhat greater that at 16 °C for both nutrient conditions. At 8 °C, growth is considerably slower. Growth rates are shown in Table 11.



Table 10a: The effect of various light intensities on the growth of *Dictyosphaerium pulchellum* at an N:P ratio of 10:1

| Time Days                               | High Light | Medium Light | Low Light |
|---|------------|--------------|-----------|
| Cell Density (x10 <sup>8</sup> Cells/L) |            |              |           |
| 0                                       | 0.93       | 0.93         | 0.57      |
| 5                                       | 7.38       | 9.98         | 11.13     |
| 10                                      | 30.57      | 29.42        | 31.29     |
| 14                                      | 41.80      | 44.25        | 45.55     |
| 23                                      | 75.93      | 76.94        | 81.84     |

Table 10b: The effect of various temperatures on the growth of *Dictyosphaerium pulchellum* at an N:P ratio of 10:1

| Time Days                               | High Temperature<br>24° C | Medium Temperature<br>16° C | Low Temperature<br>8° C |
|---|---------------------------|-----------------------------|-------------------------|
| Cell Density (x10 <sup>8</sup> Cells/L) |                           |                             |                         |
| 0                                       | 1.24                      | 1.24                        | 1.24                    |
| 4                                       | 10.12                     | 5.37                        | 2.87                    |
| 10                                      | 31.40                     | 26.75                       | 7.31                    |
| 14                                      | 40.25                     | 40.90                       | 10.77                   |
| 20                                      | 60.02                     | 55.91                       | 22.65                   |
| 22                                      | 67.15                     | 62.83                       | 22.97                   |

Table 10c: Changes in Carbohydrate Concentration for *Dictyosphaerium pulchellum* at an N:P ratio of 10:1

| Time Days  | High Temperature<br>24° C | Medium Temperature<br>16° C | Low Temperature<br>8° C |
|--|---------------------------|-----------------------------|-------------------------|
| Carbohydrate Concentration (µg glucose/L)                      |                           |                             |                         |
| 0  | 9.70                      | 9.70                        | 9.70                    |
| 4  | 17.99                     | 15.89                       | 15.87                   |
| 8  | 26.73                     | 24.92                       | 22.90                   |
| 14   | 35.73                     | 36.42                       | 24.94                   |
| 18   | 46.45                     | 44.88                       | 30.75                   |
| 22   | 64.73                     | 54.70                       | 34.11                   |
| Carbohydrate Concentration (µg glucose/ 10 <sup>8</sup> Cells) |                           |                             |                         |
| 0  | 7.80                      | 7.80                        | 7.80                    |
| 4  | 1.78                      | 2.96                        | 5.54                    |
| 8  | 1.07                      | 1.27                        | 4.35                    |
| 14   | 0.89                      | 0.89                        | 2.32                    |
| 18   | 0.96                      | 0.92                        | 1.94                    |
| 22   | 0.96                      | 0.87                        | 1.48                    |

In general, the Control Treatment has a slightly greater growth rate than the Field Simulation, with the exception of the 8 °C results (Table 11). Final cell densities after 22 days growth were similar for both the Control and Field Simulation Treatments and suggest that in the active growth phase, the nutrient ratio is not a major variable affecting growth rate.

Table 11: Growth Rates (as divisions/day) of *Dictyosphaerium* at various temperatures, based on cell densities.

| Temperature (°C) | Control (N:P = 10:1)<br>Growth Rate | Field Simulation (N:P = 1:1)<br>Growth Rate |
|------------------|-------------------------------------|---|
| 24               | 0.541                               | 0.487                                       |
| 16               | 0.497                               | 0.464                                       |
| 8                | 0.259                               | 0.306                                       |

Carbohydrate production increased with time for all temperatures and treatments (Table 10c). There was no difference in carbohydrate production between the 24 and 16 °C temperature experiments. The 8 °C temperature experiment had carbohydrate concentrations about half that at 16 °C after 22 days.

Carbohydrate content/cell decreased rapidly to a limiting value of about 1 : g glucose/10<sup>8</sup> cells after 8 days for both the 24 and 16 °C temperature experiments (Table 10c). Over the first 10 days, carbohydrate content/cell decreased more rapidly at 24 °C than at 16 °C. At 8 °C, the carbohydrate production was significantly higher than at higher temperatures, decreasing at a much slower rate, and never reaching a limiting value over the duration of the experiment.

In summary, although the 24 °C growth (in terms of both cell density and carbohydrate production) was initially greater than the 16 °C over the first 10 days of growth, there was little difference after that time. Growth rates at 8 °C were significantly slower than at 16 °C, while the amount of carbohydrate produced by each cell was significantly greater. Finally, the growth rate for the Control Treatment (N:P = 10:1) was slightly greater than for the Treatment simulating field conditions (N:P = 1:1).

#### 4.1.5 Nutrient Ratios and Mucilage Production

The growth rate, i.e., the rate at which cells are produced, appeared to be affected by the nutrient ratio. The next possible effect could be the production of mucilage, which was addressed with the next set of experiments, discussed in detail in Kalin and Olaveson (1996).

Mucilage production is measured by determination of carbohydrate concentrations. The number of cells in the experiments are quantified by measuring Optical Density. Based on a calibration curve of the two parameters, cell density and mucilage production can be related.

Nutrient stress was simulated by increasing the nutrient supply of one of the nutrients to very high concentrations such that growth could only be limited by either N or P, respectively. In addition, a treatment was added which mimicked the 1:1 N:P ratio observed in the pit over the 1994 and 1995 field seasons.

The results, representing the cell densities after calibration of Optical Density (OD), and then taking the natural log of the cell densities, are illustrated in Figure 26a. Growth was very slow over the first 7 days, probably due to the dilute cell inoculum used at the beginning of the experiment. This resulted in readings which were barely detectable by

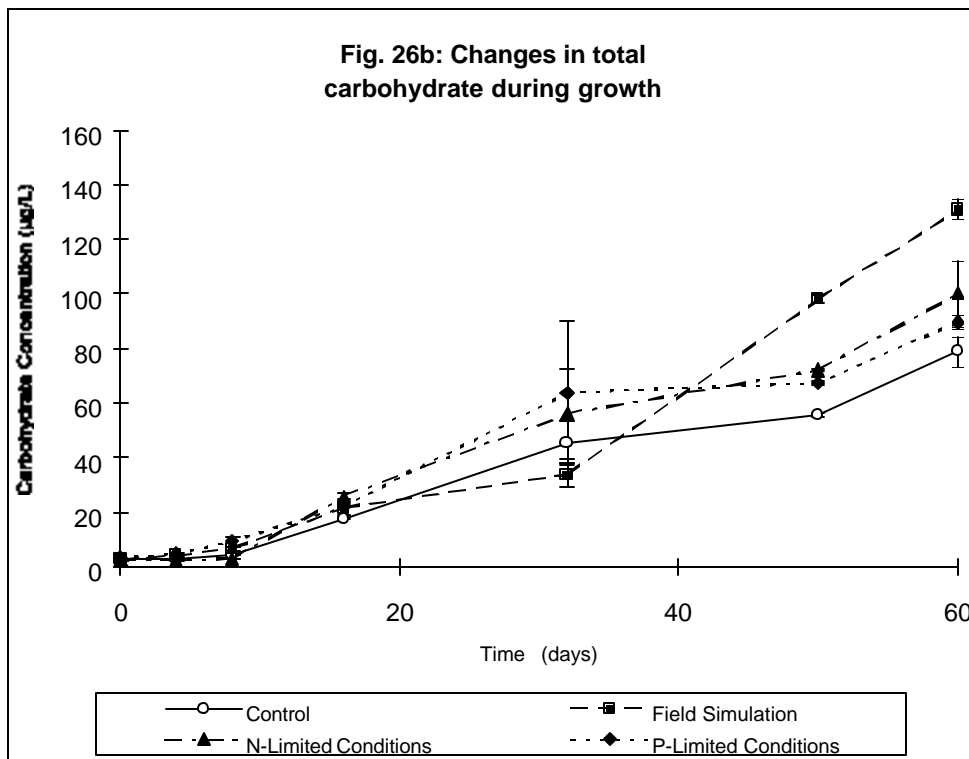
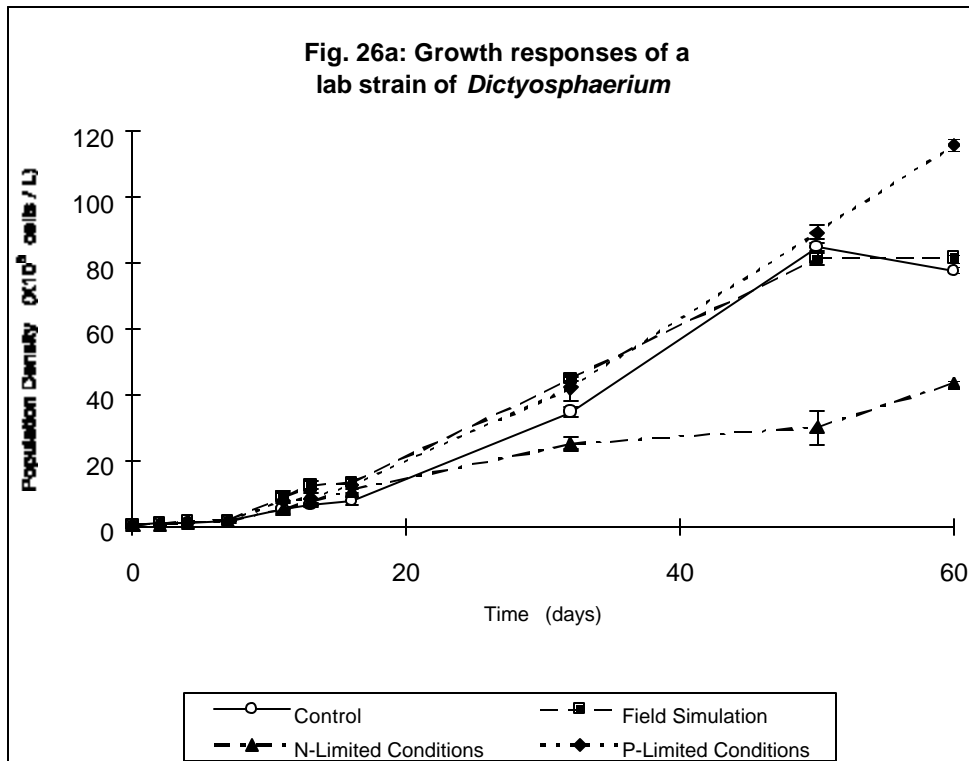
the optical density method used to quantify growth measurement. After day 11, however, all treatments showed growth. The growth rates are based on the log transform of cell densities over two time intervals, from day 2 to day 11, and from day 1 to day 31. These are summarized in Table 12.

Table 12: Growth rates (as divisions@day<sup>-1</sup>) of the lab strain of *Dictyosphaerium* grown under nutrient stress.

| Treatment           | N:P Ratio | <i>D. pulchellum</i><br>(UTEX 70)<br>Day 2 - Day 11 | <i>D. pulchellum</i><br>(UTEX 70)<br>Day 1 - Day 31 |
|---------------------|-----------|---|---|
| P-Limited Condition | 100:1     | 0.349±0.048   | 0.137   |
| Control             | 10:1      | 0.284± 0.025  | 0.126   |
| Field Simulation    | 1:1       | 0.337± 0.050  | 0.135   |
| N-Limited Condition | 0.1:1     | 0.279± 0.170  | 0.117   |

None of the growth rates reported here are significantly different during the exponential phase of growth (approximately up to day 30), but the onset of the stationary phase (after day 30) and the physiological responses to nutrient limitation are very different among the four treatments, as was previously noted with the temperature experiments.

The earlier onset of stationary phase leads to significant differences in the final population densities achieved. The error bars indicate significant differences among all treatments, with the N-Limited Condition having the lowest densities, followed by moderate densities in the Control and Field Simulation, which are similar, and finally, to the highest density achieved in the culture with the P-Limited Condition. It would appear that the N limited culture entered stationary phase at 30 days, whereas the Control and the Field treatment reached this growth phase in 50 days. The P limited growth never entered stationary phase (Figure 26a).

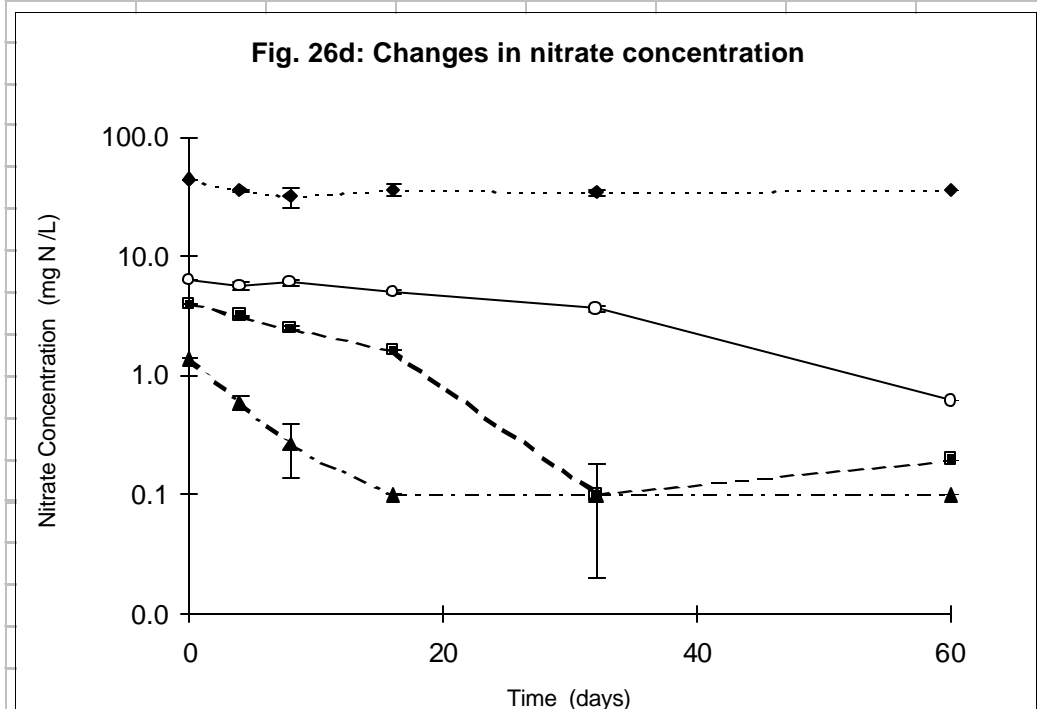
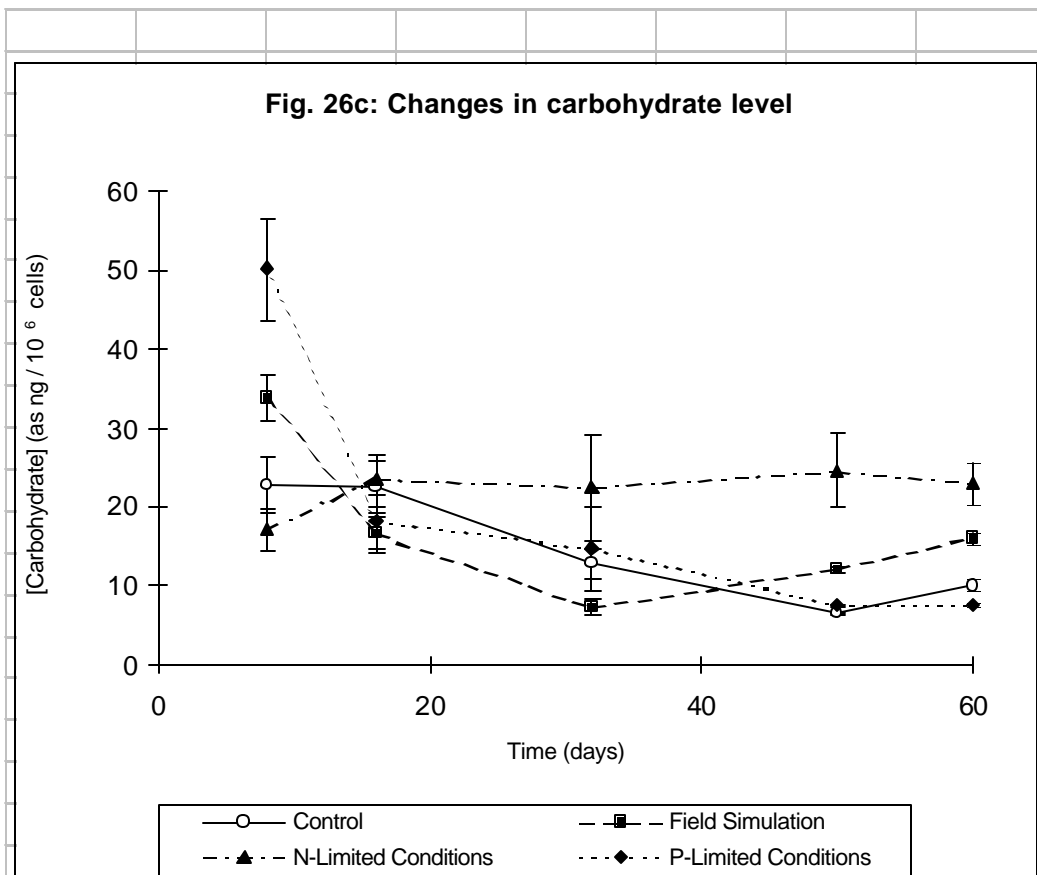


The physiological responses, especially with regard to carbohydrate production, are particularly striking among the four treatments in nutrient stress. The carbohydrate levels ( $\text{g}\cdot\text{mL}^{-1}$ ), which are used as an indicator of extracellular polysaccharide production, increased in all treatments throughout the duration of the experiment (Figure 26b).

Carbohydrate levels in the culture medium are expected to be a good indicator of extracellular polysaccharide production since, in *D. pulchellum*, the bulk of the carbohydrate associated with the cells is in the extracellular mucilaginous matrix. The very small size of the individual *D. pulchellum* cells would contribute little to the carbohydrate concentration. Once exponential growth begins at about day 7, carbohydrate levels ( $\text{g}\cdot\text{mL}^{-1}$ ) begin to increase rapidly in conjunction with growth.

The nutrient stressed treatments (N-Limited Condition and P-Limited Condition) show more rapid carbohydrate production than the Control, although the differences are not significant until after day 32. The Field Simulation shows the lowest rates of carbohydrate production ( $\text{g}\cdot\text{mL}^{-1}$ ) in the early stages of growth but after day 32, carbohydrate levels rise sharply. By the end of the experiment (day 60), the highest carbohydrate concentrations are found in the Field Simulation. The Control has the lowest concentrations of carbohydrate at the end of the experiment. A low excretion of extracellular polysaccharides would be expected from healthy growing cells as the excretion is the expected stress response to nutrient limiting conditions.

The carbohydrate concentrations as a function of the population density during growth are shown in Figure 26c. Once exponential growth is established (after day 7), a more stable pattern of carbohydrate per cell is apparent. The Field Simulation behaved in a similar fashion to the control in the early phases of growth but, after day 32, began to produce carbohydrates at a significantly greater rate, leading to the highest carbohydrate/cell ratio after the N-Limited Condition. This result suggests that, after day 32, the Field Simulation is also severely nitrogen-limited. The N-Limited Condition had the highest overall



carbohydrate/cell values. These cells continued to produce extracellular carbohydrate long after the cultures stopped growing.

Microscopic examination revealed healthy, typical colonies although, as the experiment progressed and cultures became more nutrient-stressed, there were fewer 4- and 8-colonies; most were present as single cells or 2-cell groups. The N-Limited Condition became increasingly yellow then cream-coloured during the experiment. Microscopically, there were few if any colonies. Individual cells, rather than colonies, dominated and, in many cases, empty mucilaginous globules were evident. Few viable cells were present at the end of the experiment. The Field Simulation samples became greenish-yellow in colour during the experiment. There was a decrease in the number of colonies and an increase in the number of 1- and 2- celled groups. The cells also became enlarged with obvious swelling of the internal vacuoles, a sac-like space containing gas. These observations corroborate those made on the field cultures, where with depth the colonies deteriorated (Appendix B).

The results of this experiment indicate that nitrogen limitation in particular leads to significant increases in the production of carbohydrates in cultures of axenic ( bacteria-free) *Dictyosphaerium*. This information can be used as a guide for understanding and ultimately controlling the production of carbohydrates in the field.

#### *Nutrient Ratios During Growth:*

The monitoring data from the pit indicated that phosphate concentrations remained relatively high throughout the ice-free season when *D. pulchellum* is most abundant. However, during the mid-summer bloom which is followed by intensive mucilage production, the nitrate concentrations decline (Appendix A). This trend continued in 1995 and 1996. For 1995, the nitrate concentrations decreased above the thermocline from 0.33 mg@L<sup>-1</sup> in June to 0.14 mg@L<sup>-1</sup> in August, and in 1996 the reduction in concentrations was 0.66 mg@L<sup>-1</sup> to 0.1 mg@L<sup>-1</sup>



in October. It is not clear at the present time what process could have lead to the increase in nitrate over the ice covered season. At the end of growing season other algal species become more abundant in the pit, namely species with the ability to fix  $N_2$ . If indeed nitrogen fixation by the cyanophytes can bring about such a large change may have to be assessed if it reoccurs in 1997.

As the carbohydrate or mucilage production was affected by the nutrient conditions, and those concentrations will affect particle movement in the pit, it was necessary to determine that these nutrient ratio changes, which could be noted for the pit, were also taking place in the cultures of the Nutrient Stress Experiments.

Nitrate and phosphate concentrations were monitored periodically to confirm that the expected nutrient limitation was indeed occurring and could be related to the growth and carbohydrate production rates. In Figure 26d, the changes in nitrate concentrations in each of the four treatments over the 60-day period are presented. Note that results are reported as  $mg\ N\ L^{-1}$ , and not in  $mg\ NO_3\ L^{-1}$  as they are presented in Appendix A and elsewhere in the report.

The nitrate levels in the N-Limited Condition drop steadily for the first 16 days and then level off at approximately  $0.1\ mg\ N\ L^{-1}$ , or  $0.44\ mg\ N\ L^{-1}$  nitrate as  $NO_3$  corresponding to the period when growth rates slow down (Figure 26a) and carbohydrate production per cell begins to increase (Figure 26c). The Field Simulation showed a similar pattern, although it took approximately 30 days to achieve a plateau at the  $0.1\ mg\ N\ L^{-1}$  level. Nitrate levels remained low for the remainder of the experiment. The Control approached nitrate limitation but the progression into limitation was much more gradual. The nitrate levels remained high in the P-Limited Condition suggesting that the treatment was not nitrate-limited but achieved phosphate limitation as desired. It should be noted that the levels of nitrate in the pit are actually less than in these experiments, including the laboratory N-Limited treatment.

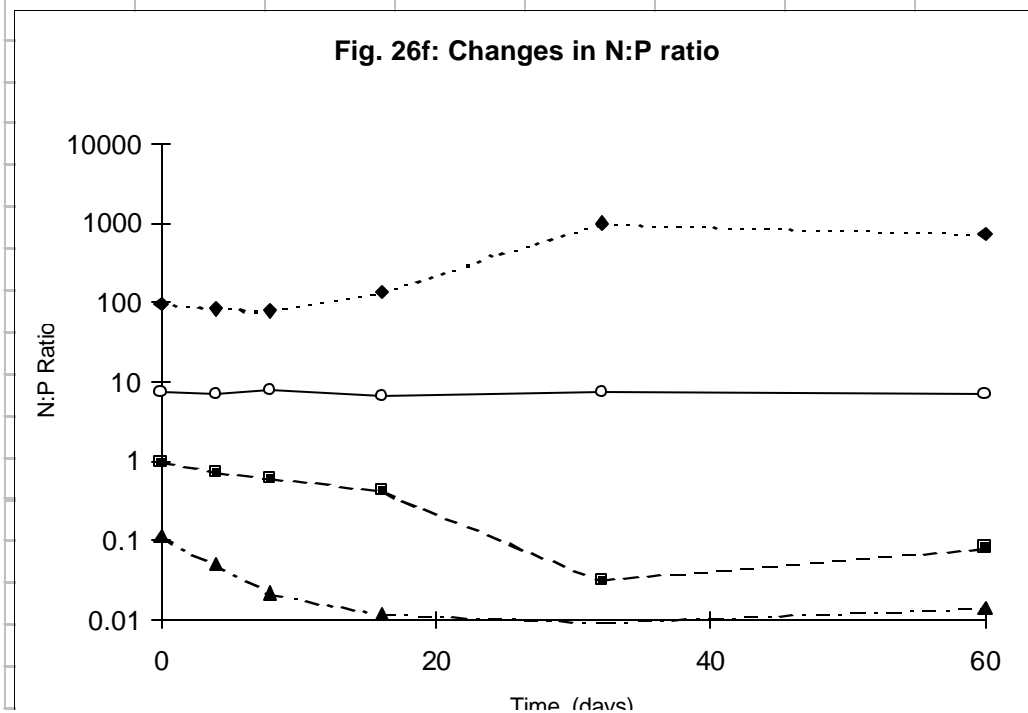
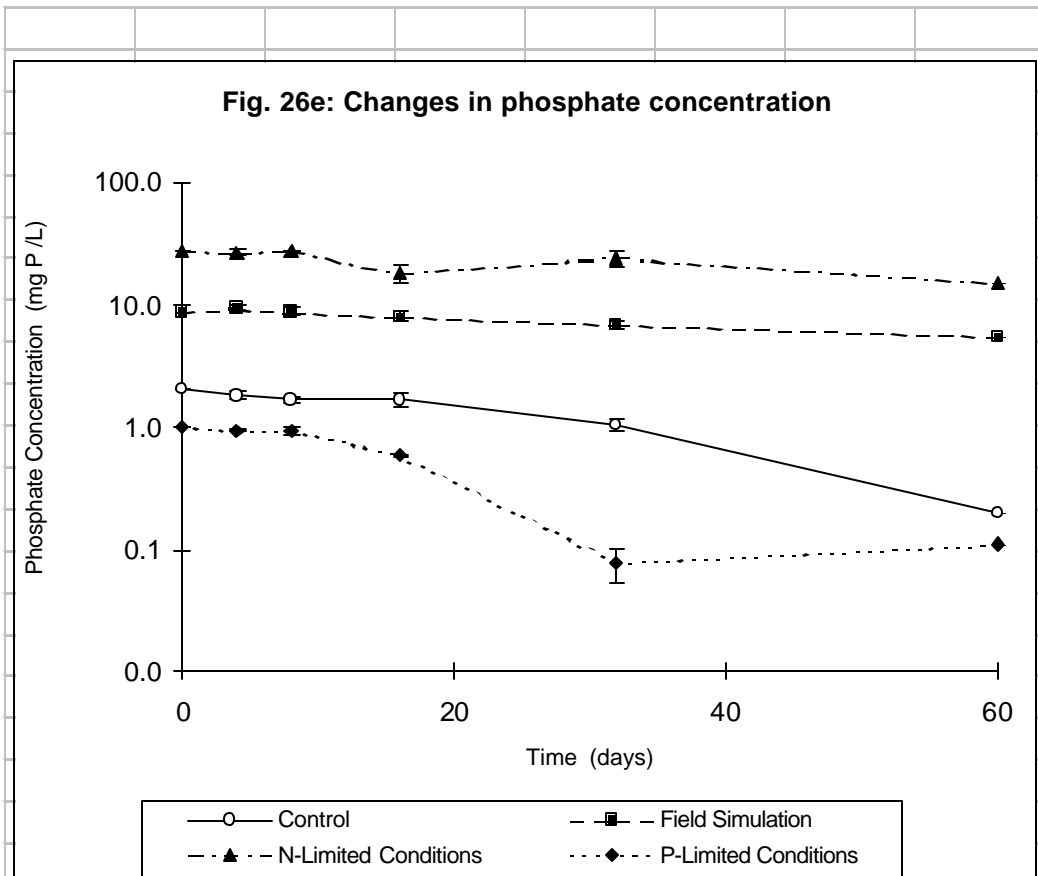
Figure 26e shows the changes in phosphate levels over the course of the experiment. In

the treatments, the P-Limited Condition achieved phosphorus limitation in the medium by day 30. This was much later than the levelling off of nitrate in the N-Limited Condition, and suggests that phosphorus storage within the algae delays the onset of the nutrient stress condition. The concentration levelled out at about  $0.1 \text{ mg P @ L}^{-1}$ ; although this concentration is a low value, it is not as low as phosphorus concentrations typical of natural freshwater, which sometimes is as low as  $1 \text{ : g PO}_4 \text{ @ L}^{-1}$  (Wetzel, 1983). Growth continued in this culture probably at the expense of internal phosphorus storage pools.

Overall, phosphorus depletion was not achieved in the experiment. However, the Control treatment showed some reduction in phosphorus concentrations, and its N:P ratio more closely resembled the "ideal" N:P ratio suggested by Redfield (1958). It appears that the onset of stationary phase, the point at which exponential growth ceases, corresponds to the simultaneous depletion of several other media components. The Field Simulation and N-Limited Condition maintain relatively high phosphorus levels throughout the experiment. Given the high concentrations of phosphorus in the pit ( $0.4 \text{ mg @ L}^{-1} \text{ PO}_4$ ) along with no seasonal changes in its concentrations (Table 1a and Table 1b), the nutrient limitation due to nitrogen is confirmed.

The changes in the N:P ratio during the Nutrient Stress Experiment are shown in Figure 26f. The P-Limited Condition is confirmed by a significant increase in the N:P ratio during the experiment. During the exponential growth period, phosphorus is consumed, driving the N:P ratio upward (to values  $>100$ ). In the Control, the N:P ratio remains relatively constant throughout the 60-day experiment, suggesting that both of these nutrients are being consumed proportionately during growth. In both the Field Simulation and P-Limited Condition, the N:P ratio indicates that nitrate is being utilized faster than the available phosphorus. Again the N-Limited Condition shows the greater nitrate depletion stress.

The changes in nutrient ratios noted in the pit and the nutrient ratio changes which took place during the experiments indicate that the field situation was relatively well simulated by the experiment.



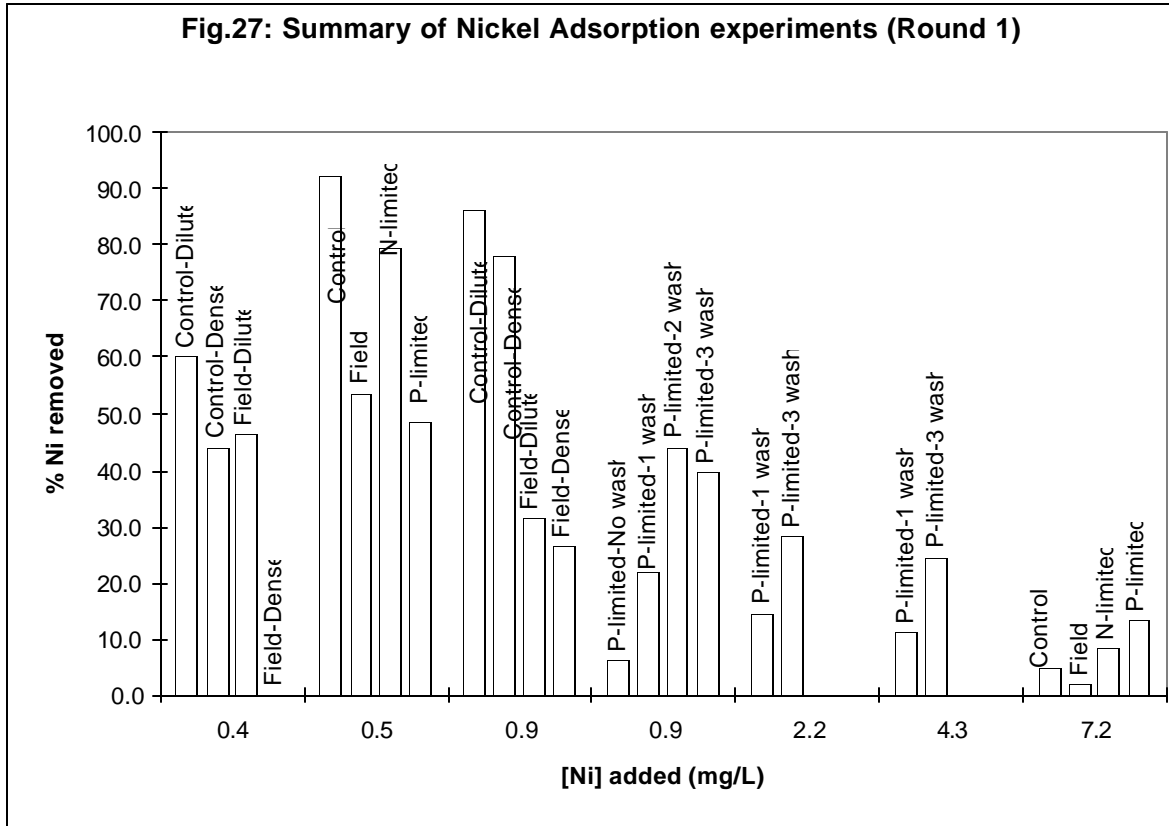
#### 4.1.6 Nickel and Arsenic Adsorption on *Dictyosphaerium pulchellum*

The biology of the dominant algae was studied along with the growth controlling factors, as this unique small algae is dominant in the pit, and contributes about 70% to the primary productivity of the pit. It was initially suggested that the mucilage produced by the algae could assist in contaminant removal, as a jelly-like biomass accumulates in the 2 m sedimentation trap. In order to determine the role of the algae with respect to the annual decrease in surface water contaminant concentration, the first question to be answered is:

Can the algae and the mucilage indeed serve as a sorbant at these low concentrations in the pit for either of the contaminants, nickel likely prevailing in the cationic form and arsenic in the anionic form? Adsorption experiments would assist in improving an understanding the role of algae in the pit, albeit the culture conditions would not necessarily reflect those in the pit.

Two series of experiments were carried out. The first round of experiments used the cultures from the nutrient stress experiments. Appendix C contains the details of the nickel and arsenic adsorption experiment. The data for the first round of experiments are presented as percent nickel removed at the various concentrations of nickel added (Figure 27). From these results, it is clear that the nutrient status of the culture has an effect on the ability of the algal cells to adsorb nickel. The control grown algae, with a relatively low concentration of carbohydrate, clearly showed the greatest ability to removal nickel in the first round of experiments.

The first round of adsorption experiments was limited by the amount of culture material available for the tests, which reduced the range of concentrations which could be tested. The unexpected differences in % Ni removal observed between the nutrient stress cultures and the healthy cultures at the concentration of 0.5 mg/L, prompted a series of follow-up tests using the remaining algal cells. The density of the culture solution was changed in the



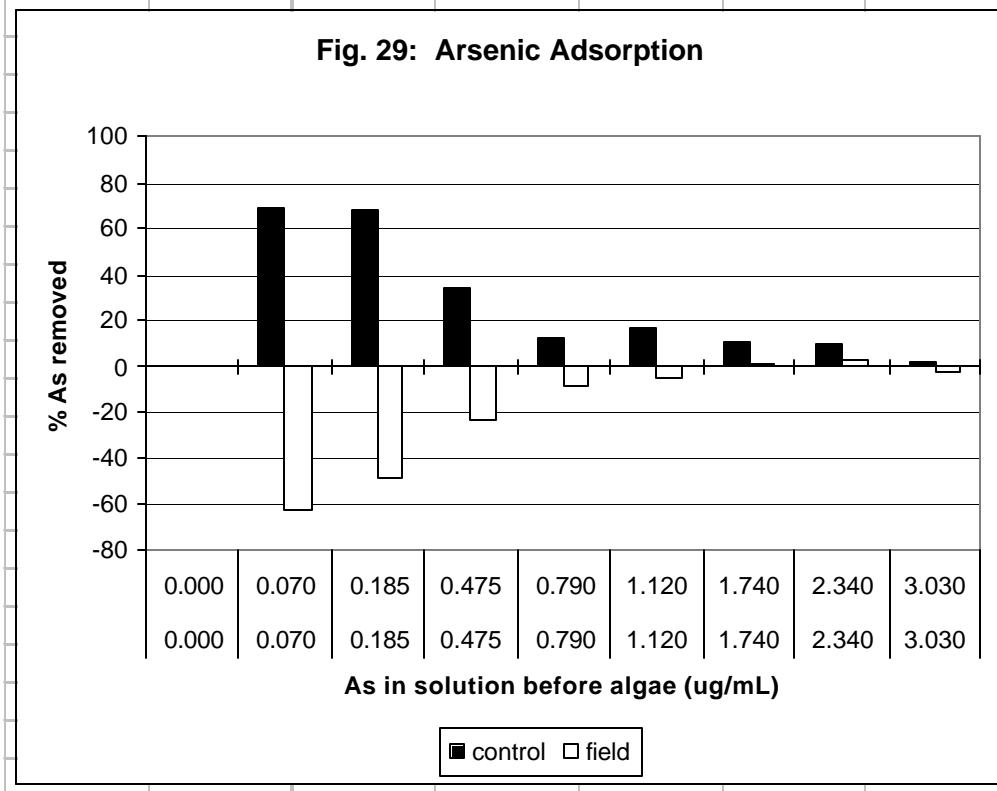
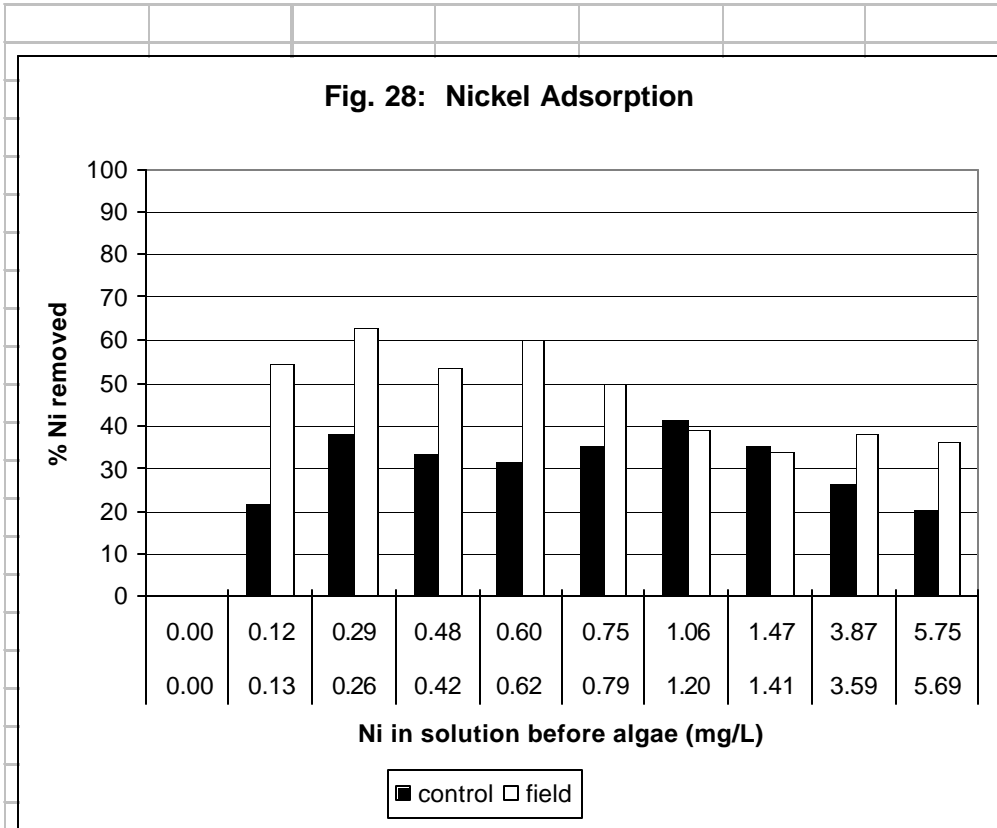
adsorption experiment and the cells were washed with distilled water to remove the carbohydrates (Figure 27). The washing of the cells using distilled water was followed by centrifuging the cells into a pellet which was resuspended before further nickel was added and monitoring of Ni removal commenced.

The amount of nickel removed by the cell/carbohydrate suspension was determined by centrifuging the solution after 2 hours and analysing the supernatant. The effects of washing were demonstrated with cells grown under the P-limited cultures. Washing improved the % Ni removal. These results indicated that carbohydrates influenced the removal process of nickel. The removal of As was also tested, but it could not be quantified due to the inability of the colorimetric analytical method used to differentiate the low concentrations.

Follow-up work was carried out under a joint contract with CANMET and is included as Appendix C in this report. Axenic (bacteria free) cultures were derived using algae from the B-Zone Pit. The previous experiments were carried out with cultures obtained from a culture collection. Details of the experiments are given in Appendix C. The second study provided a clearer understanding of adsorption of As and Ni with the mucilage-producing algae. It was concluded that, essentially, the adsorption of nickel follows Freundlich Isotherm and arsenic adsorption was better described by Langmuir. Freundlich isotherms will only show saturation of surface sites at extremely high concentrations whereas Langmuir shows saturation of surface sites at low concentrations.

Whether these isotherms strictly apply in the conditions of the pit is likely less important than the fact the data for both contaminants could be fitted to a meaningful adsorption isotherm. The role of the algae and the mucilage in relation to As and Ni removal could not have been proposed if this would not have been the case. In fact, the findings from the adsorption experiments did lead to some very important conclusions. In Figure 28 and 29, the results are summarized as % removal for the concentration ranges used for nickel and arsenic, respectively. The data are not adjusted for cell density or for carbohydrate concentration, and are thus comparable only on an absolute level in relation to the concentration added in the experiments.

Nickel removal on an absolute percentage was lower with the healthy cells than with the nutrients stressed cells. Carbohydrate concentrations during adsorption were assisting in the removal. As the concentrations of Ni added increased in the experiment, the similar % removal was maintained. This suggested that the system was not saturated with nickel at the concentrations provided (Figure 28). For As, the % removal is low and the effect of carbohydrate in the stressed cell treatments is clearly inhibiting the already low adsorption. In fact, removal by nutrient stressed cells is negative, reflecting either analytical error or desorption. With increasing concentrations added in the adsorption experiment, % As removal diminishes to nil (Figure 29).



The picture which emerges from these results is relatively clear. For nickel, healthy algal cells and carbohydrates both adsorb nickel. For arsenic, if the cells are nutrient stressed the already low As adsorption capacity of the cells is even further diminished.

The cationic form of nickel used in the experiment gets adsorbed on both cells and carbohydrates. Therefore, it is likely that, in the B-Zone Pit, the large fraction of the nickel can be present either associated with carbohydrates or adsorbed onto algal cells. Downward movement of nickel in the pit in the presence of algae is likely the result of settling of algal cells and larger organic particles carrying bound nickel. The adsorption experiment also suggests that, with higher algal production, more nickel will leave the surface water.

While Ni adsorption onto stressed cells and carbohydrates is evident from the experiment, for As this is not the case, as only healthy cells showed any affinity towards arsenic. In relation to the B-Zone Pit, with a healthy (non-nutrient stressed) algal population, an increase in As removal can be expected from the surface water. Arsenic is only removed by healthy cells and by a very limited of sites on the cell surfaces which are specific enough to adsorb arsenic, facilitating As removal from the solution. The anionic form of As added to the cell/carbohydrate solutions in the experiment is likely being removed only by aggregates of cells and carbohydrates which capture some of the As during the aggregation process. Healthy cells likely aggregate better than nutrient stressed cells. Since only a small amount of aggregates formed in the solution to which As is added, with increasing concentrations of added As, the amount of As removed from the solution diminishes.

With respect to the surface water conditions in the flooded pit, healthy algal cells are preferable over those under nutrient stress. It is well documented that algal cells, especially small species common in phytoplankton communities, excrete low molecular weight organic compounds (e.g. glycolate, citrate, etc.). These substances' diameters are well below the 0.45  $\mu\text{m}$  range and represent particles which have adsorption sites (Schematic 2).



Many of these substances have been shown to have trace metal chelating abilities. Under nutrient stress, when the cells' normal metabolism is disturbed, the excretion of such compounds can increase significantly (Hellebust, 1974). If the interference of DOC (dissolved organic carbon) with adsorption can indeed be confirmed for the conditions in the pit, it would suggest that nutrient stress (and the associated mucilage production which results in soluble organic compounds) are detrimental to all types of treatments (chemical and biotechnologically-enhanced treatments). These substances interfere with the settling of adsorbent materials as well as eliminate adsorption sites on hydroxides used in arsenic removal. That this interference exists was evident from the results obtained with nickel adsorption in the treatments with washed cells in the first round of experiments (Figure 27). In other words, the originally anticipated positive impact of mucilage production (higher surface areas, more and possibly better adsorption sites) is offset by the negative impacts of the mucilage (hindering of settling and obstruction of adsorption sites).

For an in-situ treatment As and Ni in the pit, the overriding conclusion is that it is highly likely that geochemically predicted forms of As and Ni which are associated with adsorption isotherms do not prevail in the pit. Contaminant removal has to be considered for the pit in the context of the aggregation of particles, or flocculation of the organically-bound or complexed forms of As and Ni and shifting in the bottom of the pit to adsorption processes dominated more by the behaviour with iron oxides. Although these studies have provided a good background on the expected transport mechanisms the work was complemented with some experiments of a pragmatic nature, namely additions of iron salts and bentonite to pit water, with or without algae. These will be presented in the next section.

#### 4.1.7 B-Zone Flooded Pit Limnology: Summary of 1995 Productivity Conditions

From the productivity estimates which have been discussed in detail, both based on the pit chemistry and algal growth, the dynamics in which biological processes change the pit limnology has become evident. If the biological processes are to be utilized to remove As and

Ni, the sequence of events, which take place in the pit, from dormant or low growth (in the ice covered part of the season) to a rapid growth period, changes in the euphotic zone as the season progresses, through to continuing decomposition, a month-by-month event sequence will clearly identify the optimal time to use these processes. Such a sequence is presented below using the 1995 data.

In 1995 the Secchi depth is approximately 1 m. The depth of euphotic zone (depth below which there is net loss of cell carbon because respiration exceeds photosynthesis) is therefore only 2 m, based on general limnological principles. Although measurements of the degree of mixing of the epilimnion of the pit are not available, it can be assumed that if more than approximately 10 m deep mixing takes place, there is a net loss of phytoplankton carbon in the water column. Also, if the mixing is more than 4-5 m deep, the overall rate of productivity will be very low (Raymont, JEG, 1963). Using these well defined limnological principles, the conditions for primary productivity in the Pit April - October, 1995 are summarized for each month.

**April:** Heavy ice cover; 0.5 °C at surface, rest of water column at approximately 3.5 °C. Combination of low levels and low temperature means negligible productivity rates.

**May:** (Assumed conditions from May 9, 1996 data). Ice cover about 2 ft thick; 0.8 °C at surface, rest of water column at approximately 3.5 °C. Very low productivity rates possible in May, except for near end of month when ice presumably disappears. However, at that point water mass is essentially at same temperature (3.5 °C) throughout water column, and is therefore easily mixed from top to bottom by any wind action.

**June:** No ice. The thermocline was at about 2 - 5 m with temperature in a very stable 2 m to 3 m thick epilimnion of about 16 °C with lots of light and high concentrations of major nutrients (8 : M $\mu$ L<sup>-1</sup> N (nitrate + ammonium) and 5 : M $\mu$ L<sup>-1</sup> of phosphate). High rates of primary productivity expected in epilimnion, and reasonable rates in the thermocline (2 m to 5 m; 16 -

8 °C) and in the upper layers of the hypolimnion. This is reflected in already high cell densities of the dominant phytoplankton species *Dictyosphaerium pulchellum* with  $5.5 \times 10^8$  cells  $\text{L}^{-1}$  in the upper 2 m, and about  $2 \times 10^8$  cells  $\text{L}^{-1}$  at 12 m depth.

**July:** No data are available, but by interpolation of data for June and August, one can assume that the thermocline has moved down to 6 - 8 m with the epilimnion being a very stable 6 m layer with a temperature of about 11 °C. Productivity is expected to be low below the thermocline, at about 10 m because of severe light limitation.

**August:** Main thermocline is at 7 - 12 m, with a very shallow (unstable) thermocline at about 2 m. The temperature of the top transient 2 m layer was about 14 °C, and the temperature of the main epilimnion down to 7 m was 12 °C. High rates of productivity can be expected in the epilimnion about 7 m with little or no productivity below about 10 m. Nutrient concentration in the epilimnion are still high (about  $4.4 \text{ M} \text{L}^{-1}$  of combined nitrate and ammonium; nitrate concentrations have decreased considerably from June). The concentrations of phytoplankton cells (mainly *D. Pulchellum*) is very high in the upper 10 m; about  $10 \times 10^8$  cells  $\text{L}^{-1}$ . At 12 m depth the cell concentration was about  $6 \times 10^8$  cells  $\text{L}^{-1}$ , and at 22 and 32 m,  $0.9$  and  $0.5 \times 10^8$  cells  $\text{L}^{-1}$ , respectively. It represents actively growing cells, as this is at the base of the thermocline and light level is too low for net productivity (well below the euphotic zone). The distribution of cells at this, and lower levels, is strong evidence for sinking of cells out of the euphotic zone during times of high productivity in the epilimnion.

**September:** By interpolation of August and October limnological date, one can assume that the thermocline has moved down to 14 - 18 m, with an average epilimnion temperature of about 10 °C. The mixing of the epilimnion is now quite deep (down to about 14 m), so that the overall primary productivity can be expected to be low due to light limitation. The *D. pulchellum* cell concentration in the epilimnion is now only about 2 to  $3 \times 10^8$  cells  $\text{L}^{-1}$ , and there obviously has been a net loss of cells due to sinking, grazing and/or decomposition.

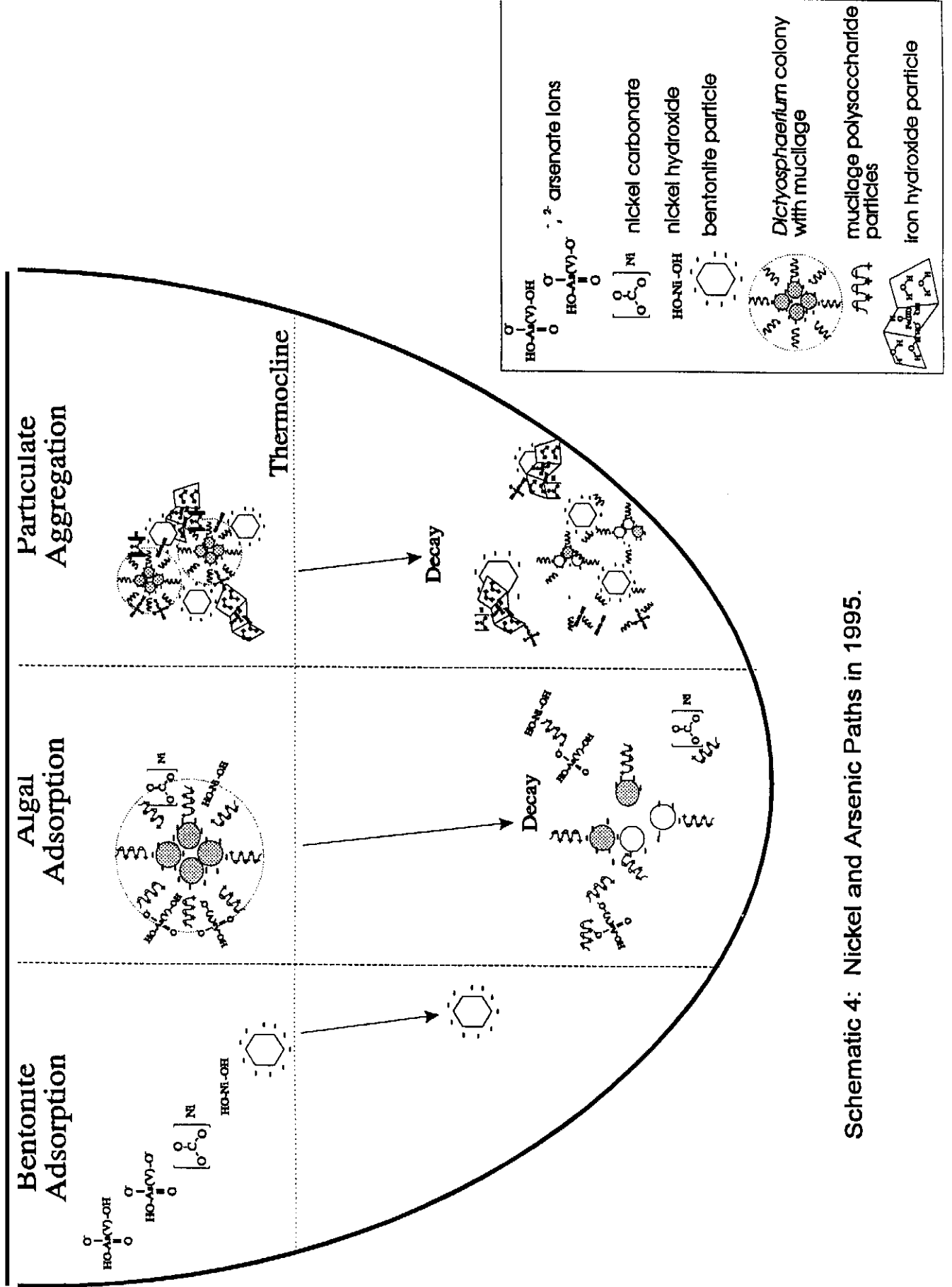
**October:** The thermocline has moved down to 18 - 24 m, with a temperature of 7 °C in the epilimnion and 4-4.5 °C in the hypolimnion. The mixing of the epilimnion is now obviously too deep for net primary productivity to take place. The nitrate concentration is very low in the epilimnion (approximately 2 :  $\text{M}\mu\text{L}^{-1}$ ; down from 8.7 :  $\text{M}\mu\text{L}^{-1}$  in April) and the phosphate concentration about 3.8 :  $\text{M}\mu\text{L}^{-1}$  (down from about 4.3 :  $\text{M}\mu\text{L}^{-1}$  in April), providing evidence for nutrient depletion due to algal productivity over the summer months. Ammonium levels, however, are quite high in the epilimnion in October (approximately 3 :  $\text{M}\mu\text{L}^{-1}$ ). This probably is due to decomposition/grazing of algal cells with release of ammonium, coupled with slow rates of denitrification.

From these considerations of the pit growth dynamics, the timing of fertilizer additions, which may be considered to produce more algal growth, and the reductions in productivity noted in 1996, is critical and likely best, just after ice breakup.

#### 4.1.8. Nickel and Arsenic Pathways in the Flooded Pit

Based on the interpretation of both field data (and the chemical analysis) and laboratory results derived from the growth experiments, with comparison to the pit conditions a dynamic model, describing the overall processes believed to be taking place in the pit, can be derived. A description of the model is presented in point form and should be read together with Schematic 4, which gives a pictorial representation of the ongoing sorption processes.

C The algal growth produces two types of organic material which is affecting surface charges. One type of organic material is the healthy cells or cell aggregations, with cell walls which are negatively charged due to their association with carboxyl groups. The second type of organic material is the polysaccharides which produce, depending on the stage of the decay, positively or negatively charged organic molecules and through their aggregation, could end up as a neutral organic particle. The surface charge depends on the number of hydroxides or their stage of hydration.



Schematic 4: Nickel and Arsenic Paths in 1995.

The mucilage production of the algae therefore produces a variety of small organic compounds (see Schematic 2 for size range), but they will alter the nature of the clearly negatively charged healthy cells and the negatively charged arsenate, prevailing in the oxygenated water. They will stick to the surfaces and change thereby the adsorption characteristics.

These organic materials, healthy cells predominantly, in the beginning of the growing season move the Ni which is either present as a  $\text{Ni}^{2+}$  ion or as a hydroxide or carbonate, which adsorb to the negatively charged cell walls into the deeper portions of the pit. It was noted that arsenic, which is likely prevailing in different fractions as either  $\text{H}_2\text{AsO}_4^-$  or  $\text{HAsO}_4^{2-}$  depending on the pH (see Appendix A-4) is moved from the surface waters later than Ni in the growing season. As both these arsenic forms are negatively charged, the attachment of the organics from the decay of mucilage will probably alter the surface charge and facilitate better particle aggregation during later parts of the growing season. Thus the two types of organics play very different but important roles in the alterations of surface charges and subsequent particle aggregation. In Schematic 4, the function of organic molecules is outlined for three conditions, the interactions with clay or bentonite particles, that with the algae and finally the role in particle aggregation.

C Lab results on the adsorption of arsenic by the algae *Dictyosphaerium pulchellum* indicated, that some adsorption of As is possible just by mucilage alone, and healthy cells appeared to showing the best removal. These findings are used to support the role of the organics in As and Ni transport from the surface water.

The organics circulate in the epilimnion (that layer of water above the thermocline) during the growing season, and find it difficult to settle past the thermocline by themselves, using the settling rates calculated from sedimentation trap results. The extracellular polysaccharides excreted by the algae hinder settling (see Plates 1 and 2) and from the settling rates of algal material alone. This does suggest, that not only does the thermocline control the physical movement of particles, but very little movement of particles will take place as long as the

thermocline exists. Only at the end of the summer season, when the thermocline breaks down and turnover occurs, can those particles, which have made it to the bottom of the pit, settle out to the sediment. Thus any particle, which has not made it to the bottom of the pit, i.e. was not able to be aggregated into particles large enough to overcome the hydrodynamic forces in the pit and settle, will be resuspended with turnover.

These conclusions are derived from the fact, that only a small portion of the As and Ni is actually removed to the bottom, where increases in As and Ni concentrations are only noted after thermocline establishment, i.e. later in the growing season. Also, physical water movement below the thermocline is likely less and it is certainly lower when the pit is ice covered. Unfortunately, the monitoring data collection is such, that some of the proposed physical changes can only be expected, but not documented, as only one measurement is available for the conditions underneath the ice.

C Ammonia concentration increases below the thermocline in June as well as in August, indicating that organic decay is occurring there. The decay results in either some release of the adsorbed nickel and arsenic or the separation of particulates. This is evident from the increases in nickel and arsenic concentration below the thermocline during the growing season, being greatest at the bottom of the flooded pit. The respiration of bacterial growth, particularly heterotrophs, allows for the decomposition of some of the organic molecules to smaller and smaller organic molecules, ultimately resulting in inorganic carbon. This again, will alter the surface charges of material carrying As and Ni.

C Inorganic particulates/clays or oxides in the upper part of the water column being associated with organics, loose their organic association as they reach the lower portions of the pit. SIMS (Secondary Ion Mass Spectroscopy) analysis of the sedimented particulates at depths of 2 m and 32 m showed that the thickness of the layer on the particle, where arsenic and nickel were located, was thinner at the bottom,

and at the bottom, both contaminants were associated with Fe-Si-O particles.

The sequential extractions done on sediments at 22 and 32 m depths indicate that the arsenic is associated entirely (100%) with the oxide fraction. At 22 m depth, sequential extraction of the nickel indicate the 31% is soluble, 27% is organic and 42% is associated with the oxide fraction. At 32 m depth, 100% of the nickel is associated with the oxide fraction. Thus the role of organic material in the transport mechanism is decreasing with depth and sorption processes dominated by oxides take over the transport. The large decrease in arsenic concentration noted in October, 1995 to depths below the thermocline, coincided with a two-fold increase in TSS. It was postulated that an intense storm late in the summer lead to the large increase in TSS, from run-off.

Sedimentation trap data also show a moderate increase in the sedimentation rate (September, 1995) relative to the rate determined earlier in the year. A second set of data, which support the dominant oxide sorption mechanism at the bottom, is the fact that with time, i.e. aging of the oxides in the bottom of the pit, the arsenic concentrations in the bottom sedimentation material has been increasing. This could be interpreted two fold. The longer the oxides are exposed to decomposition of the organics, the more and more sites become available which are specific to arsenic. On the other hand, the surface characteristics of the oxides are changing with time collecting more arsenic, or the arsenic form is changing in the bottom of the pit, altering its sorption characteristics. All these processes can be taking place at the same time and to varying degrees.

From the literature on co-flocculation, the surface charges of both clay and algae are negative. The only potentially positive metal ion is nickel, and thus it will be attracted to both surfaces, if it is indeed present as a free  $Ni^{2+}$  ion. The surface charge of the clay particles can be confirmed relatively easily with sufficient quantity of material slurried and the slurry being exposed to leads from a battery. This however was only done for the bentonite experiment



(discussed later) and not for other particles in the pit. This may represent a possibility to confirm the surface charges of the particles found at various depth in the pit as depicted in Schematic 4.

With the understanding of the transport mechanism in the pit, of both As and Ni, at hand, it was considered useful to carry out some experiments which would further substantiate the surface charges associated with the contaminants and the role of the organics (cells and mucilage) in the pit. The hydrodynamic changes, which will facilitate settling of particles or true relegation of material to the bottom of the pit, are difficult to simulate with experimentation. However, two sets of experiments were possible.

The bentonite experiment, simulating negatively charged clay particles, was used with water from different depths of the pit and supplemented with algae, grown directly in pit water with supplements of nutrients. This experiment would indicate, if either Ni or As is present in the pit as a positively charged particle or iron, the bentonite should remove the contaminants.

The second experiment was treating the water with iron salts, which should remove at least As based on conventional treatment technology. At the same time, the settleability of the produced hydroxides will be assessed and the chemical changes which would be expected due to iron additions are determined. These experiments are presented in the following section.

## **4.2 Physically mediated contaminant removal**

From the understanding of the pit contaminant profiles, accumulation in the bottom of the pit of As and Ni laden particles were to be dominated by the presence of oxides. Depending on the type of oxide, the surface charges could be positive or negative. The contaminants, depending on what form they are present, would respond to a clearly negative or positive surface. It translated into the following potential scenario for treatment. If particles, such as bentonite, could

be added to the bottom of the pit, removal could be expedited (if the surface charge was known of the material at depth).

Furthermore a brief literature review revealed that a considerable amount of information is available on co-flocculation of algae and clay, a process clearly of interest for the pit. There was the possibility that algae, enriched in contaminant (nickel or arsenic), would co-flocculate with the clay particles and settle to the bottom as sediment. During the subsequent decay process, contaminant would be released from the algae. However, because of the intimate contact between the clay and algal particles, the released contaminant would be immediately transferred to the clay surfaces in a form which was stable. Thus, co-flocculation was seen as a process which could possibly assist in relegating more contaminants to the bottom of the pit.

The literature suggests that the aggregation is attributed to the presence of extracellular polymers, especially polysaccharides. Both microbial-clay flocculation and microbial-microbial flocculation are affected by the presence of electrolytes. Some investigators have suggested that polyvalent cations are essential if flocculation is to occur, assuming that these ions form complex bridges between two negatively charged particles. Algae also secrete large amounts of polysaccharides and other polymers. Thus, an effective aggregation of algae and clay particles could be expected.

The development of the idea of using algae or algal byproduct to flocculate clay-based reservoir turbidity was first critically tested in 1982 by Avnimelech. Algae-clay aggregates were formed when algal and clay suspensions were mixed in the presence of an electrolyte. The maximum ratio of clay to algae in the aggregates depended upon the organism, ranging from 1.7 milligram clay per milligram algae (wet weight) for *Anabaena*, to 0.03 mg clay per mg algae for *Chlorella sp.* This suggested that adsorption behaviour changes, similar to those observed in our experiments, or the type of algae are not a new phenomenon being confirmed with the relatively large ranges of algae/clay ratios reported. However, the authors did not indicate, if all algal types used in the experiments were at the same stage of growth.

Avnimelech et al. (1982) further suggest that the aggregates formed at divalent  $\text{Ca}^{2+}$  concentrations higher than  $5 \times 10^{-4}$  M. In the case of the monovalent  $\text{Na}^+$  ion, the concentration threshold was 40 times greater, at  $2 \times 10^{-2}$  M. Although for the pit, the interactions of these ions have not been taken into account, since their concentrations do not change throughout the pit profile. This interpretation on the algal clay co-flocculation indirectly supports the view that the same mechanisms are involved in algal-clay co-flocculation as in microbial-clay aggregation. That is, the two negatively charged surfaces, that of the clay and that of the algae, co-flocculate bound by the cations, forming complex bridges between them. In the case of the pit, this function is attributed to the small mucilage polysaccharide particles (Schematic 4).

It was suggested that the variable flocculating potential of different algae depends on the composition and properties of the cell wall, as well as the extent and type of secretions, among other factors. This is supported by observations using an electron microscope which suggests in several publications a high affinity between clay and *Anabaena*, often referred to as extracellular flocculating agents. Based on the electron microscopy there are essentially three types of clay-algal co-flocculation identified: (a) **clay-algal co-flocculation** between *Anabaena* and clay (Avnimelech et al. 1982.) ; (b) **small clay particles coating algae**, based on extensive clay deposits cumulating around the periphyton (Burkholder and Cuker, 1991) and (c) **mineral particles aggregating** on algal cell walls (Søballe and Threlkeld, 1988). Here numerous individual mineral particles or aggregations of mineral particles attached to each algal cell or colony, even at very low mineral concentrations, are reported. In the electron microscopic work of Lawson (1997) the B-zone pit particles had strikingly similar characteristics to those described with process (c).

Avnimelech (1984) followed up his laboratory study with a field study on two pairs of turbid ponds in Oklahoma. One pond of each pair was given fertilizer treatments at various intervals throughout the growing season. The other pond of each pair was acting as a control. Turbidity levels in one of the treated ponds dropped from 180 to 7 NTU over a period from April to July. Turbidity levels in the other treated pond dropped from 92 to 20 NTU over a period from February to July. These results show that most of the suspension was removed and deposited as sediment. The fertilizer treatments acted to increase the algal populations which, in turn, co-flocculated with the fine clay particles. The key work by Avnimelech et al. (1982 and 1984) was followed by a series of further work which confirmed the general trends as follows.

The addition of nutrients (fertilizer) will decrease clay-based turbidity, increase the number of types of organisms, and increase the biomass of algae (both phytoplankton and periphyton). However, clay additions have the opposite effect of fertilizer additions, i.e., they increase turbidity, decrease the number of type of organisms and their populations.

It is therefore suggested, that the effect of additions of fertilizer and clay would be intermediate to that of fertilizer only or clay only additions. One exception was reported by Burkholder (1991), where fertilizer plus clay additions resulted in greater benthic algal growth than the fertilizer only addition. These results suggest, that the timing of the additions of either fertilizer and/or clay is important, and possibly also the sequence in which they are added. Furthermore, there appears to be an optimal ratio of fertilizer/clay which results in an optimal charge balance for co-flocculation.

To summarize briefly, the literature supports the postulated mechanisms which take place in the pit. The surface of the algal cells is negatively-charged as is the surface of the extracellular polysaccharides, while in the form of an intact mucilaginous sheath. When the clay surface is negatively charged, the addition of divalent cations (or higher concentrations of monovalent cations) will act as a bridge to bind the clay and either the algal cell or the excreted

polysaccharide surfaces, creating flocculants. The characteristics of the bridging agent is given by the surface charge of the clay type and the algal growth state, or the cell wall characteristics of the species.

#### 4.2.1 Bentonite and Algal Biomass Additions to pit water

In Figures 30a-30d, the results of the bentonite addition treatments are presented for arsenic. Some arsenic removal was observed when a very high concentration of bentonite ( $1 \text{ g}\cdot\text{L}^{-1}$ ) was added. It is interesting that when algal bloom biomass was added, similar As removal was observed with an addition of a lower concentration of bentonite (0.1 g/L).

The pattern of nickel removal with bentonite addition, and bentonite plus algal bloom biomass addition (Figures 31a - 31d) was similar to arsenic. Nickel removal took place only in treatments where the largest additions of bentonite were made, but in the presence of added algal biomass, less bentonite was required. These observations support the mechanism of As removal suggested earlier; arsenic is captured between organic and inorganic particles during aggregation. As the bentonite used was clearly negatively charged, tested with a battery suspended in a bentonite and pit water slurry, the failure to aggregate particles and/or enhanced contaminant removal does suggest that the metals are associated with organics and are not present in ionic form. The results of the bentonite experiment therefore further substantiate the proposed removal or transport mechanism of As and Ni in the pit.

#### 4.2.2 Iron Salts Additions to pit water

At the outset, geochemical simulation using the PHREEQE program was carried out to determine the effect of specific iron salt treatments on the pH, Eh and potential for precipitate formation of various minerals. It was not surprising that the pH depressions were severe and based on the assumption that Ni and As were present in ionic form, the

**Fig. 30b: Arsenic experiment  
40 m water + Bentonite**

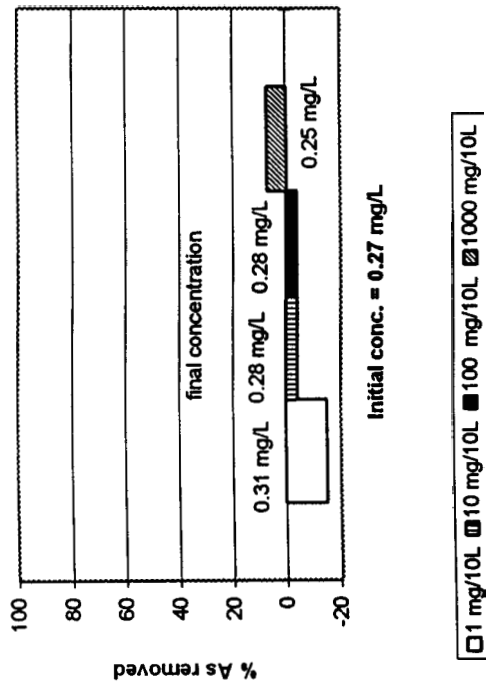


**Fig. 30d: Arsenic experiment  
2 m water + Bentonite**

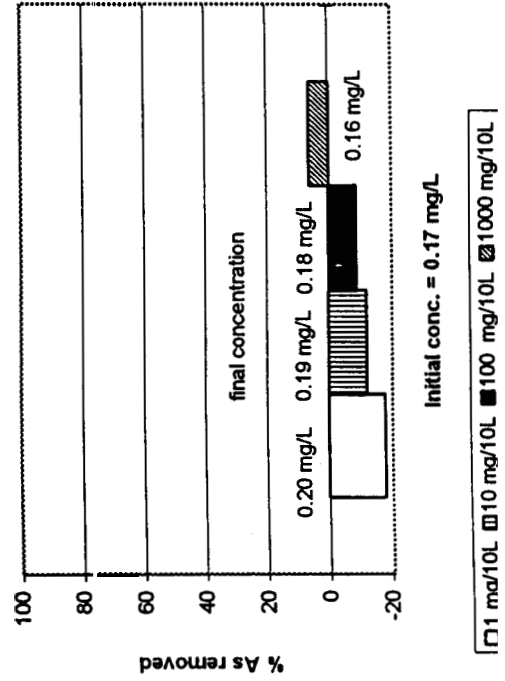


**Fig. 30a: Arsenic experiment  
40 m water + algal biomass + Bentonite**

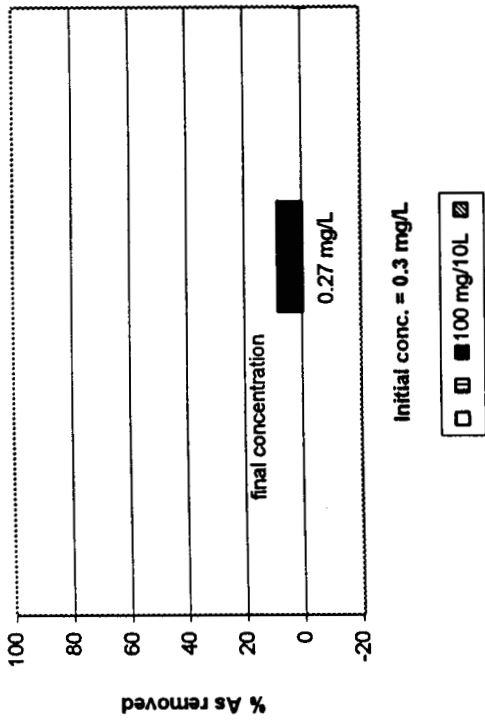


**Fig. 30c: Arsenic experiment  
15 m water + Bentonite**

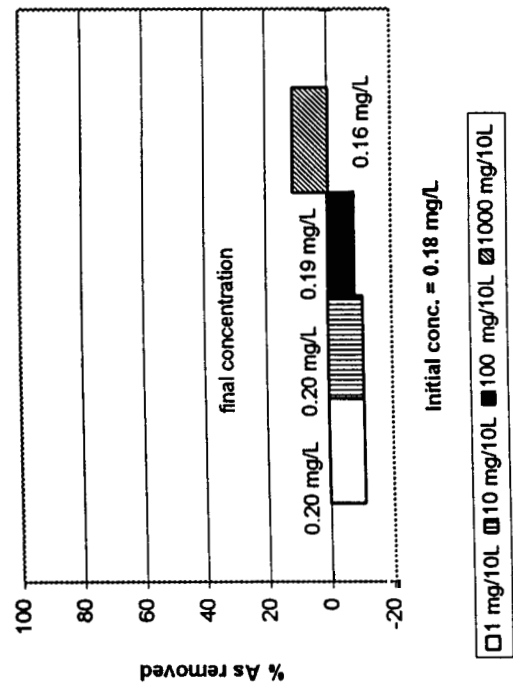
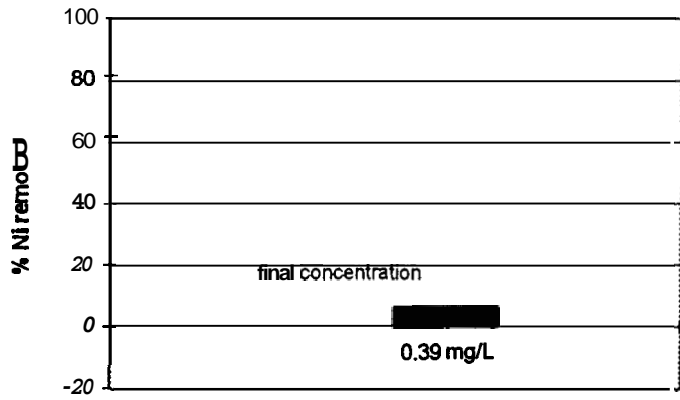
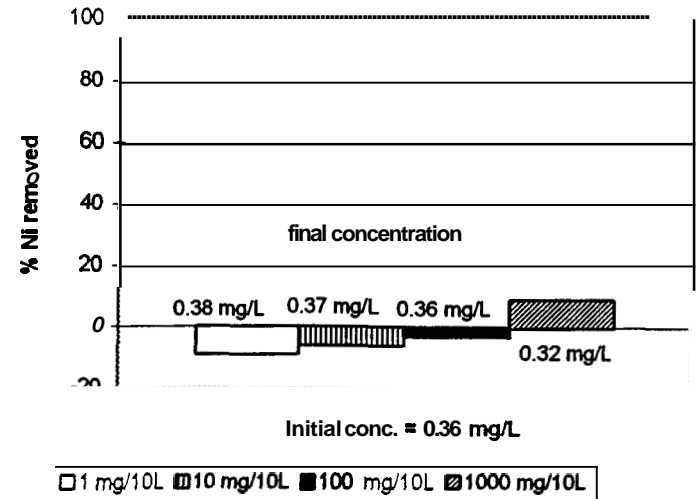


**Fig. 31a: Nickel experiment  
 40 m water + algal biomass + Bentonite**



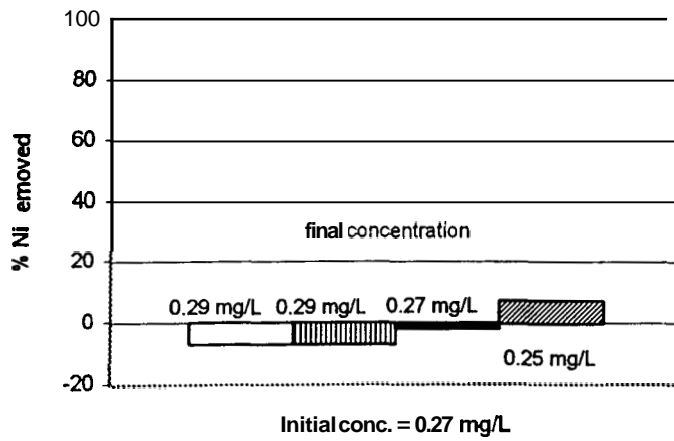
|   |    |     |      |
|---|----|-----|------|
| 0 | 10 | 100 | 1000 |
|---|----|-----|------|

**Fig. 31b: Nickel experiment  
 40 m water + Bentonite**



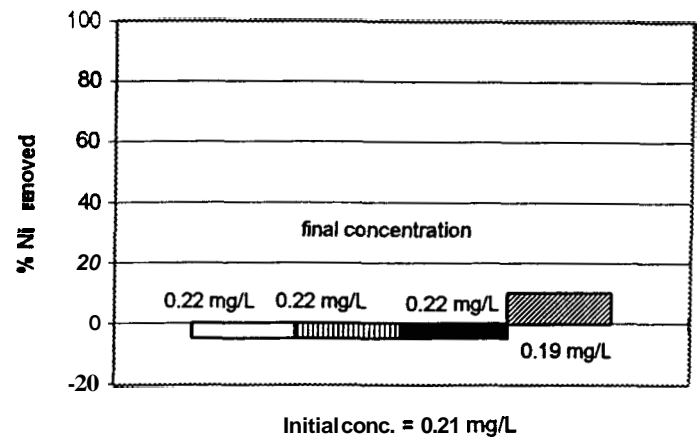
|   |    |     |      |
|---|----|-----|------|
| 0 | 10 | 100 | 1000 |
|---|----|-----|------|

**Fig. 31c: Nickel experiment  
 15 m water + Bentonite**



|   |    |     |      |
|---|----|-----|------|
| 0 | 10 | 100 | 1000 |
|---|----|-----|------|

**Fig. 31d: Nickel experiment  
 2 m water + Bentonite**



|   |    |     |      |
|---|----|-----|------|
| 0 | 10 | 100 | 1000 |
|---|----|-----|------|

concentration ranges required to form precipitates appeared very high. Since it was likely that iron salts will act as flocculating agents, an empirical approach was taken and low additions of these salts were added. Details of the methodology are given in Appendix A, along with a detailed commentary on each salt addition.

The experiments were carried out with samples of B-Zone Pit water collected from a depth of 20 m at Stn 6.72 on September 16, 1995. Water was sampled from below the thermocline, since arsenic and nickel concentrations are typically higher, and temperatures lower, than in the epilimnion. The experiment was conducted in late fall outdoors when ambient temperatures ranged from 0 to 4 °C.

Using a submersible pump attached to a plastic hose, 250 L of water from a depth of 20 m was collected. Twenty-five (25) plastic buckets were lined with clear plastic bags and 10 L of pit water was dispensed into each bucket. Six salt additions were tested, including ferric sulphate, ferrous sulphate, ammonium sulphate, ammonium phosphate, ferrous ammonium sulphate and ferric chloride, each at four concentrations (0.01, 0.1, 1 and 10 mM $\text{L}^{-1}$ ). The following discussion examines the results of ferric chloride and ferrous ammonium sulphate additions, while further details of the experiment are given in Appendix A.

The results of arsenic and nickel removal upon addition of ferric chloride (0.1 and 1 mM $\text{L}^{-1}$ ) and ferrous ammonium sulphate (1 and 10 mM $\text{L}^{-1}$ ) are summarized in Figures 32a, 32b and Figures 33a and 33b. Upon addition of flocculating/coagulating compounds such as iron salts, two general processes can be anticipated. First, sufficiently large particles of iron compounds may form flocculants which adsorb As and Ni onto their surfaces. If this occurs, lower 'dissolved' As and Ni concentrations can be anticipated in treated solutions following filtration through 0.45  $\mu\text{m}$  membranes. Second, the As and Ni-bearing flocculants may coagulate into larger particles which readily settle in the treatments during the course of the experiment. If this occurs, As and Ni concentrations in whole (unfiltered) samples should diminish.



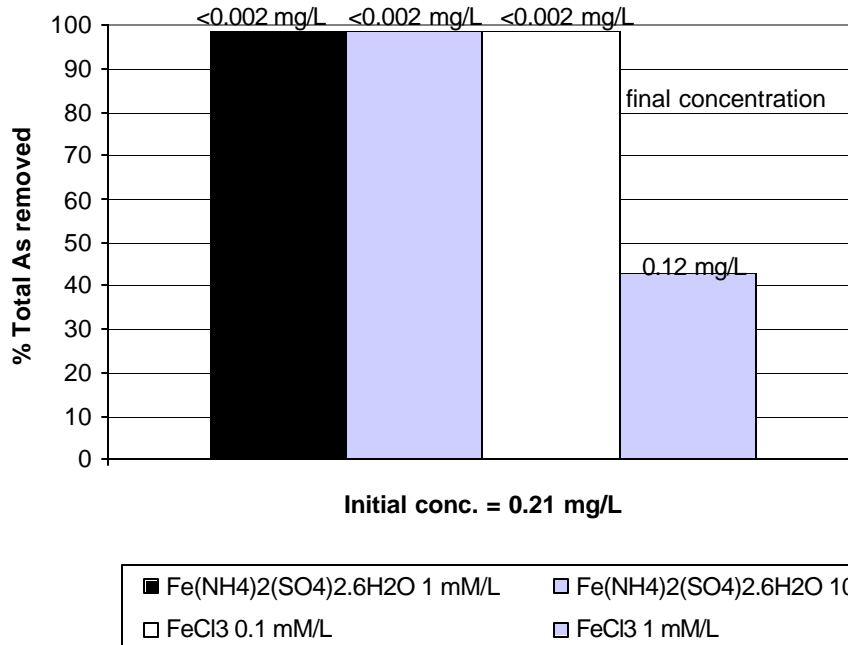
The additions of salts which did not produce any flocculant and hence no removal of As and Ni as could be expected, were not analyzed further (Ammonium Sulphate and Ammonium Phosphate). The addition of iron salts results in changes in the pH of the solutions. With addition of ferric sulphate the pit water was down to a pH of 2.8 at concentrations of 0.1 mM and lower concentrations produced less flocculant which took a long time to settle. A pH depression is also evident with ferric chloride, at concentrations of 0.5 mM the pH dropped to 3.0 after 266 hours. Details of the flocculant formation and changes in chemistry of the water are given in Appendix A-1.

Although the iron salt additions will result in removal of As in the dilute pit waters, the process of settling of the flocculants or precipitates is complex to predict, as can be seen from the preliminary run of salt addition. The salt additions shift the dissolved arsenic to a suspended arsenic, but then only a fraction reports as a settled solid.

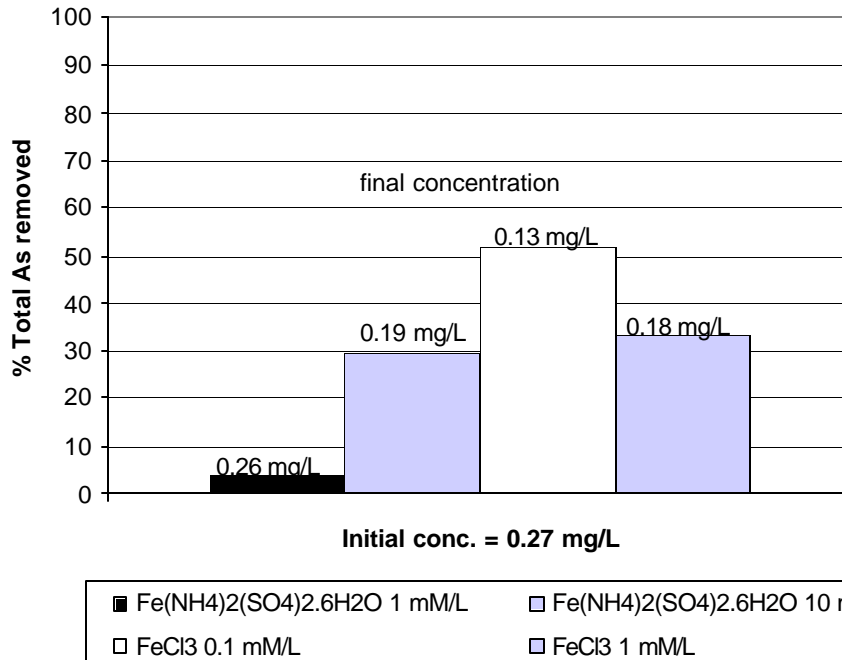
In Figure 32a, the percentages of dissolved As removed following treatment with the iron salts are presented. Both concentrations, of ferrous ammonium sulphate and the lower concentration of ferric chloride, resulted in almost complete removal of dissolved As in the treatments. The higher concentration of ferric chloride ( $1 \text{ mM@L}^{-1}$ ) was less effective in removing dissolved As (42 %). The high ferric chloride concentration reduced the pH such that ferric iron remained dissolved in solution and less particles were formed. Overall, transfer of As from solution to filterable particles was complete in three of the four treatments.

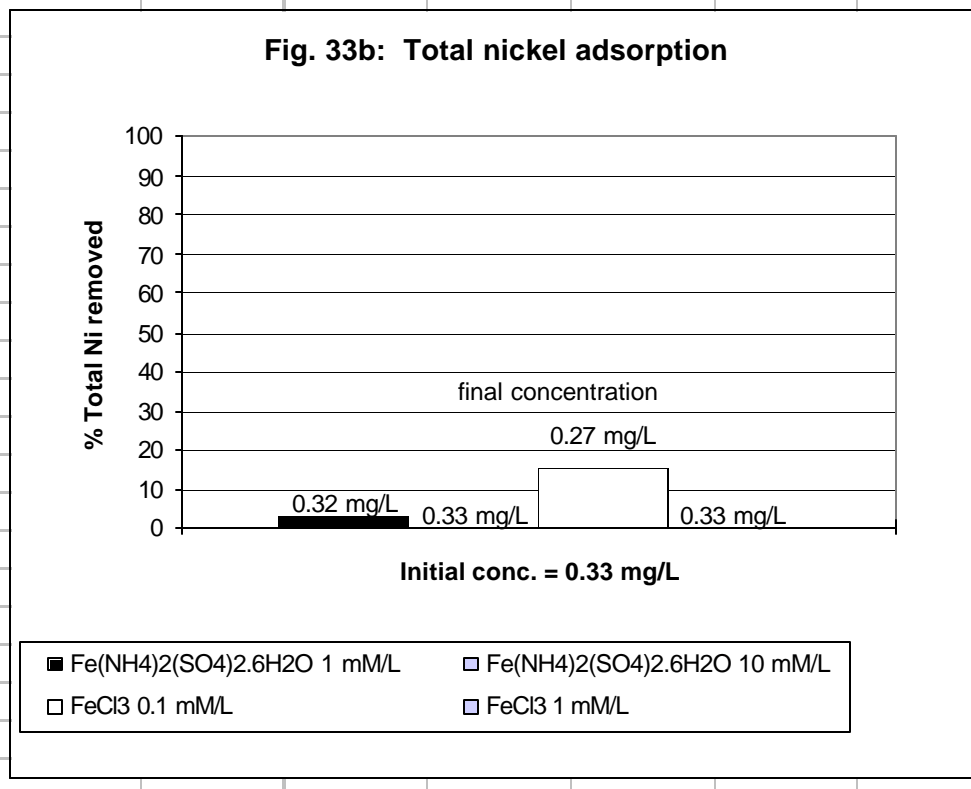
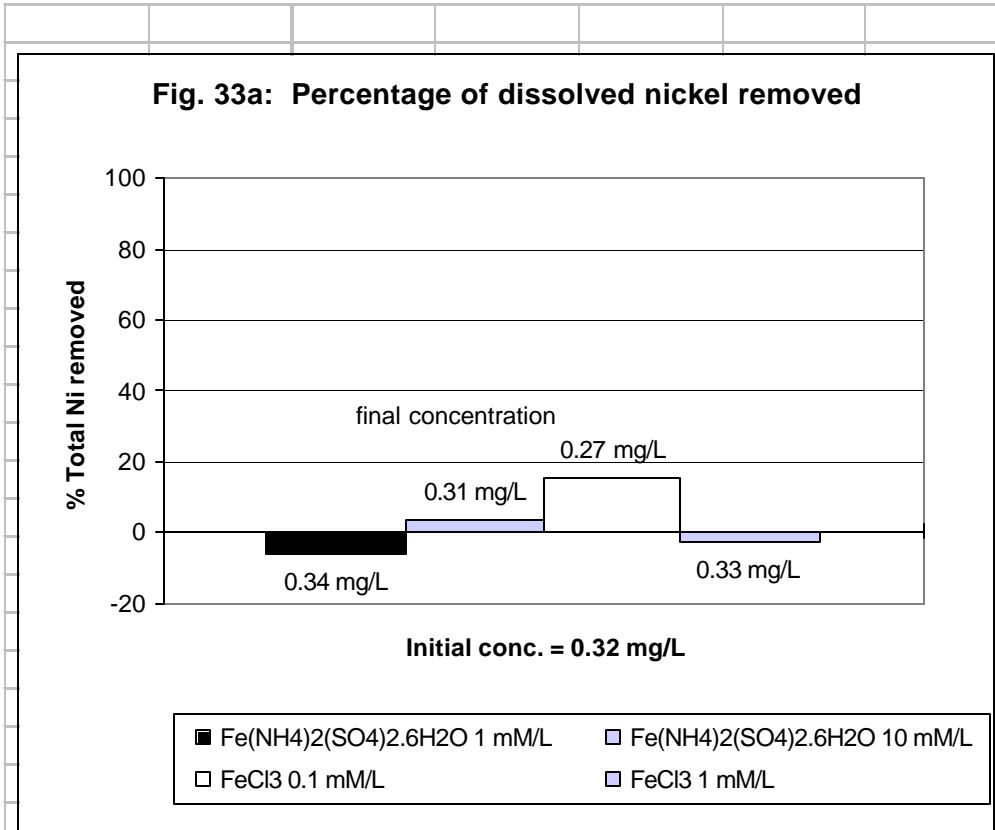
In Figure 32b, the percentage of total As removed in the treatments upon addition of the iron salts is presented. The  $0.1 \text{ mM@L}^{-1}$  ferric chloride addition was responsible for the highest As removal (50 %), while the higher ferric chloride ( $1 \text{ mM@L}^{-1}$ ) and the higher ferrous ammonium sulphate ( $10 \text{ mM@L}^{-1}$ ) were less effective in reducing the total As concentration in the solutions. Following addition of the low concentration ferrous ammonium sulphate treatment ( $1 \text{ mM@L}^{-1}$ ), sufficiently dense As-bearing particles were not formed which could settle within the time frame of the experiment.

**Fig. 32a: Percentage of dissolved arsenic removed**



**Fig. 32b: Total arsenic adsorption**





In summary, upon addition of either iron compounds, flocculants formed which captured dissolved As. However, only a fraction of these flocculants coagulated into particles large enough to settle in the time provided.

Effective contaminant removal and settlement upon additions of iron salts seen for As where not replicated for Ni. Less than 20 % of the dissolved nickel was adsorbed onto filterable (0.45 : m) particles at best (0.1 mM@L<sup>-1</sup> ferric chloride; Figure 33a). Negligible or no dissolved Ni was removed by the other three treatments. However, most of particles formed following the addition of 0.1 mM@L<sup>-1</sup> ferric chloride coagulated into settleable particles, and total Ni removal was about 15 % (Figure 33b).

At best, Ni removal following addition of iron salts was in the same range (15 % removal) as achieved following addition of algal biomass in the laboratory experiments. For total As, 50 % removal was achieved by addition of 0.1 mM@L<sup>-1</sup> ferric chloride.

A mass balance was performed based on the mass of arsenic, iron and nickel reporting as settled flocculants as well as those solids still in suspension. The suspended solids were determined by filtration from the supernatant of the 0.4 litre solution taken from the 10 litre buckets. This mass was converted to a 10 litre basis by multiplying by 25, and is listed as "filtered solids" in Table 13. The treated, unfiltered water analysis was not used in the mass balance. However, it may be used as a check of the mass balance by comparing the masses of arsenic, iron and nickel with the masses for these elements listed as "Left in 10 L" (by multiplying the total metal masses in the pit water analysis by 10).

**Ferric Sulphate and Ferrous Sulphate Treatments:** On the basis of settled and suspended solids, the 0.01 mM@L<sup>-1</sup> ferric sulphate gathered 47% of the arsenic, and the 10 mM@L<sup>-1</sup> ferrous sulphate treatment gathered 26.5%. In both cases, virtually all of the nickel remained in solution. As well, extremely high quantities of iron from the iron salt addition remained in solution. The percent iron removed is based on the initial pit water concentration of iron. Amounts of iron added through iron-salt additions were not factored in. Thus, percent removal of iron greater than 100% result.

Table 13: B-ZONE PIT ARSENIC FIELD EXPERIMENT RESULTS, September 19, 1995

| Concentration of material added (mM/L) | CONTROL | A-1 Ferric Sulphate<br>0.01 | B-2 Ferrous Sulphate<br>0.1 | B-4 Ferrous Sulphate<br>10 | E-3 Ferrous Ammonium Sulphate<br>1 | E-4 Ferrous Ammonium Sulphate<br>10 | F-2 Ferric Chloride<br>0.1 | F-3 Ferric Chloride<br>1 |
|--|---------|-----------------------------|-----------------------------|----------------------------|------------------------------------|-------------------------------------|----------------------------|--------------------------|
| <b>WATER (mg/L)</b>                    |         |                             |                             |                            |                                    |                                     |                            |                          |
| As, total                              | 0.27    |                             |                             |                            | 0.26                               | 0.19                                | 0.13                       | 0.18                     |
| As, diss.                              | 0.21    |                             |                             |                            | <0.002                             | <0.002                              | <0.002                     | 0.12                     |
| Fe, total                              | 0.54    |                             |                             |                            | 65                                 | 660                                 | 2.7                        | 49                       |
| Fe, diss.                              | 0.76    |                             |                             |                            | 58                                 | 620                                 | 0.47                       | 45                       |
| Ni, total                              | 0.33    |                             |                             |                            | 0.32                               | 0.33                                | 0.28                       | 0.33                     |
| Ni, diss.                              | 0.32    |                             |                             |                            | 0.34                               | 0.31                                | 0.27                       | 0.33                     |
| <b>FILTER PAPER (ug/filter)</b>        |         |                             |                             |                            |                                    |                                     |                            |                          |
| As                                     | 14.8    | 25.9                        |                             | 25.4                       | 94.8                               | 93.7                                | 22.7                       | 94.1                     |
| Fe                                     | 120     | 185                         |                             | 2062                       | 2402                               | 3930                                | 1286                       | 1764                     |
| Ni                                     | 4.8     | 5.1                         |                             | 1.8                        | 6.2                                | 3.7                                 | 2                          | 7.4                      |
| <b>SOLIDS (ug/g)</b>                   |         |                             |                             |                            |                                    |                                     |                            |                          |
| AS                                     |         | 32100                       | 11800                       | <2                         | 4590                               | 4560                                | 26400                      | 8680                     |
| Fe                                     |         | 165000                      | 43800                       | 145000                     | 154000                             | 252000                              | 229000                     | 198000                   |
| Ni                                     |         | 973                         | 806                         | 166                        | 333                                | 127                                 | 732                        | 384                      |
| Content in 10L                         |         |                             |                             |                            |                                    |                                     |                            |                          |
| As (mg)                                | 2.4     |                             |                             |                            |                                    |                                     |                            |                          |
| Fe (mg)                                | 6.5     |                             |                             |                            |                                    |                                     |                            |                          |
| Ni (mg)                                | 3.3     |                             |                             |                            |                                    |                                     |                            |                          |
| Dry Flocc Weight(g)                    |         | 0.015                       | 0.007                       | 0.140                      | 0.005                              | 0.029                               | 0.064                      | 0.034                    |
| Content in solids                      |         |                             |                             |                            |                                    |                                     |                            |                          |
| As (mg)                                |         | 0.482                       | 0.083                       | 0.0003                     | 0.023                              | 0.132                               | 1.690                      | 0.295                    |
| Fe (mg)                                |         | 2.475                       | 0.307                       | 20.300                     | 0.770                              | 7.308                               | 14.656                     | 6.732                    |
| Ni (mg)                                |         | 0.015                       | 0.006                       | 0.023                      | 0.002                              | 0.004                               | 0.047                      | 0.013                    |
| Left in 10L                            |         |                             |                             |                            |                                    |                                     |                            |                          |
| As (mg)                                |         | 1.92                        | 2.32                        | 2.40                       | 2.38                               | 2.27                                | 0.71                       | 2.10                     |
| Fe (mg)                                |         | 4.03                        | 6.19                        | -13.80                     | 5.73                               | -0.81                               | -8.16                      | -0.23                    |
| Ni (mg)                                |         | 3.24                        | 3.24                        | 3.23                       | 3.25                               | 3.25                                | 3.20                       | 3.24                     |
| Filtered out of 10L                    |         |                             |                             |                            |                                    |                                     |                            |                          |
| As (mg)                                | 0.37    | 0.65                        |                             | 0.64                       | 2.37                               | 2.34                                | 0.57                       | 2.35                     |
| Fe (mg)                                | 3.01    | 4.63                        |                             | 51.55                      | 60.04                              | 98.26                               | 32.15                      | 44.10                    |
| Ni (mg)                                | 0.12    | 0.13                        |                             | 0.05                       | 0.16                               | 0.09                                | 0.05                       | 0.19                     |
| Left after filtration                  |         |                             |                             |                            |                                    |                                     |                            |                          |
| As (mg)                                |         | 1.27                        |                             | 1.76                       | 0.01                               | -0.07                               | 0.14                       | -0.25                    |
| Fe (mg)                                |         | -0.60                       |                             | -65                        | -54                                | -99                                 | -40                        | -44                      |
| Ni (mg)                                |         | 3.11                        |                             | 3.18                       | 3.09                               | 3.15                                | 3.15                       | 3.05                     |
| <b>As</b>                              |         |                             |                             |                            |                                    |                                     |                            |                          |
| solid (%)                              |         | 20.1                        | 3.4                         | 0.01                       | 0.96                               | 5.51                                | 70.40                      | 12.30                    |
| suspended (%)                          |         | 27.0                        |                             | 26.5                       | 98.8                               | 97.6                                | 23.6                       | 98.0                     |
| total (%)                              |         | 47.0                        |                             | 26.5                       | 99.7                               | 103.1                               | 94.0                       | 110.3                    |
| <b>Fe</b>                              |         |                             |                             |                            |                                    |                                     |                            |                          |
| solid (%)                              |         | 38.1                        | 4.7                         | 312                        | 11.8                               | 112                                 | 225                        | 104                      |
| suspended (%)                          |         | 71.2                        |                             | 793                        | 924                                | 1512                                | 495                        | 678                      |
| total (%)                              |         | 109                         |                             | 1105                       | 936                                | 1624                                | 720                        | 782                      |
| <b>Ni</b>                              |         |                             |                             |                            |                                    |                                     |                            |                          |
| solid (%)                              |         | 0.4                         | 0.2                         | 0.7                        | 0.1                                | 0.1                                 | 1.4                        | 0.4                      |
| suspended (%)                          |         | 3.9                         | 0.0                         | 1.4                        | 4.8                                | 2.8                                 | 1.5                        | 5.7                      |
| total (%)                              |         | 4.4                         | 0.2                         | 2.1                        | 4.8                                | 3.0                                 | 3.0                        | 6.1                      |

**Ferrous Ammonium Sulphate Treatment:** On the basis of settled and suspended solids, the 1 mM@L<sup>-1</sup> and 10 mM@L<sup>-1</sup> ferrous ammonium sulphate treatment gathered all of the arsenic (99.7% and 103.1% respectively). Again, virtually no nickel reported as a solid fraction, remaining almost entirely in solution. Although substantial amounts of iron reports as solids, extremely high levels remained in solution (58 and 620 mg@L<sup>-1</sup> respectively, as compared with 0.76 mg@L<sup>-1</sup> in the untreated pit water).

**Ferric Chloride Treatment:** On the basis of settled floc and suspended solids, the 0.1 mM@L<sup>-1</sup> ferric chloride solution gathered all of the arsenic. Again, virtually none of the nickel reported as a solid fraction, remaining in solution. However, the amounts of iron remaining in solution was much lower than any of the other treatments (0.47 mg@L<sup>-1</sup>, which is essentially the same as that of the untreated pit water concentration for iron of 0.76 mg@L<sup>-1</sup>).

A mass balance for the 1 mM@L<sup>-1</sup> ferric chloride treatment was not achieved. Although all of the arsenic reported as a solid (110.3%), treated water analysis indicated that 0.12 mg@L<sup>-1</sup> of arsenic remain in solution. This may be anomalous result, or solids weight / solids arsenic content may be in error. Almost none of the nickel reported as a solid. The remaining iron in solution was extremely high at 45 mg@L<sup>-1</sup>.

Some additional cautionary notes should be made with respect to the 0.1 mM@L<sup>-1</sup> concentration of FeCl<sub>3</sub>. First, the pH response of the 0.05 mM@L<sup>-1</sup> concentration was significantly greater than that for the 0.1 mM@L<sup>-1</sup> treatment. Retesting should first be carried out to determine if this is an anomalous result or related to some precipitation effect. Second, the amount of iron and arsenic remaining in solution is very dependent upon concentration of FeCl<sub>3</sub>, and the precipitation conditions (temperature; concentration of nucleation sites equal to particulates; variability of pit water chemistry due to depth; time of the year). Any treatment program would have to accommodate the range in variability of the flooded pit water expected, and would have to effectively deal with pH effects to avoid leaching additional arsenic and nickel from pit side

walls, and waste materials located in the bottom of the pit. A larger scale test program examining these effects should be considered prior to full scale treatment.

In order to translate the results of these salt additions to the pit in-situ treatment, many considerations have to be made, prior to application. Although the salts effectively transferred dissolved As to suspended arsenic, no reduction in Ni concentration could be achieved. Due to the anticipated changes in pH, the pit would have to be neutralized. The iron would report with the precipitate to the bottom of the pit. These sludges would be a source of iron, which though oxidation-reduction reactions could be a long term source of acidification of pit surface water. Reduced iron from the bottom, would be turned over annually and be available to oxidize at the surface after ice breakup, a reaction which produces hydrogen ions.

The complexities of an in-situ iron salt addition to the pit , based on the observations of this preliminary experiment, are as follows. The pit biology would change, the arsenic forms would change due to pH changes and new metals would be released from the pit walls. The long term implications of salt additions lay in potential acidification of the pit water, due to iron release of the sludge as well as in the difficulty to predict the long term stability of the precipitates formed through the chemical additions. Given these scenarios it was considered prudent to evaluate the cost associated with salt additions, presented in the next section.

#### 4.2.3 Treatment Costs for Arsenic Removal By Iron Salt Additions to B-Zone Pit

An approximate costing for the chemical additions for the whole pit were performed (prices are as of February 1996). Conversions from molar quantities to grams for various additions is given in Table 14. Cost estimates were made based upon the concentration which produced good arsenic removal (Table 15).

**Table 14: Interconversion of mM/L, M/L and mg/L for Various Compounds.**

| mM/L | M/L     | M.W., g | Ferric Sulphate  | Ferrous Sulphate                          | Ammonium Sulphate             | Ammonium Phosphate             | Ferrous Ammonium Sulphate  | Ferric Chloride    |
|------|---------|---------|--|---|-------------------------------|--------------------------------|--|--------------------|
|      |         |         | $\text{Fe}_2(\text{SO}_4)_3 \cdot 9\text{H}_2\text{O}$ | $\text{FeSO}_4 \cdot 7\text{H}_2\text{O}$ | $(\text{NH}_4)_2 \text{SO}_4$ | $(\text{NH}_4)_2 \text{HPO}_4$ | $\text{Fe}(\text{NH}_4)_2 (\text{SO}_4)_2 \cdot 6\text{H}_2\text{O}$ | $\text{FeCl}_3$    |
|      |         |         | 562.01   | 278.05                                    | 132.14                        | 132.05                         | 392.14   | 162.21             |
|      |         |         | mg.L <sup>-1</sup>                                     | mg.L <sup>-1</sup>                        | mg.L <sup>-1</sup>            | mg.L <sup>-1</sup>             | mg.L <sup>-1</sup>   | mg.L <sup>-1</sup> |
| 0.01 | 0.00001 |         |  | 2.8                                       | 1.3                           | 1.3                            | 3.9  | 1.6                |
| 0.05 | 0.00005 |         |  | 14  | 7                             | 7                              | 20   | 8                  |
| 0.1  | 0.00010 |         |  | 28  | 13                            | 13                             | 39   | 16                 |
| 1    | 0.00100 |         |  | 278                                       | 132                           | 132                            | 392  | 162                |
| 5    | 0.00500 |         |  | 1,390                                     | 66                            | 660                            | 1,961  | 811                |
| 10   | 0.01000 |         |  | 2,781                                     | 1,321                         | 1,321                          | 3,921  | 1,622              |
| 100  | 0.10000 |         |  | 27,805                                    | 13,214                        | 13,205                         | 39,214   | 16,221             |
| 1000 | 1.00000 |         | 562,010  | 278,050                                   | 132,140                       | 132,050                        | 392,140  | 162,210            |



Table 15: Approximate Chemical Cost of Iron Salt Treatment of B-Zone Flooded Pit for Arsenic Removal  
Volume of flooded pit is approximately  $5 \times 10^6 \text{m}^3$ .

| Treatment  | Form                          | Cost (to site)       | Cost/g. mole | Treatment Concentration | Cost of Treating Flooded Pit     |
|--|-------------------------------|----------------------|--------------|-------------------------|----------------------------------|
| Ferric Sulphate<br>$\text{Fe}_2(\text{SO}_4)_7\text{OH}^1$                                       | Solution<br>12-12.5% Fe by wt | \$0.4473/kg solution | \$1.04       | 0.1 mM·L <sup>-1</sup>  | \$220,000                        |
| Ferrous Ammonium Sulphate<br>$\text{Fe}(\text{NH}_4)_2(\text{SO}_4)_2 \cdot 9\text{H}_2\text{O}$ | Solid                         | \$3.30-5.50 (US)/kg  | \$1.28-2.13  | 1.0 mM·L <sup>-1</sup>  | \$6,600,000-<br>\$11,000,00 (US) |
| $\text{FeCl}_3$  | Solid                         | \$ 0.658/kg solid    | \$0.180      | 0.1 mM·L <sup>-1</sup>  | \$94,000                         |
| $\text{FeCl}_3$  | Solution<br>10-10.5 %Fe by wt | \$ 0.286/kg solution | \$0.160      | 0.1 mM·L <sup>-1</sup>  | \$84,000                         |

1. Ferric sulphate is available as  $\text{Fe}_2(\text{SO}_4)_7\text{OH}$  rather than  $\text{Fe}_2(\text{SO}_4)_3 \cdot 9\text{H}_2\text{O}$ . Calculation is based on assumption that type and amount of precipitate and effectiveness of metal adsorption is the same for  $\text{Fe}_2(\text{SO}_4)_7\text{OH}$  and  $\text{Fe}_2(\text{SO}_4)_3 \cdot 9\text{H}_2\text{O}$  on an equivalent Fe basis (2.5 g  $\text{Fe}_2(\text{SO}_4)_3 \cdot 9\text{H}_2\text{O}$  is equivalent to 1 g  $\text{Fe}_2(\text{SO}_4)_7\text{OH}$ ).

Ferric sulphate is available in a hydroxylated form of  $\text{Fe}_5(\text{SO}_4)_7\text{OH}$  rather than as  $\text{Fe}_2(\text{SO}_4)_3 \cdot 9\text{H}_2\text{O}$  which was used in the field experiments. This has the advantage of having 0% free acid, although the pH of the solution is  $< 1$ . It is assumed that the type and amount of precipitate and effectiveness of metal adsorption is the same for  $\text{Fe}_5(\text{SO}_4)_7\text{OH}$  and  $\text{Fe}_2(\text{SO}_4)_3 \cdot 9\text{H}_2\text{O}$  on an equivalent Fe basis (2.5 g  $\text{Fe}_2(\text{SO}_4)_3 \cdot 9\text{H}_2\text{O}$  is equivalent to 1 g  $\text{Fe}_5(\text{SO}_4)_7\text{OH}$ ). The best removal concentration for ferric sulphate was with  $0.1 \text{ mM} \cdot \text{L}^{-1}$ , which removed only 47% of the arsenic. Pit treatment chemical cost for this concentration is \$220,000.

Ferrous ammonium sulphate is far too costly because of its base cost per gram mole and the higher concentrations that would have to be used ( $1 \text{ mM} \cdot \text{L}^{-1}$ ).

Ferric chloride was the least expensive of all the iron salt treatments. It is available in two forms, as a solid and in solution. The solution is slightly less expensive but it typically contains 0.5-0.6% free acid (HCl). Based on an optimal treatment concentration of  $0.1 \text{ mM} \cdot \text{L}^{-1}$  where all of the arsenic is removed, the chemical cost for treating a volume equivalent to the flooded pit volume is \$84,000.

Cost estimates given are only approximate and allow the relative costs between the various iron salt treatments to be compared. These costs do not include any additional chemical costs to offset the pH suppression effects resulting from addition of acidic solution to water with very little buffering capacity.

## 5.0 CONCLUSIONS

The main focus of summarizing the work carried out in the B-zone pit was to arrive at treatment options for As and Ni. These options should be economically achievable and above all present a long term environmentally sustainable approach providing protection to aquatic life. The concentrations of both contaminants are generally low. A pit, which appears to be well isolated from Collins Bay, containing water in concentration ranges of 0.2-0.3 mg Ni@L<sup>-1</sup> and similar low concentrations of As does not pose an environmental risk. The key issues for the decommissioning of the pit are only long term environmental implications from breaching the containment structures.

An extensive monitoring effort was carried out between 1991 and 1996 to collect regularly all chemical and biological parameter required to document the evolution of pit limnology and chemistry since flooding. This effort was complemented by an equally extensive amount of auxiliary work, culminating in four reports. A detailed understanding of the growth of the dominant algae in the pit, its role in contaminant transport and the nature of both inorganic and organic particulates was developed. The interpretation of all this information has lead to a comprehensive understanding of pit biology, limnology and its effect on chemistry of the pit waters. It can be concluded that a credible model is presented for the pit, which describes the behaviour of the water body, the seasonal trends of various chemical parameters are explained through the growth dynamics using the data derived from the dominant algae in the pit.

The transport of As and Ni from the surface water to the thermocline, which can extend to a depth of 8 to 10 m, is brought about by the algal biomass. The concentrations of As and Ni in the pit are decreasing slightly overall from year to year. The physical conditions, i.e. the complete turn over of the water body during the winter months and the decomposition of the organic material in the lower portion of the pit lead to re-release of the contaminants to the surface water, removed during the summer months. Through the investigation of the solid material, both organic and inorganic collected in sedimentation traps positioned at different depths in the pit, slight reduction in contaminants year-by-year could be explained.

The reduction is brought about by the small fraction of As and Ni, which are binding to iron/silica oxide particles present in the bottom of the pit. However only that fraction can drop out of the water column which was able to aggregate to particles large enough to overcome the hydrodynamic conditions prevailing in the pit. As the particles are all very small, those conditions are only achieved over the brief period when the pit is not stratified underneath the ice. Hence a larger fraction of As and Ni is recirculated back to the surface water, ready to be adsorbed by the new crop of biomass. Lower biomass or productivity would result in less transport of Ni and As from the surface to the deeper portion of the pit, as evidenced in 1996 surface concentrations, and presumably result in a lower rate of overall reduction.

The transport mechanism of As and Ni in the pit is substantiated through interpretation of the pit limnological profiles, where significant changes are evident in As and Ni concentrations comparing the surface and the bottom water and they change seasonally and over the years. The role of biology on the pit limnology is truly remarkable in its predictability. The reduction in algal density, predicted from the nutrient depletion noted in 1995 was borne out in 1996, with the expected reductions in biological activity.

The approach taken in the data interpretation essentially considered the pit as a large closed vessel, only altered by internal processes, no input or output of water. Quantification of biological growth dynamics could directly reflect the chemical changes noted in pit water. This strongly support the fact, that pit is in effect a closed water body where no further contaminants are released from the pit walls. All alterations in pit profile chemistry are accounted for by internal processes, driven by photosynthesis of algae and bacterial respiration and the physical process induced by temperature govern the hydrodynamics of particle settling to the sediment.

Through experimentation with pit water from various depth, adding algal suspensions, bentonite and various iron salts, the chemical/physical forms of the contaminants are as well defined as the methodologies available. The surface charges of particulates are affected by Eh, pH and their aggregations are governed by the decay products of the organics.

The investigations and the experiments lead to the realisation the generally accepted differentiation of dissolved material below the filter size of 0.45 µm is not valid for the conditions in the pit, as organically complexed Ni and As are likely prevailing forms of particulates. In addition the size fraction of the particulates, which is associated with As and Ni is very small. The key factors affecting surface charges of particles and govern particle aggregations and or colloidal growth undergo changes with depth in the pit, which in turn results in seasonally varying settling characteristics of particles.

The preliminary experiments of iron salt and bentonite additions to pit water lead to the conclusions, that from iron salt additions as expected, transfer of As from the dissolved form, defined by 0.45 µm, to a suspended form will take place. This leaves the questions of its settling behaviour of these new particulates open. In addition the long term behaviour of the resulting sludge is mainly unpredictable, as the physical conditions of the pit will not be altered. The ability to predict the effect of the additions of surface active material, such as bentonite or other flocculating agents, is clearly impaired by the presence of the organic material.

With the understanding of the pit gained through the interpretation of the information available the conclusion that the pit should not be treated chemically presents itself as the most environmentally sound approach. Biological / natural recovery of pit water quality to SSWQ objectives will likely be a slow process but could possibly be assisted with nutrient additions as reduction in growth will reduce the transport of contaminants to lower parts of the water body. A very preliminary first cut on the required additions of nitrate, based on the 1995 conditions where growth was reasonable, in order to increase the nitrate concentration in the epilimnion back to 0.4 mg@L<sup>-1</sup> (0.4 g@m<sup>-3</sup>) in the epilimnion (1.8 x 10<sup>6</sup> m<sup>3</sup>) would require 720 kg of nitrate addition.

## 6.0 REFERENCES

Antia, N.J., C.D. McAllister, T.R. Parsons, K. Stephens and J.D.H. Strickland, 1963. Further measurements of primary production using a large-volume plastic sphere. **Limnology and Oceanography** 8:166-183.

Arad, S., O. Friedman and A. Rotem, 1988. Effect of nitrogen on polysaccharide production in a *Porphyridium* sp. **Applied and Environmental Microbiology**. 54:2411-2414.

Avnimelech, Y., B.W. Troeger and L.W. Reed, 1982. Mutual flocculation of algae and clay. Evidence and Implications. In: **Science** 216:63-65.

Avnimelech, Y., and R.G. Menzel, 1984. Co-flocculation of algae and clay to clarify turbid impoundments. **Journal of Soil and Water Conservation**. pp. 200-203.

Boojum Research Limited, January 1995. **The Decommissioning of the B-Zone Flooded Pit With Ecological Engineering**. Submitted to CAMECO Corporation.

Burkholder, J.M. and B.E. Cuker, 1991. **J. Phycol.** 27: 373-384.

CAMECO Corporation, July 1993. **Collins Bay B-Zone Decommissioning Year 1-Proposed Target Levels**. Appendix A4.

CAMECO Corporation, January 1995. **Collins Bay, A-Zone, D-Zone and Eagle Point Waste Management Plan**.

Appendix E.

Davison, W and R. DeVitre, 1995. Iron Particles in Freshwater. In: Buffle, J and HP van Leeuwen (eds.) **Environmental Particles Vol. 1**. Lewis Publishers, Boca Raton. p. 315-355.

Hellebust, J.A. 1974. Extracellular products. In: Stewart, W.D.P. (ed.). **Algal Physiology and Biochemistry**. Blackwell Scientific Pub. Oxford. p. 838-863.

Kalin, M., and m. Olaveson, 1996. **Controlling factors in the production of extracellular polysaccharides in phytoplankton**. CANMET contract # 23440-5-1136/01 SQ.

Kalin, M. 1997. **Nickel and arsenic adsorption onto mucilage producing algal colonies**. CANMET Biotechnology, pp 28, CANMET Contract # 23440-6-1011/001/SQ.

Kalin, M., W.N. Wheeler and M.P. Smith, 1997. **The role of Picoplankton as primary producers in mining waste water effluents**. CANMET Contract # 23440-5-1302/001/SQ.

Klapper, H. 1992. Eutrophierung und Gewässer-schutz. Gustav Fischer Verlag Jena, Stuttgart.

Koren, D.W. 1992. **Biocoagulation/Bioflocculation - A Literature Review**. CANMET Mineral Sciences Division Report MSL 92-36.

Lowson, E.A., 1997. **Chemical, Physical, and Biological Characteristics of Particulates Formed in Mine Drainage Systems**. University of Toronto, MSc. Thesis under supervision of F.G. Ferris.

Mangi, J.I. and Schumacher, G.J. 1979. Physiological significance of copper-slime interactions in *Mesotaenium* (Zygnemetales, Chlorophyta). **Am. Mid. Nat.** 102: 134-139.

Raymont, J.E.G., 1963. **Plankton and Productivity in the Oceans**. Pergamon Press, Oxford, p. 211.

Redfield, A.C. 1958. The biological control of chemical factors in the environment. **American Scientist**. 206-221.

Rodie, A., J.J.P. Gerits and J.M. Azcue 1995. Biogeochemical pathways of arsenic in lakes. **Environ. Rev.** 3: 304-317.

Ruttner, F. 1963. **Fundamentals of Limnology**. University of Toronto Press. University of Toronto Press, Toronto. 295 p.

Ryther, J.H. and Dunstan, W.M. 1971. Nitrogen, phosphorus, and eutrophication in the coastal marine environment. **Science** 171: 1008-1013.

Ruttner, F. 1963. Fundamentals of limnology. University of Toronto Press. University of Toronto Press, Toronto. 295p.

Schanz, F. and Wälti, K. 1982. Primary productivity in freshwater environments. In: Mitsui, A. and Black, C.C. (eds). **CRC Handbook of Biosolar Resources: Basic Principles**. Vol. 1, Part 2. CRC Press, Boca Raton. p. 389-394.

Shuter, B. 1979. A model of physiological adaptation in unicellular algae. **Journal Theoretical Biology**. 78: 519-552.

Søballe, D.M. and S.T. Threlkeld, 1988. **Ver. Internat. Verein. Limnol.** 23: 750-754.

Stockner, J.G. 1988. Phototrophic picoplankton: an overview from marine and freshwater ecosystems. **Limnol. Oceanogr.** 33: 765-775



Theis, T.L., and R.O. Richter 1980. Adsorption Reactions of Nickel Species at Oxide Surfaces  
In: **Particulates in Water**.

Wetzel, R.G. 1983. **Limnology**. W.B. Saunders Co. Toronto. 767 pp.

**APPENDIX A:**

PART 1: IRON SALT TREATMENT FOR REMOVAL OF ARSENIC AND NICKEL

PART 2: BENTONITE ADDITION FOR REMOVAL OF ARSENIC AND NICKEL

PART 3: B-ZONE PIT WATER CHEMISTRY AND SEDIMENTATION TRAP SOLIDS  
ANALYSES

PART 4: BIOGEOCHEMICAL PATHWAYS OF ARSENIC IN LAKES  
ADSORPTION REACTIONS OF NICKEL SPECIES AT OXIDE SURFACES

## APPENDIX A

### PART 1 IRON SALT TREATMENT FOR REMOVAL OF ARSENIC AND NICKEL

Iron salt treatments of pit water were investigated to determine their effectiveness in removing arsenic and nickel from solution. The mechanism of removal is thought to be adsorption of the arsenic and nickel by the iron precipitates, in particular the iron oxyhydroxides.

First, a geochemical simulation, using the PHREEQE program, was carried out to determine which specific iron salt would be realistic to use in order to form precipitates, and what changes would be associated with the use of the salt on the pH and Eh. The initial water chemistry used was that of the flooded pit in April 1994.

Based on these results iron salt treatments were then applied in buckets to water samples from the flooded pit to determine their effectiveness in removing arsenic and nickel from solution.

The overall objective of this field experiment was to examine the feasibility of an *in-situ* iron salt treatment to remove arsenic and nickel from solution in the flooded pit.

#### **Field Experiments: Methods and Materials**

The purpose of this experiment was twofold. The first objective was to quantify the amount of settled floc for various iron salt treatments of the B-Zone pit water collected from the hypolimnion (20 m). The second objective was to determine the effectiveness of the formed precipitates in reducing the arsenic and nickel concentration of the flooded pit water.

The limnological profile of the B-Zone flooded pit (Stn 6.72, 40 m deep) measured on September 16, 1995 indicated that the water column was still stratified, with a warmer (10.6° C), 9 m thick circulating layer of water (epilimnion) overlying a layer of colder (4.2° C to 4.7° C) layer of water (hypolimnion, 13 m to 40 m). Since arsenic and nickel concentrations are typically higher in the hypolimnion, this water was selected for the experiment.

Using a submersible pump attached to a plastic hose, 250 L of water from a depth of 20 m were collected. Twenty-five (25) plastic buckets were lined with clear plastic bags and 10 L of pit water were dispensed into each bucket. The 25 samples were returned to, and set up outside of, the Rabbit Lake environmental lab.

Experiments using six chemicals (ferric sulphate, ferrous sulphate, ammonium sulphate, ammonium phosphate, ferrous ammonium sulphate and ferric chloride), each at four concentrations (0.01, 0.1, 1 and 10 mM $\text{L}^{-1}$ ) were carried out in 24 ten litre bucket samples. Each treatment was stirred 25 rotations with a plastic rod. A 10 L control (no addition of chemical) was also set up.

The pH, temperature, conductivity and redox potential (Eh) were measured at times of 0.25 hour, 18 hours and 38.5 hours following the addition of the chemicals. Observations of water colour and clarity were made after 39 hours (Table A1-1).

All of the 10 litre samples were brought into the laboratory in Rabbit Lake after 39 hours and were allowed to settle for two hours. A 0.4 litre sample of solution was taken from each of the buckets, filtered through Sartorius 0.45 : m filter papers, and then preserved with 1 % HNO<sub>3</sub>. The filter papers were then dried (110° C for 24 hours) and analyzed for arsenic, iron and nickel. A second and third set of water samples (0.5 L) was also taken, and preserved with H<sub>2</sub>SO<sub>4</sub> or HNO<sub>3</sub>. These were then chemically analyzed for total and dissolved arsenic, iron and nickel. A fourth set of water samples (0.5 L) was collected and left untreated.

Table A1-1: B-Zone pit water arse

| Chemical<br>Addition   | mM/L<br>M.W.<br>added | Temperature, C |             |              |             | pH       |             |              |                     | APPEARANCE               |                     | Floc<br>Wet Vc<br>mL/10l |
|--|-----------------------|----------------|-------------|--------------|-------------|----------|-------------|--------------|---------------------|--------------------------|---------------------|--------------------------|
|  |                       | Field          |             | After set-up |             | Field    |             | After set-up |                     | Solution, 39 hrs         | Filtered Sol'n      |                          |
|  |                       | 0<br>hrs       | 0.25<br>hrs | 18<br>hrs    | 38.5<br>hrs | 0<br>hrs | 0.25<br>hrs | 18<br>hrs    | 38.5<br>hrs         |                          |                     |                          |
| <b>Control. No Addition</b>  | Control               | 4.4            | 4.6         | 0.9          | 0.1         | 7.11     | 6.38        | 6.22         | 7.45                | clear                    | clear               |                          |
| Fe <sub>2</sub> (SO <sub>4</sub> ) <sub>3</sub> .9H <sub>2</sub> O<br>Lab*<br>Ferric Sulphate  | 0.01                  |                | 4.8         | 0.7          | 0.0         |          | 6.38        | 6.29         | 7.44                | light yellow             | clear               | < 1 ml                   |
|  | 0.05                  |                |             |              | 7.6         |          |             |              | 5.48                |                          | orange              | 5                        |
|  | 0.1                   |                | 4.6         | 0.6          | 0.0         |          | 3.81        | 3.70         | 3.66                | light yellow             | clear               | 21                       |
|  | 1                     |                | 4.8         | 1.1          | 0.0         |          | 2.85        | 2.76         | 2.82                | light orange             | light orange        | 26                       |
| FeSO <sub>4</sub> .7H <sub>2</sub> O<br>Ferrous Sulphate   | 10                    |                | 4.9         | 1.1          | 0.0         |          | 2.26        | 2.20         | 2.23                | orange, clear            | medium orange       |                          |
|  | 0.01                  |                | 4.6         | 0.9          | 0.1         |          | 6.38        | 5.64         | 5.44                | light yellow, clear      | light yellow        | < 1 ml                   |
|  | 0.1                   |                | 4.3         | 1.5          | 0.0         |          | 5.90        | 5.73         | 5.44                | medium yellow, clear     | light yellow        |                          |
|  | 1                     |                | 4.8         | 1.0          | 0.1         |          | 5.82        | 5.55         | 5.28                | orange, milky            | clear               |                          |
| (NH <sub>4</sub> ) <sub>2</sub> SO <sub>4</sub><br>Immonium Sulphate   | 10                    |                | 4.7         | 1.4          | 0.1         |          | 5.62        | 4.90         | 4.46                | yellow, clear            | clear               | 17                       |
|  | 0.01                  |                | 4.7         | 1.1          | 0.1         |          | 6.39        | 5.93         | 5.63                | light yellow, clear      | light yellow, clear |                          |
|  | 0.1                   |                | 4.9         | 1.3          | 0.0         |          | 5.77        | 5.91         | 5.65                | light yellow, clear      | light yellow, clear |                          |
|  | 1                     |                | 4.8         | 0.9          | 0.0         |          | 5.70        | 5.68         | 5.66                | light yellow, clear      | light yellow, clear |                          |
| 10   |                       | 4.8            | 1.3         | 0.0          |             | 5.81     | 5.39        | 5.62         | light yellow, clear | light yellow, clear      |                     |                          |
| (NH <sub>4</sub> ) <sub>2</sub> HPO <sub>4</sub><br>Immonium Phosphate   | 0.01                  |                | 4.7         | 1.1          | 0.1         |          | 6.41        | 6.53         | 6.54                | light yellow, clear      | light yellow, clear |                          |
|  | 0.1                   |                | 4.7         | 1.1          | 0.0         |          | 6.66        | 6.54         | 6.83                | light yellow, clear      | light yellow, clear |                          |
|  | 1                     |                | 4.6         | 0.8          | 0.1         |          | 7.47        | 7.38         | 7.31                | light yellow, clear      | light yellow, clear |                          |
|  | 10                    |                | 4.7         | 1.4          | 0.0         |          | 8.06        | 7.92         | 7.80                | light yellow, clear      | light yellow, clear |                          |
| Fe(NH <sub>4</sub> ) <sub>2</sub> (SO <sub>4</sub> ) <sub>2</sub> .6H <sub>2</sub> O<br>Ferrous Ammonium<br>Lab*<br>Lab*<br>Sulphate | 0.01                  |                | 4.7         | 1.0          | 0.1         |          | 6.41        | 7.91         | 7.84                | medium yellow, clear     |                     | -                        |
|  | 0.1                   |                | 4.8         | 1.3          | 0.0         |          | 7.20        | 7.51         | 7.54                | dark yellow, clear       |                     | -                        |
|  | 1                     |                | 4.5         | 1.5          | 0.1         |          | 6.89        | 6.87         | 6.75                | orange-brown, milky      |                     | <0.5 ml                  |
|  | 1                     |                |             |              | 22.8        |          |             |              | 5.2                 | orange                   |                     | 30                       |
|  | 5                     |                |             |              | 6.2         |          |             |              | 5.1                 | orange                   |                     | 10                       |
|  | 10                    |                | 4.5         | 1.1          | 0.1         |          | 6.34        | 5.95         | 5.82                | orange-brown, milky      |                     | 2.5                      |
| FeCl <sub>3</sub><br>Lab*<br>Lab*<br>Ferric Chloride   | 0.01                  |                | 4.7         | 1.0          | 0.1         |          | 6.46        | 7.26         | 7.09                | light yellow, clear      |                     | < 1                      |
|  | 0.05                  |                |             |              | 4.2         |          |             |              | 5.81                | white                    |                     |                          |
|  | 0.1                   |                | 4.8         | 1.5          | 0.1         |          | 6.95        | 7.15         | 7.09                | very light yellow, clear |                     |                          |
|  | 0.5                   |                |             |              | 2.9         |          |             |              | 3.26                | orange, very loose       |                     |                          |
|  | 1                     |                | 4.6         | 2.0          | 0.0         |          | 3.26        | 2.88         | 2.90                | orange, clear            |                     |                          |
| 10   |                       | 4.5            | 1.6         | 0.1          |             | 2.39     | 2.35        | 2.40         | orange-brown, clear |                          |                     |                          |

- follow up laboratory study results

Approximately 8 L of water remained following water sampling. Approximately 7.5 L of the remaining water was carefully decanted in such a manner as to not re-suspend solids which had settled to the bottom in each treatment. The 0.5 L sample containing solids was slurried, settled in graduated cylinders and the wet volumes recorded. The samples were then filtered, dried and analyzed for arsenic, iron and nickel.

### **Follow-up Laboratory Experiment: Methods and Materials**

Based upon the floc produced from the field experiments, a small lab experiment (supplementing the field work in the buckets) was set up to examine whether precipitates would also form at intermediate concentrations. B-Zone pit water collected from 12, 22 32 and 40 m depth were combined on September 16, 1995, and homogenized in order that 6 litres of water of the same quality were available for a lab experiment.

Ferric sulphate was added to a 1 L sample of pit water at a concentration of 0.05 mM and refrigerated to simulate field temperatures. Ferrous ammonium sulphate was added at 1 mM (room temperature) and 5 mM (refrigerated). Ferric chloride was added at 0.05 and 0.5 mM (both refrigerated).

### **Results**

In the field experiment additions are given in mM. All treatments are summarized in Table A1-1.

#### *Ferric Sulphate*

Floc amounts for the ferric sulphate field experiments for concentrations of 0.01, 0.1, 1 and 10 mM ferric sulphate were <1, 21, 26 and nil ml wet volume floc/10 L pit water respectively. A follow-up lab experiment of 0.05 mM concentration of ferric sulphate resulted in floc wet

volume of 5 mL/10 L.

Comparisons of the predicted pH from the geochemical simulations with the field experiment after 38 hours at a concentration of 1 mM $\text{L}^{-1}$  concentration (0.001 M $\text{L}^{-1}$ ) of ferric sulphate were good, being 2.52 and 2.82 respectively. The geochemical simulation also showed the highest positive saturation index (SI) for hematite at all concentrations except for the 0.001 M $\text{L}^{-1}$  concentration.

The most promising floc wet volume for the least amount of addition is at a concentration of 0.1 mM $\text{L}^{-1}$ . However, the application of a concentration of 0.1 mM $\text{L}^{-1}$  to the pit is questionable, since the pH depression is significant (pH = 3.66).

### *Ferrous Sulphate*

Among the ferrous sulphate treatments, the 0.1 mM $\text{L}^{-1}$  treatment produced a minute amount of floc (<1 mL wet floc per 10 L pit water), while the 10 mM $\text{L}^{-1}$  treatment produced 17 mL wet floc per 10 L of pit water. At a concentration between these two, (1 mM $\text{L}^{-1}$  treatment), floc formation which settled would have been anticipated. However, the solution remained "milky", indicating the formation of fine precipitates which did not settle during the 38 hours of the experiment.

The effect of ferrous sulphate additions on the pH is significantly less than for ferric sulphate. At concentrations of 1 mM $\text{L}^{-1}$ , the actual pH (after 38 hours) and that predicted from the geochemical simulation (hematite precipitation) were 5.28 and 5.67 respectively. Again, the geochemical simulation showed the highest positive SI for hematite. Allowing the hematite to precipitate resulted in high positive SI values for orpiment ( $\text{As}_2\text{S}_3$ ), pyrite ( $\text{FeS}_2$ ), and millerite ( $\text{NiS}$ ). In other words, arsenic and nickel precipitation are feasible.

### *Ammonium Sulphate*

There was no precipitation at any of the concentrations of ammonium sulphate (the geochemical simulation predicted a high positive SI for hematite for all concentrations and precipitation would have been expected. However, the solutions from the field experiment were clear, with no evidence of any suspension). Therefore, this chemical addition would require significantly higher concentrations to be added.

There was little effect of ammonium sulphate concentration on the pH of the field experiment (5.62-5.66) which was also evident in the geochemical simulation predictions (pH = 6.09 at a concentration of  $.001 \text{ M}\text{L}^{-1}$  ammonium sulphate).

### *Ammonium Phosphate*

There was no precipitation at any of the concentrations of ammonium phosphate (as in the case for ammonium sulphate, the geochemical simulation predicted a high positive SI for hematite for all concentrations, and precipitation would have been expected. However, the solutions from the field experiment were clear, with no evidence of any suspension).

The pH of the field experiments increased with increasing concentrations of ammonium phosphate concentration, which agreed with the trend predicted from the geochemical simulations. However the amount of actual increase was significantly less than predicted (7.31 and 9.37 respectively at  $1 \text{ mM}\text{L}^{-1}$  concentration). It could be that precipitation was slow in starting, and that once started would result in additional significant increases in pH. Such a delayed effect was noted in the ferrous ammonium sulphate experiments.



## *Ferrous Ammonium Phosphate*

From the field experiments, settled wet floc volume for concentrations of ferrous ammonium sulphate of 0.01, 0.1, 1 and 10  $\text{mM}\cdot\text{L}^{-1}$  were nil, nil, < 0.5 and 2.5 mL/10 L pit water respectively. The solutions at concentrations of 0.01 and 0.1 were clear. The solutions at concentrations of 1 and 10 were "milky" in appearance, indicating that a very fine precipitated suspension had formed which did not settle.

Follow-up laboratory experiments at 1 and 5  $\text{mM}\cdot\text{L}^{-1}$  concentration of ferrous ammonium sulphate showed much larger amount of settled wet floc, with 30 and 10 mL/10 L pit water forming respectively (Table A1-2a).

The effect of temperature on the amount of settled floc was seen from the results of the field experiment ( $T=0.1\text{ }^{\circ}\text{C}$ ) after 38 hours and that of the laboratory experiment ( $T=22.8^{\circ}\text{C}$ ) after 48 hours, at the same concentration (1  $\text{mM}\cdot\text{L}^{-1}$ ) ferrous ammonium sulphate. At  $0.1^{\circ}\text{C}$ , precipitation occurred, as evident from the milky appearance of the solution, but very little settled (<0.5 mL/10 L pit water). At  $22.8^{\circ}\text{C}$ , settled floc was over 60 times greater (30 mL/10 L pit water), with the remaining solution losing much of its milky appearance. The temperature affects the size of the precipitates formed and consequently their settling rates. At low temperatures, the precipitates are so fine that settling occurs extremely slowly.

Time for precipitation is another significant factor on floc formation as well as final pH of the treater pit water. This is evident from Table A1-2a and A1-2b. After 48 h, the 1 and 5  $\text{mM}\cdot\text{L}^{-1}$  concentration of ferrous ammonium sulphate formed 30 and 10 mL wet floc/10 L pit water, and had a pH of 5.25 and 5.16 respectively. After an additional 8 days (240 hours total), an additional 29 mL wet floc/10 L pit water settled out, with the pH dropping dramatically to 2.93 and 3.75 for the 1 and 5  $\text{mM}\cdot\text{L}^{-1}$  concentrations respectively (Table A1-2b).

Application of concentrations of 1  $\text{mM}\cdot\text{L}^{-1}$  is questionable because of the reaction times, temperature sensitivity of floc settling rates, delayed reaction times and the final resultant pH level of the treated pit water (2.93).

Table A1-2a: B-Zone pit water precipite formation in laboratory, September 22 - 25, 1995.

| Chemical Addition   | M.W.   | mM/L added | g/L added | Temperature Conditions | 12:00 pm, 25-Sep-95  |                           | T.S.S. mg/L (dry) | 10:30 am, September 24, 1995, = 47 hrs |          |              |         |                    |
|---|--------|------------|-----------|------------------------|----------------------|---------------------------|-------------------|--|----------|--------------|---------|--------------------|
|   |        |            |           |                        | mL wet precip. per L | Appearance of precipitate |                   | pH                                     | Temp (C) | Cond (uS/cm) | Em (mV) | Eh (mV) (Temp.Cor) |
| CONTROL   |        |            |           | Fridge                 |                      |                           | 6.6               | 6.36                                   | 4.4      | 69.6         | 149     | 404                |
| Fe <sub>2</sub> (SO <sub>4</sub> ) <sub>3</sub> ·9H <sub>2</sub> O<br>Ferric Sulphate                             | 562.01 | 0.05       | 0.02810   | Fridge                 | 0.5 mL/L             | orange                    | 10.3              | 5.48                                   | 7.6      | 86           | 216     | 468                |
| Fe(NH <sub>4</sub> ) <sub>2</sub> (SO <sub>4</sub> ) <sub>2</sub> ·6H <sub>2</sub> O<br>Ferrous Ammonium Sulphate | 392.14 | 1          | 0.39214   | Room                   | 3.0 mL/L             | orange                    | 4.1               | 5.25                                   | 22.8     | 407          | 216     | 458                |
|   |        | 5          | 1.96070   | Fridge                 | 1.0 mL/L             | orange                    | 18.5              | 5.16                                   | 6.2      | 1055         | 229     | 482                |
| FeCl <sub>3</sub><br>Ferric Chloride  | 162.21 | 0.05       | 0.00811   | Fridge                 | <0.1 mL/L            | white                     | 11.1              | 5.81                                   | 4.2      | 77           | 180     | 435                |
|   |        | 0.5        | 0.08111   | Fridge                 | 10 mL/L              | orange,very loose         | 24.6              | 3.26                                   | 2.9      | 372          | 292     | 548                |

- 1) B-Zone pit water collected 16/9/95.
- 2) Samples from 12, 22, 32 and 40 m combined to make up 5 L of water (mixed).
- 3) 1 L systems set up in cold room, 2 - 4 C, light, except 1 mM Ferrous Ammonium Sulphate treatment
- 4) Jars stirred for 10 seconds.
- 5) Chemicals added 11:40 am, 22/9/95.

Table A1-2b: B-Zone pit water precipite formation in laboratory, September 25 - October 3, 1995.

| Chemical Addition   | M.W.   | mM/L added | g/L added | Temperature Conditions | 12:30 pm, 03-Oct-95         |                                 |                           |                     | 12:30 am, October 3, 1995, = 266 hrs |          |              |         |                    |
|---|--------|------------|-----------|------------------------|-----------------------------|---------------------------------|---------------------------|---------------------|--------------------------------------|----------|--------------|---------|--------------------|
|   |        |            |           |                        | mL wet precip. per L<br>NEW | mL wet precip. per L<br>To Date | Appearance of precipitate | Appearance of Sol'n | pH                                   | Temp (C) | Cond (uS/cm) | Em (mV) | Eh (mV) (Temp.Cor) |
| CONTROL   |        |            |           | Fridge                 |                             |                                 |                           | green, algae        | 5.89                                 | 22.6     | 78.4         | 280     | 523                |
| Fe <sub>2</sub> (SO <sub>4</sub> ) <sub>3</sub> ·9H <sub>2</sub> O<br>Ferric Sulphate                             | 562.01 | 0.05       | 0.02810   | Fridge                 |                             | 0.5 mL/L                        | small am't<br>white floc  | light yellow        | 5.70                                 | 21.5     | 118          | 198     | 441                |
| Fe(NH <sub>4</sub> ) <sub>2</sub> (SO <sub>4</sub> ) <sub>2</sub> ·6H <sub>2</sub> O<br>Ferrous Ammonium Sulphate | 392.14 | 1          | 0.39214   | Room                   | 2.9 mL/L                    | 5.9 mL/L                        | orange                    | orange precip       | 2.93                                 | 22.0     | 894          | 438     | 681                |
|   |        | 5          | 1.96070   | Fridge                 | 2.9 mL/L                    | 3.9 mL/L                        | orange                    | orange precip       | 3.75                                 | 22.1     | 2180         | 220     | 463                |
| FeCl <sub>3</sub><br>Ferric Chloride  | 162.21 | 0.05       | 0.00811   | Fridge                 |                             | <0.1 mL/L                       |                           | slight yellow       | 5.79                                 | 22.3     | 92           | 296     | 539                |
|   |        | 0.5        | 0.08111   | Fridge                 |                             | 10 mL/L                         | red film                  | medium yellow       | 3.09                                 | 22.3     | 417          | 414     | 657                |

- 1) All treatments moved to Room temperature on September 25, 1995
- 2) Wet precipitate volumes measured on 0.75 L, corrected to 1 L.
- 3) New floc in 1 and 5 mM Ferrous Ammonium Sulphate newly formed, indicated by floc formation by Oct. 3 following filtration of samples on September 24

## *Ferric Chloride*

The field experiments for treatments of 0.01, 0.1, 1 and 10 mM $\text{L}^{-1}$  concentration of ferric chloride yielded nil, 45, 30 and nil mL wet floc / 10 L pit water respectively. Follow-up laboratory experiments at concentrations of 0.05 and 0.5 mM $\text{L}^{-1}$  yielded settled floc amounts of <1 and 100 mL wet floc / 10 L pit water.

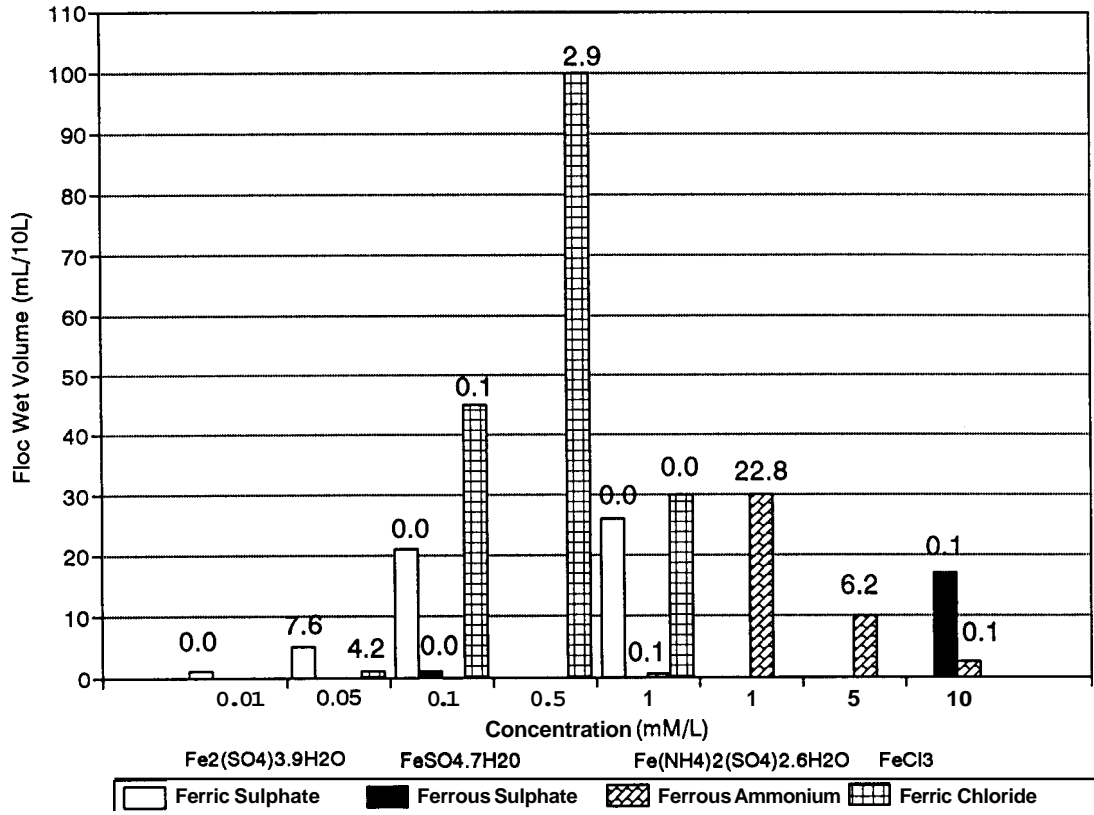
No geochemical simulation was carried out for ferric chloride. The pH levels were a little erratic. The pH of the 0.05 mM $\text{L}^{-1}$  laboratory experiment yielded a pH value of 5.81. However the 0.1 mM $\text{L}^{-1}$  field experiment yielded a less acidic pH value of 7.09. Increasing the concentration further to 0.5 mM $\text{L}^{-1}$  (lab experiment) produced a significant reduction in pH to a much more acidic value of 3.26. This fluctuation is difficult to explain, but may be indicative of a hypersensitive response of the pH level to treatment conditions.

### **Summary of Floc Formation Experiments**

A summary of the effect of type and concentration of various treatments on the amount of settled floc produced is shown in Figure A1-1. The numbers above the bars represent the treatment temperature. The graph does not represent the amount of precipitate produced, only the amounts produced which were able to settle within the time taken for the bucket experiment.

The ferric sulphate concentration which was most effective was of 1.0 mM $\text{L}^{-1}$ , however 0.1 mM $\text{L}^{-1}$  produced similar results. The ferrous sulphate required 100 times this concentration (10 mM $\text{L}^{-1}$ ) to achieve similar settled floc volumes. Ferrous ammonium sulphate was most effective at concentrations of 1.0 mM $\text{L}^{-1}$  when the precipitation temperature was 22.8 °C. At the same concentration, but at a temperature of 0.1 °C, there was virtually no settled floc. Ferric chloride had the optimal response of all treatments in terms of floc volume, with 0.5 mM $\text{L}^{-1}$  concentration resulting in twice the floc volume as the 0.1 mM $\text{L}^{-1}$  concentration.

Fig. A1-1: B-Zone Pit Precipitation E x ~



Chemical analysis was carried out on the most promising floc results, and these are presented in the Section 4.2

What also is important in the precipitation process is the precipitate size and settling rates. It was noted for the ferrous ammonium phosphate treatment that the difference between the 0.1 °C and the 22.8 °C results at 0.1 mM·L<sup>-1</sup> concentration was that much of the precipitate remains in solution at 0.1 °C as a very fine suspension. In contrast, floc did form and settle at 22.8 °C (although the reaction rates were extremely slow), leaving a solution without the "milky" appearance of the 0.1 °C experiment.

## Chemical Analysis of Selected Field Experiments

Chemical analysis on the most successful iron salt treatments (in terms of settled floc volume) was carried out. The settled floc at the bottom of the 10 litre buckets was separated from the supernatant and chemically analyzed for arsenic, iron and nickel. Suspended solids were determined from a 0.4 litre sample of the supernatant which was filtered, dried and chemically analyzed for the same elements. Analysis of the supernatant, including suspended solids, was taken from another 0.5 litre sample, and chemically analyzed for total and suspended arsenic, iron and nickel.

### *Treated and Unfiltered Pit Water*

Little dissolved arsenic ( $<.002 \text{ mg@L}^{-1}$ ) remained in the  $1 \text{ mM@L}^{-1}$  and  $10 \text{ mM@L}^{-1}$  ferrous ammonium sulphate treatment, as well as the  $0.1 \text{ mM@L}^{-1}$  ferric chloride treatment. In the  $1 \text{ mM@L}^{-1}$  ferric chloride treatment chemical analysis suggests that, only half of the dissolved arsenic was removed ( $0.12 \text{ mg@L}^{-1}$  remained from an initial pit water concentration of  $0.21 \text{ mg@L}^{-1}$ ).

Little iron was left in solution in the  $0.1 \text{ mM@L}^{-1}$  ferric chloride treatment. In other words, most of the added iron from the salt treatment reports as settled floc. The dissolved iron remaining in all of the other treatments was two to three orders of magnitude greater than the untreated pit water concentration ( $0.76 \text{ mg@L}^{-1}$ ).

Virtually all of the nickel remained in solution for all of the iron salt treatments.

## **PART 2 BENTONITE ADDITION FOR REMOVAL OF ARSENIC AND NICKEL**

### **Introduction**

The purpose of this experiment was to determine if arsenic and nickel could be removed from solution by (a) adsorption directly onto the surface of the bentonite particles, and (b) by co-flocculation of algae and bentonite particles. In addition, given that bentonite is negatively charged, the surface charge of particles with As and Ni, will be identified.

Because of the fine size of the bentonite particles, settling times are extremely slow. Typical sizes of clay particles range both above and below 0.45  $\mu\text{m}$ , is the filter size used this experiment, i.e. the finer fraction of bentonite particle would pass through the filter and be reported with the "dissolved" fraction. Centrifugation would perhaps be a better method for separating the fine clay particles from the solution. The short duration for the field experiment (3 days) facilitates to determine if the operative mechanism, in principle only, which transports the contaminants.

These bentonite experiments were carried out in late August of 1996. At that time the B-Zone flooded pit contained dissolved As (0.17 to 0.27  $\text{mg}\cdot\text{L}^{-1}$ ) and Ni (0.21 to 0.35  $\text{mg}\cdot\text{L}^{-1}$ ), based on samples collected for the test work.

### **Methods and Materials**

Briefly, four concentrations of bentonite were applied to flooded pit waters taken from three depths. Identification was as follows. Bentonite additions of 1, 10, 100 and 100  $\text{mg}$  dry weight per 10 L flooded pit water were labelled as series 2, 3, 4 and 5 respectively (series 1 = control, no addition). Pit water taken at depths of 40, 15 and 2 m were labelled as series C, D and E respectively. Series A and B had fertilizer added (0.5  $\text{mg}$  ammonium nitrate: 34-0-0) in addition to the bentonite additions. Series A was given a longer growth period (> two weeks). Series

B had an algal supplement added in order to simulate high algal density and the addition of bentonite at the same time.

In Series B, algae present in 30 L of surface pit water was supplemented with nitrogen fertilizer and grown for 4 days prior to the bentonite additions (a further 3 days). This solution was filtered and the filter cakes comprised of algal biomass were resuspended in three 10 L volumes of flooded pit from 40 m. Bentonite (100 mg/10 L) was added to each of two 10 L volumes (B2-A, B2-B) while the third 10 L volume with algae was left as a control. After three days, water samples were filtered through 0.45 : m filters and the water was submitted to SRC for determination of dissolved As and dissolved Ni.

After three days, the experiment was terminated and water samples were filtered through 0.45 : m filters and the filtered water was submitted to SRC for determination of dissolved As and dissolved Ni.

**Notes on Analyses:** SRC reports a detection limit for As of  $0.0002 \text{ mg@L}^{-1}$ . For Ni, the detection limit is  $0.001 \text{ mg@L}^{-1}$ . The dissolved As concentrations range from 0.16 to  $0.31 \text{ mg@L}^{-1}$ . The dissolved Ni concentrations range from 0.19 to  $0.41 \text{ mg@L}^{-1}$ . Both As and Ni measured concentrations are two orders of magnitude higher than the detection limits.

## Results

The results of these four series of treatment are presented in Table A2-1. The following observations can be made:

### General Observations

1. Visible turbidity was present in the 100 mg and 1000 mg bentonite treatments. On September 3, the day of sampling, a very thin film of sediment was present on the bottom of 1000 mg treatments.
2. Additions of 1 mg, 10 mg, 100 mg and 1000 mg of bentonite per 10 L treatment had little effect on the general chemistry of the samples (see Table A2-1). Only conductivity was slightly higher (3-4 :  $\text{S}\cdot\text{cm}^{-1}$ ) in the 1000 mg treatments, compared to the remainder of treatment.
3. Additions of algae filtered from the 30 L of pit surface water with fertilizer, set up in advance of the site visit and grown for 4 days, visibly increased the phytoplankton concentration in these treatments. A 250 mL sample of the algal culture was filtered through a 0.45 : m filter paper for estimating the algal biomass per litre of culture solution. The total number of cells  $\cdot\text{L}^{-1}$  for B-1, C-1 and D-1 were determined to be  $5.1\cdot 10^7$ ,  $2.8\cdot 10^6$ , and  $8.4\cdot 10^6$  respectively.
4. The measured As concentrations in the controls (water stored at room temperature for 3 days in open, plastic bag-lined buckets) were  $0.17 \text{ mg}\cdot\text{L}^{-1}$  (2 m: E1),  $0.18 \text{ mg}\cdot\text{L}^{-1}$  (15 m: D1) and  $0.27 \text{ mg}\cdot\text{L}^{-1}$  (40 m: C1). Overall, As concentrations in the flooded pit increase with depth, as seen in past surveys of pit water quality.
5. The measured Ni concentrations in the controls (water stored at room temperature for 3 days in open, plastic bag-lined buckets) were  $0.21 \text{ mg}\cdot\text{L}^{-1}$  (2 m: E1),  $0.27 \text{ mg}\cdot\text{L}^{-1}$  (15 m: D1) and  $0.35 \text{ mg}\cdot\text{L}^{-1}$  (40 m: C1). Ni concentrations also increase with depth, again seen in past surveys of pit water quality.



Table A2-1: SRC results of analyses of filtered **g** **o** population Experiment, September 3, 1996.

| 1  |                              | 40 m water+algal biom.<br>+ Bentonite |       |       | 40 m water+Bentonite |      |       |        |        |        |
|----|------------------------------|---------------------------------------|-------|-------|----------------------|------|-------|--------|--------|--------|
| 2  |                              | B1                                    | B2-A  | B2-B  | C1                   | c2   | c3    | C4-A   | C4-B   | c5     |
| 3  | Water Source: depth, m       | 40                                    | 40    | 40    | 40                   | 40   | 40    | 40     | 40     | 40     |
| 4  | Algal Addition, L filt / 10L | 7.1                                   | 7.0   | 8.0   |                      |      |       |        |        |        |
| 5  | Equiv. mg algae added        | 37                                    | 36    | 41    |                      |      |       |        |        |        |
| 6  | Bentonite Add'n, mg/ 10L     | 0                                     | 100   | 100   | 0                    | 1    | 10    | 100    | 100    | 1000   |
| 7  | Diss. As, d.l. 0.0002 mg/L   | 0.3                                   | 0.27  | 0.28  | 0.27                 | 0.31 | 0.28  | 0.28   | 0.28   | 0.25   |
| 8  | % As removed                 |                                       | 10%   | 7%    |                      | -15% | -4%   | 4%     | 4%     | 7%     |
| 9  | mg As removed/mg algae       |                                       | 0.008 | 0.005 |                      |      |       |        |        |        |
| 10 | mg As removed/mg Bent.       |                                       | 0.003 | 0.002 |                      | -0.4 | -0.01 | -0.001 | -0.001 | 0.0002 |
| 11 | Diss. Ni, d.l.= 0.001 mg/L   | 0.41                                  | 0.39  | 0.38  | 0.35                 | 0.38 | 0.37  | 0.36   | 0.36   | 0.32   |
| 12 | % Ni Removed                 |                                       | 5%    | 7%    |                      | -9%  | -6%   | -3%    | -3%    | 9%     |
| 13 | mg Ni removed/mg Bent.       |                                       | 0.002 | 0.003 |                      | -0.3 | -0.02 | -0.001 | -0.001 | 0.0003 |

| 1  |                              | 15 m water+Bentonite |       |        |        |        |        | 2 m water+Bentonite |      |       |        |        |        |
|----|------------------------------|----------------------|-------|--------|--------|--------|--------|---------------------|------|-------|--------|--------|--------|
| 2  |                              | D1                   | D2    | D3     | D4-A   | D4-B   | D5     | E1                  | E2   | E3    | E4-A   | E4-B   | E5     |
| 3  | Water Source: depth, m       | 15                   | 15    | 15     | 15     | 15     | 15     | 2                   | 2    | 2     | 2      | 2      | 2      |
| 4  | Algal Addition, L filt / 10L |                      |       |        |        |        |        |                     |      |       |        |        |        |
| 5  | Equiv. mg algae added        |                      |       |        |        |        |        |                     |      |       |        |        |        |
| 6  | Bentonite Add'n, mg/ 10L     | 0                    | 1     | 10     | 100    | 100    | 1000   | 0                   | 1    | 10    | 100    | 100    | 1000   |
| 7  | Diss. As, d.l. 0.0002mg/L    | 0.18                 | 0.2   | 0.2    | 0.2    | 0.19   | 0.16   | 0.17                | 0.2  | 0.19  | 0.19   | 0.18   | 0.16   |
| 8  | % As removed                 |                      | -11%  | -11%   | -11%   | -6%    | 11%    |                     | -18% | -12%  | -12%   | -6%    | 6%     |
| 9  | mg As removed/mg algae       |                      |       |        |        |        |        |                     |      |       |        |        |        |
| 10 | mg As removed/mg Bent.       |                      | -0.02 | -0.002 | -0.002 | -0.000 | 0.0002 |                     | -0.3 | -0.02 | -0.002 | -0.001 | 0.0001 |
| 11 | Diss. Ni, d.l.= 0.001 mg/L   | 0.27                 | 0.29  | 0.29   | 0.28   | 0.27   | 0.25   | 0.21                | 0.22 | 0.22  | 0.22   | 0.22   | 0.19   |
| 12 | % Ni Removed                 |                      | -7%   | -7%    | 4%     | 0%     | 7%     |                     | -5%  | -5%   | -5%    | -5%    | 10%    |
| 13 | mg Ni removed/mg Bent.       |                      | -0.2  | -0.02  | -0.001 | 0.000  | 0.0002 |                     | -0.1 | -0.01 | -0.001 | -0.001 | 0.0002 |

### **B-Series (100 mg dw/10 L bentonite plus algal biomass supplement plus fertilizer)**

The arsenic concentration in the solution supplemented with algal biomass (B1) was  $0.30 \text{ mg@L}^{-1}$ ,  $0.03 \text{ mg@L}^{-1}$  higher than the C1 control with no algal biomass supplement. The Ni concentration in the solution supplemented with algal biomass (B1) was  $0.41 \text{ mg@L}^{-1}$ ,  $0.06 \text{ mg@L}^{-1}$  higher than the C1 control. The higher concentrations may be due to As and Ni release from the algal biomass filter cake added to B1, B2-A and B2-B. The pressure filtration may have caused cell disruption.

Addition of 100 mg bentonite to 10 L of 40 m pit water supplemented with algal biomass (B2-A and B2-B) reduced the dissolved As concentration by 0.02 to  $0.03 \text{ mg@L}^{-1}$ , compared to the B1 control (7% to 10% reduction). Similarly, Ni concentrations decreased by 0.02 to  $0.03 \text{ mg@L}^{-1}$ , compared to the B1 control (5% to 7% reduction).

### **C-Series (40 m depth flooded pit water)**

Addition of 1, 10 and 100 mg of Bentonite to 40 m pit water (C2, C3, C4-A and C4-B) apparently increased dissolved As concentrations by 0.01 to  $0.04 \text{ mg@L}^{-1}$ , compared to the C1 control (4% to 15% increase). These Bentonite additions also increased Ni concentrations by 0.01 to  $0.03 \text{ mg@L}^{-1}$  (3% to 9% increase).

Addition of 1000 mg Bentonite to 40 m pit water (C5) apparently decreased the dissolved As concentration by  $0.02 \text{ mg@L}^{-1}$ , compared to the control C1 (7% decrease), and the dissolved Ni concentration by  $0.03 \text{ mg@L}^{-1}$  (9% decrease).

### **D-Series (15 m depth flooded pit water)**

As seen in the C-Series, 1, 10 and 100 mg additions (D2, D3, D4-A and D4-B) of Bentonite to the 10 L samples of 15 m pit water slightly increased dissolved As (6% to 11% increase)

and Ni (0.5 to 7% increase) concentrations. Addition of 1000 mg of Bentonite (D5) decreased the dissolved As concentration by  $0.02 \text{ mg}\cdot\text{L}^{-1}$  and the dissolved Ni concentration by  $0.02 \text{ mg}\cdot\text{L}^{-1}$ . This was the same trend seen in the C-S series experiments.

### **E-Series (2 m depth flooded pit water)**

The 1, 10 and 100 mg (E2, E3, E4-A, E4-B) bentonite treatments showed the same trend, with increased dissolved As concentrations by 0.01 to  $0.03 \text{ mg}\cdot\text{L}^{-1}$ , and the dissolved Ni concentrations by  $0.01 \text{ mg}\cdot\text{L}^{-1}$ . The 1000 mg Bentonite treatment (E5) reduced the dissolved As concentration by  $0.01 \text{ mg}\cdot\text{L}^{-1}$  and dissolved Ni concentration by  $0.02 \text{ mg}\cdot\text{L}^{-1}$ .

### **C-,D-,E-Series**

Observed dissolved As and Ni concentrations in the 2, 3, 4-A and 4-B treatments did not increase proportionally with the amount of Bentonite added (1, 10, 100 mg per 10 L).

The effects of Bentonite additions did not vary with the depth from which flooded pit water samples were collected.

The greatest dissolved metal concentration decrease observed, with respect to the Controls (C1, D2, E1) was the  $0.03 \text{ mg}\cdot\text{L}^{-1}$  Ni decrease (9% decrease) in the C5 treatment.

### **Discussion**

The results show that the highest bentonite addition ( $1000 \text{ mg dw (dry weight)}\cdot\text{L}^{-1}$  bentonite) resulted in 6-11% removal of arsenic and 7-10% removal of nickel. Neither depth of water nor concentration of As and Ni in the water made a difference in the amount of contaminant removed. At the higher concentration, from the deeper portions of the pit, a very thin film of sediment was present on the bottom of the containers. This film was not noted at lesser concentrations of bentonite treatments or at lower contaminant concentrations.

At the highest concentration (1000 mg dw/10L) of bentonite, some flocculation of the clay particles with one another seemed to be occurring, resulting in a larger particle size which settled out during the three days of the experiment, and were larger than the filter size of 0.45 : m.

Removal occurred for the combination of 100 mg dw<sup>d</sup>L<sup>-1</sup> bentonite and algal biomass supplement. The amount of arsenic removed was 7-10% , and 5-7% for the nickel. With no biomass supplement and the same bentonite addition, no detectable arsenic or nickel was removed. It appears that some co-flocculation occurred between the algae and the bentonite particles, resulting in a larger particles size, and thus facilitating settling. The importance of this result is that removal of arsenic and nickel from solution by co-flocculation of the algae and clay is taking place, at lower clay loadings than with clay additions alone.

Reports from the literature on co-flocculation of clay and algae (to decrease turbidity of water reservoirs, such as ponds, etc) show substantial removal of algae and clay particles over the course of the growing season (>90% reduction in the turbidity). In other words, these processes are slow, but result ultimately in substantial removal of clay and algae from suspension. The above experiment shows that arsenic and nickel from solution does adsorb onto particles, by the two proposed mechanisms: directly to the bentonite surfaces by adsorption; and by co-flocculation of algae/organics and bentonite.

It should be pointed out that the proposed mechanisms do not suggest that arsenic and nickel will be removed permanently. This would have to be determined as a next step.

**PART 3      B-ZONE PIT WATER CHEMISTRY AND SEDIMENTATION TRAP SOLIDS  
ANALYSES**

Table A3-1a: Nutrient status, major ions and contaminants in the flooded pit (1992).

| Date    | Depth       | Nutrients, mg/L |                 |                 |       | Dissolved Ion Concentrations, mg/l |     |     |     |      |                 |     |                  |       |       | TD5 Sum |      |
|---------|-------------|-----------------|-----------------|-----------------|-------|------------------------------------|-----|-----|-----|------|-----------------|-----|------------------|-------|-------|---------|------|
|         |             | PO <sub>4</sub> | NO <sub>3</sub> | NH <sub>4</sub> | N,TKN | K                                  | Ca  | Mg  | Na  | Fe   | SO <sub>4</sub> | Cl  | HCO <sub>3</sub> | As    | Ni    |         |      |
| July 23 | Collins Bay | 0.15            | 0.04            | 0.07            | 0.16  | 1.4                                | 2.3 | 0.9 | 1.1 | 0.02 | 3.0             | 0.7 | 11               | 0.001 | 3.005 | 20.9    |      |
| June 21 | Above       | 2               | 0.46            | 0.35            | 0.07  |                                    |     |     |     |      | 4.5             |     |                  | 0.113 | 0.18  | 5.7'    |      |
|         | Below       | 12              | 0.49            | 0.40            | 0.08  |                                    |     |     |     |      | 4.5             |     |                  | 0.113 | 0.22  | 5.8'    |      |
|         | Thermo-c    | 32              | 0.61            | 0.35            | 0.07  |                                    |     |     |     |      | 4.8             |     |                  | 0.107 | 0.15  | 6.1'    |      |
|         | cline       | 50              | 1.10            | 0.44            | 0.10  |                                    |     |     |     |      | 5.4             |     |                  | 0.150 | 0.17  | 7.4*    |      |
| June 30 |             | 5               | 0.40            |                 | <0.01 |                                    | 1.1 | 3.4 | 1.6 | 1.7  | 0.20            | 4.7 | 0.4              | 12    | 0.118 | 0.12    | 54   |
|         |             | 10              | 0.46            |                 | 0.05  |                                    | 1.1 | 3.4 | 1.6 | 1.8  | 0.16            | 4.7 | 0.4              | 12    | 0.114 | 0.12    | 54   |
|         |             | 15              | 0.43            |                 | 0.05  |                                    | 1.1 | 3.3 | 1.6 | 1.8  | 0.18            | 4.6 | 0.4              | 12    | 0.099 | 0.14    | 55   |
|         |             | 20              | 0.37            |                 | 0.09  |                                    | 1.3 | 3.4 | 1.6 | 1.8  | 0.21            | 4.7 | 0.4              | 12    | 0.106 | 0.14    | 56   |
|         |             | 25              | 0.43            |                 | 0.07  |                                    | 1.2 | 3.4 | 1.7 | 1.8  | 0.22            | 4.8 | 0.4              | 12    | 0.118 | 0.15    | 46   |
|         |             | 30              | 0.49            |                 | 0.07  |                                    | 1.2 | 3.5 | 1.7 | 1.8  | 0.24            | 5.0 | 0.4              | 12    | 0.129 | 0.15    | 51   |
|         |             | 35              | 0.55            |                 | 0.05  |                                    | 1.2 | 3.6 | 1.8 | 1.8  | 0.23            | 5.6 | 0.4              | 12    | 0.137 | 0.18    | 48   |
|         |             | 40              | 0.61            |                 | 0.05  |                                    | 1.3 | 3.6 | 1.8 | 1.8  | 0.22            | 5.8 | 0.4              | 12    | 0.162 | 0.18    | 54   |
|         |             | 45              | 0.58            |                 | 0.07  |                                    | 1.4 | 3.6 | 1.9 | 1.9  | 0.24            | 6.5 | 0.4              | 13    | 0.213 | 0.21    | 57   |
|         |             | 50              | 0.74            |                 | 0.03  |                                    | 1.5 | 3.6 | 2.0 | 1.8  | 0.25            | 6.1 | 0.4              | 12    | 0.220 | 0.22    | 56   |
| July 23 | Above       | 0               | 0.34            | 0.13            | 0.01  | 0.31                               | 3.0 | 3.0 | 1.2 | 1.6  | 0.08            | 4.9 | 0.5              | 13    | 0.125 | 0.12    | 28.3 |
|         | Below       | 2               | 0.18            | 0.13            | 0.05  | 0.28                               | 1.8 | 3.1 | 1.3 | 1.6  | 0.36            | 5   | 0.5              | 13    | 0.125 | 0.13    | 27.6 |
|         | Thermo-     | 12              | 0.25            | 0.22            | 0.07  | 0.20                               | 1.7 | 3.0 | 1.2 | 1.7  | 0.15            | 4.7 | 0.4              | 12    | 0.097 | 0.17    | 25.8 |
|         | cline       | 22              | 0.46            | 0.31            | 0.07  | 0.41                               | 1.8 | 3.0 | 1.2 | 1.7  | 0.14            | 5.3 | 0.4              | 13    | 0.118 | 0.18    | 28.1 |
|         |             | 32              | 0.58            | 0.09            | 0.08  | 0.31                               | 1.8 | 3.2 | 1.3 | 1.7  | 0.15            | 6.1 | 0.4              | 13    | 0.164 | 0.21    | 29.1 |
|         |             | 48              | 0.86            | 0.04            | 0.08  | 0.24                               | 4.0 | 3.6 | 1.5 | 1.8  | 0.19            | 9.2 | 1.2              | 20    | 0.337 | 0.31    | 43.4 |
| Sept 1  | Above       | 0               | 0.12            |                 | <0.01 |                                    | 1.0 | 3.0 | 1.3 | 1.7  | 0.36            | 5.2 | 0.5              | 13    | 0.170 | 0.12    | 43   |
|         | Below       | 2               | 0.28            |                 | <0.01 |                                    | 1.0 | 3.1 | 1.3 | 1.6  | 0.34            | 5.2 | 0.3              | 13    | 0.151 | 0.12    | 34   |
|         | Thermo-     | 10              | 0.43            |                 | <0.01 |                                    | 1.0 | 3.1 | 1.4 | 1.7  | 0.31            | 5.2 | 0.3              | 12    | 0.131 | 0.15    | 28   |
|         | cline       | 15              | 0.49            |                 | 0.03  |                                    | 1.1 | 3.3 | 1.5 | 1.7  | 0.32            | 6.0 | 0.3              | 12    | 0.196 | 0.22    | 40   |
|         |             | 20              | 1.44            |                 | 0.04  |                                    | 1.2 | 3.4 | 1.6 | 1.8  | 0.31            | 6.5 | 0.3              | 12    | 0.191 | 0.23    | 38   |
|         |             | 25              | 0.06            |                 | 0.03  |                                    | 1.3 | 3.5 | 1.6 | 1.8  | 0.32            | 7.1 | 0.3              | 12    | 0.255 | 0.24    | 41   |
|         |             | 30              | 0.64            |                 | 0.03  |                                    | 1.3 | 3.6 | 1.7 | 1.8  | 0.35            | 7.5 | 1.3              | 12    | 0.266 | 0.25    | 46   |
|         |             | 35              | 0.12            |                 | 0.04  |                                    | 1.3 | 3.6 | 1.8 | 1.9  | 0.29            | 8.0 | 0.3              | 12    | 0.300 | 0.30    | 38   |
|         |             | 40              | 0.67            |                 | 0.04  |                                    | 1.4 | 3.8 | 1.9 | 1.9  | 0.28            | 9.1 | 0.3              | 12    | 0.361 | 0.35    | 46   |
|         |             | 45              | 0.74            |                 | 0.04  |                                    | 1.4 | 3.9 | 1.9 | 1.8  | 0.28            | 9.6 | 0.3              | 12    | 0.402 | 0.35    | 40   |
| Sept 17 | Above       | 0               | 0.34            | 0.44            | 0.01  | 0.61                               | 0.2 | 3.3 | 1.3 | 1.6  | 0.13            | 5.5 | 0.5              | 12    | 0.160 | 0.14    | 26.2 |
|         | Below       | 2               | 0.37            | 0.49            | 0.03  | 0.37                               | 1.1 | 3.1 | 1.2 | 1.8  | 0.10            | 5.3 | 0.8              | 12    | 0.127 | 0.20    | 27   |
|         | Thermo-     | 12              | 0.34            | 0.49            | 0.03  | 0.38                               | 1.0 | 3.3 | 1.2 | 1.6  | 0.08            | 5.4 | 0.4              | 12    | 0.192 | 0.13    | 26.5 |
|         | cline       | 22              | 1.35            | 0.92            | 0.04  | 0.96                               | 2.5 | 3.3 | 1.3 | 1.7  | 0.11            | 7.7 | 1.6              | 12    | 0.206 | 0.21    | 33.9 |
|         |             | 32              | 0.74            | 1.00            | 0.05  | 0.25                               | 1.5 | 3.4 | 1.2 | 1.8  | 0.09            | 8.6 | 0.8              | 12    | 0.322 | 0.27    | 32   |
|         |             | 41              | 0.71            | 1.10            | 0.05  | 0.35                               | 2.2 | 3.7 | 1.4 | 2    | 0.10            | 9.4 | 1.3              | 12    | 0.374 | 0.33    | 35   |
| Oct. 1  | Above       | 0               | 0.40            |                 | 0.03  |                                    | 1.1 | 3.9 | 1.8 | 1.8  | 0.46            | 6.9 | 0.3              | 12    | 0.256 | 0.22    | 43   |
|         | Below       | 5               | 0.43            |                 | 0.03  |                                    | 1.1 | 3.9 | 1.8 | 1.8  | 0.49            | 6.9 | 0.3              | 12    | 0.263 | 0.22    | 53   |
|         | Thermo-     | 10              | 0.46            |                 | 0.03  |                                    | 1.1 | 4.0 | 1.8 | 2    | 0.46            | 6.6 | 0.5              | 12    | 0.255 | 0.22    | 54   |
|         | cline       | 15              | <0.03           |                 | 0.04  |                                    | 1.1 | 4.0 | 1.8 | 1.8  | 0.37            | 7.0 | 0.4              | 11    | 0.240 | 0.20    | 59   |
|         |             | 20              | 0.25            |                 | 0.01  |                                    | 1.1 | 3.7 | 1.8 | 1.8  | 0.39            | 7.0 | 0.4              | 12    | 0.267 | 0.20    | 60   |
|         |             | 25              | 0.34            |                 | 0.04  |                                    | 1.2 | 3.8 | 1.8 | 1.8  | 0.33            | 6.9 | 0.5              | 12    | 0.216 | 0.21    | 57   |
|         |             | 30              | 0.28            |                 | 0.03  |                                    | 1.1 | 3.8 | 1.8 | 1.8  | 0.36            | 7.0 | 0.4              | 12    | 0.223 | 0.21    | 57   |
|         |             | 35              | 0.40            |                 | 0.04  |                                    | 1.1 | 3.8 | 1.8 | 1.8  | 0.37            | 7.0 | 0.4              | 12    | 0.260 | 0.20    | 55   |
|         |             | 40              | 0.40            |                 | 0.03  |                                    | 1.1 | 3.8 | 1.7 | 1.8  | 0.34            | 7.0 | 0.4              | 12    | 0.192 | 0.19    | 55   |
|         |             | 45              | <0.03           |                 | 0.03  |                                    | 1.2 | 4.0 | 1.8 | 2.1  | 0.34            | 6.5 | 0.4              | 11    | 0.215 | 0.21    | 58   |

\* Incomplete dataset

Table A3-1b: Nutrient status, major ions and contaminants in the flooded pit (1993)

|  | Depth | Nutrients, mg/L |                 |                 |                    | Dissolved Ion Concentrations, mg/L |     |     |      |      |                 |     |                  |       |      | DS<br>um |
|--|-------|-----------------|-----------------|-----------------|--------------------|------------------------------------|-----|-----|------|------|-----------------|-----|------------------|-------|------|----------|
|  |       | PO <sub>4</sub> | NO <sub>3</sub> | NH <sub>4</sub> | V <sub>1</sub> TKN | K                                  | Ca  | Mg  | Na   | Fe   | SO <sub>4</sub> | Cl  | HCO <sub>3</sub> | As    | Ni   |          |
| March 7<br><br>Inverse Stratification        | 0     | 0.46            |                 | 0.01            |                    | 1.6                                | 6.0 | 2.0 | 2.2  | 0.38 | 8.0             | 2.0 | 14               | 0.242 | 0.28 | 65       |
|  | 5     | 0.34            |                 | 0.01            |                    | 1.4                                | 4.0 | 2.0 | 2.0  | 0.35 | 7.0             | 2.0 | 12               | 0.211 | 0.26 | 60       |
|  | 10    | 0.25            |                 | 0.03            |                    | 1.3                                | 5.0 | 2.0 | 1.9  | 0.35 | 7.0             | 2.0 | 12               | 0.179 | 0.24 | 59       |
|  | 15    | 0.40            |                 | 0.03            |                    | 1.3                                | 5.0 | 2.0 | 1.8  | 0.37 | 7.0             | 2.0 | 12               | 0.173 | 0.24 | 67       |
|  | 20    | 0.21            |                 | 0.03            |                    | 1.3                                | 5.0 | 2.0 | 1.8  | 0.39 | 8.0             | 2.0 | 12               | 0.168 | 0.27 | 67       |
|  | 25    | 0.28            |                 | 0.01            |                    | 1.3                                | 5.0 | 2.0 | 1.8  | 0.37 | 7.0             | 2.0 | 12               | 0.177 | 0.26 | 64       |
|  | 30    | 0.28            |                 | 0.01            |                    | 1.3                                | 5.0 | 2.0 | 1.8  | 0.36 | 8.0             | 2.0 | 12               | 0.208 | 0.24 | 64       |
|  | 35    | 0.31            |                 | 0.01            |                    | 1.3                                | 5.0 | 2.0 | 1.8  | 0.38 | 8.0             | 2.0 | 11               | 0.230 | 0.27 | 61       |
|  | 40    | 0.34            |                 | 0.01            |                    | 1.4                                | 5.0 | 2.0 | 2.0  | 0.36 | 8.0             | 2.0 | 12               | 0.237 | 0.31 | 64       |
|  | 45    | 1.84            |                 | 0.03            |                    | 2.4                                | 9.0 | 5.0 | 2.8  | 0.32 | 28.0            | 2.0 | 11               | 0.249 | 1.20 | 96       |
| June 11<br><br>Above<br>Below<br>Thermocline | 0     | 1.41            | 0.75            | < 0.01          | 0.20               | 1.3                                | 4.0 | 1.7 | 1.8  | 0.10 | 9.2             | 0.4 | 13               | 0.210 | 0.30 | 50       |
|  | 2     | 1.10            | 0.75            | < 0.01          | 0.49               | 1.3                                | 3.7 | 1.6 | 1.8  | 0.22 | 8.8             | 0.4 | 14               | 0.240 | 0.27 | 50       |
|  | 12    | 1.90            | 0.75            | < 0.01          | 0.33               | 1.3                                | 3.8 | 1.6 | 1.7  | 0.18 | 9.0             | 0.5 | 14               | 0.240 | 0.27 | 46       |
|  | 22    | 0.98            | 0.71            | < 0.01          | 0.75               | 1.4                                | 3.7 | 1.6 | 1.8  | 0.19 | 9.0             | 0.5 | 14               | 0.230 | 0.26 | 48       |
|  | 32    | 1.04            | 0.71            | < 0.01          | 0.48               | 1.5                                | 3.8 | 1.6 | 1.8  | 0.19 | 9.0             | 0.6 | 13               | 0.230 | 0.25 | 50       |
|  | 40    | 0.92            | 0.84            | < 0.01          | 0.37               | 1.7                                | 3.8 | 1.6 | 1.8  | 0.20 | 9.1             | 0.8 | 13               | 0.230 | 0.27 | 51       |
| June 29<br><br>Above<br>Below<br>Thermo-     | 0     | 1.66            |                 | < 0.01          |                    | 1.3                                | 5.0 | 3.0 | 2.0  | 0.35 | 9.0             | < 1 | 14               | 0.270 | 0.23 | 52       |
|  | 5     | 1.17            |                 | 0.01            |                    | 1.3                                | 5.0 | 3.0 | 1.7  | 0.37 | 9.0             | < 1 | 15               | 0.360 | 0.25 | 57       |
|  | 10    | 1.59            |                 | 0.03            |                    | 1.4                                | 4.0 | 3.0 | 2.0  | 0.40 | 9.0             | < 1 | 13               | 0.230 | 0.27 | 61       |
|  | 15    | 1.93            |                 | 0.03            |                    | 1.4                                | 4.0 | 3.0 | 1.8  | 0.37 | 9.0             | < 1 | 13               | 0.220 | 0.27 | 59       |
|  | 20    | 1.29            |                 | 0.03            |                    | 1.4                                | 4.0 | 3.0 | 1.8  | 0.45 | 9.0             | < 1 | 13               | 0.260 | 0.27 | 59       |
|  | 25    | 1.26            |                 | 0.01            |                    | 1.3                                | 4.0 | 4.0 | 1.8  | 0.41 | 9.0             | < 1 | 13               | 0.300 | 0.29 | 62       |
|  | 30    | 0.80            |                 | 0.31            |                    | 1.4                                | 5.0 | 4.0 | 1.8  | 0.41 | 9.0             | < 1 | 13               | 0.240 | 0.28 | 59       |
| 35   | 1.04  |                 | 0.01            |                 | 1.4                | 5.0                                | 4.0 | 1.8 | 0.43 | 9.0  | < 1             | 13  | 0.250            | 0.28  | 55   |          |
| Aug. 22<br><br>Above<br>Below<br>Thermocline | 0     | 0.31            |                 | < 0.01          |                    | 1.3                                | 3.7 | 1.6 | 1.7  | 0.07 | 10.0            | 3.0 | 13               | 0.268 | 0.15 | 45       |
|  | 5     | 0.34            |                 | < 0.01          |                    | 1.6                                | 3.9 | 1.6 | 1.7  | 0.08 | 10.0            | 3.0 | 13               | 0.309 | 0.17 | 48       |
|  | 10    | 0.34            |                 | 0.01            |                    | 1.5                                | 4.0 | 1.7 | 1.8  | 0.29 | 10.0            | 3.0 | 13               | 0.320 | 0.27 | 48       |
|  | 15    | 0.49            |                 | 0.01            |                    | 1.7                                | 4.1 | 1.8 | 1.8  | 0.27 | 9.0             | 3.0 | 13               | 0.277 | 0.29 | 51       |
|  | 20    | 0.40            |                 | 0.01            |                    | 1.6                                | 4.2 | 1.8 | 1.8  | 0.24 | 9.0             | 3.0 | 14               | 0.329 | 0.28 | 49       |
|  | 25    | 0.55            |                 | 0.01            |                    | 1.7                                | 4.2 | 1.8 | 1.9  | 0.29 | 9.0             | 3.0 | 13               | 0.313 | 0.29 | 50       |
|  | 30    | 0.49            |                 | 0.01            |                    | 1.8                                | 4.4 | 1.8 | 1.9  | 0.26 | 10.0            | 3.0 | 13               | 0.350 | 0.31 | 51       |
|  | 35    | 0.49            |                 | 0.01            |                    | 2.0                                | 4.1 | 1.7 | 1.8  | 0.27 | 10.0            | 3.0 | 13               | 0.376 | 0.33 | 53       |
| Oct. 9<br><br>Circulation                    | 0     | 0.46            |                 | < 0.01          |                    | 1.3                                | 5.0 | 2.0 | 1.6  |      | 10.0            | 1.0 | 14               | 0.316 | 0.25 |          |
|  | 5     | 0.46            |                 | < 0.01          |                    | 1.3                                | 5.0 | 2.0 | 1.6  |      | 10.0            | < 1 | 14               | 0.328 | 0.26 |          |
|  | 10    | 0.46            |                 | < 0.01          |                    | 1.3                                | 5.0 | 2.0 | 1.6  |      | 10.0            | 2.0 | 14               | 0.324 | 0.27 |          |
|  | 15    | 0.49            |                 | < 0.01          |                    | 1.3                                | 5.0 | 2.0 | 1.6  |      | 10.0            | 1.0 | 14               | 0.312 | 0.30 |          |
|  | 20    | 0.43            |                 | < 0.01          |                    | 1.3                                | 5.0 | 2.0 | 1.6  |      | 10.0            | < 1 | 14               | 0.300 | 0.29 |          |
|  | 25    | 0.34            |                 | < 0.01          |                    | 1.3                                | 5.0 | 3.0 | 1.6  |      | 10.0            | 1.0 | 14               | 0.288 | 0.27 |          |
|  | 30    | 0.34            |                 | < 0.01          |                    | 1.3                                | 6.0 | 2.0 | 1.6  |      | 10.0            | 1.0 | 14               | 0.318 | 0.29 |          |
|  | 35    | 0.43            |                 | < 0.01          |                    | 1.3                                | 5.0 | 1.0 | 1.6  |      | 10.0            | < 1 | 14               | 0.304 | 0.29 |          |
|  | 40    | 0.4             |                 | < 0.01          |                    | 1.3                                | 6.0 | 3.0 | 1.6  |      | 10.1            | 1.0 | 14               | 0.294 | 0.29 |          |
|  | 45    | 0.46            |                 | < 0.01          |                    | 1.2                                | 6.0 | 2.0 | 1.6  |      | 10.0            | 1.0 | 14               | 0.318 | 0.29 |          |

\* Multiple discontinuity layers

Table A3-1c: Nutrient status, major ions and contaminants in the flooded pit (1994).

|                  | Depth   | Nutrients, mg/L |                 |                 |       | Dissolved Ion Concentrations, mg/L |     |      |     |                 |    |                  |         |         |      | DS<br>µm |
|------------------|---------|-----------------|-----------------|-----------------|-------|------------------------------------|-----|------|-----|-----------------|----|------------------|---------|---------|------|----------|
|                  |         | PO <sub>4</sub> | NO <sub>3</sub> | NH <sub>4</sub> |       | Ca                                 | Mg  | Na   | Fe  | SO <sub>4</sub> | Cl | HCO <sub>3</sub> | As      | Ni      |      |          |
| April 17         | 0       | 0.40            |                 | 0.01            |       | 7                                  | 3   | 2.4  |     | 11              | <1 | 16               | 0.370   | 0.26    | 56   |          |
|                  | 5       | 0.43            |                 | 0.01            |       | 6                                  | 2   | 2.6  |     | 11              | <1 | 16               | 0.380   | 0.28    | 52   |          |
|                  | 10      | 0.43            |                 | 0.01            |       | 5                                  | 3   | 2.3  |     | 11              | <1 | 17               | 0.380   | 0.20    | 53   |          |
|                  | 15      | 0.40            |                 | <0.01           |       | 5                                  | 2   | 2.1  |     | 12              | <1 | 16               | 0.350   | 0.20    | 52   |          |
|                  | 20      | 0.37            |                 | <0.01           |       | 5                                  | 2   | 2    |     | 11              | <1 | 16               | 0.310   | 0.26    | 52   |          |
|                  | 25      | 0.40            |                 | <0.01           |       | 5                                  | 3   | 2.1  |     | 10              |    | 16               | 0.310   | 0.27    | 49   |          |
|                  | 30      | 0.40            |                 | <0.01           |       | 5                                  | 2   | 1.8  |     | 10              | <1 | 15               | 0.310   | 0.26    | 50   |          |
|                  | 35      | 0.43            |                 | <0.01           |       | 6                                  | 3   | 1.8  |     | 11              | <1 | 16               | 0.360   | 0.30    | 51   |          |
|                  | 40      | 0.49            |                 | <0.01           |       | 7                                  | 3   | 1.8  |     | 12              | <1 | 16               | 0.400   | 0.32    | 56   |          |
| 45               | 1.29    |                 | <0.01           |                 | 8     | 5                                  | 2.8 |      | 22  | <1              | 17 | 0.720            | 0.67    | 75      |      |          |
| June 26          | 0       | 0.49            | 0.09            | <0.013          |       |                                    |     |      |     |                 |    |                  |         |         | 55   |          |
| Above            | 2       | 0.43            | 0.13            | <0.013          |       |                                    |     |      |     |                 |    |                  |         |         | 54   |          |
| Below            | 12      | 0.34            | 0.53            | <0.013          |       |                                    |     |      |     |                 |    |                  |         |         | 54   |          |
| Thermo-<br>cline | 22      | 0.43            | 0.48            | <0.013          |       |                                    |     |      |     |                 |    |                  |         |         | 53   |          |
|                  | 32      | 0.40            | 0.53            |                 |       |                                    |     |      |     |                 |    |                  |         |         | 57   |          |
|                  | 43      | 0.46            | 0.62            |                 |       |                                    |     |      |     |                 |    |                  |         |         | 60   |          |
|                  |         |                 |                 |                 |       |                                    |     | 1.8  |     | 11              |    |                  |         |         |      |          |
|                  |         |                 |                 |                 |       |                                    |     |      |     |                 |    |                  |         |         |      |          |
| June 28          | 0       | 0.43            | 0.40            | <0.01           |       | 6                                  | 2   |      |     | <1              | 15 | 0.390            | 0.24    | 51      |      |          |
| Above            | 5       | 0.43            | 0.75            | <0.01           |       | 5                                  | 2   |      |     | <1              | 15 | 0.390            | 0.32    | 49      |      |          |
| Below            | 10      | 0.43            | 0.88            | <0.01           |       | 5                                  | 2   | 1.8  |     | 10              | 1  | 15               | 0.400   | 0.29    | 50   |          |
| Thermo-<br>cline | 15      | 0.46            | 0.88            | <0.01           |       | 5                                  | 2   | 2    |     | 10              | <1 | 15               | 0.410   | 0.32    | 61   |          |
|                  | 20      | 0.40            | 0.84            | <0.01           |       | 5                                  | 2   | 2    |     | 10              | <1 | 15               | 0.400   | 0.30    | 54   |          |
|                  | 25      | 0.43            | 0.92            | <0.01           |       | 5                                  | 2   | 2    |     | 10              | <1 | 15               | 0.39(*) | 0.29(*) | 61   |          |
|                  | 30      | 0.68            | 0.92            | <0.01           |       | 5                                  | 2   | 1.8  |     | 10              | <1 | 15               | 0.380   | 0.27    | 64   |          |
|                  | 35      | 0.49            | 0.92            | <0.01           |       | 5                                  | 2   | 2    |     | 10              | <1 | 15               | 0.390   | 0.30    | 56   |          |
|                  | 40      | 0.34            | 0.92            | <0.01           |       | 5                                  | 2   | 2    |     | 11              | <1 | 15               | 0.400   | 0.28    | 56   |          |
|                  | 45      | 0.46            | 0.97            | <0.01           |       | 6                                  | 2   | 2    |     | 11              | <1 | 15               | 0.420   | 0.28    | 55   |          |
|                  | 47      | 0.31            | 0.97            | <0.01           |       | 6                                  | 2   | 2    |     | 11              | <1 | 15               | 0.410   | 0.32    | 58   |          |
|                  | Aug. 16 | 0               | 0.49            | 0.04            | <0.01 |                                    | 6   | 2    | 1.6 |                 | 11 | <1               | 15      | 0.290   | 0.12 | 63       |
| Above            | 5       | 0.49            | <0.04           | <0.01           |       | 7                                  | <1  | 2.3  |     | 11              | <1 | 15               | 0.300   | 0.12    | 54   |          |
| Below            | 10      | 0.46            | 0.70            | 0.02            |       | 6                                  | 2   | 2.2  |     | 10              | <1 | 14               | 0.290   | 0.28    | 53   |          |
| Thermo-<br>cline | 15      | 0.49            | 0.79            | <0.01           |       | 6                                  | 2   | 2    |     | 10              | <1 | 14               | 0.270   | 0.28    | 49   |          |
|                  | 20      | 0.46            | 0.79            | <0.01           |       | 6                                  | 2   | 2    |     | 10              | <1 | 15               | 0.280   | 0.28    | 52   |          |
|                  | 25      | 0.43            | 0.79            | <0.01           |       | 6                                  | <1  | 2.2  |     | 10              | <1 | 15               | 0.240   | 0.32    | 50   |          |
|                  | 30      | 0.46            | 0.79            | 0.01            |       | 6                                  | 1   | 2.2  |     | 10              | <1 | 15               | 0.270   | 0.30    | 49   |          |
|                  | 35      | 0.49            | 0.84            | 0.01            |       | 7                                  | <1  | 2.3  |     | 10              | <1 | 15               | 0.280   | 0.34    | 49   |          |
|                  | 40      | 0.52            | 0.84            | 0.01            |       | 6                                  | <1  | 2.3  |     | 10              | <1 | 15               | 0.280   | 0.36    | 52   |          |
|                  | 45      | 0.58            | 0.88            | 0.02            |       | 6                                  | 1   | 2.3  |     | 12              | <1 | 15               | 0.320   | 0.40    | 53   |          |
| Sept. 9          | 0       | 0.46            | <0.04           | 0.68            |       |                                    |     |      |     |                 |    |                  | 0.240   | 0.13    |      |          |
| Above            | 2       | 0.43            | <0.04           | 0.01            |       |                                    |     |      |     |                 |    |                  | 0.270   | 0.13    |      |          |
| Below            | 12      | 0.43            | 0.75            | 0.08            |       |                                    |     |      |     |                 |    |                  | 0.250   | 0.27    |      |          |
| Thermo-<br>cline | 22      | 0.46            | 0.79            | 0.05            |       |                                    |     |      |     |                 |    |                  | 0.240   | 0.30    |      |          |
|                  | 32      | 0.46            | 0.84            | 0.05            |       |                                    |     | 0.24 |     |                 |    |                  | 0.250   | 0.29    |      |          |
|                  | 42      | 0.67            | 0.82            | 0.05            |       |                                    |     | 0.22 |     |                 |    |                  | 0.260   | 0.29    |      |          |
|                  |         |                 |                 |                 |       |                                    |     |      |     |                 |    |                  |         |         |      |          |
|                  |         |                 |                 |                 |       |                                    |     |      |     |                 |    |                  |         |         |      |          |
| Oct. 9           | 0       | 0.55            | <0.04           | <0.01           |       | 6                                  | 3   | 2    |     | 11              | <1 | 15               | 0.260   | 0.17    | 54   |          |
|                  | 5       | 0.37            | <0.04           | <0.01           |       | 6                                  | 3   | 2.1  |     | 11              | <1 | 14               | 0.240   | 0.15    | 51   |          |
|                  | 10      | 0.40            | <0.04           | <0.01           | 1.3   | 6                                  | 4   | 2.1  |     | 11              | <1 | 14               | 0.250   | 0.16    | 58   |          |
| Above            | 15      | 0.40            | <0.04           | <0.01           | 1.2   | 3                                  | 3   | 1.6  |     | 11              | <1 | 14               | 0.280   | 0.17    | 50   |          |
| Below            | 20      | 0.43            | 0.70            | 0.01            | 1.5   | 3                                  | 2   | 2.2  |     | 11              | <1 | 14               | 0.260   | 0.31    | 51   |          |
| Thermo-<br>cline | 25      | 0.43            | 0.79            | 0.02            | 1.2   | 3                                  | 3   | 1.6  |     | 11              | <1 | 14               | 0.250   | 0.26    | 49   |          |
|                  | 30      | 0.37            | 0.79            | 0.03            | 1.2   | 3                                  | 2   | 1.6  |     | 11              | 1  | 14               | 0.260   | 0.27    | 53   |          |
|                  | 35      | 0.58            | 0.84            | 0.02            | 1.2   | 3                                  | 2   | 2    |     | 12              | <1 | 14               | 0.280   | 0.26    | 54   |          |
|                  | 40      | 0.49            | 0.88            | 0.01            | 1.3   | 3                                  | 3   | 2    |     | 12              | <1 | 14               | 0.310   | 0.34    | 54   |          |
|                  | 43      | 0.52            | 0.88            | 0.02            | 1.3   | 3                                  | 4   | 2.1  |     | 13              | 2  | 14               | 0.350   | 0.31    | 59   |          |

iv) n above and below water samples reported.



Table A3-1d: Nutrient status, major ions and contaminants in the flooded pit (1995).

|          | Depth   | Nutrients, mg/L |                 |                 |       | Dissolved Ion Concentrations, mg/L |     |    |     |      |                 |    |                  |       |       | DS<br>um |    |
|----------|---------|-----------------|-----------------|-----------------|-------|------------------------------------|-----|----|-----|------|-----------------|----|------------------|-------|-------|----------|----|
|          |         | PO <sub>4</sub> | NO <sub>3</sub> | NH <sub>4</sub> | N,TKN | K                                  | Ca  | Mg | Na  | Fe   | SO <sub>4</sub> | Cl | HCO <sub>3</sub> | As    | Ni    |          |    |
| April 12 | 0       | 0.46            | 0.44            | 0.01            |       | 1.6                                | 6   | 3  | 23  | 0.29 | 11              | <1 | 20               | 0.280 | 0.29  | 61       |    |
|          | 5       | 0.43            | 0.44            | 0.03            |       | 1.5                                | 5   | 2  | 22  | 0.27 | 11              | <1 | 19               | 0.260 | 0.28  | 58       |    |
|          | 10      | 0.40            | 0.4             | 0.01            |       | 1.5                                | 5   | 2  | 21  | 0.27 | 10              | <1 | 19               | 0.280 | 0.27  | 48       |    |
|          | 15      | 0.40            | 0.35            | 0.03            |       | 1.4                                | 6   | 2  | 21  | 0.29 | 10              | <1 | 19               | 0.250 | 0.25  | 59       |    |
|          | 20      | 0.40            | 0.44            | 0.03            |       | 1.3                                | 6   | 3  | 21  | 0.37 | 10              | <1 | 20               | 0.220 | 0.26  | 59       |    |
|          | 25      | 0.40            | 0.57            | 0.03            |       | 1.3                                | 4   | 3  | 26  | 0.36 | 10              | <1 | 19               | 0.230 | 0.24  | 60       |    |
|          | 30      | 0.37            | 0.4             | 0.01            |       | 1.2                                | 6   | 3  | 2   | 0.33 | 10              | <1 | 20               | 0.240 | 0.25  | 60       |    |
|          | 35      | 0.37            | 0.53            | 0.03            |       | 1.5                                | 6   | 2  | 22  | 0.34 | 10              | <1 | 19               | 0.240 | 0.26  | 58       |    |
|          | 40      | 0.49            | 0.7             | 0.01            |       | 1.6                                | 6   | 2  | 22  | 0.38 | 11              | <1 | 20               | 0.300 | 0.30  | 70       |    |
|          | 45      |                 |                 | 0.04            |       | 1.8                                | 5   | 3  | 24  |      | 15              | <1 | 22               |       |       |          |    |
| June 14  | 0       | 0.40            | 0.13            | 0.05            | 0.24  | 1.3                                | 5   | 3  | 2   | 0.29 | 10              | <1 | 19               | 0.224 | 0.22  | 61       |    |
|          | 5       |                 | 0.53            |                 |       | 1.2                                | 5   | 3  | 2   | 0.29 | 10              | <1 | 19               | 0.290 | 0.25  | 64       |    |
|          | Above   | 10              | 1.38            | 0.35            | 0.05  | 0.14                               | 1.4 | 4  | 2   | 2    | 0.29            | 11 | <1               | 19    | 0.326 | 0.27     | 65 |
|          | Below   | 15              | 0.28            | 0.40            | 0.08  | 0.31                               | 1.4 | 5  | 2   | 2    | 0.31            | 10 | <1               | 19    | 0.197 | 0.27     | 64 |
|          | Thermo- | 20              | 0.21            | 0.35            | 0.03  | 0.16                               | 1.4 | 5  | 2   | 2    | 0.31            | 10 | <1               | 19    | 0.192 | 0.29     | 60 |
|          | cline   | 25              | 0.28            | 0.40            | 0.12  | 0.24                               | 1.4 | 5  | 3   | 2    | 0.34            | 10 | <1               | 19    | 0.221 | 0.29     | 60 |
|          |         | 30              | 0.40            | 0.40            | 0.1   | 0.63                               | 1.4 | 5  | 2   | 1.7  | 0.32            | 10 | <1               | 19    | 0.256 | 0.28     | 59 |
|          |         | 35              | 0.46            | 0.35            | 0.03  | 0.8                                | 1.3 | 5  | 2   | 2.1  | 0.37            | 11 | <1               | 19    | 0.247 | 0.31     | 56 |
|          |         | 40              | 0.49            | 0.44            | 0.07  | 0.27                               | 1.5 | 6  | 3   | 1.8  | 0.38            | 11 | <1               | 20    | 0.266 | 0.31     | 62 |
| Aug. 17  | 0       | 0.38            | 0.04            | 0.1             |       | 1.4                                | 5   | 3  | 2.1 |      | 10              | 1  | 19               | 0.270 | 0.17  | 58       |    |
|          | 5       | 0.46            | 0.04            | 0.05            |       | 1.4                                | 5   | 3  | 2.1 |      | 10              | 1  | 18               | 0.260 | 0.18  | 56       |    |
|          | Above   | 10              | 0.77            | 0.35            | 0.05  |                                    | 1.4 | 5  | 3   | 2.1  |                 | 10 | <1               | 19    | 0.280 | 0.24     | 57 |
|          | Below   | 15              | 0.37            | 0.31            | 0.04  |                                    | 1.4 | 5  | 3   | 2.1  |                 | 10 | <1               | 19    | 0.280 | 0.25     | 56 |
|          | Thermo- | 20              | 0.40            | 0.35            | 0.05  |                                    | 1.4 | 5  | 3   | 2.1  |                 | 10 | <1               | 19    | 0.220 | 0.26     | 56 |
|          | cline   | 25              | 0.52            | 0.44            | 0.18  |                                    | 1.4 | 6  | 3   | 2.2  |                 | 10 | <1               | 19    | 0.230 | 0.26     | 58 |
|          |         | 30              | 0.52            | 0.48            | 0.09  |                                    | 1.5 | 6  | 3   | 2.1  |                 | 10 | 1                | 19    | 0.240 | 0.28     | 58 |
|          |         | 35              | 0.61            | 0.40            | 0.13  |                                    | 1.5 | 6  | 3   | 2.2  |                 | 11 | 2                | 19    | 0.290 | 0.29     | 57 |
|          |         | 40              | 0.64            | 0.62            | 0.22  |                                    | 1.4 | 5  | 3   | 2.2  |                 | 10 | 1                | 19    | 0.310 | 0.32     | 56 |
|          |         | 45              | 0.77            | 0.40            | 0.04  |                                    | 1.5 | 6  | 3   | 2.8  |                 | 11 | 1                | 19    | 0.370 | 0.36     | 58 |
| Oct. 14  | 0       | 0.37            | 0.13            | 0.05            |       | 1.4                                | 5   | 2  | 2   |      | 10              | <1 | 21               | 0.100 | 0.24  | 59       |    |
|          | 5       | 0.43            | 0.09            | 0.03            |       | 1.4                                | 5   | 3  | 2   |      | 11              | <1 | 21               | 0.190 | 0.24  | 58       |    |
|          | 10      | 0.31            | 0.09            | 0.05            |       | 1.4                                | 5   | 3  | 1.8 |      | 10              | <1 | 21               | 0.170 | 0.22  | 58       |    |
|          | 15      | 0.28            | 0.18            | 0.03            |       | 1.4                                | 5   | 3  | 1.8 |      | 10              | <1 | 21               | 0.180 | 0.22  | 60       |    |
|          | Above   | 20              | 0.43            | 0.09            | 0.03  |                                    | 1.4 | 5  | 2   | 2.1  |                 | 10 | <1               | 21    | 0.240 | 0.24     | 66 |
|          | Below   | 25              | 0.18            | 0.31            | 0.08  |                                    | 1.4 | 5  | 3   | 1.8  |                 | 11 | <1               | 21    | 0.140 | 0.24     | 91 |
|          | Thermo- | 30              | 0.31            | 0.48            | 0.03  |                                    | 1.4 | 5  | 3   | 1.9  |                 | 11 | <1               | 22    | 0.250 | 0.29     | 63 |
|          | cline   | 35              | 0.43            | 0.48            | 0.03  |                                    | 1.4 | 6  | 2   | 2.1  |                 | 11 | <1               | 21    | 0.270 | 0.33     | 66 |
|          | 40      | 0.49            | 0.44            | 0.03            |       | 1.4                                | 5   | 3  | 1.9 |      | 13              | <1 | 22               | 0.340 | 0.31  | 67       |    |

Table A3-1e: Nutrient status, major ions and contaminants in the flooded pit (1996)

| Depth   | Nutrients, mg/L  |                 |                 |       | Dissolved Ion Concentrations, mg/L |     |     |     |     |                 |     |                  |       |       | DS<br>um |      |    |
|---------|------------------|-----------------|-----------------|-------|------------------------------------|-----|-----|-----|-----|-----------------|-----|------------------|-------|-------|----------|------|----|
|         | PO <sub>4</sub>  | NO <sub>3</sub> | NH <sub>4</sub> | N,TKN | K                                  | Ca  | Mg  | Na  | Fe  | SO <sub>4</sub> | Cl  | HCO <sub>3</sub> | As    | Ni    |          |      |    |
| Layer 9 | 0                | 0.40            | 0.66            | 0.03  |                                    | 1.2 | 5.5 | 2.5 | 1.9 |                 | 12  | 0.5              | 21    | 0.230 | 0.28     | 70   |    |
|         | 5                | 0.40            | 0.75            | 0.01  |                                    | 1.3 | 5.5 | 2.4 | 2.2 |                 | 12  | 0.5              | 21    | 0.230 | 0.28     | 67   |    |
|         | 10               | 0.37            | 0.75            | 0.03  |                                    | 1.2 | 5.7 | 2.4 | 2.3 |                 | 12  | 0.5              | 22    | 0.220 | 0.27     | 68   |    |
|         | 15               | 0.40            | 0.48            | 0.03  |                                    | 1.2 | 5.6 | 2.4 | 2.3 |                 | 12  | 0.5              | 21    | 0.210 | 0.28     | 88   |    |
|         | 20               | 0.40            | 0.48            | 0.03  |                                    | 0.7 | 5.6 | 2.4 | 2.2 |                 | 12  | 0.4              | 21    | 0.190 | 0.27     | 82   |    |
|         | 25               | 0.40            | 0.53            | 0.03  |                                    | 1   | 5.6 | 2.4 | 2.2 |                 | 12  | 0.4              | 22    | 0.190 | 0.27     | 83   |    |
|         | 30               | 0.31            | 0.57            | 0.04  |                                    | 1.7 | 5.7 | 2.4 | 2.1 |                 | 12  | 0.4              | 22    | 0.200 | 0.28     | 81   |    |
|         | 35               | 0.37            | 0.35            | 0.04  |                                    | 1.7 | 5.6 | 2.4 | 2.2 |                 | 12  | 0.4              | 23    | 0.200 | 0.28     | 78   |    |
|         | 40               | 0.40            | 0.18            | 0.04  |                                    | 1.4 | 5.8 | 2.5 | 2.2 |                 | 13  | 0.5              | 22    | 0.240 | 0.31     | 64   |    |
| Aug. 26 | 0                | 0.24            | 0.04            | 0.05  |                                    | 1.6 | 5.8 | 2.3 | 2.2 |                 | 12  | 0.5              | 21    | 0.190 | 0.22     | 54   |    |
|         | Above            | 5               | 0.21            | 0.04  | 0.03                               |     | 2.3 | 5.9 | 2.4 | 2               |     | 13               | 0.5   | 21    | 0.200    | 0.22 | 49 |
|         | Below            | 10              | 0.21            | 0.04  | 0.02                               |     | 1.8 | 5.7 | 2.4 | 2.1             |     | 13               | 0.5   | 21    | 0.200    | 0.27 | 52 |
|         | Thermo-<br>cline | 15              | 0.21            | 0.04  | 0.01                               |     | 2.3 | 5.9 | 2.4 | 2.1             |     | 13               | 0.6   | 21    | 0.200    | 0.28 | 49 |
|         |                  | 20              | 0.24            | 0.04  | 0.05                               |     | 2.2 | 6.1 | 2.5 | 2.2             |     | 13               | 0.5   | 21    | 0.210    | 0.29 | 53 |
|         |                  | 25              | 0.21            | 0.04  | 0.1                                |     | 2   | 5.2 | 2.1 | 1.9             |     | 11               | 0.6   | 21    | 0.180    | 0.27 | 55 |
|         |                  | 30              | 0.21            | 0.04  | 0.04                               |     | 1.9 | 5.3 | 2.1 | 1.9             |     | 11               | 0.6   | 21    | 0.220    | 0.27 | 51 |
|         |                  | 35              | 0.31            | 0.09  | 0.03                               |     | 1.9 | 5.6 | 2.3 | 1.9             |     | 12               | 0.5   | 22    | 0.280    | 0.33 | 52 |
| 40      | 0.37             | 0.13            | 0.04            |       | 2.1                                | 5.8 | 2.4 | 2.1 |     | 13              | 0.6 | 22               | 0.310 | 0.32  | 61       |      |    |
| Oct. 28 | 0                | 0.34            | 0.13            | 0.01  |                                    | 2   | 5.8 | 2.6 | 2.2 |                 | 13  | 0.5              | 22    | 0.220 | 0.27     | 50   |    |
|         | 5                | 0.31            | 0.18            | 0.04  |                                    | 1.9 | 5.9 | 2.6 | 2.2 |                 | 13  | 0.5              | 22    | 0.200 | 0.27     | 51   |    |
|         | 10               | 0.31            | 0.13            | 0.01  |                                    | 1.3 | 5.9 | 2.6 | 2.1 |                 | 13  | 0.5              | 22    | 0.200 | 0.25     | 51   |    |
|         | 15               | 0.31            | 0.09            | 0.05  |                                    | 1.8 | 5.9 | 2.6 | 2.2 |                 | 13  | 0.5              | 22    | 0.200 | 0.26     | 51   |    |
|         | 20               | 0.31            | 0.22            | 0.03  |                                    | 1.4 | 5.9 | 2.6 | 2.3 |                 | 13  | 0.5              | 22    | 0.210 | 0.27     | 49   |    |
|         | 25               | 0.31            | 0.13            | 0.01  |                                    | 1.7 | 5.8 | 2.6 | 2.3 |                 | 13  | 0.5              | 21    | 0.200 | 0.27     | 50   |    |
|         | 30               | 0.31            | 0.18            | 0.01  |                                    | 2.3 | 5.8 | 2.6 | 2.3 |                 | 13  | 0.6              | 21    | 0.210 | 0.26     | 52   |    |
|         | 35               | 0.37            | 0.13            | 0.01  |                                    | 1.7 | 5.9 | 2.6 | 2.4 |                 | 13  | 0.5              | 21    | 0.200 | 0.26     | 53   |    |
|         | 40               | 0.64            | 0.04            | 0.05  |                                    | 1.2 | 6   | 2.7 | 2.3 |                 | 13  | 0.6              | 21    | 0.180 | 0.25     | 53   |    |

Table A3-2: Major elements in material in sedimentation traps ( $\mu\text{g/g}$  dry weight basis)

| Year | 1992   |        | 1993 |        | 1994   |        |        | 1995   |        |        |        |        | 1996   |        |        |        |
|------|--------|--------|------|--------|--------|--------|--------|--------|--------|--------|--------|--------|--------|--------|--------|--------|
|      | Date   | Sedim. | Trap | Sedim. | Trap   | Sedim. | Algae  | 10-Aug | 10-Aug | 16-Sep | 16-Sep | 16-Sep | 26-Jun | 30-Aug | 30-Aug | 30-Aug |
|      | 25-Jul | Sedim. | Trap | 17-Aug | Sedim. | Trap   | 10-Sep | 10-Sep | 08-Sep | 10-Aug | 16-Sep | 16-Sep | 16-Sep | 30-Aug | 30-Aug | 30-Aug |
|      | 32 m   |        | 2 m  | 32 m   | 2 m    | 32 m   | 2 m    | 2 m    | 32 m   | 32 m   | 2 m    | 32 m   | Bottom | 2 m    | 12 m   | 22 m   |
| Al   | 15400  | 7190   | 7360 | na     | na     | 8980   | 5700   | 5810   | 3740   | 7210   | 6960   | 9620   | 16900  | 16200  | 14300  |        |
| As   | 144    | 323    | 363  | 150    | 520    | 1880   | 360    | 1910   | 143    | 729    | 3480   | 143    | 1250   | 1820   | 2090   |        |
| Ca   | 3280   | na     | na   | 3300   | 7300   | na     | na     | na     | na     | na     | na     | 2290   | 3870   | 3090   | 3190   |        |
| Fe   | 17600  | 9420   | 9480 | 13100  | 3800   | 14300  | 7900   | 12000  | 5610   | 9410   | 14000  | 10800  | 19800  | 20100  | 20200  |        |
| Mg   | 5580   | na     | na   | 3600   | 3400   | na     | na     | na     | na     | na     | na     | 2790   | 5640   | 5060   | 4570   |        |
| Mn   | 386    | 492    | 303  | 420    | 8800   | 608    | 415    | 455    | 687    | 634    | 548    | 160    | 2140   | 611    | 927    |        |
| Ni   | 166    | 1420   | 450  | 2300   | 1700   | 1070   | 1310   | 778    | 1180   | 916    | 668    | 149    | 1820   | 729    | 715    |        |
| P    | 758    | na     | na   | 600    | 1000   | na     | na     | na     | na     | na     | na     | 488    | 544    | 620    | 616    |        |
| S    | 117    | na     | na   | na     | na     | na     | na     | na     | na     | na     | na     | 570    | 726    | 632    | 655    |        |
| Si   | 644    | na     | na   | na     | na     | na     | na     | na     | na     | na     | na     | na     | na     | na     | na     |        |

na - not analyzed

Table A3-3: Major elements in material collected on 0.45 µm filter paper after filtering 2L of water ( µg/g dry weight basis)

| Sampling date: 16-June-199: |      |       |       |       |
|-----------------------------|------|-------|-------|-------|
| Sample                      | 2 m  | 12 m  | 22 m  | 32 m  |
| Element                     |      |       |       |       |
| Al                          | 5956 | 12980 | 10385 | 8222  |
| As                          | 235  | 1206  | 2117  | 1741  |
| Ca                          | 1131 | 2246  | 1690  | 1430  |
| Fe                          | 7432 | 20955 | 21115 | 17493 |
| Mg                          | 2306 | 5065  | 4362  | 3293  |
| Mn                          | 159  | 392   | 560   | 394   |
| Ni                          | 273  | 859   | 727   | 468   |
| P                           | 1077 | 1839  | 1996  | 2248  |
| S                           | na   | na    | na    | na    |
| Si                          | 3661 | 9045  | 6231  | 5117  |

na - not analyzed

**PART 4: BIOGEOCHEMICAL PATHWAYS OF ARSENIC IN LAKES  
ADSORPTION REACTIONS OF NICKEL SPECIES AT OXIDE SURFACES**

# Biogeochemical pathways of arsenic in lakes

Andrew Rodie, Jan J.P. Gerits, and Jose M. Azcue

**Abstract:** Owing to various human activities, arsenic (As) concentrations have increased in lakes and other aquatic ecosystems around the world. This increase of As concentrations has become a concern because of the known toxic, carcinogenic, mutagenic, and teratogenic effects of As on ecosystem organisms and humans. Understanding the biogeochemistry of As in the aquatic environment is therefore a topic of fundamental interest. This study presents a review of the major biogeochemical processes controlling the concentration of solid and dissolved As in freshwater lakes. These processes are dynamic and vary both temporally and spatially because of a complex relationship between microbial activity and various geochemical processes. Particularly the oxidation of As sulphides and the reduction of Fe and Mn oxyhydroxides at the sediment-water interface play an important role in the mobilization of As. These and other interactions among the various biogeochemical processes are synthesized in a conceptual model of As mobility in lakes.

*Key words:* arsenic cycling, biogeochemistry, freshwater lakes.

**Résumé :** Sous l'influence de diverses activités humaines, les teneurs en arsenic (As) ont augmenté dans les lacs et autres écosystèmes aquatiques dans le monde. Cette augmentation des teneurs en As devient un problème, compte tenu des effets toxiques, carcinogènes, mutagènes et tératogènes de l'As sur les organismes et les humains des écosystèmes. La compréhension de la biogéochimie de l'As dans les milieux aquatiques devient donc un sujet d'intérêt fondamental. Les auteurs présentent une revue des principaux processus biogéochimiques qui contrôlent les teneurs en As solide et dissout dans les lacs d'eau douce. Ces processus sont dynamiques et varient à la fois dans le temps et dans l'espace, impliquant de façon complexe l'activité microbienne et les différents processus géochimiques. L'oxydation des sulfures d'As et la réduction des oxyhydroxydes de Fe et de Mn, à l'interface du sédiment et de l'eau, joue un rôle particulièrement important dans la mobilisation de l'As. Dans un modèle conceptuel de la mobilité de l'As dans les lacs, les auteurs synthétisent cette interaction ainsi que d'autres impliquant divers processus biogéochimiques.

*Mots clés :* cyclage de l'arsenic, biogéochimie, lacs d'eau douce.

[Traduire par la rédaction]

## Introduction

Arsenic (As) compounds have been apparently known and used since about 3000 B.C. (Azcue and Nriagu 1994). Only in this century, with the advent of analytical technology, have we observed the contamination and poisoning of natural water systems by As. The concern for human health has been the impetus for much scientific research on As contamination in natural water systems. The specific toxic effect of As depends on its valency state (Hindmarsh

and McCurdy 1986). Arsenate ( $\text{AsO}_4^{3-}$ ), an analogue of phosphate, is taken up by most organisms via the phosphate transport system, whereas arsenite ( $\text{AsO}_3^{3-}$ ) forms covalent bonds with sulfur atoms present on active sites of many enzymes.

The main sources of As in lakes are summarized in Table 1. Rocks containing As minerals (sulphides and sulpho-salts) constitute the major natural source of As in lakes (Schaufelberger 1993). Weathered As compounds may be retained in the solid phase (soils, sediments) or dissolved in the liquid phase (water) and subsequently transported. Approximately 60% of the emission of As into the atmosphere is from natural sources: volcanism, forest wildfires, and volatilization (Walsh et al. 1979). Domestic and industrial waste waters, electric power plants, metal mining, smelting, and atmospheric fallout are the major direct sources of As in lakes. The main indirect sources of As are leaching of mine wastes and residues of agricultural chemicals. Despite the immense controversy, the major use of As (about 75% of the total consumption)

Received May 8, 1995.

A. Rodie and J.J.P. Gerits, University of Toronto, Geography Department, Toronto, ON M5S 1A1, Canada.  
J.M. Azcue, National Water Research Institute, P.O. Box 5050, Burlington, ON L7R 4A6, Canada.

Author to whom all correspondence should be sent at the following address: University of Toronto, Sidney Smith Hall, 100 St. George St., Toronto, ON M5S 1A1, Canada (e-mail: gerits@geog.utoronto.ca).

**Table 1.** Main sources of arsenic in lakes

| Natural                           | Anthropogenic  |
|-----------------------------------|--|
| Weathering of As-containing rocks | Base metal mining  |
| Volcanic emissions                | Smelting and refining  |
| Geothermal                        | Manufacturing processes  |
| Atmospheric deposition            | Atmospheric fallout  |
| Biological activity               | Agricultural runoff (herbicides, wood preservatives, insecticides) |
|                                   | Dumping of sewage sludge   |
|                                   | Domestic wastewater  |

is in the agricultural field (Nriagu and Azcue 1990). The high-pressure spraying techniques widely employed in the application of As herbicides and pesticides result in the contamination of soils, air, and surface waters. Arsenic is still used in wood preservatives and for debarking trees. The commonly used monosodium methanoarsenate and arsenous acid are highly soluble in water and easily leach from soils.

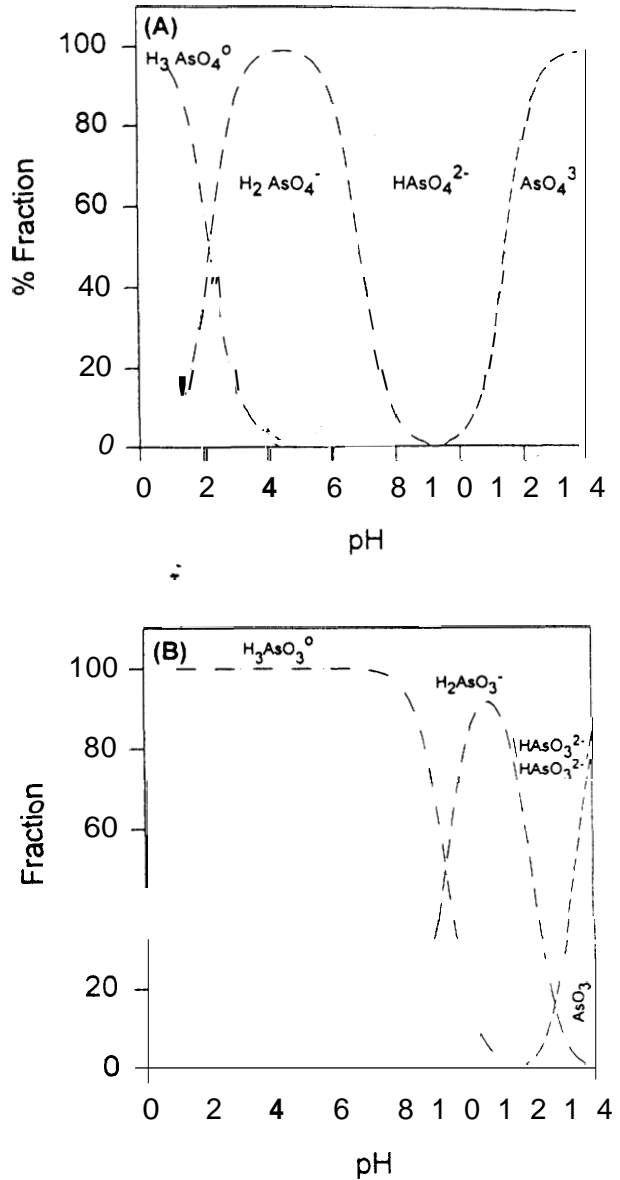
Reported concentrations of dissolved As in lakes in different parts of the world are listed in Table 2. Arsenic concentrations in uncontaminated lakes may vary from 0.1 to 20 µg·L<sup>-1</sup>, depending on bedrock geology, runoff, and evaporation. Assessment of the impact of specific contaminant sources has been the main reason for many studies. Dissolved arsenic concentrations in lake waters near a gold smelter in Yellowknife (Canada) ranged from 700 to 5500 µg·L<sup>-1</sup> (Wagemann 1978). Total As contents as high as 2780 µg·L<sup>-1</sup> have been reported in Union Lake, N.J. The source of contamination in the latter case is the industrial manufacture of As compounds (Faust et al. 1983). Recently, Anderson and Bruland (1991) reported dissolved As concentrations of 17 232 µg·L<sup>-1</sup> in Mono Lake, Calif. Although organic As species (methyl-As) have been found in some lakes (Abdel-Moatti 1990; Anderson and Bruland 1991; Braman and Foreback 1973), inorganic As species have been shown to be the dominant form of As in almost all lake waters.

The distribution of solid and dissolved As in lakes depends on biotic and abiotic reactions in the As cycle. The concentration of dissolved As is determined by aqueous complexation, surface complexation, dissolution, (co)precipitation, and redox reactions. The bioavailability of As is not only related to its dissolved, free ionic concentration (oxyanion) but also to the metabolism and affinity of organisms to assimilate As (Tessier and Campbell 1991). A detailed knowledge of the biogeochemical cycle is therefore required to predict the fate and impact of As in lakes. This paper presents a review of the biogeochemistry of As in lakes using a conceptual model of As mobility.

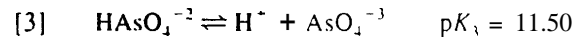
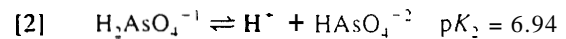
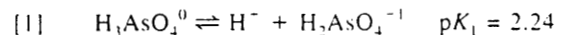
**Aqueous speciation**

Arsenic, a group VA elemental metalloid, has four oxidation states (-3, 0, +3, and +5). Similar to phosphorous, As forms a triprotic acid in aqueous solution and is therefore

**Fig. 1.** Fraction distribution diagram for (A) arsenic acid and (B) arsenous acid.



anionic in nature. The predominant form of As in oxic waters is As(V) as the triprotic arsenic acid:



Under anoxic conditions, usually within the sediment column, the most predominant form of As is As(III) as the triprotic arsenous acid:

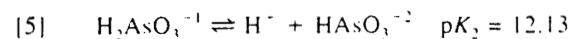


Figure 1 shows fraction distribution diagrams for arsenic

**Table 2.** Reported concentrations of dissolved arsenic ( $\mu\text{g}\cdot\text{L}^{-1}$ ) in different lake waters.

| Locations                 | Total dissolved |           | Inorganic | Methyl-As | Sources of As       | Ref                              |
|---------------------------|-----------------|-----------|-----------|-----------|---------------------|----------------------------------|
|                           | Average         | Range     |           |           |                     |                                  |
| <b>Canada</b>             |                 |           |           |           |                     |                                  |
| 9 Lakes in Sudbury        | 0.31            | 0.1-0.65  | —         | —         | Smelters            | Nriagu 1983                      |
| 6 Lakes Nova Scotia       | 1.64            | 0.2-5.8   | —         | —         | Mining              | Mudroch and Clair 1986           |
| Moirs Lake, Ontario       | 75              | —         | —         | —         | Mining              | Mudroch and Capobianco 1980      |
| Ossisko Lake, Quebec      | 1.2             | —         | —         | —         | Smelting            | Arafat 1985                      |
| 4 Lakes Northwest Territ. | 1 160           | 10-5500   | —         | —         | Mining              | Wagemann et al. 1978             |
| Thompson Lake             | 5               | 2-40      | —         | —         | Mining              | Moore 1981                       |
| Great Lakes               | 0.55            | 0.01-0.9  | —         | —         | Mix                 | Rossmann and Barres (1988)       |
| Jack of Clubs Lake, B.C.  | 0.38            | <0.2-0.41 | —         | —         | Mining              | Azcue et al 1994a                |
| <b>U S A</b>              |                 |           |           |           |                     |                                  |
| Lake Tahoe                | 1.12            | —         | 1.12      | 0.37      | u.i.*               | Anderson and Bruland 1991        |
| Lake Berreyssa            | 0.67            | —         | 0.6       | 0.06      | u.i.                | Anderson and Bruland 1991        |
| Lahe Ruth                 | 12              | —         | 11.2      | 0.77      | u.i.                | Anderson and Bruland 1991        |
| Mono Lake                 | 17 232          | —         | 17 232    | <7        | u.i.                | Anderson and Bruland 1991        |
| Pyramid Lake              | 97.4            | —         | 97.4      | 1.12      | u.i.                | Anderson and Bruland 1991        |
| Lake Ontario              | 0.52            | —         | 0.32      | 0.2       | u.i.                | Anderson and Bruland 1991        |
| Union Lake                | 1 895           | 28-2780   | 1224      | 1171      | As manufacture      | Faust et al. 1983                |
| Lake Echols               | 3.58            | —         | 3.15      | 0.43      | Mix                 | Braman and Foreback 1973         |
| Lake Magdalena            | 1.75            | —         | 1.38      | 0.37      | Mix                 | Braman and Foreback 1973         |
| Lake Wisconsin            | —               | 2-56      | —         | —         | —                   | Chamberland and Shapiro 1969     |
| 10 Minnesota Lakes        | 77.8            | 7-224     | —         | —         | —                   | Shapiro 1971                     |
| Chautauqua Lake           | 15.1            | 3.5-43.4  | —         | —         | Herbicides          | Lis and Hopke 1973               |
| Chaurauqua Lake           | —               | 10-14 600 | —         | —         | Herbicides          | Ullman et al. 1961               |
| Donner Lake               | 0.15            | —         | 0.135     | 0.011     | u.i.                | Andreae 1978                     |
| Saddlebag Lake            | 0.08            | —         | 0.07      | 0.008     | u.i.                | Andreae 1978                     |
| Squaw Lake                | 3.7             | —         | 3.56      | 0.102     | u.i.                | Andreae 1978                     |
| Lake Michigan             | 0.69            | 0.48-1.3  | —         | —         | Mix                 | Rossmann 1984                    |
| <b>Other</b>              |                 |           |           |           |                     |                                  |
| Lake Pavin, France        | 4.3             | —         | 4.55      | —         | u.i.                | Seyler and Martin 1989           |
| Lakes in Grece            | 12.9            | 1.3-54.5  | —         | —         | Mix                 | Baur and Onishi 1978             |
| Lakes in Japan            | 0.80            | 0.16-1.9  | —         | —         | Mix                 | Baur and Onishi 1978             |
| Nilo Delta Lakes, Egypt   | 3.63            | 1.2-18.2  | 95%       | 1-8%      | Herbicides + sewage | Abdel-Moati 1990                 |
| El-Temsah Lake, Egypt     | 0.29            | 0.22-0.58 | —         | —         | Sewage              | Abo-El-Wafa and Abdel-Shafy 1987 |

\*u.i., unidentified sources.

acid and arsenous acid based on thermodynamic data from Sadiq and Lindsay (1981). The first acid ionization constant of arsenous acid,  $\text{p}K_1 = 9.23$ , is well above the pH range of normal freshwater lakes. Therefore, the dominant arsenite acid species under anoxic conditions in lakes is the neutral aqueous species  $\text{H}_3\text{AsO}_3^0$ . A typical distribution of As(III) and As(V) species in the interstitial water of Moira Lake, Ont., is shown in Fig. 2 (Azcue et al. 1994b). Using the redox potential ( $E_h$ ) and assuming thermodynamic equilibrium, the distribution of As(III) and As(V) species concentrations can be estimated with

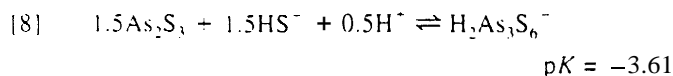
$$[7] \quad \log\left(\frac{[\text{As}^{3+}]}{[\text{As}^{5+}]}\right) = \frac{-E_h}{29.6} - 6.46$$

The distribution of As species in the As- $\text{H}_2\text{O}$  system is illustrated in Fig. 3. Added to this diagram are the redox boundaries for  $\text{MnO}_2/\text{Mn}^{2+}$  and  $\text{Fe}(\text{OH})_3/\text{Fe}^{2+}$ . Notice that only As(s) exists at a redox potential less than  $-200$  mV. It is also important to note that amorphous iron hydroxide dissolves reductively at  $E_h$  values at which arsenous acid is dominant. This implies that during reductive dissolution of amorphous iron hydroxides, adsorbed arsenic or arsenous acid will be released into the dissolved phase.

Under reduced conditions, in the presence of sulphide, As forms an aqueous thioarsenite complex (Webster 1990; Cherry et al. 1979; Wagemann 1978). Until recently, it was suggested that the thioarsenate complex was  $\text{AsS}_2^-$ , but the orpiment solubility studies of Webster (1990)



concluded that the most stable thioarsenite species was  $H_2As_3S_6^-$ .

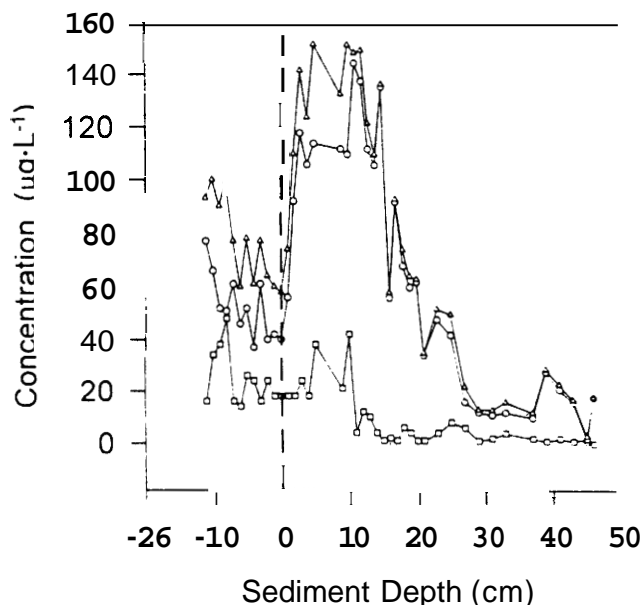


The aqueous organic chemistry of **As** is dominated by methylation and oxidation, by predominantly bacteria and to some extent algae. Under oxic freshwater conditions, inorganic arsenate is the dominant form of dissolved **As**, with arsenite, methylarsonic acid (MAA), and dimethylarsonic acid (DMAA) comprising a small part of the total dissolved As concentration (Ferguson and Gavis 1972; Braman and Foreback 1973; Andreae 1978, 1979; Sanders 1980). Under certain conditions, heterotrophic bacteria can oxidize up to 96% of arsenite to arsenate (Tamaki and Frankenberger 1992). Apparently this is a detoxification process because arsenite is approximately 10 times more toxic to bacteria than arsenate. In the methylation process methanogenic bacteria methylate inorganic **As** to volatile dimethylarsine,  $(CH_3)_2AsH$  (Tamaki and Frankenberger 1992; McBride et al. 1978). The intermediate products of this process include MAA  $(CH_3AsO(OH)_2)$  and DMAA  $((CH_3)_2AsOOH)$ .

The biomethylation process (Fig. 4) starts with the reduction of arsenate to arsenite, followed by the methylation of arsenite by methylcobalamin and the cofactor coenzyme 2,2'-dithiodiethane sulfonic acid (McBride et al. 1978). The methanobacterium can use arsenate, arsenite, and methylarsonic acid to produce dimethylarsinic acid and dimethylarsine (Tamaki and Frankenberger 1992). Methylarsonic acid and dimethylarsinic acid are diprotic ( $pK_1 = 4.1$ ,  $pK_2 = 8.7$ ) and monoprotic ( $pK_a = 6.2$ ) acids, respectively (Lemmo et al. 1983). Methylcobalamin, similar to vitamin B<sub>12</sub> except that all CN groups are replaced by CH<sub>3</sub> groups, serves as a methyl donor. The final product of this biomethylation process is dimethylarsine, which only exists under strongly reduced conditions. Dimethylarsine is rapidly oxidized and has a strong affinity for sulphhydryl functional groups found on particulates (sulphides and organic matter) (Tamaki and Frankenberger 1992; Jernelev and Martin 1975).

Methylation of As is greatest in the pH range of 3.5–5.5 (Baker et al. 1983). This pH dependence suggests that **As** methylation is more prominent in acidic lakes (e.g., receiving acid mine drainage) than in neutral or alkaline lakes. Algae have been reported to produce methylarsonic acid and dimethylarsinic acid under aerobic conditions. A study by Creed (1988), which examined the metabolism of arsenate by five strains of the freshwater alga *Chlorella vulgaris*, revealed that this species of algae did produce minor amounts of methylarsonic acid and dimethylarsinic acid, but that these methylated As species were more toxic to the algae than arsenite or arsenate. Other, similar studies demonstrated that methylated species of As constituted only a minor proportion of the total extracellular As (Andrea and Klumpp 1979; Budd and Craig 1981). Because the methylated As compounds were toxic to all *Chlorella vulgaris* strains studied, Creed (1988) concluded that the methylated forms of As were metabolites rather than products of detoxification.

**Fig. 2.** Total dissolved As(III) and As(V) in Moira Lake sediment interstitial water (adapted from Azcue et al 1994b). ○, total dissolved As(III); □, total dissolved As(V); ▲, total dissolved As(III) + As(V)



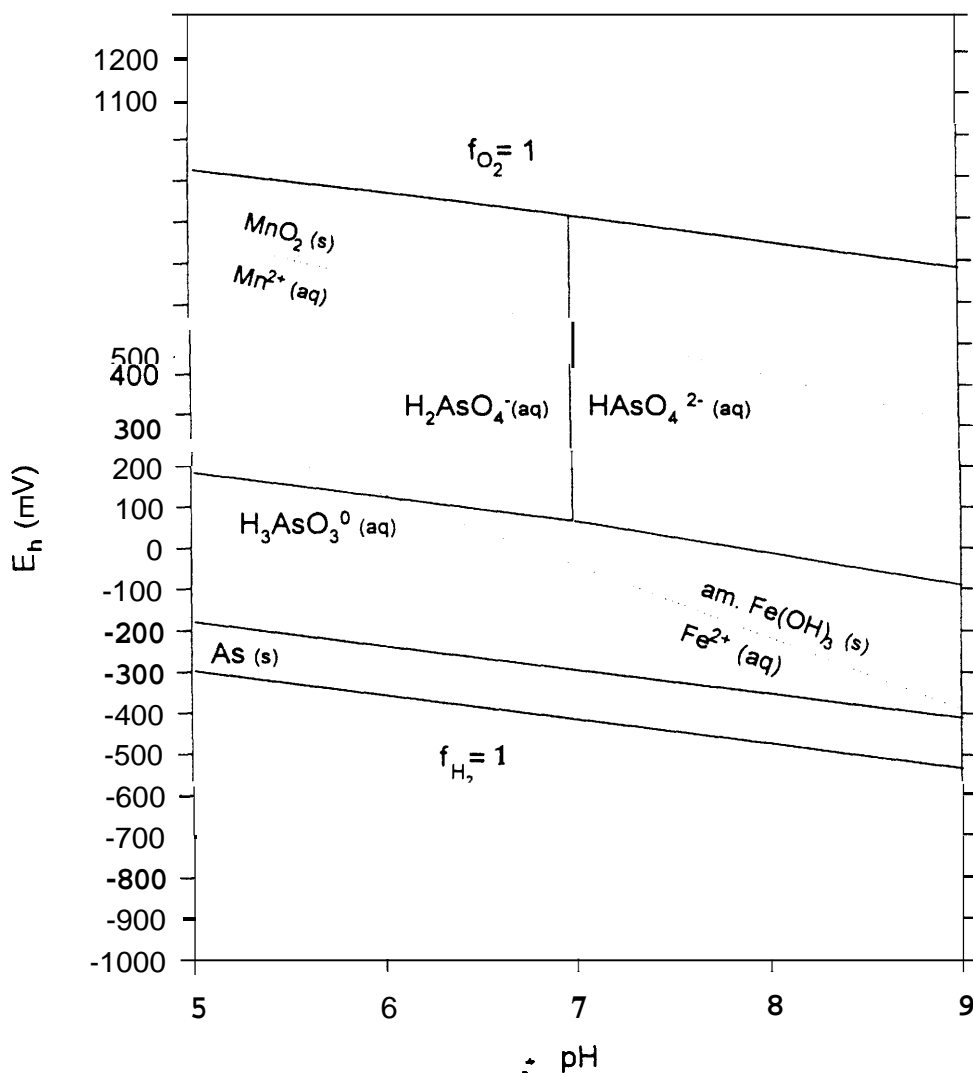
## Dissolution and precipitation

Dissolution and precipitation reactions are two of the major geochemical processes that control the concentration of dissolved As in the aquatic environment. Studies of sediments from different areas have shown that at least 50% of the arsenic in sediments occurs in the sulphide and residual fractions (Azcue and Nriagu 1993; Cornett and Chant 1986; Cornett et al. 1992; Moore et al. 1988).

Most arsenic minerals are either sulphides (As(III)) or metal arsenates (Sadiq and Lindsay 1979; Sadiq 1990; Essington 1988a). Organic arsenical solids are too unstable to exist in natural waters (Ferguson and Gavis 1972; Wagemann 1978). Realgar (AsS) and orpiment (As<sub>2</sub>S<sub>3</sub>) are the most common As(III) sulphides formed under anoxic conditions, whereas a large variety of metal arsenates ( $M_x(AsO_4)_y$ ) can be formed under oxic conditions. The solubility product constants ( $K_{sp}$ ) of a number of As minerals, calculated with thermodynamic data from different sources, are listed in Table 3.

In environments with a heterogeneous composition of inorganic contaminants (e.g., trace metals), the solid-phase activity of **As** minerals ( $M_x(AsO_4)_y$ ) has not always a unit value. Coprecipitation of metal arsenates and the formation of solid solutions ( $M_x \dots M_y(AsO_4)_y$ ) may occur and result in solubility product constants ( $K_{sp}$ ) different from those reported in Table 3. The solubility product constants of the solid solutions can be calculated once the specific composition of the solid solutions are known (Stumm 1992). However, determination of the specific chemical composition of the coprecipitate (e.g., by energy dispersive X-ray (EDX)) may be a major problem considering the low concentrations of trace metals and the variability in the chemical composition of the solid solutions. The preceding implies that the use of solubility product constants of As

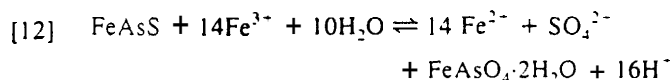
Fig. 3.  $E_h$ -pH diagram for the As—O—H<sub>2</sub>O system.  $A_{S_T} = 10^{-6.176}$  M.  $a_{Fe^{2+}} = 10^{-6}$ .  
 $a_{Mn^{2+}} = 10^{-5}$ .



minerals (e.g., Table 3) to determine if the concentration of dissolved arsenic is governed by a particular solid phase of **As** is not always warranted.

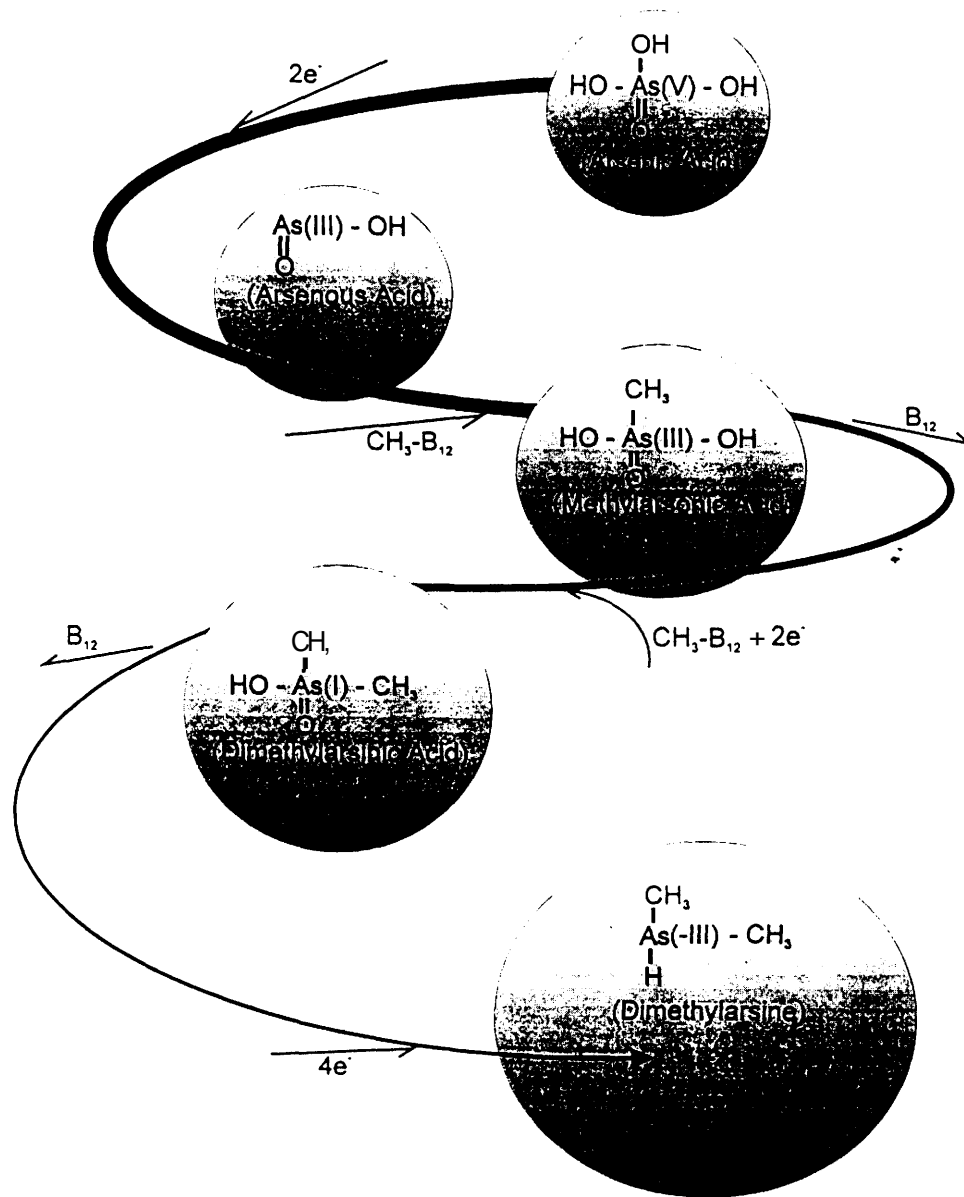
Examining metal arsenates in a marine environment, Sadiq (1990) found that the most stable arsenate mineral was  $Fe_3(AsO_4)_2$ , followed by  $Mn_3(AsO_4)_2$  and  $Ca_3(AsO_4)_2$ . Analogous to the formation of iron phosphates, he also suggested that arsenate is first adsorbed at the surface of ferrous oxide (surface complexation) before forming an  $Fe_3(AsO_4)_2$  surface precipitate. A suspected metal arsenate in freshwater environments is  $Ba_3(AsO_4)_2$ . Previous research indicated that the concentration of dissolved **As** in many freshwaters is governed by  $Ba_3(AsO_4)_2$  because of its small solubility product constant ( $pK_{sp} = 50.11$ ) (Wagemann 1978). However, recent experimental work has revealed new solubility product constants for  $Ba_3(AsO_4)_2$  ( $pK_{sp} = 21.62$ ) and  $BaHAsO_4 \cdot H_2O$  ( $pK_{sp} = 24.64$ ) and suggests that jarium arsenate is a much less stable mineral than previously considered (Essington 19886). Arsenopyrite is a mineral often found in aquatic environments contaminated by

mining activity. Microbial oxidation of arsenopyrite materials may greatly enhance the release of **As** into the dissolved phase. A recent study by Carlson et al. (1992) has demonstrated that sulphide-oxidizing bacteria generate an acidic leachate (pH  $\approx$  1) containing barely soluble scodorite ( $FeAsO_4 \cdot 2H_2O$ ):



The reaction is catalyzed by bacterial oxidation of the ferrous iron. Scodorite is only stable at pH < 1.5 and arsenate concentrations greater than 0.01 M, which is not within the natural conditions of freshwater (Dove and Rimstidt 1985). Reducing conditions can also lead to the formation of manganese arsenates. Masscheleyn et al. (1991) were able to demonstrate that under reduced conditions, following reductive dissolution of manganese oxides, the dissolved phase became supersaturated with respect to manganese arsenate.

**Fig. 4.** Anaerobic biomethylation pathway for dimethylarsine production by *Methanobacterium* sp. (adapted from McBride and Wolf 1971, cited in Tamaki and Frankenberger 1992). B<sub>12</sub>, vitamin B<sub>12</sub>.



## Sorption

Adsorption and coprecipitation are probably the most important processes that control the concentration of dissolved **As** in oxic freshwater environments (Holm et al. 1979; Belzile and Tessier 1990). The effects of adsorption and coprecipitation on the accumulation of contaminants in the solid phase are difficult to distinguish (Sposito 1986). Both processes are therefore often collectively called sorption. Ligand exchange and ternary surface complexation are the main adsorption mechanisms by which **As** is complexed by surface hydroxyl groups (aluminol, type **A** hydroxyl) and Lewis acid sites on metal oxides, (oxy)-hydroxides, clay minerals, organic matter, and amorphous silicates (Sposito 1984; Stumm 1992).

In oxic waters, arsenate sorbed by amorphous iron oxyhydroxide (ferrihydrite,  $\text{Fe}(\text{OH})_3$ ) and aluminum hydroxide can constitute a large portion of the total **As** (Rancourt and Tessier 1993; Elkhatib et al. 1984; Fordham and Norrish 1979; Brannon and Patrick 1987; Seyler and Martin 1989; Masscheleyn et al. 1991; Moore et al. 1988; Huang and Liaw 1979). Arsenite is also sorbed by iron and aluminum (oxy)hydroxides (Pierce and Moore 1980, 1982; Elkhatib et al. 1984). However, reductive dissolution of the adsorbent or oxidation of the adsorbate would lead to, respectively, desorption of arsenite or adsorption of arsenate (Goldberg and Glaubig 1988). Studies by Belzile and Tessier (1990) revealed that arsenate, not arsenite, is sorbed by iron (oxy)hydroxides in lake sediments. In general, arsenate is

**Table 3.** Dissolution and precipitation equilibria.

| Reaction  | $pK_{sp}$                |
|---|--------------------------|
| $As_2O_3$ (arsenolite) + $5H_2O \rightleftharpoons 2AsO_4^{3-} + 10H^+ + 4e^-$          | 81.72                    |
| $As_2O_3$ (claudenite) + $5H_2O \rightleftharpoons 2AsO_4^{3-} + 10H^+ + 4e^-$          | 81.85                    |
| $As_2O_3 + 3H_2O \rightleftharpoons 2AsO_4^{2-} + 6H^+$                                 | 34.97                    |
| $AsS$ (realgar) + $3H_2O \rightleftharpoons H_3AsO_3^0 + HS^- + 2H^+$                   | 16.13 <sup>u</sup>       |
| $0.5As_2S_3$ (orpiment) + $3H_2O \rightleftharpoons H_3AsO_3^0 + 1.5HS^- + 1.5H^+$      | 23.11 <sup>b</sup>       |
| $AlAsO_4$ (s) $\rightleftharpoons Al^{3+} + AsO_4^{3-}$                                 | 25.14                    |
| $AlAsO_4 \cdot 2H_2O$ (s) $\rightleftharpoons Al^{3+} + AsO_4^{3-} + 2H_2O$             | 18.55                    |
| $K_3AsO_4$ (s) $\rightleftharpoons 3K^+ + AsO_4^{3-}$                                   | -0.33                    |
| $Ag_3AsO_4$ (s) $\rightleftharpoons 3Ag^+ + AsO_4^{3-}$                                 | -8.14                    |
| $Na_3AsO_4$ (s) $\rightleftharpoons 3Na^+ + AsO_4^{3-}$                                 | 3.91                     |
| $Li_3AsO_4$ (s) $\rightleftharpoons 3Li^+ + AsO_4^{3-}$                                 | 9.35                     |
| $Ca_3(AsO_4)_2$ (s) $\rightleftharpoons 3Ca^{2+} + 2AsO_4^{3-}$                         | 24.91                    |
| $Ca_3(AsO_4)_2 \cdot 4H_2O$ (s) $\rightleftharpoons 3Ca^{2+} + 2AsO_4^{3-} + 4H_2O$     | <b>19.78<sup>c</sup></b> |
| $Ca_3(AsO_4)_2 \cdot 14H_2O$ (s) $\rightleftharpoons 3Ca^{2+} + 2AsO_4^{3-} + 14H_2O$   | 18.55 <sup>c</sup>       |
| $Cd_3(AsO_4)_2$ (s) $\rightleftharpoons 3Cd^{2+} + 2AsO_4^{3-}$                         | <b>32.4</b>              |
| $Cu_3(AsO_4)_2$ (s) $\rightleftharpoons 3Cu^{2+} + 2AsO_4^{3-}$                         | <b>37.97</b>             |
| $Cu_3(AsO_4)_2 \cdot 6H_2O$ (s) $\rightleftharpoons 3Cu^{2+} + 2AsO_4^{3-} + 6H_2O$     | 36.41 <sup>c</sup>       |
| $Mn_3(AsO_4)_2$ (s) $\rightleftharpoons 3Mn^{2+} + 2AsO_4^{3-}$                         | 31.39                    |
| $Mn_3(AsO_4)_2 \cdot 8H_2O$ (s) $\rightleftharpoons 3Mn^{2+} + 2AsO_4^{3-} + 8H_2O$     | 29.02 <sup>c</sup>       |
| $Mg_3(AsO_4)_2$ (s) $\rightleftharpoons 3Mg^{2+} + 2AsO_4^{3-}$                         | 30.02                    |
| $Ni_3(AsO_4)_2$ (s) $\rightleftharpoons 3Ni^{2+} + 2AsO_4^{3-}$                         | 25.21                    |
| $Ni_3(AsO_4)_2 \cdot 8H_2O$ (s) $\rightleftharpoons 3Ni^{2+} + 2AsO_4^{3-} + 8H_2O$     | <b>26.07.</b>            |
| $Co_3(AsO_4)_2$ (s) $\rightleftharpoons 3Co^{2+} + 2AsO_4^{3-}$                         | <b>34.74<sup>c</sup></b> |
| $Co_3(AsO_4)_2 \cdot 8H_2O$ (s) $\rightleftharpoons 3Co^{2+} + 2AsO_4^{3-} + 8H_2O$     | 36.63 <sup>d</sup>       |
| $Pb_3(AsO_4)_2$ (s) $\rightleftharpoons 3Pb^{2+} + 2AsO_4^{3-}$                         | <b>32.07</b>             |
| $Pb_3(AsO_4)_2 \cdot 4H_2O$ (s) $\rightleftharpoons 3Pb^{2+} + 2AsO_4^{3-} + 4H_2O$     | 44.28                    |
| $Zn_3(AsO_4)_2$ (s) $\rightleftharpoons 3Zn^{2+} + 2AsO_4^{3-}$                         | 31.20 <sup>c</sup>       |
| $Zn_3(AsO_4)_2 \cdot 2.5H_2O$ (s) $\rightleftharpoons 3Zn^{2+} + 2AsO_4^{3-} + 2.5H_2O$ | 48.81 <sup>c</sup>       |
| $BaHAsO_4 \cdot H_2O$ (s) $\rightleftharpoons Ba^{2+} + HAsO_4^{2-} + H_2O$             | <b>36.13<sup>c</sup></b> |
| $Ba_3(AsO_4)_2$ (s) $\rightleftharpoons 3Ba^{2+} + 2AsO_4^{3-}$                         | 21.62 <sup>c</sup>       |
| $Be_3(AsO_4)_2$ (s) $\rightleftharpoons 3Be^{2+} + 2AsO_4^{3-}$                         | 38.29                    |
| $Fe_3(AsO_4)_2$ (s) $\rightleftharpoons 3Fe^{2+} + 2AsO_4^{3-}$                         | 34.41                    |
| $FeAsO_4 \cdot 2H_2O$ (s) $\rightleftharpoons Fe^{3+} + AsO_4^{3-} + 2H_2O$             | 21.70                    |

Note: The Gibbs free energy of formation for aqueous ions used in calculating estimated solubility product constants were taken from Sadiq and Lindsay (1979), Sadiq and Lindsay (1981), and Essington (1988a, 1988b).

<sup>u</sup>Value was calculated using Gibbs free energies of formation in Sadiq and Lindsay (1979) and Webrer (1990).

<sup>c</sup>Equilibrium constant reported by Webster (1990).

<sup>b</sup>Values were calculated from Gibbs free energy of formation values (STP) from Essington (1988b).

<sup>d</sup>Essington (1988b) estimated the average Gibbs free energy of formation for hydration of metal arsenates to be  $-241.37 \text{ kJ} \cdot \text{mol}^{-1} \pm 16.85 \text{ kJ} \cdot \text{mol}^{-1}$ . This standard deviation was too great, so the calculated value of hydration of  $Ni_3(AsO_4)_2 \cdot 8H_2O$  from Essington's (1988a) list was used for the same structure of Co ( $-238.48 \text{ kJ} \cdot \text{mol}^{-1}$ ) in calculating and estimated Gibbs free energy of formation for this mineral.

<sup>e</sup>Essington (1988a).

more strongly adsorbed (ca. 50% greater) than arsenite (Brewster 1992). The primary reason for this is that arsenite has a stronger affinity for protons that arsenate. This competition for surface sites reduces arsenite surface complexation (ligand exchange) and arsenite adsorption occurs almost entirely by (nonspecific) electrostatic or hydrogen bonds (Brewster 1992).

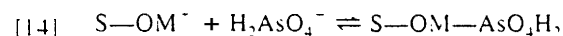
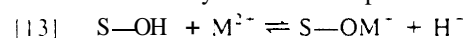
Using sequential extractions, several studies have shown that as much as 56–64% of the total solid As in lake sediments was bound in the Fe and Mn oxide fraction (Tessier

et al. 1979; Azcue and Nriagu 1993; Cornett and Chant 1986). Particularly Al and Fe oxides play an important role in the adsorption of arsenate because of their high point of zero charge (PZC). The approximate PZC of amorphous  $Fe(OH)_3$  (ferrihydrite) is at pH 8.5 and for  $\gamma\text{-AlOOH}$  (boehmite) it is at pH 8.2 (Stumm and Morgan 1981). Below PZC, surface hydroxyls (S—OH) become protonated and form very reactive Lewis acid sites (S—OH<sub>2</sub><sup>+</sup>), which complex arsenate (e.g., S—AsO<sub>4</sub>H<sub>2</sub>) by ligand exchange (Sposito 1984; Stumm 1992).

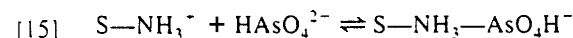
Manganese oxides do not play a significant role in the adsorption of arsenate (Huang et al. 1982). The PZC of birnessite ( $[\text{Na,Ca}]\text{Mn}_7\text{O}_{14}\cdot 2.8\text{H}_2\text{O}$ ), the most common manganese oxide, is at pH 2 (Stumm and Morgan 1981). Under the normal pH range of most natural waters, surface hydroxyls of birnessite will deprotonate ( $\text{S}-\text{O}^-$ ) and the chance of surface complexation of arsenate by ligand exchange will be greatly reduced. Considering this, it appears that the As bound in the Fe/Mn fraction of the sediments as reported by Azcue and Nriagu (1993) and Cornett and Chant (1986) is most probably bound to Fe oxides (Belzile and Tessier 1990; De Vitre et al. 1991). However, at  $\text{pH} > \text{PZC}$  and only in the presence of divalent (metal) cations, ternary surface complexes of arsenate (e.g.,  $\text{S}-\text{OCu}-\text{AsO}_4\text{H}_2$ ) can be formed on manganese oxides (McBride 1989). Takamatsu et al. (1985) demonstrated that if divalent cations are adsorbed at the surface of manganese oxide (e.g.,  $\text{S}-\text{OCu}^+$ ), adsorption of arsenate is enhanced.

A similar surface complexation reaction is possible between organic matter and arsenate. Studies of the St. Johns River, Nfld., by Waslenchuk and Windom (1978), showed that arsenate was complexed by dissolved organic matter (DOM) ( $\text{MW} < 10\,000$ ). On average  $22\text{ mg}\cdot\text{L}^{-1}$  of dissolved organic carbon complexed approximately  $0.71\text{ }\mu\text{g}\cdot\text{L}^{-1}$  of arsenate. Considering the presence of DOM in lakes, it is quite possible that this process might also occur in lakes.

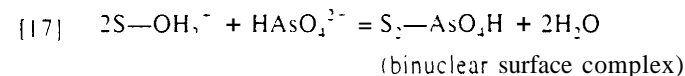
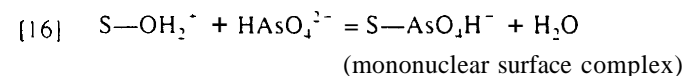
Possible surface complexation reactions could be (i) metal and ternary surface complex formation,



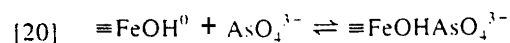
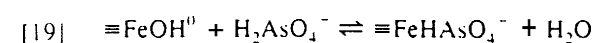
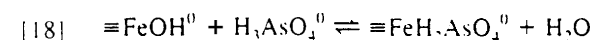
and (ii) surface complexation by positively charged amine or sulphur groups on organic matter.



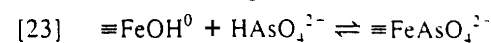
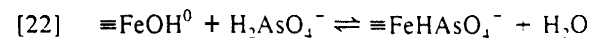
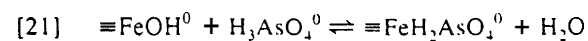
Using extended X-ray absorption fine structure (EXAFS) spectroscopy, Waychunas et al. (1993) were able to conclude that arsenate, like phosphate, forms predominantly inner-sphere binuclear surface complexes rather than inner-sphere mononuclear surface complexes. Only 30% of all surface complexes on ferrihydrite were mononuclear, the rest being binuclear.



In modeling surface complexation of arsenate, the choice of surface complexation reactions may have a strong effect on the results. Using data from Pierce and Moore (1982) and Leckie et al. (1980), Dzombak and Morel (1990) attempted to model the adsorption of arsenate on ferrihydrite with a generalized two-layer model and the optimization program FITEQL (Westall and Morel 1977). They assumed the following surface complexation reactions:



The failure of their model to fit the observed results of Pierce and Moore (1982) and Leckie et al. (1980) could be due to the variability problems with the data from the respective authors. However, using the constant capacitance model (Stumm et al. 1970) and FITEQL, Goldberg (1986) obtained much better results in modeling arsenate adsorption on aluminum and iron oxides. She used the following surface complexation reactions:



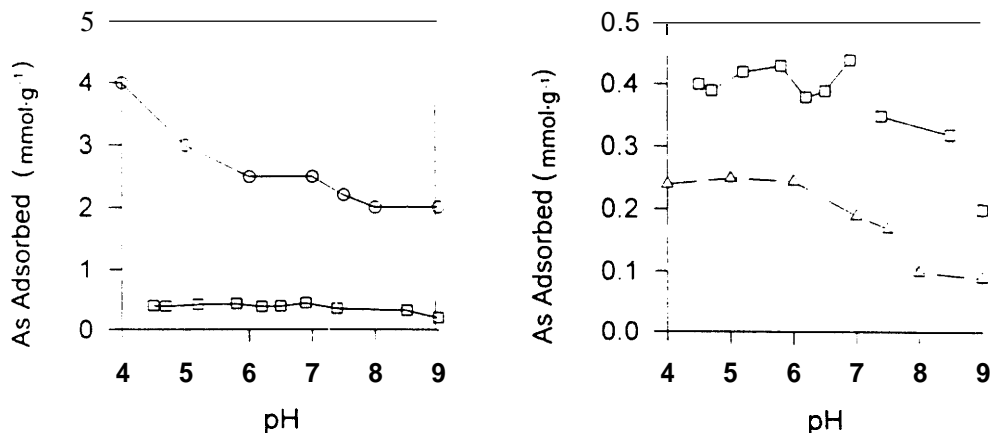
The disparity between the results of Dzombak and Morel (1990) and Goldberg (1986) raises the question whether the choice of adsorption model or experimental data is responsible for the failure or success of their modeling attempts, respectively. One interesting point, not considered previously, is the fact that in their adsorption models, only mononuclear surface complexes are used. In reality over 70% of surface arsenate-iron oxyhydroxide surface complexes are binuclear (Waychunas et al. 1993).

Work by Belzile and Tessier (1990) has demonstrated that by plotting  $\log K_A$  (apparent equilibrium constant) against pH, the surface complexation type can be identified. They suggest that between pH 4 and 7, the dominant surface complexation type is  $\text{FeAsO}_4\text{H}^-$ , and above pH 7, the dominant surface complexation type is  $\text{FeAsO}_4^{2-}$ . Both surface complexes are consistent with the theory on the aqueous complexation of As (Fig. 1A).

In several studies on arsenate adsorption to Fe and Al (oxy)hydroxides in the natural aquatic environment, the adsorption behaviour could be described by the Langmuir adsorption isotherm (Huang and Liaw 1979; Oscarson et al. 1980, 1981, 1983; Kersten 1988; Malotky and Anderson 1976; Ferguson and Gavis 1972; Pierce and Moore 1982, 1980). The capacity for arsenic acid adsorption is much greater for ferrihydrite than gibbsite (Fig. 5). Though the illustrated trend (Fig. 5) for adsorption of As on gibbsite is somewhat erratic, it is discernible that maximum arsenate adsorption occurs around pH 7 with minima at pH 4 and 9 (Anderson et al. 1976). Considering the relative high solubility of gibbsite at low pH, the minimum adsorption of arsenate at low pH is probably due to adsorbent dissolution. The general decrease in adsorbed arsenate results in the decrease of protonated surface functional groups with increasing pH. The adsorption of arsenate on amorphous iron hydroxide exhibits a maximum at low pH (ca. pH 4-5) and decreases as pH increases (Pierce and Moore 1982). The maximum at low pH could be due to the protonation of surface functional groups (formation of surface hydroxyls and Lewis acid sites) resulting in an increased potential for ligand exchange.

Without specific chemical analytical methods or spectroscopic methods, it is difficult to differentiate between adsorption and coprecipitation (Sposito 1986). Using EDTA, Aggett and Roberts (1986) were able to demonstrate that As in Lake Ohakuri sediments (New Zealand) was coprecipitated with iron oxyhydroxides. As the rate of oxyhydroxide dissolution by EDTA was slow (ca. 48 h), the observation

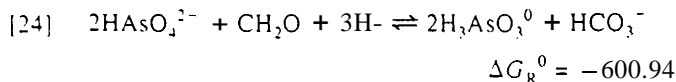
Fig. 5. Arsenate adsorption per unit mass adsorbate as a function of equilibrium pH adapted from Pierce and Moore 1982 and Anderson et al. 1976). □, 66.7 μmol As·L<sup>-1</sup> (5 ppm) and 0.00445 g am. Fe(OH)<sub>3</sub>·L<sup>-1</sup> (Pierce and Moore 1982); △, 66.7 μmol As·L<sup>-1</sup> (5 ppm) and 0.16 g Al(OH)<sub>3</sub>·L<sup>-1</sup> (Anderson et al. 1976); ○, 1.33 pmol As·L<sup>-1</sup> (100 ppb) and 0.00445 g am. Fe(OH)<sub>3</sub>·L<sup>-1</sup> (Pierce and Moore 1982).



of constant, dissolved Fe:As ratios during the dissolution process revealed that As was coprecipitated rather than adsorbed. The work by Waychunas et al. (1993) indicated that the adsorption density of As on ferrihydrite is about 0.25 mol·mol Fe(III)<sup>-1</sup>, and 0.7 mol·mol Fe(III)<sup>-1</sup> during coprecipitation. Arsenic adsorption equilibria can be affected by changes in pH, ionic strength, and competitive anions such as phosphate (Peryea 1991). The As locked up within the matrix of ferrihydrite becomes only (bio)available if the coprecipitate dissolves or with aging, as the iron oxide forms a more ordered structure and As is forced out of the structure (Waychunas et al. 1993).

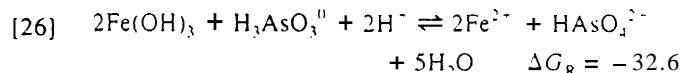
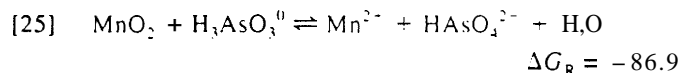
## Redox processes

Oscarson et al. (1980) has shown that in aquatic sediment predominantly abiotic processes are responsible for the oxidation of arsenite to arsenate and biotic oxidation mechanisms play a subordinate role. However, studies by Tamaki and Frankenberger (1992), showed that bacteria can play a significant role in the oxidation of arsenite to arsenate. Arsenate was effectively reduced during microbial oxidation of organic matter in a flooded soil (Masscheleyn et al. 1991). The following reaction equation shows that the reduction of arsenate to arsenite using organic carbon as the reductant is thermodynamically favourable:



The Gibbs free energy of the reaction ( $\Delta G_R^0$ ) was calculated using the Gibbs free energy of formation for  $\alpha$ -D-glucose (aq) from Fenchel and Blackburn (1979). The Gibbs free energy of formation for the As species and the bicarbonate ion were taken, respectively, from Sadiq and Lindsay (1979) and Sadiq and Lindsay (1981). The dominance of abiotic or biotic redox processes will depend on the quality (resistance to decomposition) and quantity of the organic matter in sediments.

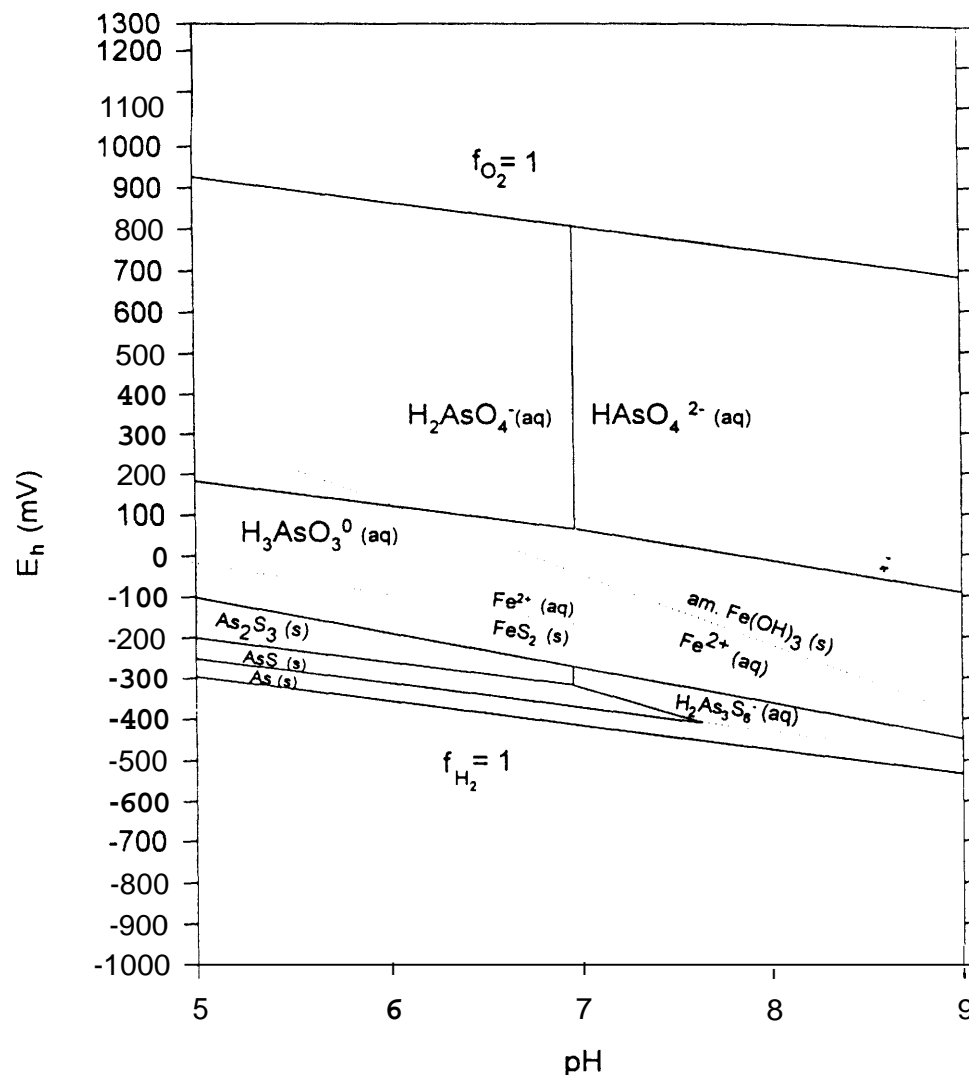
Mn(IV) and Fe(III) oxides are major and minor sediment components, respectively, involved in the abiotic oxidation of As(III) to As(V) (Oscarson et al. 1980). The  $\Delta G_R$  values from the following reactions show that MnO<sub>2</sub> is favoured thermodynamically over amorphous Fe(OH)<sub>3</sub> as an electron acceptor in the oxidation of arsenious acid to arsenic acid (Belzile and Tessier 1990).



Despite being thermodynamically favoured, unpublished data referred to by Oscarson et al. (1980) revealed that the oxidation of As(III) to As(V) by Fe(III) oxyhydroxides did not occur within 72 h. No mention was made by Oscarson et al. (1980) of the experimental conditions or the type of synthetic iron oxyhydroxide (amorphous or crystalline). Considering this and other experimental data, Oscarson et al. (1980) assumed oxidation to be controlled by Mn(IV) oxides.

A common constituent of anoxic sediment in aquatic environments is reduced sulphur or sulphide. If As is in contact with sulphur in reduced environments, relatively insoluble arsenic-sulphur compounds are formed. The As-S-O-H<sub>2</sub>O system is illustrated in the  $E_h$ -pH diagram of Fig. 6. The stability areas occupied by orpiment (As<sub>2</sub>S<sub>3</sub>) and realgar (AsS) represent conditions at which the concentration of dissolved As species is less than 5 μg·L<sup>-1</sup> (Cherry et al. 1979). The low concentration of dissolved As in these stability areas is regulated by the highly insoluble As sulphides. Presented in Fig. 6 are the dotted lines representing stability zones for Fe<sup>2+</sup> (aq), Fe(OH)<sub>3</sub> (s), and FeS<sub>2</sub> (s). The dotted equilibrium line for Fe<sup>2+</sup> (aq) and FeS<sub>2</sub> (s) terminates half way through the diagram owing to its solubility at higher pH values (i.e., beyond this line HS<sup>-</sup> (aq) exists). The reason for plotting this line in the

Fig. 6.  $E_h$ -pH diagram for the As—S—O—H<sub>2</sub>O system (adapted from Cherry et al. 1979 and Wagemann 1978).  $As_T = 10^{-6.176}$  M.  $S_T = 10^{-3}$  M.  $a_{Fe^{2+}} = 10^{-6}$ .



As—S—O—H<sub>2</sub>O  $E_h$ -pH diagram is to demonstrate the coexistence of a stable and dominant solid sulphide. This theoretical evidence indicates that arsenic sulphide formation does compete with iron sulphide formation with sulphide being the limiting reactant. This information also reveals that where iron sulphides are found arsenic sulphides could also be found.

### Conclusion: synthesis and application of a conceptual biogeochemical model

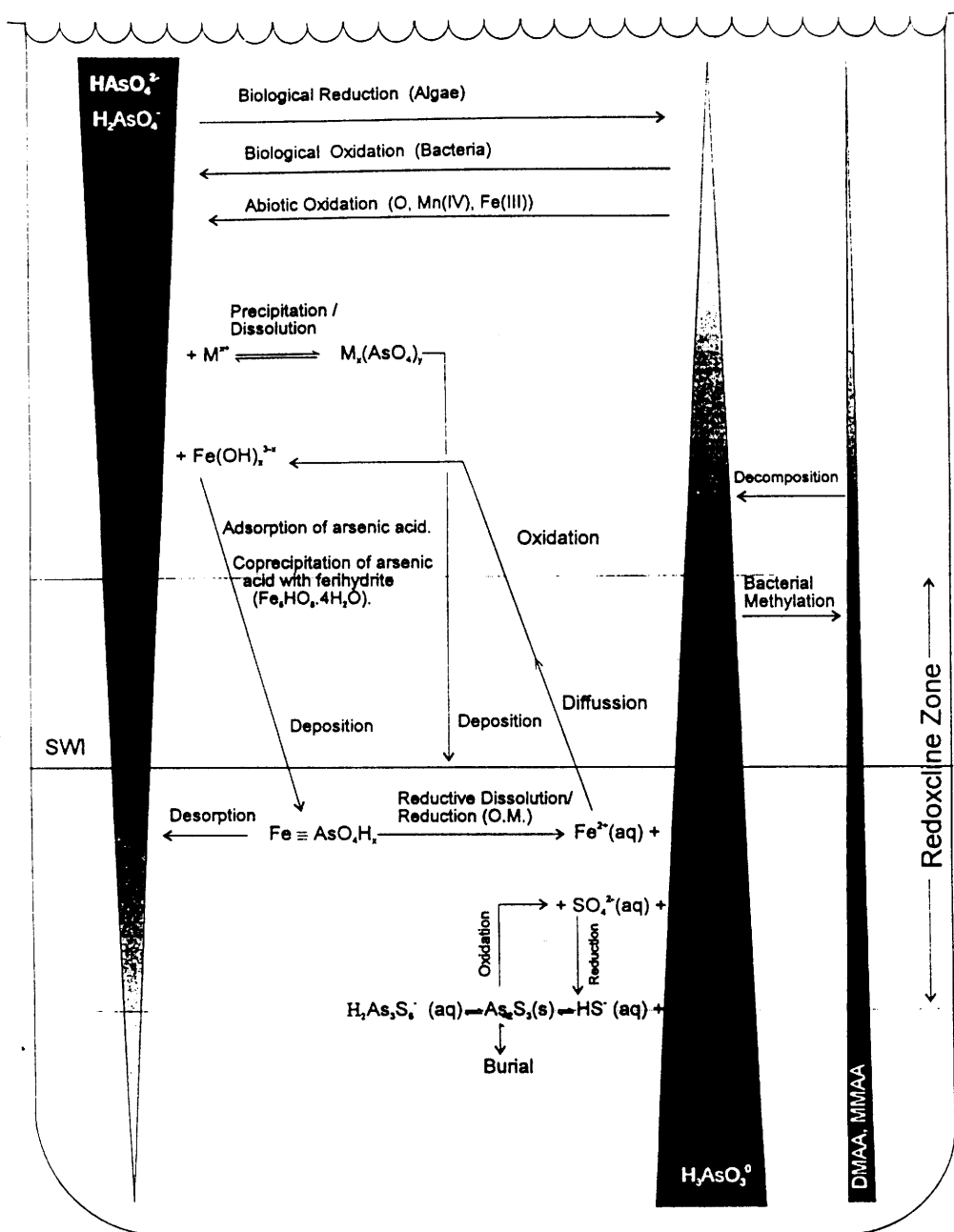
The factors and processes controlling the mobility of arsenic in lakes can best be described as extremely complex. Not only does arsenic speciate ( $H_2AsO_4^-$ ,  $HAsO_4^{2-}$ ,  $H_3AsO_3^0$ ,  $H_2As_3S_6^-$ , etc.) but it also fractionates in the solid phase between metal arsenates, adsorbates, coprecipitates, and sulphides. Speciation and solid-phase fractionation can be dependent on a multitude of factors including pH,  $E_h$ , ionic strength, biomethylation processes, activities of various

solid-forming cations, and kinetics. All of these processes are variable at any point in a lake at any time of the year. Considering this complexity, a general conceptual model of biogeochemical processes controlling As mobility in lakes is presented in Fig. 7. The figure presents a summary of the processes previously reviewed.

The large shaded spikes in Fig. 7 represent the distribution of As species (arsenic acid, arsenous acid, and MAA or DMAA), not concentration. In the oxic hypolimnion, the dominant As species is As(V) as arsenic acid, whereas in the interstitial waters As(III) arsenous acid is dominant. Since MAA and DMAA are synthesized via anaerobic methylation, they are predominantly found in anaerobic interstitial waters.

On opposite sides of the sediment-water interface (SWI) are two dotted lines representing the upper and lower boundary of the redoxcline zone. This zone represents the temporal and spatial variation in the location of the redoxcline. Depending on aerobic bacterial activity and the quantity or quality of organic matter deposition, the redoxcline

Fig. 7. Conceptual model of biogeochemical process involving As in lakes. O.M., organic matter.



could shift from below the SWI to above the SWI. The importance of a possible shift in redoxcline is revealed through the instability of the adsorbate am.  $\text{Fe}(\text{OH})_3$  (iron oxyhydroxide, i.e., ferrihydrite) under reduced conditions and arsenic sulphides ( $\text{As}_2\text{S}_3$ ) under oxic conditions. If the redoxcline exists long enough above the SWI, authigenic arsenic sulphides form at the SWI. If the redoxcline then falls below the zone where the sulphides formed, the sulphides could be exposed to oxic conditions where the sulphides are oxidized, resulting in mobile arsenous acid (see the oxidation reaction in Fig. 7. at the lower boundary of the redoxcline). If the redoxcline exists long enough below

the SWI, precipitated am.  $\text{Fe}(\text{OH})_3$  with adsorbed/coprecipitated arsenic acid will be deposited at the SWI. Should the redoxcline then shift to an area above the SWI, the am.  $\text{Fe}(\text{OH})_3$  will be exposed to an anoxic environment where it is unstable (see Fig. 5). The iron oxyhydroxide will be reduced (i.e.,  $\text{Fe}^{3+}$  to  $\text{Fe}^{2+}(\text{aq})$ ), resulting in mobilized arsenic acid (see reaction equation below SWI in Fig. 7).

Arsenic is specifically adsorbed to iron oxyhydroxides and generally not readily exchangeable. However, research by Peryea (1991) shows that As adsorption is affected by pH (i.e., aqueous arsenic speciation) and by competitive innersphere complexing anions such as phosphate.



Also illustrated in Fig. 7 is the process of metal arsenate precipitation and dissolution. It is quite possible that under the correct conditions, solid phases of metal arsenate precipitate in the hypolimnion and are deposited at the SWI. No direct evidence of this has yet been presented. Much thermodynamic chemical modelling has been done that suggests some metal arsenates such as  $Mn_3(AsO_4)_2$  probably precipitate, but no experimental evidence exists to support the modelling results. The main problem associated with gaining the required evidence stems from the fact that the solid phases exist in a part per million concentration, and are difficult to find and separate.

It is well known that arsenic acid is favoured as the dominant species of As dissolved in the oxic water of the hypolimnion. Arsenous acid is at times found in the hypolimnion, but is generally unstable and oxidized to arsenic acid. The main processes that promote the oxidation of arsenous acid are abiotic and biotic in nature (see top area of Fig. 7). The biotic process is mediated bacterially and the abiotic process of oxidation is coupled to the reduction of dissolved oxygen, Mn(IV), and Fe(III).

Below the redoxcline, arsenous acid is the most dominant form of dissolved arsenic (Fig. 7). Prior to the deposition of As (as some solid phase, i.e., an adsorbate, coprecipitate, precipitate, etc.), As occurs as As(V). This As(V) is eventually reduced to the more mobile As(III).

The process of dissolved arsenic methylation is also illustrated in Fig. 7. This process is bacterially mediated under anaerobic conditions, usually below the redoxcline. For this reason the methylated forms of arsenic are unstable in the oxic hypolimnion and decompose.

The development of a conceptual model of the biogeochemical processes controlling As mobility in lakes allows us to predict qualitatively the impact of natural and human disturbances on the potential toxicity of bioavailable forms of As. A detailed understanding of the mobility of contaminants is a first prerequisite to understand and predict the fate of toxic contaminants in the environment.

The conceptual model of the biogeochemical pathways of As can be applied to a lake that is mesotrophic during spring, winter, and fall and eutrophic during summer. During spring, winter, and fall, planktonic activity is limited in the epilimnion and little organic matter is transferred to the hypolimnion and deposited at the SWI. This could lead to a predominantly oxic water column with a redoxcline located below the SWI. During these seasons, the lack of high biological activity would promote the more abiotic pathways for As in the lake. Precipitation, adsorption, and coprecipitation of arsenic acid dominate and arsenic becomes predominantly labile.

In some eutrophic lakes (Diamond 1990; Azcue and Nriagu 1993), bioproductivity is increased during the summer and large amounts of organic matter are deposited at the SWI. Aerobic microbial decomposition of the organic matter causes increased consumption of dissolved oxygen near the SWI. This results in an anoxic zone at or above the SWI.

This changing redox condition affects arsenic mobility through the instability of am.  $Fe(OH)_3$ . Arsenic acid is sorbed to am.  $Fe(OH)_3$  in the oxic hypolimnion and deposited at the pre-seasonal (i.e., pre-summer) oxic SWI.

If the environment at the SWI becomes anoxic (less than 100 mV), the iron oxyhydroxide dissolves, releasing arsenic into the water. Under these reduced conditions arsenic sulphides are formed.

During the winter, bioproductivity is decreased, oxygen consumption is minimized, and the redoxcline is lowered at or below the SWI. When the redoxcline is lowered and the arsenic sulphides are exposed to oxic water, the sulphides are unstable and dissolve, releasing As to the water column. This dissolution process is accelerated by sulphide-oxidizing bacteria such as *Thiobacillus ferrooxidans* (Dove and Rimstidt 1985). Below the redoxcline zone sulphides are stable and arsenic is relatively immobile. Above the redoxcline zone sulphides are unstable and dissolve. Below the redoxcline arsenic sulphides are buried. During fall turnover, arsenic sulphides at the SWI are transported to the oxic hypo/epilimnion, where they are oxidized. This promotes the mobilization of As.

## Acknowledgment

Research for this paper was supported by a grant from the Natural Sciences and Engineering Research Council of Canada. Their assistance is greatly acknowledged.

## References

- Abdel-Moatti, A.R. 1990. Speciation and behavior of arsenic in the Nile Delta lakes. *Water Air Soil Pollut.* **51**: 117-132.
- Abo-El-Wafa, O., and Abdel-Shafy, H.I. 1987. Concentration of mercury and arsenic in El-Temsah Lake. *In* Proceedings of the 6th International Conference on Heavy Metals in the Environment, September 1987, New Orleans, La. CEP Consultants, Edinborough, Scotland, pp. 265-267.
- Aggett, J., and Roberts, S. 1986. Insight into the mechanism of accumulation of arsenate and phosphate in hydro lake sediments by measuring the rate of dissolution with ethylenediaminetetraacetic acid. *Environ. Sci. Technol.* **20**: 183-186.
- Anderson, L.C.D., and Bruland, K.W. 1991. Biogeochemistry of arsenic in natural waters: the importance of methylated species. *Environ. Sci. Technol.* **25**: 420-427.
- Anderson, M., Ferguson, J.F., and Gavis, J. 1976. Arsenate adsorption on amorphous aluminum hydroxide. *J. Colloid Interface Sci.* **54**: 391-399.
- Andrae, M. 1978. Distribution and speciation of arsenic in natural waters and some marine algae. *Deep-sea Res.* **25**: 391-402.
- Andrae, M. 1979. Arsenic speciation in seawater and interstitial waters: the influence of biological-chemical interaction on the chemistry of trace element. *Limnol. Oceanogr.* **24**: 440-452.
- Andrae, M., and Klumpp, D. 1979. Biosynthesis and release of organoarsenic compounds by marine algae. *Environ. Sci. Technol.* **13**: 738-741.
- Arafat, N.M. 1985. The impact of mining and smelting on trace metal distribution in lake sediments around Rouyn-Noranda, Quebec. *Water Pollut. Res. Can.* **20**: 1-8.
- Azcue, J.M., and Nriagu, J.O. 1993. Arsenic forms in mine-polluted sediments of Moira Lake, Ontario. *Environ. Int.* **19**: 405-415.
- Azcue, J.M., and Nriagu, J.O. 1994. Arsenic—historical perspectives. *In* Arsenic in the environment. *Edited by* J.O. Nriagu. John Wiley & Sons, Inc., N.Y. pp. 1-15.
- Azcue, J.M., Mudroch, A., Rosa, F., and Hall, G.E.M. 1994a. Effects of abandoned gold mine tailings on the arsenic

- concentrations in water and sediments of Jack of Clubs Lake. *B.C. Environ. Technol.* **15**: 669-678.
- Azcue, J.M., Nriagu, J.O., and Schiff, S. 1994*b*. Role of sediment porewater in the cycling of arsenic in a mine-polluted lake. *Environ. Int.* **20**: 517-527.
- Baker, M., Inniss, W., Mayfield, C., Wong, P., and Chau, Y. 1983. Effect of pH on the methylation of mercury and arsenic by sediment microorganisms. *Environ. Technol. Lett.* **4**: 459-466.
- Baur, W.H., and Onishi, H. 1978. Arsenic. *In Handbook of geochemistry*. Edited by K.H. Wedepohl. Springer-Verlag, Berlin.
- Belzile, N., and Tessier, A. 1990. Interactions between arsenic and iron oxyhydroxides in lacustrine sediments. *Geochim. Cosmochim. Acta.* **54**: 103-109.
- Braman, R., and Foreback, C. 1973. Methylated forms of arsenic in the environment. *Science (Washington, D.C.)*. **182**: 1247-1249.
- Brannon, J., and Patrick, W. 1987. Fixation, transformation, and mobilization of arsenic in sediments. *Environ. Sci. Technol.* **21**: 450-459.
- Brewster, M. 1992. Removing arsenic from contaminated wastewater. *Water Environ. Technol.* **4**: 54-57.
- Budd, K., and Craig, S. 1981. Resistance to arsenate toxicity in the blue-green alga *Synechococcus leopoliensis*. *Can. J. Bot.* **59**: 1518-1521.
- Carlson, L., Lindstrom, B., Hallberg, K., and Tuovinen, O. 1992. Solid-phase products of bacterial oxidation of arsenical pyrite. *Appl. Environ. Microbiol.* **58**: 1046-1049.
- Chamberland, W., and Shapiro, J. 1969. On the biological significance of the phosphate analysis. *Limnol. Oceanogr.* **14**: 921-927.
- Cherry, J., Shaikh, A., Tallman, D., and Nicholson, R. 1979. Arsenic species as an indicator of redox conditions in groundwater. *J. Hydrol.* **43**: 373-392.
- Cornett, J., and Chant, L. 1986. Speciation of arsenic and nickel in sediments of Moira Lake. Research report for The National Uranium Tailings Program, Canada Centre for Mineral and Energy Technology, Energy, Mines and Resources Canada. Department of Supplies and Services File No. 05GS.23241-5-17 16.
- Cornett, J., Chant, L., and Risto, B. 1992. Arsenic transport between water and sediments. *Hydrobiologia*, **235/236**: 533-544.
- Creed, I. 1988. The metabolism of arsenate in sensitive and tolerant strains of the freshwater eukaryote, *Chlorella vulgaris* (Chlorophyceae). M.Sc. thesis. Institute for Environmental Studies, University of Toronto, Toronto, Ont.
- De Vitre, R., Belzile, N., and Tessier, A. 1991. Speciation and adsorption of arsenic on diagenetic iron oxyhydroxides. *Limnol. Oceanogr.* **36**: 1480-1485.
- Diamond, M. 1990. Modelling the fate and transport of arsenic and other inorganic chemicals in lakes. Ph.D. thesis, Department of Chemical Engineering, University of Toronto, Toronto, Ont.
- Dove, P., and Rimstidt, J. 1985. The solubility and stability of scorodite.  $\text{FeAsO}_4 \cdot 2\text{H}_2\text{O}$ . *Am. Mineral.* **70**: 838-844.
- Dzombak, D., and Morel, F. 1990. Surface complexation modelling: hydrous ferrous oxide. John Wiley & Sons, Toronto.
- Elkhatib, E., Bennet, O., and Wright, R. 1984. Arsenite sorption and desorption in soils. *Soil Sci. Soc. Am. J.* **48**: 1025-1030.
- Essington, M.E. 1988*a*. Estimation of the standard free energy of formation of metal arsenates, selenates, and selenites. *Soil Sci. Soc. Am. J.* **52**: 1574-1579.
- Essington, M.E. 1988*b*. Solubility of barium arsenate. *Soil Sci. Soc. Am. J.* **52**: 1566-1570.
- Faust, S.D., Winka, A.J., Belton, T., and Tucker, R. 1983. Assessment of the chemical and biological significance of arsenical compounds in a heavily contaminated watershed. *J. Environ. Sci. Health Part A Environ. Sci. Eng.* **18**: 389-411.
- Fenchel, T., and Blackburn, T. 1979. Bacteria and mineral cycling. Academic Press, New York.
- Ferguson, J.F., and Gavis, J. 1972. A review of the arsenic cycle in natural waters. *Water Res.* **6**: 1259-1274.
- Fordham, A., and Norrish, K. 1979. Arsenate-73 uptake by components of several acidic soils and its implications for phosphate retention. *Aust. J. Soil Res.* **17**: 307-316.
- Goldberg, S. 1986. Chemical modeling of arsenate adsorption on aluminum and iron oxide minerals. *Soil Sci. Soc. Am. J.* **50**: 1154-1157.
- Goldberg, S., and Glaubig, R. 1988. Anion adsorption on a calcareous, montmorillonitic soil—arsenic. *Soil Sci. Soc. Am. J.* **52**: 1297-1300.
- Hindmarsh, J.T., and McCurdy, R.F. 1986. Clinical and environmental aspects of arsenic toxicity. *CRC Crit. Rev. Clin. Lab. Sci.* **23**: 315-317.
- Holm, T., Anderson, M., Iverson, D., and Stanforth, R. 1979. Heterogenous interactions of arsenic in aquatic systems. *In Chemical modeling in aqueous systems*. Edited by E.A. Jenne. American Chemical Society, Washington, D.C. pp. 710-736.
- Huang, P.M., and Liaw, W.K. 1979. Adsorption of arsenite by lake sediments. *Int. Rev. Gesamten Hydrobiol.* **64**: 263-271.
- Huang, P.M., Oscarson, D., Liaw, W.K., and Hammer, U.T. 1982. Dynamics and mechanisms of arsenite oxidation by freshwater lake sediments. *Hydrobiologia*. **91**: 315-322.
- Jernelov, A., and Martin, A. 1975. Ecological implication of metal metabolism by microorganisms. Swedish Water and Air Pollution Research Lab. Swedish Institute of Environmental Research, Stockholm, Sweden. pp. 61-77.
- Kersten, M. 1988. Geochemistry of priority pollutants in anoxic sludges. *In Cadmium, arsenic, methyl mercury, and chlorinated organics in chemistry and biology of solid waste, dredged materials and mine tailings*. Edited by W. Solomons and U. Forstner. Springer-Verlag, New York.
- Leckie, J., Benjamin, M., Hayes, K., Kaufman, G., Altman, S. 1980. Adsorption/coprecipitation of trace elements from water with iron oxyhydroxide. Electric Power Institute, Palo Alto, Calif. Rep. No. EPRI RP-910-1.
- Lemmo, X.V., Faust, S.D., Belton, T., and Tucker, R. 1983. Assessment of the chemical and biological significance of arsenical compounds in a heavily contaminated watershed: the fate and speciation of arsenical compounds in aquatic environments—a literature review. *J. Environ. Sci. Health Part A Environ. Sci. Eng.* **18**: 335-387.
- Lis, S.A., and Hopke, P.K. 1973. Anomalous arsenic concentrations in Chautapua Lake. *Environ. Lett.* **5**: 45-51.
- Malotky, D.T., and Anderson, M.A. 1976. The adsorption of the potential determining arsenate anion on oxide surfaces. *colloid and interface science*. Vol. IV. Hydrosols and rheology. Academic Press Inc., New York.
- Masscheleyn, P., Delaune, R., and Patrick, W. 1991. Effect of redox potential and pH on arsenic speciation and solubility in a contaminated soil. *Environ. Sci. Technol.* **25**: 1413-1419.
- McBride, M.B. 1989. Reactions controlling heavy metal solubility in soils. *Adv. Soil Sci.* **10**: 1-56.
- McBride, B.C., and Wolf, R.S. 1971. Biosynthesis of dimethylarsine by methano-bacterium. *Biochemistry*. **10**: 4312-4317.
- McBride, B.C., Merilees, H., Cullen, W.R., Pickett, W. 1978. Anaerobic and aerobic alkylation of arsenic. *In Organometals and organometalloids occurrence and fate in the environment*.

- Edited by F.E. Brickman and J.M. Bslama. ACS Symp. Ser. 82: 94-115.*
- Moore, J.W. 1981. Epipelagic algal communities in a eutrophic Northern lake contaminated with mine wastes. *Water Res.* **15**: 97-105.
- Moore, J.W., Ficklin, W., and Johns, C. 1988. Partitioning of arsenic and metals in reducing sulfidic sediments. *Environ. Sci. Technol.* **22**: 432-437.
- Mudroch, A., and Capobianco, J.A. 1980. Impact of past mining activities on aquatic sediments in Moira River basin, Ontario. *J. Gt. Lakes Res.* **6**: 121-128.
- Mudroch, A., and Clair, T.A. 1986. Transport of arsenic and mercury from gold mining activities through an aquatic ecosystem. *Sci. Total Environ.* **57**: 205-216.
- Nriagu, J.O. 1983. Arsenic enrichment in lakes near the smelters at Sudbury, Ontario. *Geochim. Cosmochim. Acta*, **47**: 1523-1526.
- Nriagu, J.O., and Azcue, J.M. 1990. Food contamination with arsenic in the environment. *In Food contamination from environmental sources. Edited by J.O. Nriagu and M.S. Simons. John Wiley & Sons. New York. pp. 121-143.*
- Oscarson, D.W., Huang, P.M., and Liaw, W.K. 1980. The oxidation of arsenite by aquatic sediments. *J. Environ. Qual.* **9**: 700-703.
- Oscarson, D.W., Huang, P.M., Defosse, C., and Herbillon, A. 1981. Oxidative power of Mn(IV) and Fe(III) oxides with respect to As(III) in terrestrial and aquatic environment. *Nature (London)*, **291**: 50-51.
- Oscarson, D.W., Huang, P.M., Hammer, U.T., and Liaw, W.K. 1983. Oxidation and sorption of arsenite by manganese dioxide as influenced by coating of iron and aluminum oxides and calcium carbonate. *Water Air Soil Pollut.* **20**: 233-244.
- Peryea, F. 1991. Phosphate induced release of arsenic from soils contaminated with lead arsenate. *Soil Sci. Soc. Am. J.* **55**: 1301-1306.
- Pierce, M., and Moore, C. 1980. Adsorption of arsenite on amorphous iron hydroxide from dilute aqueous solution. *Environ. Sci. Technol.* **14**: 214-216.
- Pierce, M., and Moore, C. 1982. Adsorption of arsenite on amorphous iron hydroxide. *Water Res.* **16**: 1247-1253.
- Rancourt, L., and Tessier, A. 1993. Adsorption of As(V) on various iron oxyhydroxides. *Heavy Metals Environ.* **1**: 385-388.
- Rossmann, R.R. 1984. Trace metal concentrations in the offshore waters of Lakes Erie and Michigan. University of Michigan, East Lansing, Mich. Spec. Rep. 108.
- Rossmann, R.R., and Barres, J. 1988. Trace element concentrations in near surface waters of the Great Lakes and methods of collection, storage and analysis. *J. Gt. Lakes Res.* **14**: 188-204.
- Sadiq, M. 1990. Arsenic chemistry in marine environments: a comparison between theoretical and field observations. *Mar. Chem.* **31**: 285-297.
- Sadiq, M., and Lindsay, W. 1979. Selection of standard free energies of formation for use in soil chemistry. Colorado State University, Fort Collins, Colo. Tech. Bull. 134.
- Sadiq, M., and Lindsay, W. 1981. Arsenic selection of standard free energies of formation for use in soil chemistry. Colorado State University, Fort Collins, Colo. Supplement to Tech. Bull. 134.
- Sanders, J.G. 1980. Arsenic cycling in marine systems. *Mar. Environ. Res.* **3**: 257-266.
- Schaeufelberger, F.A. 1994. Arsenic minerals formed at low temperatures. *In Arsenic in the environment. Edited by J.O. Nriagu. John Wiley & Sons, Inc., New York. pp. 403-413.*
- Seyler, P., and Martin, J.M. 1989. Biogeochemical processes affecting arsenic species distribution in a permanently stratified lake. *Environ. Sci. Technol.* **23**: 1258-1263.
- Shapiro, J. 1971. Arsenic and phosphate: measured by various techniques. *Science (Washington, D.C.)*. **171**: 234.
- Sposito, G. 1983. *The surface chemistry of soils.* Oxford University Press, New York.
- Sposito, G. 1986. Distinguishing adsorption from surface precipitation. *In Geochemical processes at mineral surfaces. Edited by J.A. Davis and K.F. Hayes. ACS Symp. Ser. 323: 217-228.*
- Stumm, W. 1992. *Chemistry of the solid-water interface: processes at the mineral-water and particle-water interface in natural systems.* John Wiley & Sons, Toronto.
- Stumm, W., and Morgan, J.J. 1981. *Aquatic chemistry: an introduction emphasizing chemical equilibria in natural waters.* 2nd ed. John Wiley Sons, Toronto.
- Stumm, W., Huang, C., and Jenkins, S.R. 1970. Specific chemical interaction affecting the stability of dispersed systems. *Croat. Chem. Acta.* **42**: 223-245.
- Takamatsu, T., Kawashima, M., and Koyama, M. 1985. The role of Mn<sup>2+</sup>-rich hydrous manganese oxide in the accumulation of arsenic in lake sediments. *Water Res.* **19**: 1029-1032.
- Tamaki, S., and Frankenberger, J.T. 1992. Environmental biochemistry of arsenic. *Rev. Environ. Contam. Toxicol.* **124**: 79-110.
- Tessier, A., and Campbell, P. 1991. Partitioning of trace metals in sediments and its relationship to their accumulation in benthic organisms. *In Metal speciation in the environment. NATO ASI Ser. Ser. G Ecol. Sci.* **23**: 545-570.
- Tessier, A., Campbell, P., and Bisson, M. 1979. Sequential extraction procedure for the speciation of particulate trace metals. *Anal. Chem.* **51**: 844-851.
- Ullman, W., Schaefer, R.W., and Sanderson, W.W. 1961. Arsenic accumulation by fish in lakes treated with sodium arsenite. *J. Water Pollut. Control Fed.* **33**: 416-418.
- Wagemann, R. 1978. Some theoretical aspects of stability and solubility of inorganic arsenic in the freshwater environment. *Water Resour.* **12**: 139-145.
- Wagemann, R., Snow, N.B., Rosenberg, D.H., and Lutz, A. 1978. Arsenic in sediments, water, and aquatic biota from lakes in the vicinity of Yellowknife, Northwest Territories, Canada. *Arch. Environ. Contam. Toxicol.* **7**: 169-191.
- Walsh, P.R., Duce, R.A., and Fasching, J.L. 1979. Considerations of the enrichment, sources and flux of arsenic in the troposphere. *J. Geophys. Res.* **84**: 1719-1726.
- Waslenchuck, D., and Windom, H. 1978. Factors controlling the estuarine chemistry of arsenic. *Estuarine Coastal Mar. Sci.* **7**: 455-464.
- Waychunas, G., Rea, B., Fuller, C., and Davis, J. 1993. Surface chemistry of ferrihydrite. Part 1. EXAFS studies of the geometry of coprecipitated and adsorbed arsenate. *Geochim. Cosmochim. Acta.* **57**: 2251-2269.
- Webster, J. 1990. The solubility of As<sub>2</sub>S<sub>3</sub> and speciation of As in dilute and sulphide-bearing fluids at 25 and 90°C. *Geochim. Cosmochim. Acta.* **54**: 1009-1017.
- Westall, J., and Morel, F. 1977. FITEQL: a general algorithm for the determination of metal-ligand complex stability constants from experimental data. Ralph M. Parsons Laboratory, Department of Civil Engineering, Massachusetts Institute of Technology, Cambridge, Mass. Tech. Note 19.

8. Giovanoli, R.; Burki, P.; Guiffredi, M.; Stumm, W. "Layer Structured Manganese Oxide Hydroxides, IV. The Buserite Group; Structure Stabilized by Transition Elements," *Chimia* 1975, 29, 517-520.
9. Wagman, D. D.; Evans, W. H.; Parker, V. B.; Halow, I.; Bailey, S. M.; Schumm, R. H. "Selected Values of Chemical Thermodynamic Properties," *Nat. Bur. Stand. (U.S.) Tech. Note* 1969, 270-4.
10. Naumov, C. B.; Ryzhenko, B. N.; Khodakovskiy, I. L. "Handbook of Thermodynamic Data," 1971, (translated by G. J. Soleimani) *U.S. Dept. Commer., Off. Techn. Ser., PB Rep.* 1974, PB 226 722.
11. Bolzan, J. A.; Podesta, J. J.; Arvia, A. J. "Hydrolytic Equilibrium among Metal Ions. I. The Hydrolysis of Co(II) Ion in Aqueous Solutions of  $\text{NaClO}_4$ ," *An. Asoc. Quim. Argent.* 1963, 51, 43-58.
12. Wagman, D. D.; Evans, W. H.; Parker, V. B.; Halow, I.; Bailey, S. M.; Schumm, R. H. "Selected Values of Chemical Thermodynamic Properties," *Nat. Bur. Stand. (U.S.) Tech. Note* 1968, 270-3.
13. Lind, C. J. "Polarographic Determination of Lead Hydroxide Formation Constants at Low Ionic Strength," *Environ. Sci. Technol.* 1978, 12, 1406-1410.
14. Hem, J. D. "Chemical Equilibria and Rates of Manganese Oxidation," *U.S. Geol. Surv., Water-Supply Pap.* 1963, 1667-A.
15. Hem, J. D. "Deposition and Solution of Manganese Oxides," *U.S. Geol. Surv., Water-Supply Pap.* 1964, 1667-B, 5-11.
16. Manheim, F. T. "Manganese-Iron Accumulations in the Shallow Marine Environment," *Mar. Geochem., Proc. Symp.* 1965, 13, 217-276.
17. Prigogine, I.; Defay, R. "Chemical Thermodynamics"; Wiley: New York, 1954.
18. Schweisfurth, R. "Manganoxydierend Bakterien," *Z. Allg. Mikrobiol.* 1973, 13, 341-347.
19. Garrels, R. M.; Christ, C. L. "Solutions, Minerals, and Equilibria"; Harper and Row: New York, 1965; p. 42-49.
20. Kennedy, V. C.; Zellweger, G. W.; Jones, B. F. "Pore Size Effects on the Analysis of Al, Fe, Mn, and Ti in Water," *Water Resour. Res.* 1974, 10, 785-790.
21. Wentz, D. A. "Effect of Mine Drainage on the Quality of Streams in Colorado, 1971-72"; Colorado Water Resources: 1974; Circ. 21.
22. Murray, J. W. "The Interaction of Metal Ions at the Manganese Dioxide-Solution Interface," *Geochim. Cosmochim. Acta* 1975, 39, 505-519.
23. Cronan, D. S. In "The Sea: Vol. 5, Marine Chemistry"; Goldberg, E. D., Ed.; Wiley: New York, 1974; p. 512-515.
24. Van der Weijden, C. H.; Kruissink, E. C. "Some Geochemical Controls on Lead and Barium Concentrations in Ferromanganese Deposits," *Mar. Chem.* 1977, 5, 93-112.
25. Sinha, A. P. B.; Sinjana, N. R.; Biswas, A. B. "On the Structure of Some hlanganites," *Acta Crystallogr.* 1957, 10, 439-440.
26. Hem, J. D. "Redox Processes at Surfaces of Manganese Oxide and Their Effects on Aqueous Metal Ions," *Chem. Geol.* 1978, 21, 199-218.
27. Koljonen, T.; Lahermo, P.; Carlson, L. "Origin, Mineralogy and Chemistry of Manganiferous and Ferruginous Precipitates Found in Sand and Gravel Deposits in Finland," *Bull. Geol. Soc. Finland* 1976, 48, 111-135.

RECEIVED October 24, 1978.

17 000331

4

## Adsorption Reactions of Nickel Species at Oxide Surfaces

THOMAS L. THEIS and RICHARD O. RICHTER<sup>1</sup>

Department of Civil Engineering, University of Notre Dame,  
Notre Dame, IN 46556

*Experimental adsorption isotherms of  $\text{Ni}^{2+}$  on  $\alpha$ -quartz and  $\alpha$ - $\text{FeOOH}$  (goethite) are described adequately by the solvent-ion model of adsorption. The addition of complexing ligands (in this study, sulfate, citrate, nitrilotriacetate, glycine, and cyanide) to the nickel-oxide systems alters adsorption behavior. For sulfate, citrate, and nitrilotriacetate, a competition model for free  $\text{Ni}^{2+}$  between surface and ligand can account for the observed data. Strong evidence is presented for specific adsorption of glycine- and cyanide-nickel complexes onto goethite. All adsorption reactions are discussed through analysis of theoretical nickel speciation in combination with experimental data, the nature of the oxides, and the structure of the nickel-ligand complexes*

Reactions of metal ions in aqueous media have been shown to be strongly influenced by surface sorption reactions. The adequate description of metal ion behavior in systems where particulates have been included is an important step in the application of laboratory data to natural systems of wide environmental interest. In this study, data on the adsorption of aqueous nickel,  $\text{Ni}^{2+}$ , onto oxides of silica and iron is presented. Of special interest are the effects which various ligands have on the adsorption reactions. Data are analyzed through the use of the chemical equilibrium computer model REDEQL2 making use of the solvent-ion model of adsorption.

<sup>1</sup> Current address: Department of Civil and Environmental Engineering, Washington State University, Pullman, WA 99164.

### Models of Adsorption

There are many models that describe the interaction between solute ions and surfaces. These have been reviewed by several authors (1, 2, 3) and include general ion exchange (4, 5, 6), surface complex formation (7, 8) (the "Swiss" model), and various electrostatic models (Gouy-Chapman-Stern (9), Grahame (10, 11), and James and Healy (12)). For hydrolyzable species sorbing onto hydrous oxide surfaces, the surface complex formation model and the solvent-ion interaction model of James and Healy have been shown to be in good agreement with observations. In this chapter, data are analyzed via the James and Healy model.

In this model, a distinction is drawn between electrostatic forces that arise from coulombic considerations, and those that arise from the energy required to replace (or electrically saturate) the secondary hydration sphere around the ion with the hydration layer attached to the sorbing surface. Since most hydrophobic sols have dielectrics considerably less than bulk solution, the latter energy term, known as solvation energy, is positive and opposes the adsorption reaction. In addition, the model recognizes the existence of specific interaction forces between ion and surface resulting from dipole or covalent bonding. Accordingly, the total energy of adsorption of a species *i* is given by:

$$\Delta G^{\circ}_{\text{ADS},i} = \Delta G^{\circ}_{\text{COUL},i} + \Delta G^{\circ}_{\text{SOLV},i} + \Delta G^{\circ}_{\text{CHEM},i} \quad (1)$$

A mathematical summary of the model is given in the Appendix. The use of the Nernst equation (VIII) is valid for small pH variations around the zero point of charge (ZPC). From Equation XI it can be seen that the magnitude of the solvation energy is proportional to the square of the charge, thereby decreasing fourfold upon hydrolysis of the metal ion. This agrees well with the often-observed phenomenon of increased adsorption of many metal-surface combinations at the pH corresponding to the pK of hydrolysis of the metal ion. Therefore, it is implicit that hydrolysis occurs in conjunction with adsorption.

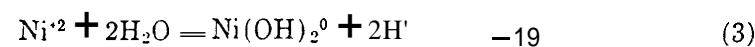
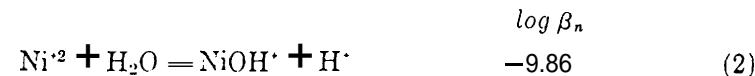
Although it has a chemical meaning in the James and Healy model, the specific chemical free energy term is in practice an experimental fitting parameter. It can be determined by measuring the extent of adsorption at the ZPC of the oxide surface; however, this method assumes that the magnitude does not change with solution pH. More commonly, theoretical adsorption isotherms of the amount of metal adsorbed vs. pH are fitted to actual data by adjusting the  $\Delta G^{\circ}_{\text{CHEM}}$  term.

### Aqueous Chemistry of Nickel

The element nickel is a Group VIII metal which is part of the first transition series. Elemental nickel has the outer sphere electron configuration  $3d^8 4s^2$  and readily yields the 4s electrons to give the divalent ion

$\text{Ni}^{2+}$ , which is the only oxidation state of importance in natural systems. Like the other elements in the first transition series (V, Cr, Mn, Fe, Co),  $\text{Ni}^{2+}$  is octahedrally coordinated in aqueous systems as  $\text{Ni}(\text{H}_2\text{O})_6^{2+}$  (13). This free aquo ion dominates the aqueous chemistry of nickel at neutral pH values; however, complexes of naturally occurring ligands are formed to a small degree ( $\text{OH}^- > \text{SO}_4^{2-} \approx \text{Cl}^- > \text{NH}_3$ ).

Among the mononuclear hydrolytic species of nickel, only the stability of  $\text{NiOH}^+$  is well documented. Baes and Mesmer (14) have compiled the following values for the hydrolysis reactions:



The literature indicates that the solubility of  $\text{Ni}(\text{OH})_2$  depends on the degree of aging of the precipitate. The solubility product is reported to range from  $10^{-14.7}$  for a fresh precipitate to  $10^{-17.2}$  for an aged one (15,16). The equilibrium relationship of the free nickel ion and hydroxide precipitate can be used in combination with Equations 2-5 to construct the log solubility vs. pH diagrams for Ni(II) as given in Figure 1.

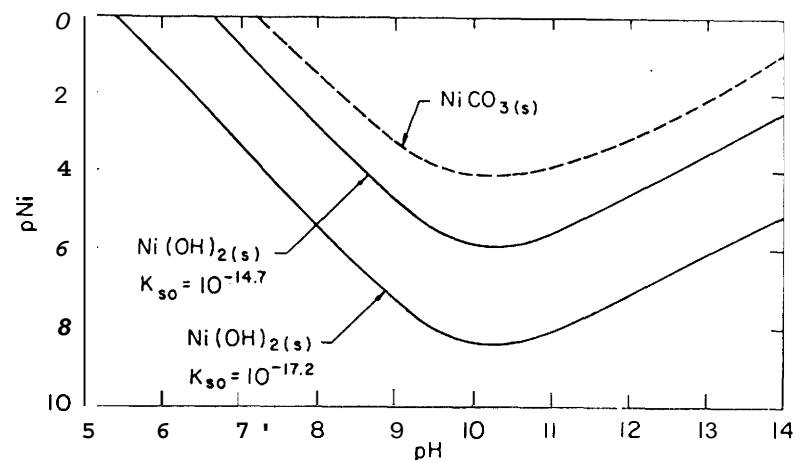


Figure 1. Comparison of solubilities of nickel carbonate ( $pK_{so} = 6.87$ ) and nickel hydroxide for active ( $pK_{so} = 14.7$ ) and aged ( $pK_{so} = 17.2$ ) precipitates ( $P_{\text{CO}_2} = 10^{-3.5} \text{ atm}$ )

Carbonate precipitates are important for some metal ions; however, the solubility of nickel carbonate ( $\log K_{so} = -6.87^{15}$ ) is sufficiently large so that it is of little consequence in natural waters. The dashed line in Figure 1 represents nickel carbonate precipitation for a system in equilibrium with  $10^{-3.5}$  atm of  $\text{CO}_2$ . Under reducing conditions the solubility of nickel would be expected to be controlled by the sulfide,  $\text{NiS}$  ( $\log K_{so} = -22.9^{15}$ ).

As indicated,  $\text{Ni}^{2+}$  forms generally weak complexes with common inorganic ligands. However, complexes of sizeable stability are formed with many organic ligands and a considerable portion of this study has been devoted to their effects on nickel-sorption reactions. Those ligands specifically studied were sulfate ( $\text{SO}_4^{2-}$ ), citrate, nitrilotriacetate (NTA), glycine, and cyanide. Appropriate data are summarized in Table I. These data were obtained from Raes and Mesmer (14), Sillen and Martell (15, 1S), and Smith and Martell (17).

#### Experimental Procedures

The oxides used in this study were  $\alpha\text{-SiO}_2$  (a-quartz), obtained commercially, and  $\alpha\text{-FeOOH}$  (goethite), which was prepared in a manner similar to that of Forbes et al. (18). The silica was washed initially in 0.1N nitric acid. Both oxides were washed with double distilled water, dried at  $100^\circ\text{C}$  for 24 hr, powdered with a mortar and pestle, and passed through a 200 mesh ( $75\ \mu\text{m}$ ) sieve. Powdered x-ray diffraction verified the existence of a-quartz and goethite. BET- $\text{N}_2$  adsorption indicated specific surface areas of  $1.7\ \text{m}^2/\text{g}$  for silica and  $85\ \text{m}^2/\text{g}$  for goethite. Corresponding ZPC values, determined by electrophoresis and turbidity measurements, were 1.7 and 5.5. Dielectrics were taken to be 4.3 for silica and 14.2 for goethite (19).

Adsorption studies were carried out in 150-mL borosilicate glass reaction vessels at room temperatures ( $22^\circ\text{--}25^\circ\text{C}$ ). The oxide was weighed to give the desired surface area per liter and then placed into the vessel. A 0.11M sodium perchlorate stock solution was added in the proper dilution to give the desired ionic strength. To this was added the appropriate amount of the nickel-ligand mixture. The pH was adjusted with strong acid or base to an initial value and then the vessel was sealed. After shaking for 3 hr, the bottle was removed and the final pH was measured. The contents were filtered through a  $0.45\text{-}\mu\text{m}$  membrane filter, and the filtrate was acidified and stored at  $4^\circ\text{C}$  prior to analysis. Samples were analyzed for total nickel by flameless atomic absorption.

Data are reported as percent nickel removed vs. pH isotherms. The James and Healy adsorption model as contained in the equilibrium computer model REDEQL2 was used to facilitate data analysis (20). In this way, an assessment of the combined effects of adsorption, complexation, and precipitation could be attempted.

#### Results

**Evaluation of Hydrolysis Data.** The application of thermodynamic models such as REDEQL2 to the type of work reported on in this chapter requires a careful assessment of the data base used. Of critical importance

in this study are the stability constants given in Table I, especially those defining hydrolysis reactions of nickel. To successfully use REDEQL2 to model laboratory reactions, it was necessary to evaluate the stability constants for  $\text{NiOH}^+$  and  $\text{Ni}(\text{OH})_2^0$ , and the solubility product of  $\text{Ni}(\text{OH})_2(s)$  for the existing conditions. Accordingly, pH values of  $10^{-4.77}\text{M}$  solutions of  $\text{Ni}^{2+}$  (at various ionic strengths ( $I$ )) were adjusted over a wide range, allowed to react for the 3-hr period, and analyzed for filterable nickel. Figure 2 shows nickel removal vs. pH for three ionic strengths tested. The curves shown are the best fit of the data and were generated using  $\log \beta_1 = -9.9$  and  $\log K_{so} = -15.2$  ( $I = 0$ ). Since residual nickel at the higher pH values was consistently below the detection limit ( $2.5\ \mu\text{g}/\text{L}$ ),  $\beta_2$ ,  $\beta_3$ , and  $\beta_4$  were assumed to be insignificant at the nickel concentrations used throughout the experimentation and multiple hydroxyl ligand complexes of nickel were ignored. Figure 3 shows the theoretical distribution of nickel(II) species in water with  $\text{Ni}_T = 10^{-4.77}\text{M}$ ,  $I = 0.01$ .

**Nickel Adsorption onto Silica and Goethite.** Figure 4 contains adsorption isotherms for nickel onto  $\alpha\text{-SiO}_2$  and  $\alpha\text{-FeOOH}$  as compared with precipitation which occurs in the absence of oxide surfaces. The lines in Figure 4, as with all figures in this chapter showing sorptive behavior, are predicted using the James and Healy model in conjunction

Table I. Acidity and Nickel Stability Constants for Complexing Ligands'

| Ligand             | Equilibrium   | Log K |
|--------------------|---|-------|
| $\text{OH}^-$      | $K_1 = \text{NiL}/\text{Ni} \cdot \text{L}$               | 4.1   |
|                    | $K_{so} = \text{Ni} \cdot \text{L}^2$                     | -15.2 |
| $\text{SO}_4^{2-}$ | $\text{HL}/\text{H} \cdot \text{L}$                       | 2.2   |
|                    | $\text{NiL}/\text{Ni} \cdot \text{L}$                     | 2.3   |
| $\text{CN}^-$      | $\text{HL}/\text{H} \cdot \text{L}$                       | 9.3   |
|                    | $\text{NiL}_4/\text{Ni} \cdot \text{L}^4$                 | 31.8  |
| $\text{GLY}^{-1}$  | $\text{HL}/\text{H} \cdot \text{L}$                       | 9.9   |
|                    | $\text{H}_2\text{L}/\text{H} \cdot \text{HL}$             | 2.3   |
|                    | $\text{NiL}/\text{Ni} \cdot \text{L}$                     | 6.3   |
| $\text{CIT}^{-4}$  | $\text{NiL}_2/\text{Ni} \cdot \text{L}^2$                 | 11.4  |
|                    | $\text{HL}/\text{H} \cdot \text{L}$                       | 16.8  |
|                    | $\text{H}_2\text{L}/\text{H} \cdot \text{HL}$             | 6.4   |
|                    | $\text{H}_3\text{L}/\text{H} \cdot \text{H}_2\text{L}$    | 4.5   |
|                    | $\text{H}_4\text{L}/\text{H} \cdot \text{H}_3\text{L}$    | 3.0   |
|                    | $\text{NiHL}/\text{Ni} \cdot \text{HL}$                   | 6.0   |
| $\text{NTA}^{-3}$  | $\text{NiH}_2\text{L}/\text{Ni} \cdot \text{H}_2\text{L}$ | 3.8   |
|                    | $\text{HL}/\text{H} \cdot \text{L}$                       | 10.5  |
|                    | $\text{H}_2\text{L}/\text{H} \cdot \text{HL}$             | 3.2   |
|                    | $\text{H}_3\text{L}/\text{H} \cdot \text{H}_2\text{L}$    | 2.2   |
|                    | $\text{NiL}/\text{Ni} \cdot \text{L}$                     | 13.1  |

'  $T = 25^\circ\text{C}, I = 0$ .

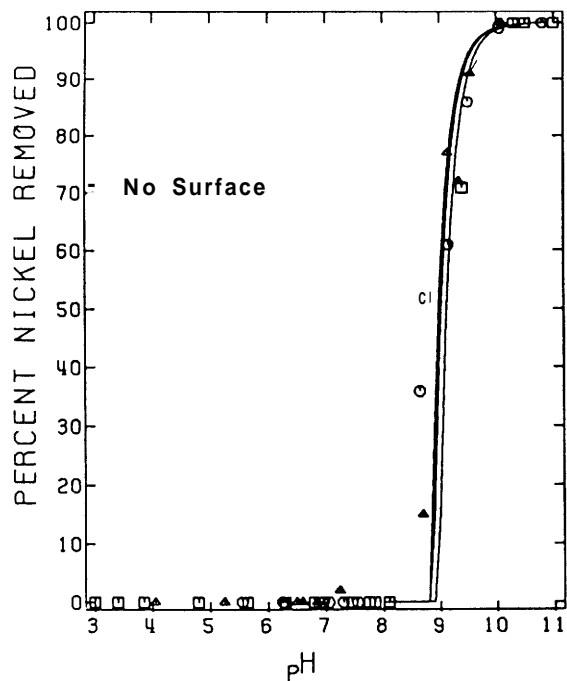


Figure 2. Nickel removal as a function of pH for varying ionic strengths (lines are predicted by REDEQL2 using  $pK_{so} = 15.2$ ,  $pNi_T = 4.77$ ; ( $\square$ )  $I = 10^{-3}$ ; ( $\circ$ )  $I = 10^{-2}$ ; ( $\Delta$ )  $I = 10^{-1}$ )

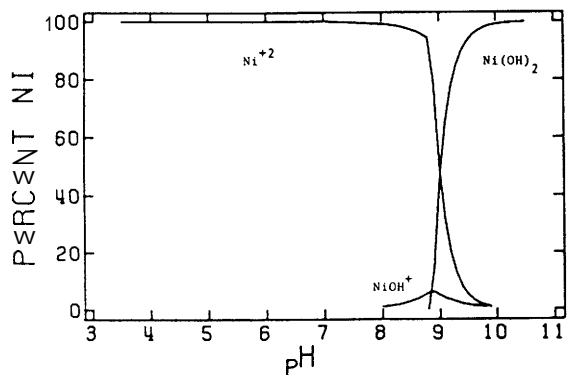


Figure 3. Theoretical distribution of nickel as a function of pH ( $\{Ni\}_T = 10^{-4.77}M$ ,  $I = 0.01$ )

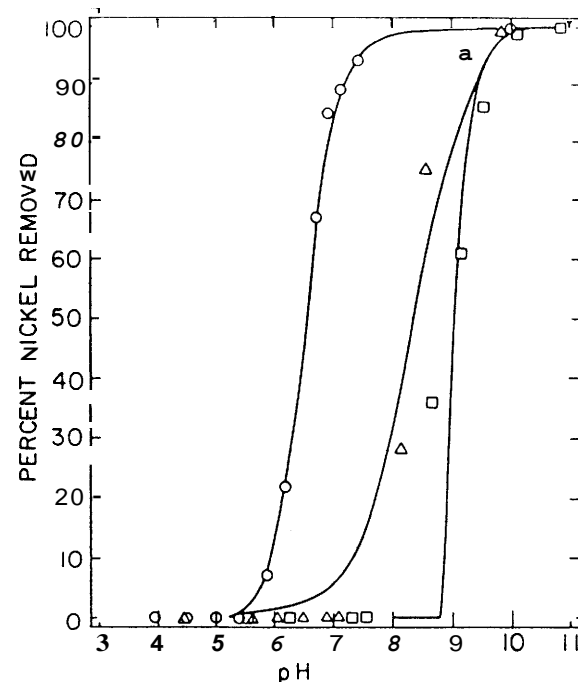


Figure 4. Nickel removal as a function of pH in the presence of oxide surfaces ( $\{Ni\}_T = 10^{-4.77}M$ ,  $I = 0.01$ ,  $\{FeOOH\} = 0.59$  g/L ( $50$  m<sup>2</sup>/L),  $\{SiO_2\} = 29.4$  g/L ( $50$  m<sup>2</sup>/L); ( $\circ$ ) Fe; ( $\Delta$ ) Si; ( $\square$ ) no solid)

with the equilibrium subroutines in REDEQL2. The isotherms generated by the model are for  $\Delta G_{CHEM}$  values of  $-6.55$  kcal/mol and  $-5.35$  kcal/mol for silica and goethite, respectively. It is apparent from Figure 4 that goethite adsorbs greater amounts of nickel at lower pH values than silica in spite of its higher ZPC. This is explained in the James and Healy model by the greater solvation-energy term for sorption onto silica attributable to its low dielectric. By comparison with Figure 3, it can be seen that most adsorption occurs in the pH range where  $Ni^{+2}$  is the dominant dissolved form for goethite and where  $NiOH^+$  is the dominant dissolved species for sorption onto silica. In the latter case, the reduced charge brings about a reduction in the oppositional solvation-energy term, shifting the overall free energy of adsorption to more negative values.

**Effects of Complexing Ligands on Adsorption.** There are basically two effects that a complexing ligand can have on the adsorption reactions being studied. If the resulting complex is not specifically adsorbed (that is,  $\Delta G_{CHEM} = 0$ ), then the effect of the ligand is to retard overall adsorption. However, in some instances the ligand has been shown to

enhance the adsorption reaction either by directly attaching the complex to the oxide surface or by altering the surface properties and sorption sites such that adsorption is favored more (21). The version of REDEQL2 that was used is based on the former conceptual model, that is, ligands compete with the surface for the metal ion. Substantial disagreement between the model and experimental data suggests that specific adsorption of the complex is occurring. Examples of both retardation and enhancement of nickel adsorption will be given.

**SULFATE.** Large amounts of sulfate ion are required to bring about significant complexation of  $\text{Ni}^{2+}$ . For  $\text{Ni}_T = 10^{-4.77}\text{M}$ ,  $10^{-1}\text{M}$  sulfate complexes approximately 50% of the nickel present as the uncharged ion pair,  $\text{NiSO}_4^0(\text{aq})$ . The resulting adsorption edges for goethite and silica are shown in Figure 5. Comparison with Figure 4 shows a slight shift of the curves to the right as would be expected. A portion of this is attributable to the higher ionic strength of the sulfate medium ( $\sim 0.1\text{M}$ ). The data can be explained adequately by the competition model used in REDEQL2.  $\Delta G_{\text{CHEM}}$  for the complex is taken to be zero.

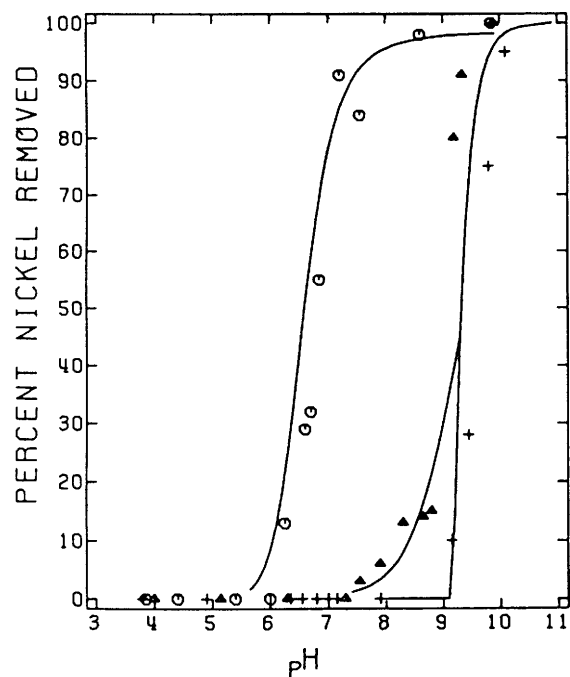


Figure 5. Nickel removal as a function of pH in the presence of sulfate and oxide surfaces ( $\{\text{Ni}\}_T = 10^{-4.77}\text{M}$ ,  $\{\text{SO}_4\}_T = 10^{-1}\text{M}$ ,  $I = 0.3$ ,  $\{\text{FeOOH}\} = 0.59\text{ g/L}$  ( $50\text{ m}^2/\text{L}$ ),  $\{\text{SiO}_2\} = 29.41\text{ g/L}$  ( $50\text{ m}^2/\text{L}$ ); (O) Fe; (A) Si; (+) no solid)

**CITRATE.** Citrate can be considered to have the generalized formula  $\text{H}_3\text{L}$ , since a fourth proton, associated with the hydroxyl group, does not ionize in the pH range of water. With  $\text{Ni}^{2+}$  it forms a stable tridentate chelate ( $\text{Ni-CIT}^{-1}$ ) which, at low pH, may be protonated. Figures 6 and 7 show the effects of adding this ligand on adsorption onto silica and goethite, respectively. For both systems, increasing the amount of citrate shifts the curves to the right. For silica, once the pH becomes high enough to produce  $\text{NiOH}^+$ , removal takes place. According to the model, at higher pH values precipitation of  $\text{Ni}(\text{OH})_{2(s)}$  plays a greater role in the removal as the ligand concentration increases. However, parallel experimental systems containing only the nickel-citrate chelate and no silica showed little precipitation. This anomaly suggests either that the oxide surface is acting as a nucleation site for  $\text{Ni}(\text{OH})_{2(s)}$  formation, or that specific adsorption of the complex is occurring.

For the nickel-citrate-goethite system (Figure 7), the oxide becomes more competitive with increasing pH because of the greater coulombic attraction predicted by the Nernst equation. Unlike silica,  $\text{Ni}^{2+}$  is the

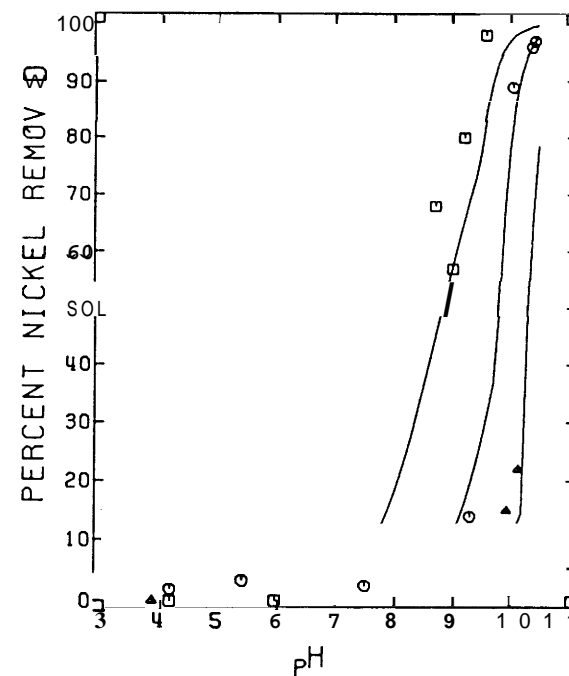


Figure 6. Nickel removal as a function of pH in the presence of silicon dioxide and citrate ( $\{\text{Ni}\}_T = 10^{-4.77}\text{M}$ ,  $I = 0.01$ ,  $\{\text{SiO}_2\} = 29.41\text{ g/L}$  ( $50\text{ m}^2/\text{L}$ ); (□)  $\text{CIT} = 10^{-5}$ ; (O)  $\text{CIT} = 10^{-4}$ ; (Δ)  $\text{CIT} = 10^{-3}$ )



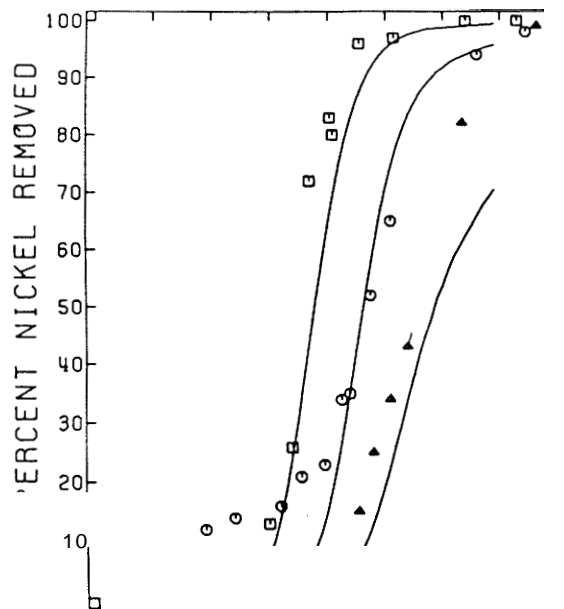


Figure 7. Nickel removal as a function of pH in the presence of iron oxide and citrate ( $\{Ni\}_T = 10^{-4.77}M$ ,  $I = 0.01$ ,  $\{FeOOH\} = 0.59$  g/L ( $50$   $m^2/L$ ); ( $\square$ )  $CIT = 10^{-3}$ ; ( $\circ$ )  $CIT = 10^{-4}$ ; ( $\Delta$ )  $CIT = 10^{-5}$ )

main species in solution. At the highest citrate concentration studied ( $10^{-3}M$ ), the data show slightly greater nickel removal than predicted by the model. As with silica, it appears possible that there is a small amount of adsorption of the nickel-citrate complex onto the oxide surface. In general, however, the competition model used is sufficient to account for pertinent data trends.

**NITRILOTRIACETATE.** Nitriilotriacetic acid (NTA) is a triprotic weak acid which is a well known sequestering agent. It forms a quadridentate chelate with  $Ni^{2+}$  of the form  $Ni-NTA^{-1}$  which is very stable ( $\log K = 13.1$ ). If sufficient NTA is added to solution, virtually complete ( $\sim 100\%$ ) chelation of  $Ni^{2+}$  takes place in the neutral and alkaline pH range. Results of the nickel-NTA-oxide systems are shown in Figures 8 and 9 for silica and goethite, respectively,

For silica, it can be seen that the effect of NTA on the adsorption of nickel is qualitatively similar to that of citrate, although, as would be expected, the extent of the adsorption shift to the right is considerably more pronounced. A limited amount of  $NiOH^+$  adsorption is deferred

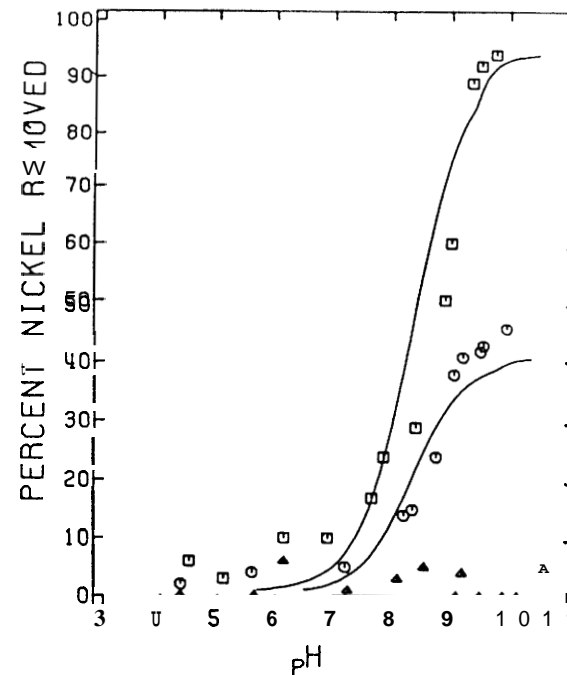


Figure 8. Nickel removal as a function of pH in the presence of silicon dioxide and NTA ( $\{Ni\}_T = 10^{-4.77}M$ ,  $I = 0.01$ ,  $\{SiO_2\} = 29.41$  g/L ( $50$   $m^2/L$ ); ( $\circ$ )  $NTA = 10^{-6}$ ; ( $\square$ )  $NTA = 10^{-5}$ ; ( $\Delta$ )  $NTA = 10^{-4}$ )

to high pH values since the nickel concentration available for adsorption is lower in the presence of the complexing ligand. At the high NTA concentration ( $10^{-4}M$ ), neither adsorption nor precipitation occurs.

As with silica, the model is able to account well for the observations made in the goethite system. The adsorption intensity between the oxide and  $Ni^{2+}$  will never increase to a point sufficient to remove the nickel from the NTA. Even though  $K_{ADS}$  increases with pH (as the oxide surface becomes more negative), the strength of the  $Ni-NTA^{-1}$  complex will increase since the amount of deprotonated NTA ( $L^{-3}$ ) will also become greater. Nickel removal in Figure 9 is slightly greater than predicted at the higher NTA concentrations, again, as with  $Ni-CIT^{-1}$ , suggesting the possibility that some adsorption of the complex takes place. However, the small discrepancies between theory and experiment in Figures 7 and 9 could just as well be explained through slight adjustments in the thermodynamic data base used.

The interactions that take place in the systems described can be viewed conveniently in a graphical manner as shown in Figure 10. Here

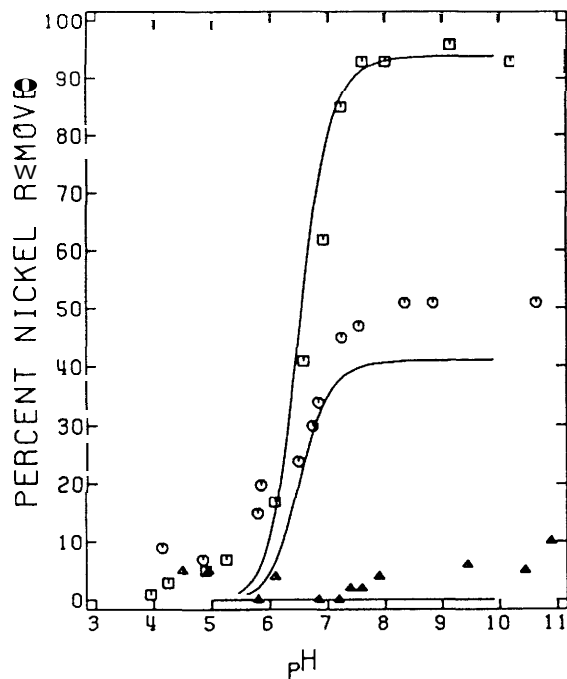


Figure 9. Nickel removal as a function of pH in the presence of iron oxide and NTA ( $\{Ni\}_T = 10^{-4.77}M$ ,  $I = 0.01$ ,  $\{FeOOH\} = 0.59 \text{ g/L}$  ( $50 \text{ m}^2/\text{L}$ ); ( $\circ$ )  $NTA = 10^{-6}$ ; ( $\square$ )  $NTA = 10^{-5}$ ; ( $\triangle$ )  $NTA = 10^{-4}$ )

the speciation of nickel in both the NTA-silica and NTA-goethite systems is given. Qualitatively similar diagrams for citrate and sulfate effects could also be made.

**GLYCINE.** Glycine, like all the amino acids, displays amphoteric properties over the pH range of interest. It can be represented as  $H_2L^+$  having two available protons. The deprotonated ligand forms both bidentate ( $Ni-GLY^+$ ) and quadridentate ( $Ni-(GLY)_2^0$ ) chelates of moderate stability with  $Ni^{2+}$ , although at the glycine-nickel ratios used in this study  $Ni-GLY^{+1}$  is the dominant complex.

The results of the addition of  $10^{-5}$  and  $10^{-4}$  mol/L of glycine to  $10^{-4.77}M$  nickel are shown in Figure 11. Both theory (solid lines) and data confirm that a tenfold increase in total glycine results in an increase of one pH unit for hydroxide precipitation. At the lower concentration of glycine, insufficient complexation takes place to defer the precipitation reaction.

When  $\alpha\text{-SiO}_2$  is added to the system, the results shown in Figure 12 are obtained. Adsorption and precipitation of nickel are affected only slightly by  $10^{-5}M$  glycine. At  $10^{-4}M$  both the model and the data suggest

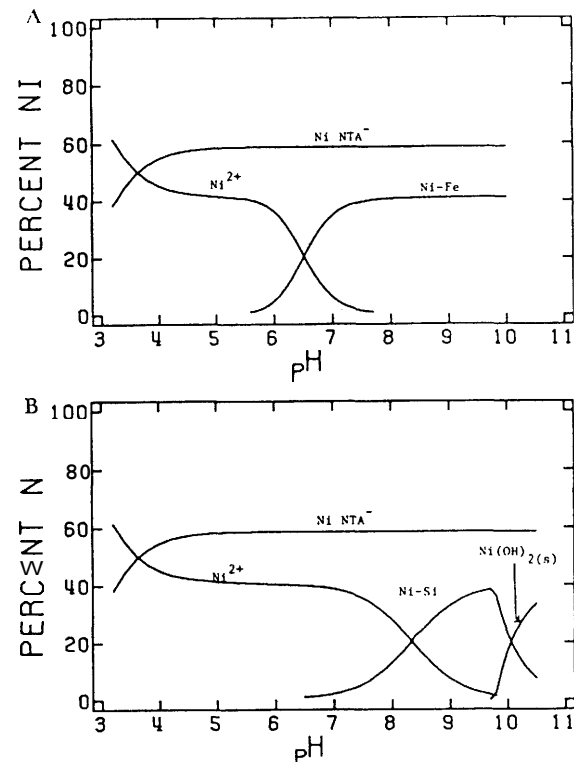


Figure 10. Theoretical distribution of nickel in the presence of (A) iron oxide and NTA ( $\{Ni\}_T = 10^{-4.77}M$ ,  $\{NTA\}_T = 10^{-5}M$ ,  $I = 0.01$ ,  $\{FeOOH\} = 0.59 \text{ g/L}$  ( $50 \text{ m}^2/\text{L}$ )) and (B) silicon dioxide and NTA ( $\{Ni\}_T = 10^{-4.77}M$ ,  $\{NTA\}_T = 10^{-5}M$ ,  $I = 0.01$ ,  $\{SiO_2\} = 29.41 \text{ g/L}$  ( $50 \text{ m}^2/\text{L}$ ))

that only  $NiOH^+$  is adsorbed up to a maximum of 15% of the total nickel at pH 8.5, with precipitation controlling above pH 10. These interactions are shown more clearly in the speciation diagram of Figure 13. The model and data are in good agreement, indicating  $Ni-GLY^+$  does not adsorb specifically onto silica.

Figure 14, when compared with Figure 4, shows that the model predicts that  $10^{-5}M$  glycine will not affect the removal of nickel by goethite. This is confirmed by the experimental data; however, for higher glycine concentrations the model and the data are in poor agreement. The theory used predicts that as the pH approaches the dissociation pH of the amino group of the glycine ( $\sim 9$ ), the extent of complexation is great enough to complex the nickel effectively and prevent adsorption of either  $Ni^{2+}$  or  $NiOH^+$  by the goethite. The model permits adsorption of these species only. However, it is likely that there is interaction between the oxide surface and the  $Ni-GLY^+$  chelate. Electrostatic attrac-

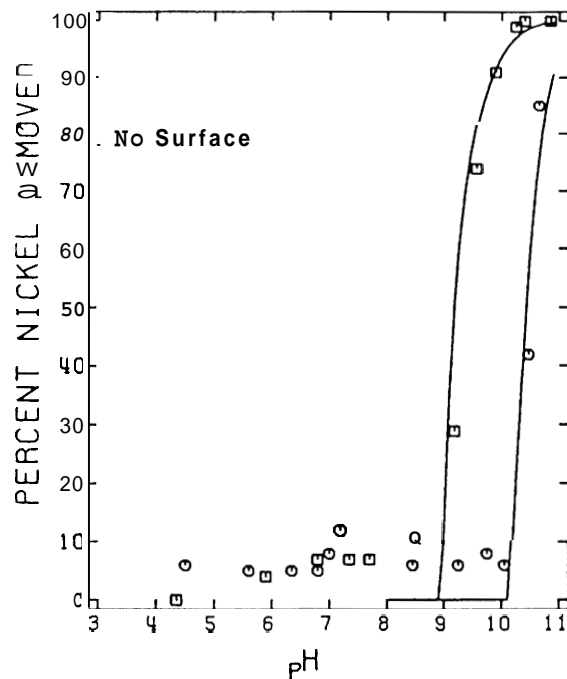


Figure 11. Nickel removal as a function of pH in presence of glycine ( $\{Ni\}_T = 10^{-4.77}M$ ,  $I = 0.01$ ; ( $\square$ )  $GLY = 10^{-5}$ ; ( $\circ$ )  $GLY = 10^{-4}$ )

tion would occur between the positively charged complex and the negative surface, but it would not be as great for  $Ni^{2+}$  since it has a lower charge. Using the equations in the Appendix it can be shown that coulombic forces are insufficient to account for the removals observed, and that a specific adsorption energy ( $\Delta G_{CHEM}$ ) of approximately  $-3$  kcal/mol for  $Ni-GLY^+$  and goethite is required.

**CYANIDE.** Hydrogen cyanide is weakly acidic ( $pK_a = 9.3$ ). Cyanide ion reacts to form complexes with many transition metals. The quaternary nickel-cyanide complex,  $Ni(CN)_4^{-2}$ , is extraordinarily stable ( $\log \beta_4 = 31.8$ ) and dominates the simple aqueous chemistry of nickel as shown in Figure 15. At total cyanide concentrations of  $10^{-4}M$  and above, hydrolysis reactions of  $Ni^{2+}$  are deferred indefinitely.

When silica is added to the nickel-cyanide system, the results are quite predictable as shown in Figure 16. At the lower cyanide concentration ( $10^{-5}M$ ) there is enough cyanide to complex about 10% of the nickel present, so adsorption of  $NiOH^+$  onto silica and precipitation of  $Ni(OH)_2(s)$  are affected only slightly. As would be expected, at higher cyanide concentrations the nickel is made completely soluble at all pH values studied.

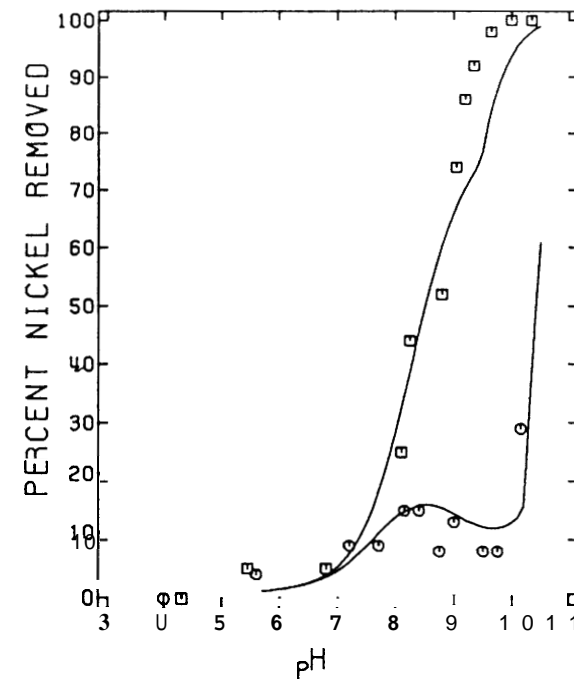


Figure 12. Nickel removal as a function of pH in the presence of silicon dioxide and glycine ( $\{Ni\}_T = 10^{-4.77}M$ ,  $I = 0.01$ ,  $\{SiO_2\} = 29.41$  g/L ( $50$  m<sup>2</sup>/L); ( $\square$ )  $GLY = 10^{-5}$ ; ( $\circ$ )  $GLY = 10^{-4}$ )

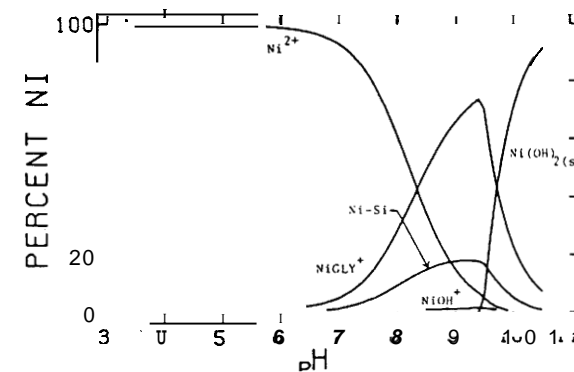


Figure 13. Theoretical distribution of nickel in the presence of silicon dioxide and glycine ( $\{Ni\}_T = 10^{-4.77}M$ ,  $\{GLY\}_T = 10^{-5}M$ ,  $I = 0.01$ ,  $\{SiO_2\} = 29.41$  g/L ( $50$  m<sup>2</sup>/L))

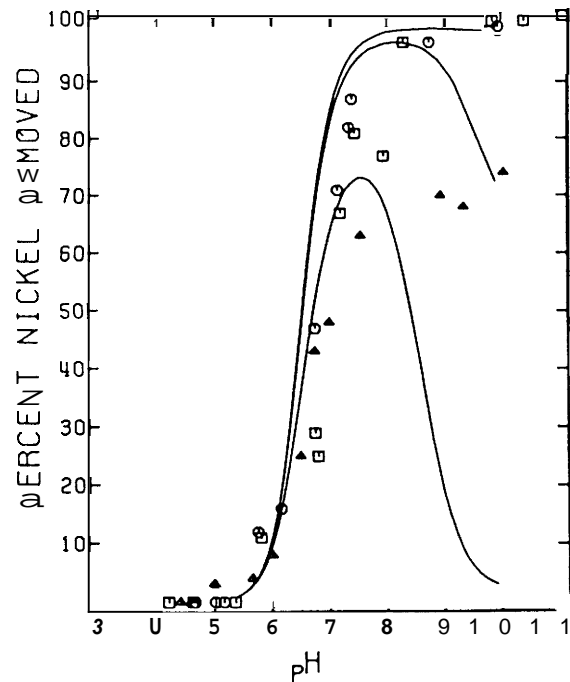


Figure 14. Nickel removal as a function of pH in the presence of iron oxide and glycine ( $\{Ni\}_T = 10^{-4.77}M$ ,  $I = 0.01$ ,  $\{FeOOH\} = 0.59$  g/L (50 m<sup>2</sup>/L); (□) CLY =  $10^{-5}$ ; (○) GLY =  $10^{-4}$ ; (△) GLY =  $10^{-3}$ )

Behavior in the goethite-nickel-cyanide system (Figure 17) is much less obvious. Agreement between model and theory exists only at the low cyanide concentration. At higher concentrations the model is able to predict only the neutral pH range in which the soluble nickel-cyanide complex does not adsorb. Of considerably greater interest is the enhanced adsorption of nickel at pH 6 and below, where no adsorption takes place in the absence of cyanide (Figure 4). The negatively charged complex will adsorb onto the now positively charged goethite surface. However, somewhat analogous to the glycine system, the favorable electrostatic gradient is not sufficient to account for the removals observed. It is apparent that  $Ni(CN)_4^{2-}$  is capable of adsorbing specifically to goethite. From the equations in the Appendix, a  $\Delta G_{CHEM}$  term of  $-7$  kcal/mol can be calculated. The slight downturn in the experimental data for the  $10^{-3}M$  cyanide case below pH 4 may be real, since it would be expected that the  $Ni(CN)_4^{2-}$  complex will break down as HCN is formed at low pH (Figure 15). The small but significant removal that occurs above pH 9 may also be attributable to specific adsorption of the complex;

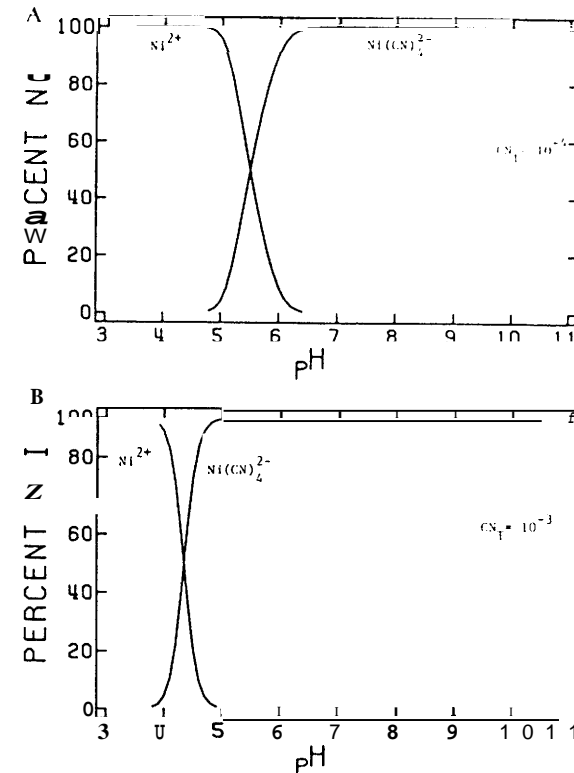


Figure 15. Theoretical distribution of nickel in the presence of (A)  $10^{-4}M$  cyanide ( $\{Ni\}_T = 10^{-4.77}M$ ,  $I = 0.01$ ) and (B)  $10^{-3}M$  cyanide ( $\{Ni\}_T = 10^{-4.77}M$ ,  $I = 0.01$ )

however, in this case the removal is much less because it is against an unfavorable electrostatic gradient. In view of this, the fact that no adsorption occurs in the neutral pH range cannot be readily explained, in spite of agreement with the model, and therefore points to the possibility that  $\Delta G_{CHEM}$  may vary with pH. Interactions among cyanide, nickel, goethite, and pH are summarized in Figure 18.

### Discussion

The results of the specific adsorption of nickel onto silica and goethite are in basic agreement with similar work reported for other metals (2, 18). The James and Healy model is capable of describing the interactions well. Similarly, when complexing ligands are added to nickel-silica systems the results can be adequately explained by a competition model in

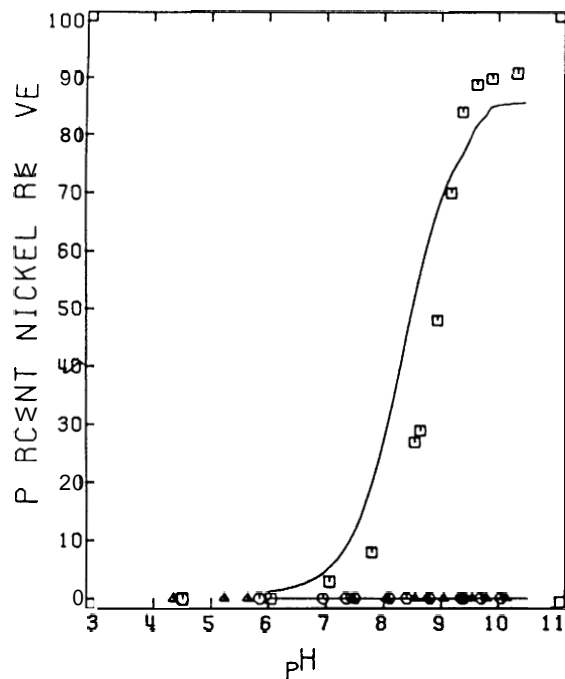


Figure 16. Nickel removal as a function of pH in the presence of silicon dioxide and cyanide ( $\{Ni\}_T = 10^{-4.77}M$ ,  $I = 0.01$ ,  $\{SiO_2\} = 29.41$  g/L ( $50$  m<sup>2</sup>/L); ( $\square$ )  $CN = 10^{-5}$ ; ( $\circ$ )  $CN = 10^{-4}$ ; ( $\Delta$ )  $CN = 10^{-3}$ )

which the nickel-ligand complex does not adsorb specifically to the silica surface.

For the case of nickel-ligand-goethite systems, the results for sulfate, citrate, and NTA could be accounted for by the model used, although some small degree of specific adsorption appeared to take place for citrate and NTA complexes. The evidence for this is not conclusive. However, for both nickel glycine and nickel cyanide, specific energies of adsorption of  $-3$  and  $-7$  kcal/mol, respectively, were calculated.

Reasons for the adsorption of a complex in one case, but not in another, are not always straightforward. In the case of silica it was shown that energetic considerations favor adsorption when  $NiOH^+$  is the dominant species in solution. Any complex that defers or eliminates the hydrolysis of  $Ni^{2+}$  would be expected to affect adsorption of nickel accordingly. Specific bonding of a complex to a surface oxygen could be via a hydrogen or a dipole effect; however, the bond energies evidently are not large enough to overcome the repulsive solvation and electrostatic forces. Direct bonding of a functional group on the complex to the silicon atom is unlikely because of the very large Si-O bond energies of silica which have a large ionic character.

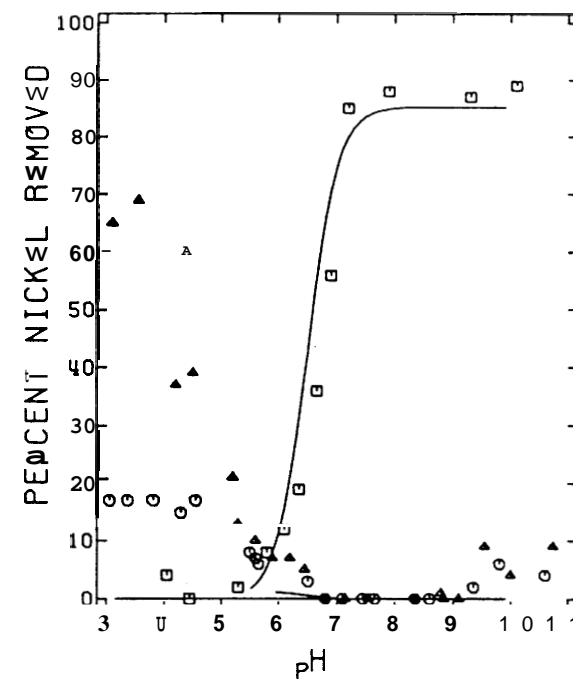


Figure 17. Nickel removal as a function of pH in the presence of iron oxide and cyanide ( $\{Ni\}_T = 10^{-4.77}M$ ,  $I = 0.01$ ,  $\{FeOOH\} = 0.59$  g/L ( $50$  m<sup>2</sup>/L); ( $\square$ )  $CN = 10^{-5}$ ; ( $\circ$ )  $CN = 10^{-4}$ ; ( $\Delta$ )  $CN = 10^{-3}$ )

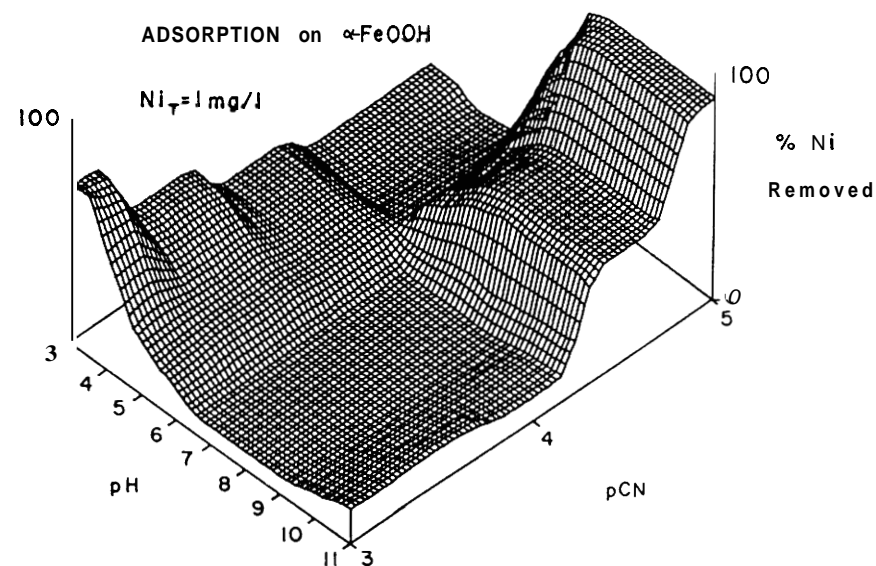


Figure 18. Three-dimensional depiction of the nickel-cyanide-goethite system (conditions as given in Figure 17)

The bonding of complexes to the surface of goethite is far more likely than to the surface of silica because of the more neutral ZPC and higher dielectric, which act to moderate electrostatic repulsion when it exists, and because of the available d orbitals of iron which extend further from the nucleus and which are capable of accepting electrons from appropriate donor atoms of the complex. The structures of the citrate, NTA, glycine, and cyanide complexes of nickel are shown in Figure 19. Nickel-citrate and nickel-NTA both have a  $-1$  charge, so at pH values above the ZPC (5.5) electrostatic repulsion takes place. In the case of Ni-NTA $^{-1}$ , the only possible bonding site is via one of the water molecules attached to the nickel. This would require deprotonation of a water molecule, bringing about a greater negative charge and more electrostatic repulsion. In contrast, the Ni-CIT $^{-1}$  chelate has an available binding site at the terminal carboxyl group. The fact that little, if any, specific adsorption of this complex takes place on goethite implies that electrostatic forces are too great to overcome.

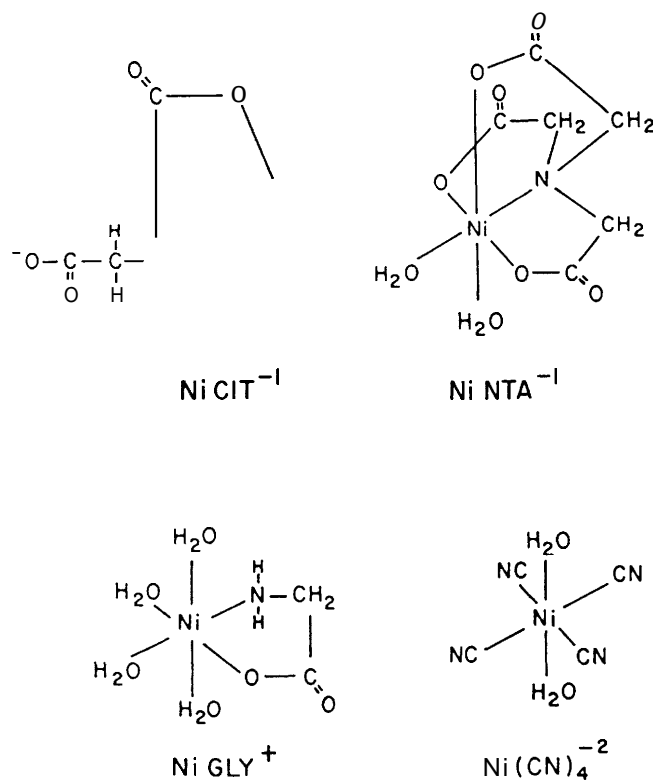
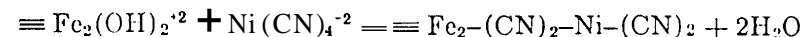


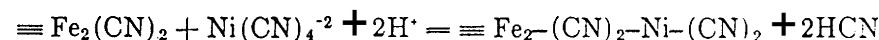
Figure 19. Conformational structures of complexes used in this study. Data from Ref. 13 (cyanide), Ref. 22 (citrate and NTA), and Ref. 23 (glycine).

For Ni-GLY $^{+}$  the electrostatic gradient is more favorable, and it appears that specific bonding to the surface through the amine group is possible either by replacement of one of the protons and formation of a covalent bond with iron or by the direct formation of a hydrogen bond with a surface oxo group. The former mechanism is more favorable for Ni-NTA $^{-1}$  since bonding can take place without disruption of the chelating ring. However, the magnitude of  $\Delta G_{\text{CHEM}}$  ( $-3$  kcal/mol) would favor the latter mechanism.

The structure of the nickel-cyanide complex is square planar—the four Ni-C bonds being of equal length at  $90^\circ$  to one another. The polar waters are slightly closer to the central nickel atom (13). The excellent electron donor properties of the nitrogen atoms that face toward the solution imply very strongly that covalent surface bonding to the iron takes place. The relatively high  $\Delta G_{\text{CHEM}}$  ( $-7$  kcal/mol) supports this. The specific adsorption which was observed at high pH, that is, against electrostatic forces, would require an even greater value. Cyanide ion is known to form metal-cyanide chains in which both the carbon and nitrogen atoms bond covalently to neighboring metal ions. It is simplest to postulate specific adsorption of the complex to two surface sites according to the reaction



An alternate mechanism which cannot be discounted based on the evidence at hand involves the replacement of surface oxo with cyano groups, thereby altering surface properties, followed by adsorption of nickel according to



The effect on nickel sorption is the same in either case. These possibilities are undergoing further study.

### Concluding Remarks

The description of natural systems is made decidedly more difficult when specific adsorption of metal complexes onto oxide surfaces occurs. It may often be possible, in a qualitative way, to predict those systems in which complex adsorption will take place; however, the quantitative extent of adsorption can be established only through direct experimentation. The number of combinations of even common metals, ligands, and surfaces is quite large, making the task a formidable one. It may be worthwhile to devise methods of estimating complex-adsorption energies similar to those used now to estimate stability constants.

### Appendix. Equations of the James and Healy Model

#### A. Adsorption Isotherm

$$\Gamma_{M,i} = \frac{\Gamma^{\text{MAX}} K_{\text{ADS},i} [M_i]}{1 + \sum K_{\text{ADS},i} [M_i]} \text{ mol/m}^2 \quad (\text{I})$$

$$\text{where } K_{\text{ADS},i} = \exp(-\Delta G^{\circ}_{\text{ADS},i}/RT) \text{ L/mol} \quad (\text{II})$$

$$\Gamma^{\text{MAX}} = \frac{1}{\pi(x)^2 N} \text{ mol/m}^2 \quad (\text{III})$$

$$\text{and } \Delta G^{\circ}_{\text{ADS},i} = \Delta G^{\circ}_{\text{COUL},i} + \Delta G^{\circ}_{\text{SOLV},i} + \Delta G^{\circ}_{\text{CHEM},i} \quad (\text{IV})$$

#### B. Coulombic Energy

$$\Delta G^{\circ}_{\text{COUL},i} = z_i F \Delta \psi_x \text{ J/mol} \quad (\text{V})$$

$$\text{where } \Delta \psi_x = 2 \frac{RT}{zF} \ln \left[ \frac{(\exp(y) + 1) + (\exp(y) - 1) \exp(-\kappa x)}{(\exp(y) + 1) - (\exp(y) - 1) \exp(-\kappa x)} \right] \quad (\text{VI})$$

$$\text{and } y = zF\psi_0/2RT \quad (\text{VII})$$

$$\psi_0 = 2.3 RT/F (\text{pH}_{\text{ZPC}} - \text{pH}) \text{ V} \quad (\text{VIII})$$

$$\kappa = 0.328 \times 10^{10} (I)^{0.5} \text{ m}^{-1} \quad (\text{IX})$$

$$x = r_i + 2r_{\text{water}} \text{ m} \quad (\text{X})$$

$z_i$  = sign and charge of adsorbing ion

$z = 1$  (for 1:1 inert electrolyte)

$I$  = ionic strength

#### C. Solvation Energy

$$\Delta G^{\circ}_{\text{SOLV},i} = \frac{(z_i e)^2 N}{16 \pi \epsilon_0} \left[ \left( \frac{1}{x} - \frac{r_i}{2x^2} \right) \left( \frac{1}{\epsilon_1} - \frac{1}{\epsilon_0} \right) + \frac{1}{2} \cdot \frac{1}{x} \left( \frac{1}{\epsilon_s} - \frac{1}{\epsilon_1} \right) \right] \text{ J/mol} \quad (\text{XI})$$

$$\text{where } \epsilon_1 = \frac{\epsilon_b - 6}{1 + B (d\psi/dx)_x^2} + 6 \quad (\text{XII})$$

$$\text{and } \frac{d\psi}{dx} = \frac{-2\kappa RT}{zF} \sinh \left( \frac{zF\Delta\psi_x}{2RT} \right) \text{ V/m} \quad (\text{XIII})$$

$$B = 1.2 \times 10^{-17}$$

#### D. Chemical Energy

$\Delta G^{\circ}_{\text{CHEM},i}$  = fitting term which is constant for the free and hydrolyzed species of a component. It represents the energy change resulting from chemical interaction forces such as van der Waals and H-bonding.

#### Acknowledgment

This research was supported in part by Grant EY-76-02-S-2727 of the Department of Energy.

#### Literature Cited

- James, R. O.; Stiglich, P. J.; Healy, T. W. "Analysis of Models of Adsorption of Metal Ions at Oxide/Water Interfaces," *Faraday Discuss. Chem. Soc.* **1975**, *59*, 142.
- James, R. O.; MacNaughton, M. G. "The Adsorption of Aqueous Heavy Metals on Inorganic Minerals," *Geochim. Cosmochim. Acta* **1977**, *41*, 154.
- Hohl, H.; Stumm, W. "Interaction of  $\text{Pb}^{2+}$  with Hydrated  $\gamma\text{-Al}_2\text{O}_3$ ," *J. Colloid Interface Sci.* **1976**, *55*, 281.
- Kurbatov, M. H.; Wood, G. B.; Kurbatov, J. D. "Application of the Maslov Law to Adsorption of Divalent Ions on Hydrated Ferric Oxide," *J. Chem. Phys.* **1951**, *19*, 258.
- Greenberg, S. A. "The Chemisorption of Calcium Oxide by Silica," *J. Phys. Chem.* **1956**, *60*, 325.
- Dugger, D. L. "The Exchange of Twenty Metal Ions with the Weakly Acidic Silanol Group of Silica Gel," *J. Phys. Chem.* **1964**, *68*, 757.
- Schindler, P. W.; Furst, B.; Dick, R.; Wolf, P. U. "Ligand Properties of Surface Silanol Groups—I. Surface Complex Formation with  $\text{Fe}^{3+}$ ,  $\text{Cu}^{2+}$ ,  $\text{Cd}^{2+}$ ,  $\text{Pb}^{2+}$ ," *J. Colloid Interface Sci.* **1976**, *55*, 469.
- Huang, C. P.; Stumm, W. "Specific Adsorption of Cations on Hydrated  $\gamma\text{-Al}_2\text{O}_3$ ," *J. Colloid Interface Sci.* **1973**, *43*, 409.
- Shaw, D. J. "Introduction to Colloid and Surface Chemistry," 2nd ed.; Butterworths: London, **1978**.
- Grahame, D. C. "The Electrical Double Layer and the Theory of Electrocapilarity," *Chem. Rev.* **1947**, *41*, 441.
- Grahame, D. C. "On the Specific Adsorption of Ions in the Electrical Double Layer," *J. Chem. Phys.* **1955**, *23*, 1166.
- James, R. O.; Healy, T. W. "Adsorption of Hydrolyzable Metal Ions at the Oxide-Water Interface—111: A Thermodynamic Model of Adsorption," *J. Colloid Interface Sci.* **1972**, *40*, 65.
- Cotton, A.; Wilkinson, G. "Advanced Inorganic Chemistry," 2nd ed.; Wiley-Interscience: New York, **1977**.
- Baes, C. F.; Mesmer, R. E. "The Hydrolysis of Cations"; Wiley-Interscience: New York, **1976**.
- Sillen, L. G.; Martell, A. E. "Stability Constants of Metal Ion Complexes"; The Chemical Society: London, **1964**.

16. Sillen, L. G.; Martell, A. E. "Stability Constants of Metal Ion Complexes, Supplement No. 1"; The Chemical Society: London, 1971.
17. Smith, R. M.; Martell, A. E. "Critical Stability Constants, IV: Inorganic Complexes"; Plenum: New York, 1976.
18. Forbes, E. A.; Posner, A. M.; Quirk, J. P. "The Specific Adsorption of Inorganic Hg(II) Species and Co(III) Complex Ions on Goethite," *J. Colloid Interface Sci.* **1974**, *49*, 403.
19. Vuceta, J. "Adsorption of Pb(II) and Cu(II) on  $\alpha$ -Quartz from Aqueous Solutions: Influence of pH, Ionic Strength, and Complexing Ligands," Ph.D. Thesis, California Institute of Technology, Pasadena, CA, **1976**.
20. McDuff, R. E.; Morel, F. M. M. "Description and Use of the Chemical Equilibrium Program REDEQL2," Technical Report EQ-73-02, W. M. Keck Laboratory, California Institute of Technology, 1973.
21. Davis, J. A.; Leckie, J. O. "Effect of Adsorbed Complexing Ligands on Trace Metal Uptake by Hydrous Oxides," *Environ. Sci. Technol.* **1978**, *12*, 1309.
22. Chaberek, S.; Martell, A. E. "Organic Sequestering Agents"; Wiley: New York, 1959.
23. Martell, A. E.; Calvin, M. "Chemistry of the Metal Chelate Compounds"; Prentice-Hall: New York, 1952.

RECEIVED December 7, 1978.

5

## Poliovirus Adsorption on Oxide Surfaces

### Correspondence with the DLVO-Lifshitz Theory of Colloid Stability

JAMES P. MURRAY<sup>1</sup> and G. A. PARKS

Departments of Geology, Medical Microbiology, and Applied Earth Sciences, Stanford University, Stanford, CA 94305

*Adsorption of enteric viruses on mineral surfaces in soil and aquatic environments is well recognized as an important mechanism controlling virus dissemination in natural systems. The adsorption of poliovirus type 1, strain LSc2ab, on oxide surfaces was studied from the standpoint of equilibrium thermodynamics. Mass-action free energies are found to agree with potentials evaluated from the DLVO-Lifshitz theory of colloid stability, the sum of electrodynamic van der Waals potentials and electrostatic double-layer interactions. The effects of pH and ionic strength as well as electrokinetic and dielectric properties of system components are developed from the model in the context of virus adsorption in extra-host systems.*

The transmission of viral disease in contaminated drinking water is a well-recognized phenomenon, recently reviewed by Berg et al. (1). Virus dissemination in soil and aquatic environments is controlled, to a large extent, by adsorption to mineral surfaces (2). The objective of this investigation is to determine the principal mechanisms that control adsorption, and to build predictive models that characterize the relevant interactions. We find good agreement between mass-action free energies and potentials evaluated from the DLVO-Lifshitz theory of colloid

<sup>1</sup> Current address: Division of Applied Sciences, Harvard University, Cambridge, MA 02138.



**APPENDIX B: REPORT ON ANALYSIS OF B-ZONE SAMPLES**

## **Report on analysis of B-zone samples 2m and 32m, September 16, 95**

### Review of Scanning Electron Microscopy/Energy Dispersive X-ray microanalysis (SEM/EDX)

(N.B. This analysis is based on micrographs and spectra provided by a third party and as such I have no way of verifying how representative they are.)

The 2m and 32m samples were prepared for SEM/EDX as dispersed sediments on filter paper. The samples were carbon-coated prior to examination. SEM of the two samples shows no distinct morphological differences between them. Both samples show a wide distribution of grain size with two broad populations (one greater than 10 micron and the other less than 1 micron). EDX of the samples shows significant variation in the chemical composition of individual grains. However, 'global' EDX of the samples show that both the 2m and 32m samples are Si rich (50%)

with Al, K, Ca and Fe being present at levels between 5 and 25%. As and Ni were not widely detected. However, given that EDX is not a surface analytical technique it is not possible to draw any firm conclusions as to the presence or absence of these two elements.

### Secondary Ion Mass Spectroscopy (SIMS)

SIMS analysis was carried out on the same samples previously examined by SEM/EDX. Figure 1 is an example of imaging SIMS for the 2m sample. The diameter of the imaged area is 150 microns. Six elemental maps are presented. O is used as a default element for general imaging of the sample. The O image shows several large grains (~10 $\mu$ m) in a matrix of fine grain (<1 $\mu$ m) sediment. Both As and Ni are clearly present. An examination of the images suggests that Ni and As are associated with Fe and S rich areas in the sample. The images also indicate that As and Ni are generally associated with the fine grain material rather than larger single grains.

Imaging SIMS of the 32m sample (figure to be included later) showed a generally similar

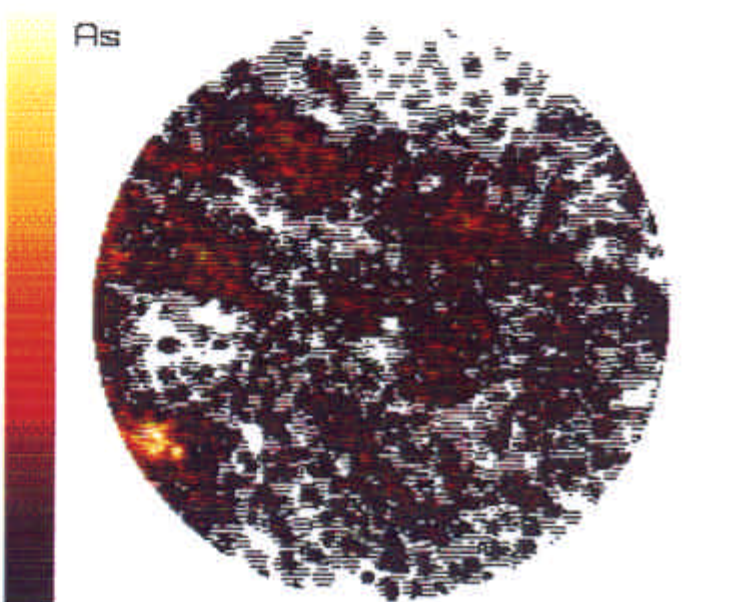
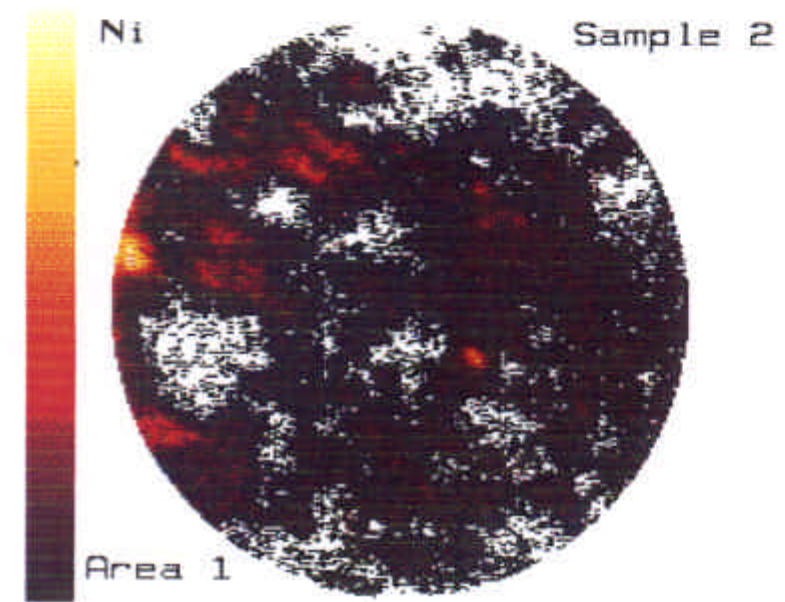
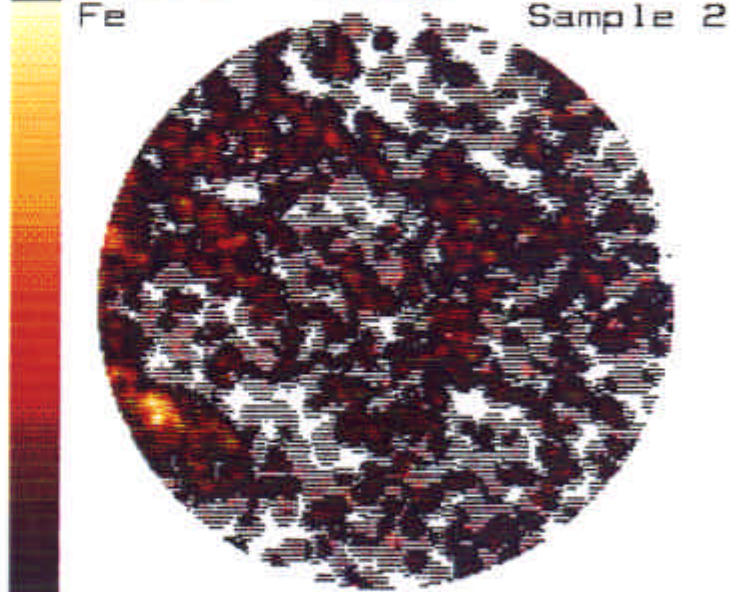
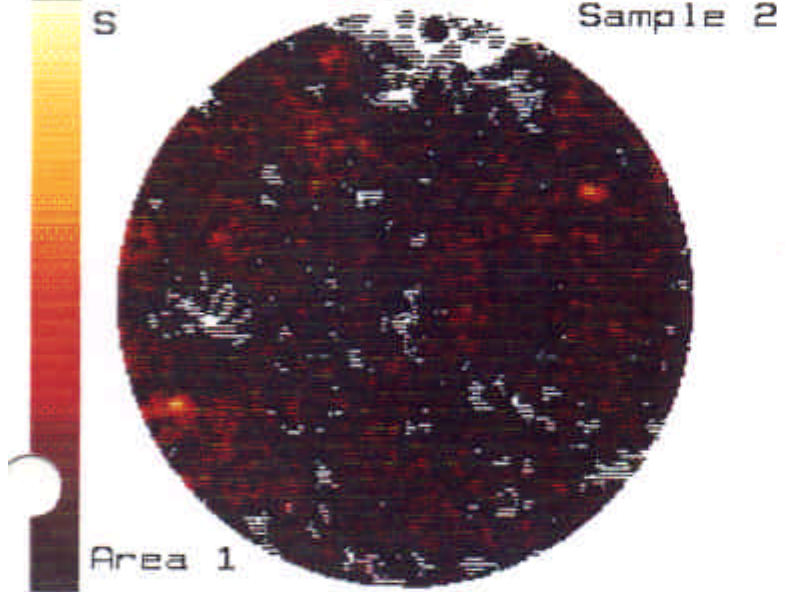
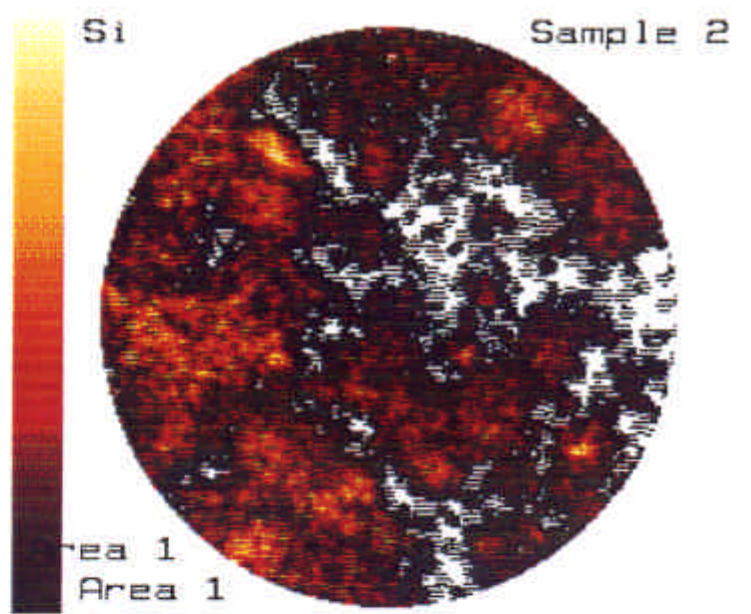
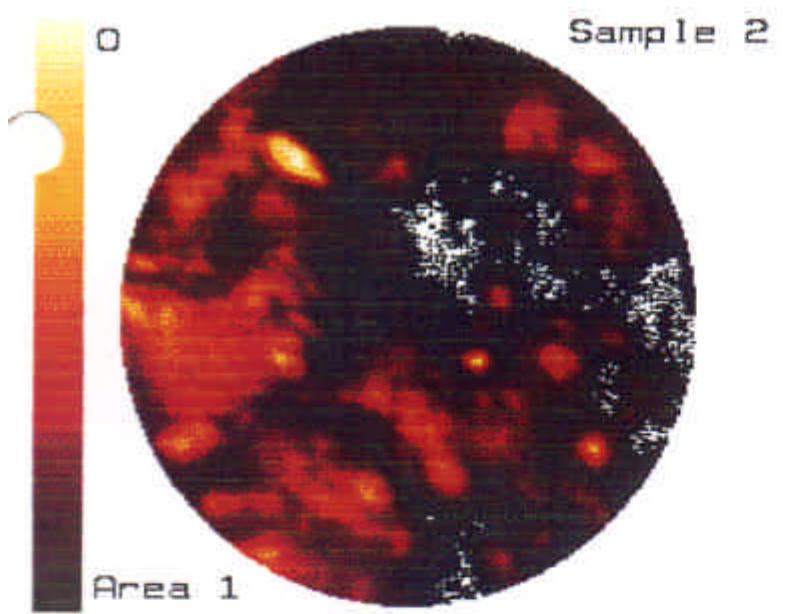
distribution pattern for Ni and As. However, the Ni content of the sample (both in terms of concentration and distribution) was greater than in the 2m sample.

In addition to elemental mapping, depth profiling was also carried out. The profiles were collected over a  $60\mu\text{m} \times 60\mu\text{m}$  area. The results are shown in figure 2 (2m sample) and figure 3 (32m sample). For the profiles, the left axis represents the surface of the sample. Profiling times fell in the range of 1000 to 1500 seconds. The sputtering rate is somewhat less than 1nm per second (greater precision is not possible with a multi-grain sample).

The depth profile for the 2m sample (figure 2) clearly shows strong signals for As and Ni. However, at a profile depth of approximately  $1\mu\text{m}$ , both the Ni and As signals dropped to zero. This clearly indicates that As and Ni exist as surface species. The 32m sample (figure 3) shows a similar surface distribution of Ni and As, but both elements appear to be limited to the first  $0.5\mu\text{m}$  of the sample surface. (N.B. since the depth profiling is averaged over a large number of grains, the apparent thickness of adsorbed Ni and As is probably greater than for any individual grain.)

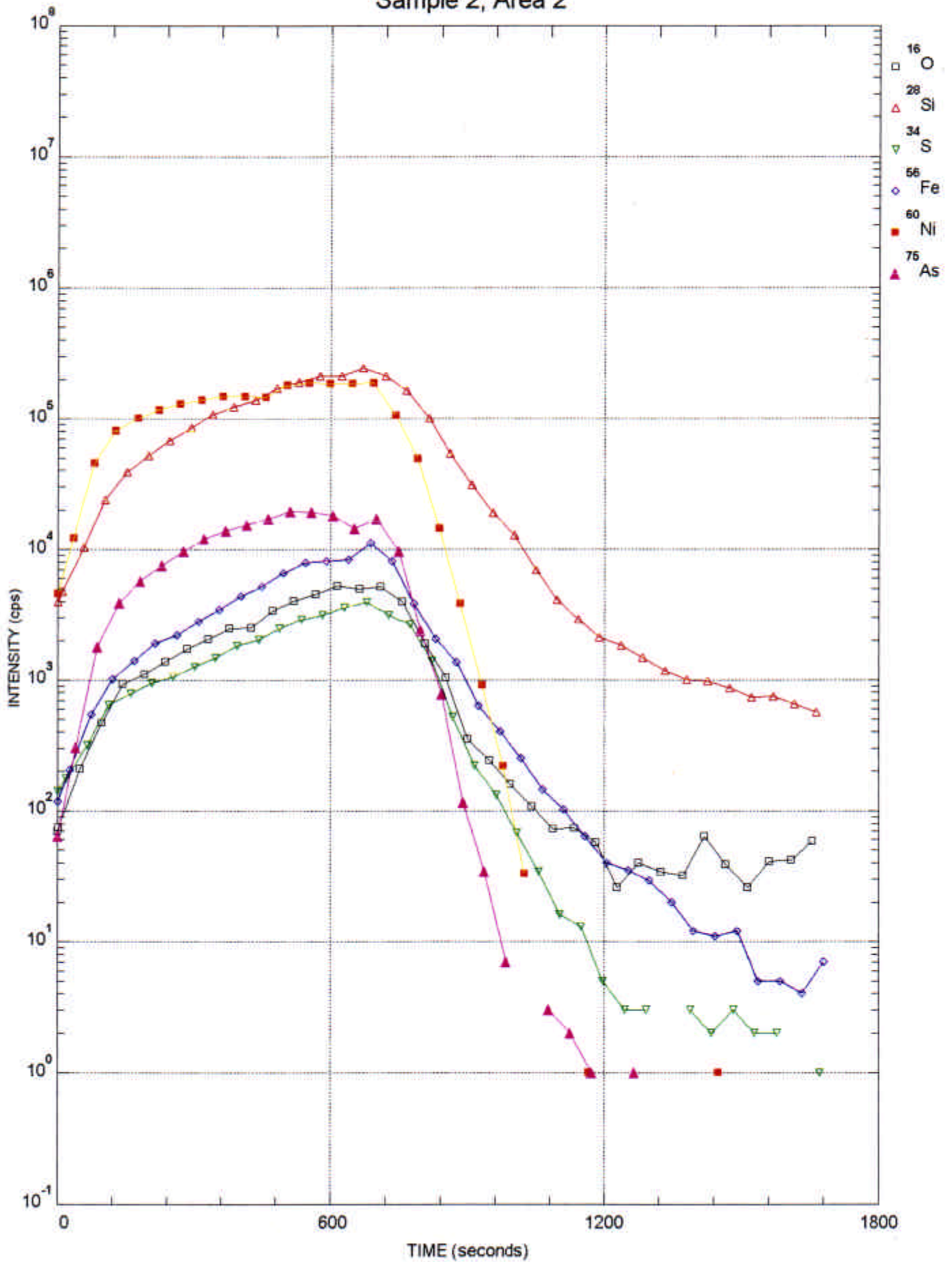
Quantitation of the As present in the depth profiles, revealed that the maximum concentration of the element in the 2m sample, was 0.2 wt% and in the 32m sample it was 0.7 wt%.

Given the limitations of time, it was not possible to obtain quantitation for the Ni present in the samples. A follow up study using gold coated samples, rather than Carbon coated, would allow for mapping of Carbon which is important in establishing any association of Ni and As with biologically derived material in the sediments.



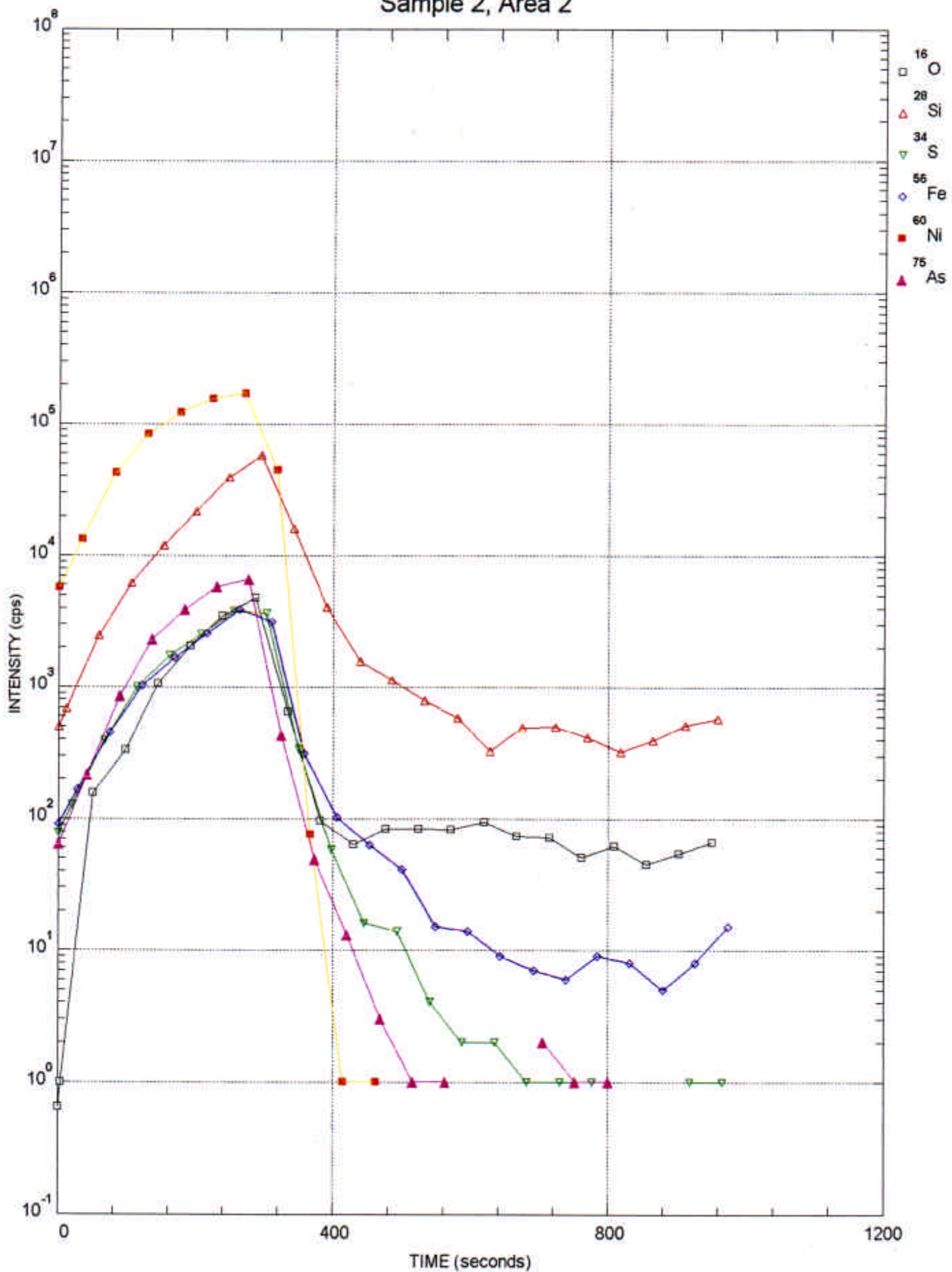


test2  
Sample 2, Area 2



s\_32a1  
Sample 2, Area 2

IS-ZONE 232



960104

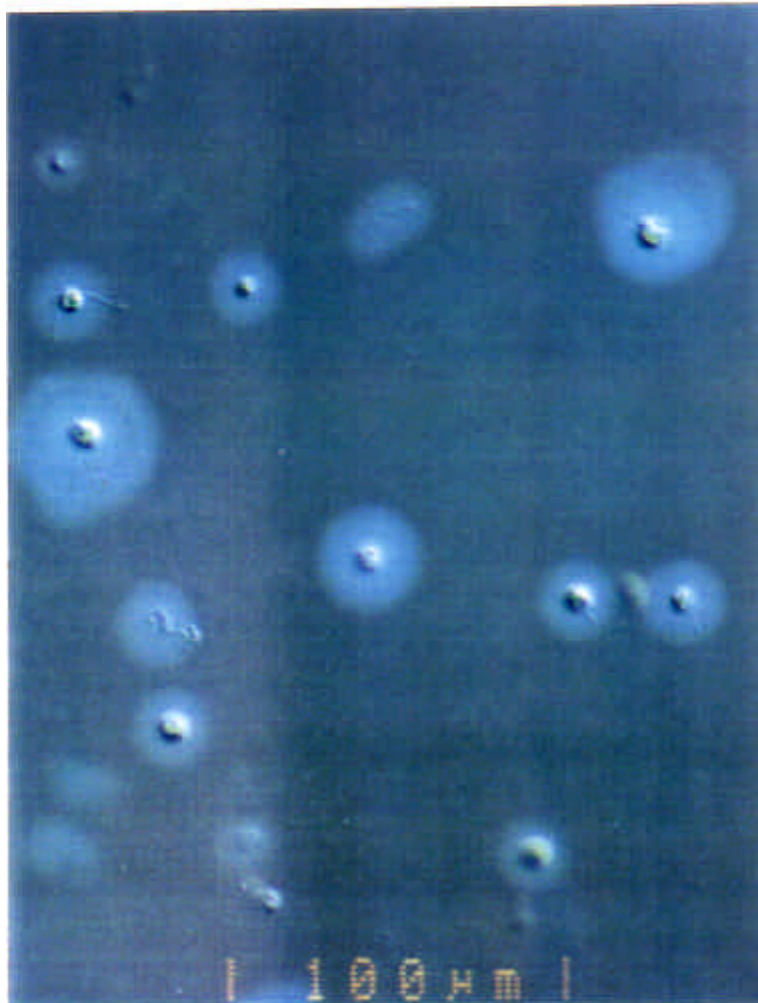
14:01:08

SSW

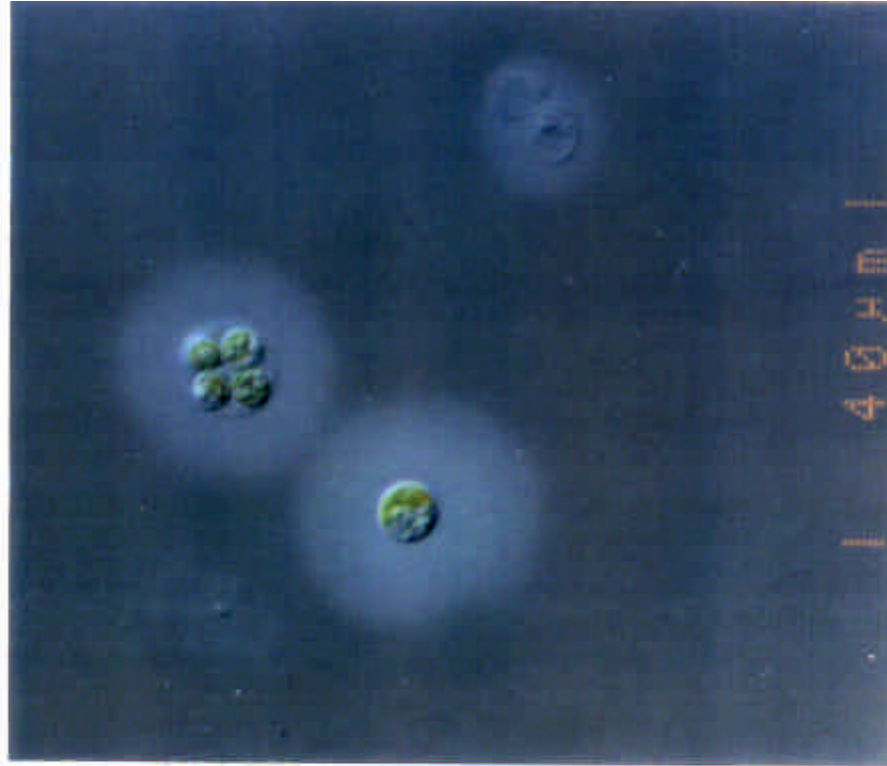
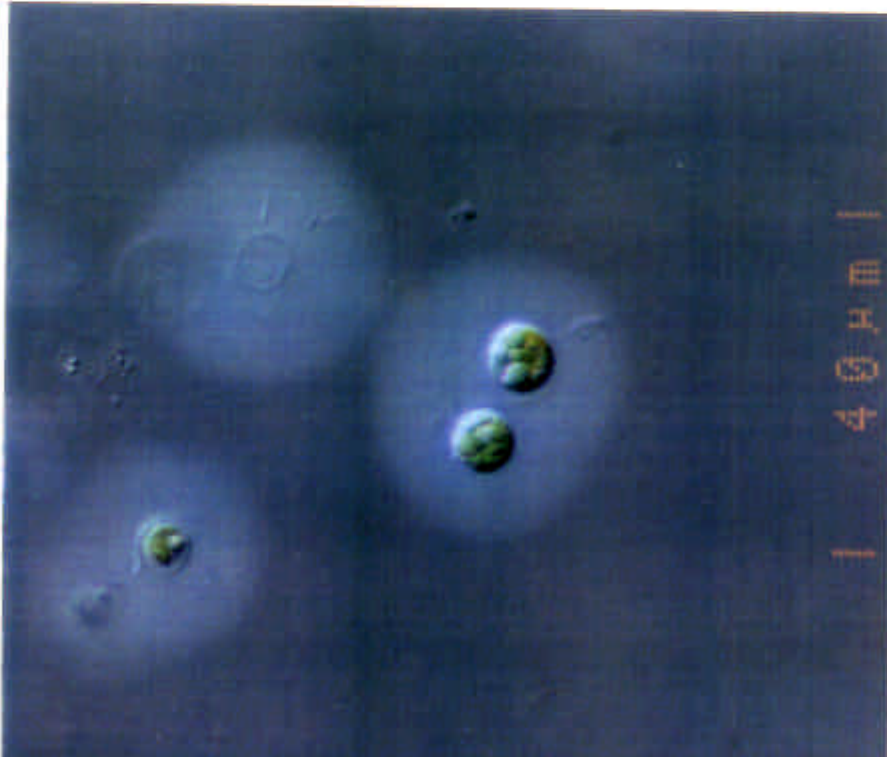
B-ZONE PIT

16/09/95

2M



B-ZONE PIT  
16/09/95  
2M



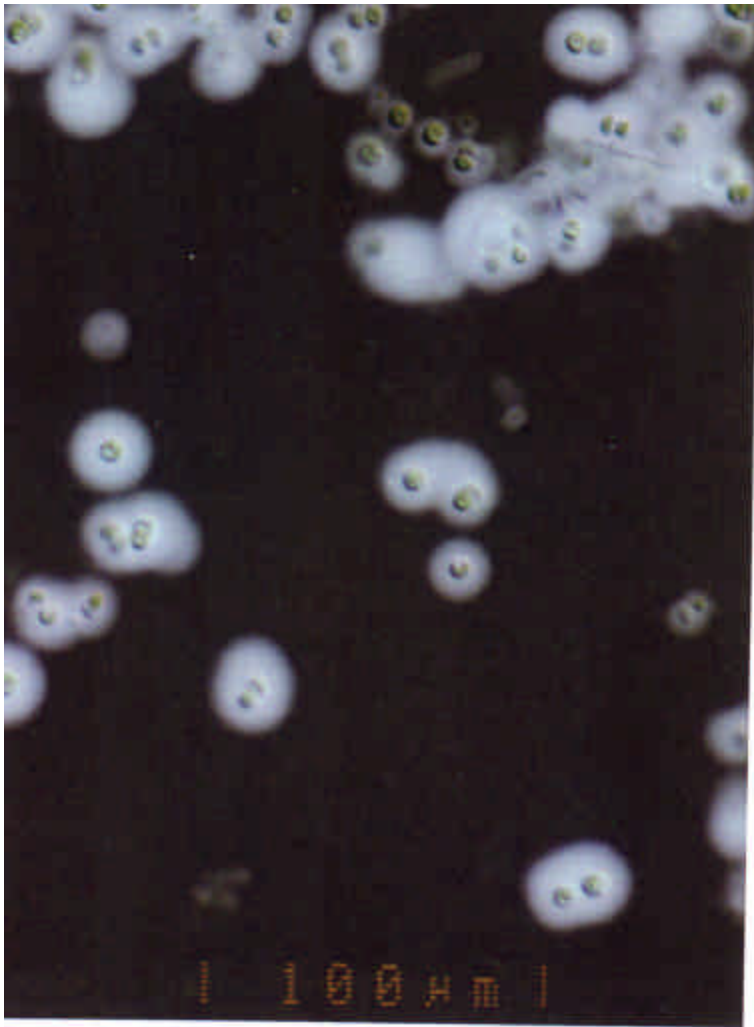




B-ZONE PIT  
16/09/95

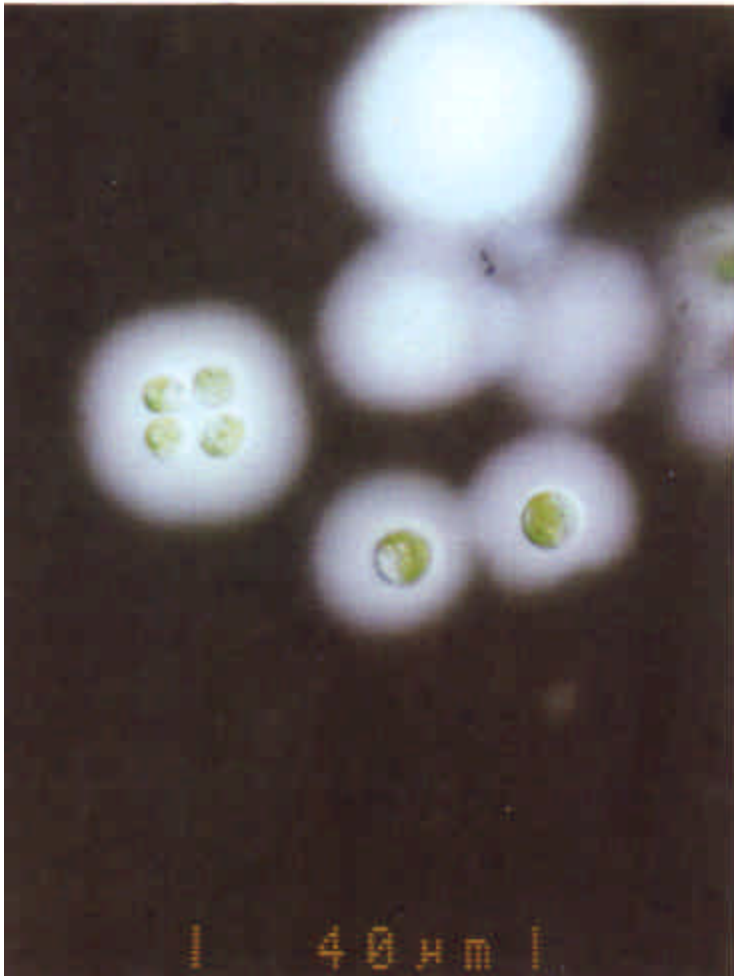
12M





B-ZONE PIT  
16/09/95

22M





B-ZONE PIT  
16/09/95

32M



## Bulk Elemental Analyses and Sequential Chemical Extractions

Following centrifugation for 20 minutes at 10,000 g and removal of the supernatant an initial bulk digestion was performed to obtain a total elemental composition for each sample. The samples were dissolved in 3.3 mL of concentrated HNO<sub>3</sub>(70%) for 24 hours and were subsequently diluted to 30 mL with ultra-pure deionized water in acid washed 60 mL Nalgene, low density polyethylene (LDPE) sample bottles to a final v/v HNO<sub>3</sub> concentration of 7.7%.

Sequential chemical digestions were performed on all samples following the methodology developed by Tessier (1979). The first fraction, representing water soluble inorganic species, was extracted for 5 hours at room temperature with 3 mL of Nanopure water and agitation every 15 to 20 minutes. Following each extraction, samples were centrifuged for 20 minutes. Following each extraction, samples were centrifuged for 20 minutes at 10,000 g the supernatant was recovered and placed in acid washed 60 mL Nalgene LDPE sample containers and diluted to 30 mL total volume. Fraction two, exchangeable metals, was then extracted from the remaining solids at room temperature for 5 hours with 3 mL of 1 M sodium acetate adjusted to pH 5.0 with acetic acid. For fraction three the residue from the sodium acetate extraction (fraction two) was treated with 3 mL of 0.04 M hydroxylamine hydrochloride in 25 % (v/v) acetic acid at 85 °C for 6 hours and frequent agitation to release inorganic species bound to metal oxides. Fraction four, inorganic species bound to organic matter, residuals from the oxide extraction (fraction three) were heated to 85 °C for 2 hours with 0.9 mL of 0.02 M HNO<sub>3</sub>, and 1.5 mL of 30% (v/v) H<sub>2</sub>O<sub>2</sub> (adjusted to pH 2.0 with HNO<sub>3</sub>). A second 0.3 mL aliquot of H<sub>2</sub>O<sub>2</sub> was then added, and the sample heated again to 85 °C for an additional 3 hours. After cooling, 1.5 mL of 3.2 M ammonium acetate in 20% (v/v) HNO<sub>3</sub>, was added and the sample was diluted to 10 mL with Nanopure water. The fifth and final extraction involved complete digestion of residual material at 60 °C in a 4 mL volume of 3:1 aqua regia (3HCl : 1 HNO<sub>3</sub>). Elemental concentrations were determined by multi-element inductively coupled plasma atomic emission spectroscopy (ICP-AES) at XRAL Laboratories in Don Mills, Ontario. Calibration was performed with NBS multi-element standards and reagent blanks for each of the extraction steps.

**APPENDIX C: NICKEL AND ARSENIC ADSORPTION ONTO MUCILAGE PRODUCING ALGAL COLONIES. ADDENDUM. 1997 CANMET REPORT**

**NICKEL AND ARSENIC ADSORPTION  
ONTO MUCILAGE PRODUCING ALGAL COLONIES  
FINAL REPORT  
CANMET, CAMECO - MARCH 1997**

All files on floppy 38.7

Text: REPORT.WPD

Copy: REPORT.CPY

Table 1: in text

Table 2: in text

Table 3: FREXTEMP.XLS

Table 4: MARYDAT2.XLS

Table 5: NICKEL.XLS

Table 6; NICKEL.XLS

Table 7: ARSEXP.WQ1

Figure 1: NIREMOV.WQ1 ASNIFIG1

Figure 2: MARYDAT2.WQ1 ASNIFIG2

Figure 3a: MARYDAT2.WQ1 ASNIFIG3A

Figure 3b: MARYDAT2.WQ1 ASNIFIG3B

Figure 4: NI-CONT1.WQ1 ASNIFIG4

Figure 5: NI-FLD1.WQ1 ASNIFIG5

Figure 6: NI-AA.WQ1 ASNIFIG6

Figure 7: NI-AA.WQ1 ASNIFIG7

Figure 8: NI-CONT.WQ1 ASNIFIG8

Figure 9: NI-CONT.WQ1 ASNIFIG9

Figure 10: NI-CONT.WQ1 ASNIFIG10

Figure 11: NI-CONT.WQ1 ASNIFIG11

Figure 12: AS.WQ1 ASNIFIG12

Figure 13: AS.WQ1 ASNIFIG13

## SUMMARY

A small multicellular green algae, *Dictyosphaerium pulchellum* is very common in mine waters with low concentrations of arsenic and nickel. In order to evaluate the potential of biotechnological treatment of low concentration mining effluents, the adsorption of nickel and arsenic on *Dictyosphaerium pulchellum* was studied in laboratory batch experiments.

Nickel and arsenic (as arsenate) can be adsorbed by biomolecules attached to the cell walls and possibly by mucilages produced by the algae under conditions of stress (nutrient, light or temperature limitations). Previous studies have estimated mucilage production (measured as carbohydrates) under a range of environmental conditions. Using that information, algae were exposed to various stress treatments prior to the adsorption experiments. Nickel adsorption on *Dictyosphaerium pulchellum*, exposed to different treatments of stress, appeared to be highly variable among the various treatments. This can be attributed to effect of mucilages produced at different amounts in the various treatments. The higher the mucilage production the larger the Ni adsorption. Although the precise mechanism is unknown, mucilage production seems to enhance Ni adsorption.

Two stress treatments were applied to the algae used in detailed adsorption experiments with arsenic and nickel: Control (N:P=10) and Field Simulation (N:P=1:1), the latter being more favourable for mucilage production. Mucilage production enhanced nickel adsorption but drastically reduced arsenic adsorption. This difference between nickel and arsenic adsorption (magnitude and shape of isotherm) can be attributed to electrostatic interactions between surface complexes and (de)protonated functional groups, and the nickel and arsenic ions in solution moving towards the interface. Nickel transport across the interface is enhanced by electrostatic attraction but arsenic transport to binding sites is reduced by repulsive electrostatic interactions. This different behaviour of nickel and arsenic not only explains their different adsorption isotherm (Freundlich versus Langmuir) but also suggests that the mucilages may have a similar effect on nickel and arsenic

adsorption as other biomolecules attached to the cell walls

Of particular interest is the deviating adsorption behaviour of nickel at high dissolved nickel concentrations: adsorbed nickel decreases sharply, sometimes even to zero. This could be due to detachment of mucilages from cell walls or colonies. Alternatively, strong organic ligands exudated by the cells at high nickel levels (detoxification mechanism) may out compete the surfaces for nickel thereby transferring nickel from the adsorbed into the dissolved phase. A comparison of the measured and predicted adsorbed nickel in the two different treatments suggests that the lower nickel adsorption at high dissolved nickel concentrations (high stress) could be due to detachment of mucilage from the cell wall or colonies. Although changes in adsorption seem to be associated with changes in mucilage production, the charge and adsorption characteristics of mucilages are not well known. These need to be more studied to assess their potential for bioremediation.



## TABLE OF CONTENTS

|     |                                      |    |
|-----|--------------------------------------|----|
| 1.0 | INTRODUCTION .....                   | 1  |
| 2.0 | DESCRIPTION OF THE EXPERIMENTS ..... | 7  |
| 3.0 | NICKEL ADSORPTION .....              | 9  |
| 4.0 | ARSENIC ADSORPTION .....             | 20 |
| 5.0 | DISCUSSION .....                     | 22 |
| 6.0 | CONCLUSIONS .....                    | 28 |

### APPENDIX I

## LIST OF TABLES

|          |  |    |
|----------|--|----|
| Table 1: | Growth Rates of the lab strain <i>Dictyosphaerium pulchellum</i> grown under nutrient stress . . . . . | 4  |
| Table 2: | Growth Rates with Temperatures . . . . .   | 5  |
| Table 3: | Temperature Experiment . . . . .   | 6  |
| Table 4: | Data Summary for All Adsorption Experiments . . . . .  | 11 |
| Table 5: | The Summary of Nickel Adsorption Experiments . . . . .   | 15 |
| Table 6: | Comparison of Spectrophotometric and AA Results . . . . .  | 18 |
| Table 7: | The Summary of Arsenic Adsorption Experiments . . . . .  | 21 |

## LIST OF FIGURES

|            |  |    |
|------------|--|----|
| Figure 1:  | % Ni Removed. All Conditions . . . . .                               | 12 |
| Figure 2:  | Ni Removed. Averages for different [Ni] . . . . .                    | 12 |
| Figure 3a: | Ni removed (ng of Ni per 10 <sup>6</sup> cells) . . . . .            | 14 |
| Figure 3b: | Ni removed (ng of Ni per µg of Carbohydrate) . . . . .               | 14 |
| Figure 4:  | % Ni Removal by <i>Dictyosphaerium</i> . Control Treatment . . . . . | 16 |

|            |  |    |
|------------|--|----|
| Figure 5:  | % Ni Removal by <i>Dictyosphaerium</i> , Field Simulation . . . . .                            | 16 |
| Figure 6:  | Nickel Adsorption, Spectrophotometric and <b>AA</b> Results<br>(per $10^6$ cells) . . . . .    | 19 |
| Figure 7:  | Nickel Adsorption, Spectrophotometric and <b>AA</b> Results<br>(per mg Carbohydrate) . . . . . | 19 |
| Figure 8:  | Adsorbed Nickel, Control Treatment, Freundlich Isotherm<br>(per $10^6$ cells) . . . . .        | 25 |
| Figure 9:  | Adsorbed Nickel, Field Simulation, Freundlich Isotherm<br>(per $10^6$ cells) . . . . .         | 25 |
| Figure 10: | Adsorbed Nickel, Control Treatment, Freundlich Isotherm<br>(per mg Carbohydrate) . . . . .     | 26 |
| Figure 11: | Adsorbed Nickel, Field Simulation, Freundlich Isotherm<br>(per mg Carbohydrate) . . . . .      | 26 |
| Figure 12: | Adsorbed Arsenic, Control Treatment, Langmuir Isotherm<br>(per $10^8$ cells) . . . . .         | 27 |
| Figure 13: | Adsorbed Arsenic, Control Treatment, Langmuir Isotherm<br>(per mg Carbohydrate) . . . . .      | 27 |

## 1.0 INTRODUCTION

In previous studies *Dicfyosphaerium pulchellum* was found to be the dominant algae, contributing about 17% of the total primary productivity in a flooded pit. As trace metals are adsorbed by these algae, it is important to know how changes in environmental conditions (e.g. nutrient stress) affect both algal growth as well as the ability of the algae to adsorb arsenic and nickel.

*Dicfyosphaerium* spp. are common members of the phytoplankton community in many lakes. This genus reportedly contains 12 species, of which 4 are commonly found: *D. pulchellum*, *D. simplex*, *D. planctonicum* and *D. ehrenbergianum*. Due to their size, their contribution to the overall biomass of phytoplankton in pristine waters is small. The species are distinguished on the basis of cell shape (e.g., spherical, ovoid, reniform). Colonies are formed when the 4 (or rarely 8) autospores remain attached through fragments of the mother-cell wall. Further taxonomic characteristics include the colonies, which are surrounded by a copious gelatinous matrix. The cells are very small (usually < 10 µm in diameter) which, combined with the mucilaginous layer, keeps this species suspended in the water column for much of the year.

Phytoplankton blooms and mucilage production are frequently connected and represent the end of the healthy growth phase for a species. Increase in cell density occurs during growth resulting in a peak cell density, referred to as a bloom. At that time nutrients become limited and mucilage production takes place. In natural, unpolluted waters blooms are usually the result of normal changes in environmental conditions, such as alterations in the relative proportions of nutrients as well as light and temperature conditions during the growing season.

Phytoplankton blooms can be viewed as a stress response if it takes place during the life cycle of phytoplankton populations and not at the end. The stress would be associated with the production of large quantities of extracellular polysaccharides. This response can be species-specific and can occur during various changes in nutrient ratios. As seasonal

environmental conditions change and induce stress on phytoplankton, each species has developed physiological and possibly, genetical adaptations to that stress in order to survive. In phytoplankton species, one of the most commonly reported adaptations to environmental stresses such as nutrient depletion or contaminant elevation, is a physiological adjustment involving the excess production of carbohydrates, variously referred to as exopolymers, extracellular polysaccharides, mucilage, mucus, slime, etc. Algal populations produce excess carbohydrates under two kinds of growth situations: (1) nutrient stress (usually phosphorus and/or nitrogen limitation); and, (2) light stress (either high light or low light). When light conditions are adequate, excess carbohydrates will be produced under nutrient stresses (e.g. nitrogen or phosphorus limitation).

Unlike phosphorus, which can be stored internally as polyphosphates for later use, algae are unable to store reserves of nitrogen. Therefore, the depletion of nitrogen in particular has serious consequences for the continued growth of algal species. Nitrogen starvation is known to cause the cessation of growth and a shift from the production of proteins to the production of carbohydrates. When nutrients are adequate and balanced, high light (at inhibitory levels) or low light (at limiting levels) may also shift the cells' metabolism in favour of carbohydrate production, but this is not common. This excretion of carbohydrates is a normal consequence of nutrient stress in small algal species. At first glance such losses of photosynthetic material appear to be negative. However, there is evidence that the excreted carbohydrates provide cells with protection from contaminants in the ecosystem. The mechanism(s) of such protection are not well understood but probably involve chelation, co-precipitation, adsorption and adhesion for contaminants such as metals. The accumulation of these complexes can lead to increases in colloidal and particulate material in the water column which, depending on the contaminant, can cause subsequent problems. However, the binding properties of this excreted material can provide a unique opportunity to remove contaminants. Therefore, a better understanding of these properties is essential in order to capitalize on the potential of planktonic microorganisms for bioremediation.

In previous studies the *Dictyosphaerium pulchellum* was grown under different light and nutrient stress conditions. **High, medium, and low light conditions** represent 1.35 - 1.50, 0.88 - 0.96, and 0.20 - 0.29 x 10<sup>16</sup> quanta cm<sup>-2</sup>sec<sup>-1</sup> respectively. The various nutrient stress conditions are: **P-Limited** (N:P=100:1), **Control** (N:P=10:1), **Field Simulation** (N:P=1:1), which mimicked the N:P ratio observed in the pit over the 1994 and 1995 field seasons, and **N-Limited** (N:P=1:10).

The light experiment showed that *Dictyosphaerium pulchellum* is able to grow over a wide range of light intensities. Growth rate of the population was slowest at the lowest light intensity, as expected. Over a 2-week period, however, the cell densities achieved were similar to those in the ambient and high light treatments.

Results of the nutrient stress treatments showed a significant increase in the N:P ratio during the P-Limited treatment. During the exponential growth period, phosphorus is consumed, driving the N:P ratio upward (to values >100). In the Control treatment the N:P ratio remains relatively constant throughout the 60-day experiment, suggesting that both nutrients are being consumed proportionately during growth. In both the Field Simulation and P-Limited treatments, the N:P ratio indicates that nitrate is being utilized faster than the available phosphorus. The N-Limited condition shows the greater nitrate stress. The changes in nutrient ratios noted in the pit and the nutrient ratio changes which took place during the experiments indicate that the field situation was relatively well simulated by the experiment.

The effect of various nutrient stress conditions on growth rates (divisions-day<sup>-1</sup>) of *Dictyosphaerium pulchellum* are summarized below (Table 1). Growth was very slow over the first 7 days, probably due to the dilute cell inoculum used at the start of the experiment; this resulted in a low optical density, barely detectable by the optical density method used to quantify growth measurement. After day 11 however, all treatments showed growth. The growth rates are based on the log transform of cell densities over two time intervals,

from day 2 to day 11, and from day 1 to day 31.

Table 1: Growth Rates of the lab strain *Dicfyosphaerium pulchellum* grown under nutrient stress.

| Treatment           | N:P Ratio | <i>D. pulchellum</i><br>(UTEX 70)<br>Day 2 -Day 11 | <i>D. pulchellum</i><br>(UTEX 70)<br>Day 1 - Day 31 |
|---------------------|-----------|--|---|
| P-Limited Condition | 100:1     | 0.349±0.048  | 0.137   |
| Control             | 10:1      | 0.284± 0.025                                       | 0.126   |
| Field Simulation    | 1:1       | 0.337± 0.050                                       | 0.135   |
| N-Limited Condition | 0.1:1     | 0.279± 0.170                                       | 0.117   |

None of the growth rates reported here are significantly different during the exponential phase of growth (approximately up to day 30), but the onset of the stationary phase (after day 30) and the physiological responses to nutrient limitation are very different among the four treatments (see below).

The earlier onset of stationary phase leads to significant differences in the final population densities achieved. The results indicate significant differences among all treatments, with the N-Limited treatment having the lowest densities, followed by moderate densities in the Control and Field Simulation, which are similar, and, finally to the highest density achieved in the culture with the P-Limited treatment.

The physiological responses, especially in regard to carbohydrate production, are particularly striking among the four treatments in nutrient stress. The carbohydrate levels ( $\mu\text{g}\cdot\text{mL}^{-1}$ ), which are used as an indicator of extracellular polysaccharide production, increase in all treatments throughout the duration of the experiment.

Carbohydrate levels in the culture medium are expected to be a good indicator of extracellular polysaccharide production since in *D. pulchellum* the bulk of the carbohydrate associated with the cells is in the extracellular mucilaginous matrix. The very small size of

the individual *D. pulchellum* cells would contribute little to the carbohydrate concentration. Once exponential growth begins at about day 7, carbohydrate levels ( $\mu\text{g}\cdot\text{mL}^{-1}$ ) begin to increase rapidly in conjunction with growth.

The nutrient stressed treatments (N-Limited and P-Limited) show more rapid carbohydrate production than the Control, although the differences are not significant until after day 32. The Field Simulation shows the lowest rates of carbohydrate production ( $\mu\text{g}\cdot\text{mL}^{-1}$ ) in the early stages of growth but after day 32, carbohydrate levels rise sharply. By the end of the experiment (day 60), the highest carbohydrate concentrations are found in the Field Simulation while the Control has the lowest concentrations of carbohydrate. A low excretion of extracellular polysaccharides would be expected from healthy growing cells as the excretion is the expected stress response.

The results of the experiment indicate that nitrogen limitation, in particular, leads to significant increases in the production of carbohydrates in cultures of *Dictyosphaerium*.

The effect of temperature on cell growth of *Dictyosphaerium pulchellum* was studied in experiments at 8, 16 and 24°C (Table 2). Two nutrient treatments were used: the Control and the Field Simulation. At 10 days of growth and after, the cell densities at temperatures of 24 and 16 °C were identical. Over the first 10 days, the growth rate at 24 °C is perceptibly greater than at 16°C for both growth solutions. At 8 °C, growth is considerably slower. Growth rates (divisions $\cdot\text{day}^{-1}$ ) are shown below.

| Temperature<br>°C | Control (N:P = 10:1)<br>Growth Rate<br>division. day <sup>-1</sup> | Field Simulation (N:P = 1:1)<br>Growth Rate<br>division. day <sup>-1</sup> |
|-------------------|--|--|
| 24                | 0.541  | <b>0.487</b>   |
| 16                | <b>0.497</b>   | <b>0.464</b>   |
|                   | 0.259  | 0.306  |



In general the Control treatment has a slightly greater growth rate than the Field Simulation (The 8 °C study was an exception to this). However final cell densities after 22 days growth were similar for both the Control and Field Simulation treatments.

The Carbohydrate production decreased with time for all temperatures and treatments (Table3). There was no difference in carbohydrate production between the 24 °C and 16°C experiments. The experiments at 8 °C produced carbohydrate concentrations about half that at 16°C after 22 days. In the control medium, carbohydrate content/cell decreased rapidly to a limiting value of about 1 µg glucose per 10<sup>8</sup> cells after 10 days for both the

Table 3: Temperature Experiment

| Dictyosphaerium grown in regular Chu 10 (10:1 N:P ratio) |                                  |                                  |                                  |
|--|----------------------------------|----------------------------------|----------------------------------|
| Days   | High Temperature (24 °C)         | Medium Temperature (16 °C)       | Low Temperature (8 °C)           |
|  | Carbohydrate Concentration       | Carbohydrate Concentration       | Carbohydrate Concentration       |
|  | (ug gluc./10 <sup>8</sup> cells) | (ug gluc./10 <sup>8</sup> cells) | (ug gluc./10 <sup>8</sup> cells) |
| 0  | 7.798                            | 7.798                            | 7.798                            |
| 4  | 1.778                            | 2.960                            | 5.536                            |
| 8  | 1.073                            | 1.270                            | 4.354                            |
| 12   | 0.843                            | 0.905                            | 2.569                            |
| 14   | 0.888                            | 0.890                            | 2.317                            |
| 18   | 0.965                            | 0.920                            | 1.941                            |
| 22   | 0.964                            | 0.871                            | 1.485                            |
| Dictyosphaerium grown in reduced Chu 10 (1:1 N:P ratio)  |                                  |                                  |                                  |
| Days   | High Temperature (24 °C)         | Medium Temperature (16 °C)       | Low Temperature (8 °C)           |
|  | Carbohydrate Concentration       | Carbohydrate Concentration       | Carbohydrate Concentration       |
|  | (ug gluc./10 <sup>8</sup> cells) | (ug gluc./10 <sup>8</sup> cells) | (ug gluc./10 <sup>8</sup> cells) |
| 0  | 7.798                            | 7.798                            | 7.798                            |
| 4  | 2.154                            | 3.666                            | 4.593                            |
| 8  | 1.258                            | 1.430                            | 3.597                            |
| 12   | 1.134                            | 1.216                            | 3.102                            |
| 14   | 1.074                            | 1.187                            | 2.366                            |
| 18   | 1.014                            | 1.105                            | 1.795                            |
| 22   | 1.242                            | 1.266                            | 1.399                            |

24°C and 16°C temperature experiments, in the cultures with nutrient stress. Over the first 10 days, carbohydrate content/cell decreased at a faster rate at 24 °C than at 16 °C. At 8 °C, the carbohydrate production was significantly higher than at higher temperatures, decreasing at a much slower rate, and never reaching a limiting value over the duration of the experiment.

In summary, although the 24 °C growth (in terms of both cell density and carbohydrate production) was initially greater than the 16 °C over the first 10 days of growth, there was little difference in growth after that time. Growth rates at 8 °C were significantly slower than at 16 °C, with the amount of carbohydrate produced by each cell being significantly greater. Finally, the growth rate for the Control Treatment (N:P = 10:1) was slightly greater than for the Treatment simulating field conditions (N:P = 1:1), or stress.

## 2.0 DESCRIPTION OF THE EXPERIMENTS

In Kalin and Olaveson (1996) experiments on nickel and arsenic adsorption onto *Dictyosphaerium pulchellum* were carried out using colorimetric determination of the As and Ni. The arsenic concentrations adsorbed onto the algae, could not be quantified, since the concentrations were at the detection limit of the test strips. The experiments were repeated using analytical methods with a lower detection limit, to quantify the adsorption of both metals.

Prior to the experiments, all glassware used was acid washed, rinsed five to six times with distilled water and oven dried. Concentrated nickel sulphate ( $\text{Ni}_2\text{SO}_4$ ) hexahydrate and arsenic ( $\text{Na}_2\text{HAsO}_4 \cdot 7\text{H}_2\text{O}$ ) stock solutions ( $2.5 \text{ g}\cdot\text{L}^{-1}$ ) with distilled, deionized water were

adjusted to pH 6.8 with 0.1M NaOH. The final test concentrations prepared with these concentrated stock solutions were: 0.01, 0.25, 0.5, 0.75, 1.0, 1.5, 2.0, 2.5 mg·L<sup>-1</sup> As and 0.01, 0.2, 0.3, 0.4, 0.5, 0.75, 1.0, 2.5, 4.0 mg·L<sup>-1</sup> Ni. A 100 mL volume of each test concentration was prepared and divided into four 25 mL aliquots, dispensed into four glass test tubes. The first 25 mL replicate was used to give the actual test concentration (e.g. no addition of algal cells). This solution was acidified with 0.1% nitric acid and stored for analysis by atomic adsorption. The remaining three 25 mL replicates of each test concentration received algal additions to test the biological adsorption of arsenic and nickel to the algal cells.

*Dictyosphaerium pulchellum* was grown in batch culture at room temperature, under constant illumination, in the Control (N:P=10:1) and Field Simulation (N:P=1:1) treatment. The cultures were allowed to grow for 20 days in order to reach the stationary phase of growth. The control (no alga cells) and different As or Ni treatments were performed in triplicate. For each replicate 50 mL of the original culture with an optical density of 0.2 (approximately  $1.5 \times 10^{10}$  cells·mL<sup>-1</sup>) was needed. Therefore, a total volume of 1350 mL of original stock culture (either Control or Field Simulation) was required. Once the algal cultures reached an optical density of 0.2, the experiment was carried out. The desired experimental density of cells was achieved by centrifuging 50 mL of original culture for 30 minutes to a pellet, removing the supernatant and resuspending the pellet in a 25 mL test solution. After resuspending the algal pellets in the 25 mL test solution, the glass tubes were shaken every 20 minutes for optimum contact between the surface area of the algae and the test solution. At the end of the two hour exposure time, each 25 mL sample with the added algal cells was centrifuged for 20 minutes. A 15 mL sample of the supernatant was removed, dispensed into scintillation vials, acidified with 0.1% nitric acid and stored for analysis. Nickel was determined with ICP and arsenic was determined using Graphite Furnace Atomic Absorption. The analytical results from the laboratory, along with the certification, are supplied in Appendix 1. The algal pellets were recentrifuged and the remaining supernatant was removed. The pellet volumes were sampled into 2 mL

Eppendorf centrifuge tubes and centrifuged in a micro-centrifuge at 10,000 rpm for 10 minutes. Any remaining supernatant was removed. The pellet volumes (approximately 1.5 mL) were stored at 4 °C for analysis of the nickel or arsenic removed from the test solution by the algal cells.

As the mucilage sheath surrounding the small cells represents the major part of the colony biovolume relative to the cells, the cells are not separate from the mucilage, when the amount of mucilage is quantified. The standard phenol-sulphuric acid test to determine carbohydrate concentrations was used to quantify changes in mucilage as carbohydrate.

### 3.0 NICKEL ADSORPTION

A summary of the results of the first round of nickel adsorption experiments conducted is presented in Table 4. Treatments included in the experiments are: different **cell densities** (50 mL culture resuspended, after centrifugation, into 50 or 25 mL distilled water) and different **washings** (removal of culture medium by several washing steps with distilled water). Running the experiments with different cell densities might reveal that the nickel adsorption is related to the mucilage. The successive washing steps would remove nickel which is not bound to the cell wall, but bound or complexed to the mucilage, as each washing step removes a portion of the mucilage.

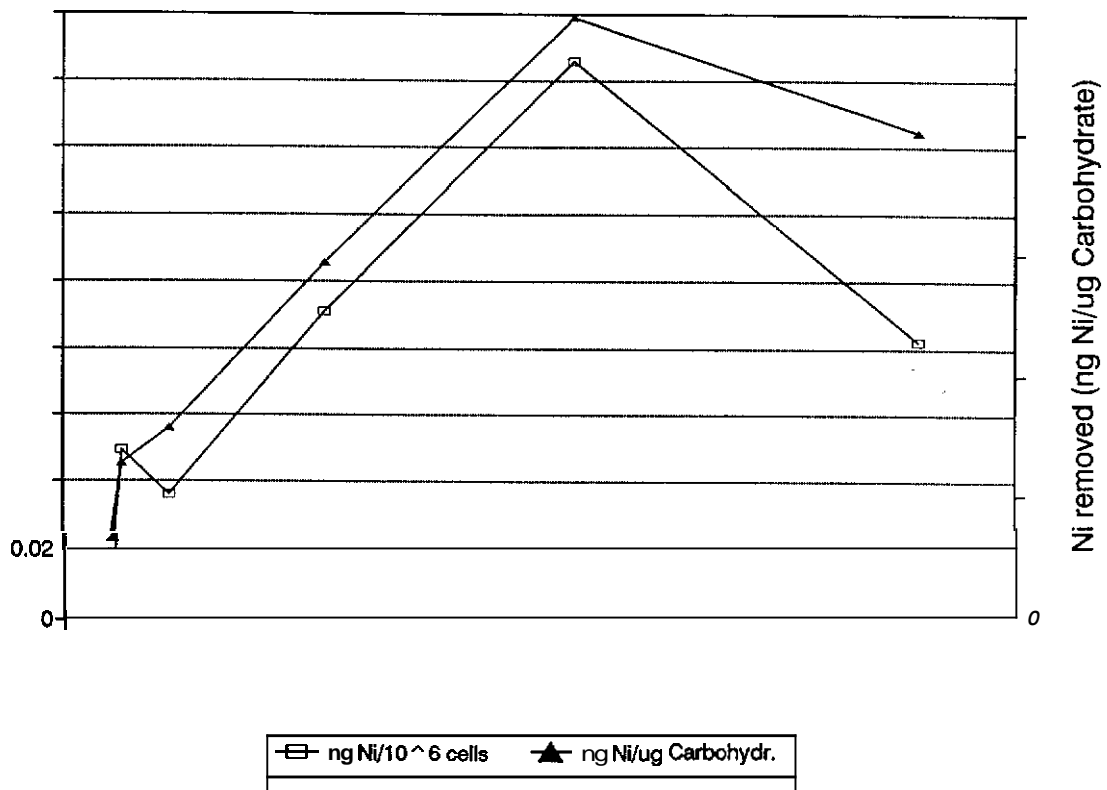
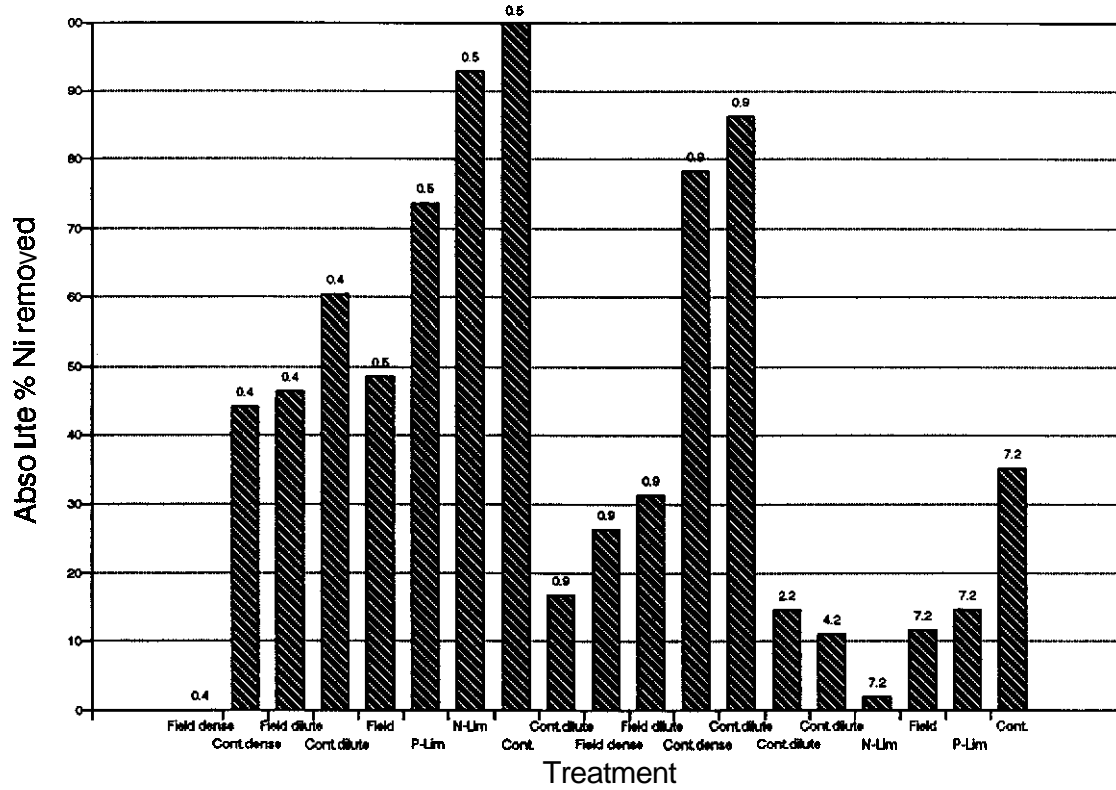
The amount of nickel removed on a per cell or per colony basis ranges throughout all experiments from 0.01 ng of Ni per  $10^6$  cells to 0.1 ng of Ni per  $10^6$  cells. The nickel removed based on carbohydrate concentration in the solution ranges from 0.6 ng of Ni to 51 ng of Ni per  $\mu\text{g}$  of carbohydrate. This suggests that both the cells and the mucilage produced on the colonies remove Ni from the water but, depending on the conditions in which the cells are growing and producing extracellular carbohydrates, the removal efficiency appears to be different. In Figure 1 the absolute % Ni removal from the test solutions is plotted for all the experiments, prior to standardizing the results for either carbohydrate or cell colony concentrations. **All** high percentages of nickel removal (up to 100 %) are obtained in the low concentration range, which suggests that saturation of available adsorption sites is reached at those low concentrations.

Due to the large range in nickel concentrations, all experimental data cannot be described by a single Langmuir or Freundlich adsorption isotherm. Averages of nickel removal in all experimental runs (Table 4) plotted against the amounts of nickel added in the various treatments are shown in Figure 2. It appears that *at* concentrations up to  $0.9 \text{ mg}\cdot\text{L}^{-1}$  Ni, the adsorbent has a much higher relative affinity for nickel (steeper slope) than at concentrations between 0.9 and  $4 \text{ mg}\cdot\text{L}^{-1}$  Ni. The adsorption behaviour of nickel is also different at low ( $0.9$  to  $4 \text{ mg}\cdot\text{L}^{-1}$  Ni) and high ( $5$  to  $7 \text{ mg}\cdot\text{L}^{-1}$  Ni) concentrations. These differences in adsorption behaviour ([low] and [high]) could indicate that only at low Ni

Table 4: Data Summary of All Adsorption Experiments

| added<br>mg/L | removed<br>ng Ni/10 <sup>6</sup> cells | Treatment             | [Ni]<br>added<br>mg/L | Ni<br>removed<br>ng Ni/ug Carbohydrate | Treatment             |
|---------------|--|-----------------------|-----------------------|--|-----------------------|
|               |  |                       | 0.4                   | 7.441                                  | Control - dilute      |
| 0.4           | 0.007                                  | Control - dense       | 0.4                   | 3.413                                  | Control - dense       |
| 0.4           | 0.015                                  | Field - dilute        | 0.4                   | 2.363                                  | Field - dilute        |
| 0.4           | 0.000                                  | Field - dense         | 0.4                   | 0.000                                  | Field - dense         |
| 0.5           | 0.049                                  | Control               | 0.5                   | 8.032                                  | Control               |
| 0.5           | 0.035                                  | Field Simulation      | 0.5                   | 2.362                                  | Field Simulation      |
| 0.5           | 0.093                                  | N - Limited           | 0.5                   | 5.442                                  | N - Limited           |
| 0.5           | 0.021                                  | P - Limited           | 0.5                   | 9.351                                  | P - Limited           |
| 0.9           | 0.062                                  | Control - dilute      | 0.9                   | 25.564                                 | Control - dilute      |
| 0.9           | 0.030                                  | Control - dense       | 0.9                   | 13.082                                 | Control - dense       |
| 0.9           | 0.022                                  | Field - dilute        | 0.9                   | 4.805                                  | Field - dilute        |
| 0.9           | 0.010                                  | Field - dense         | 0.9                   | 2.335                                  | Field - dense         |
| 0.9           | 0.007                                  | No wash, P - Limited  | 0.9                   | 0.614                                  | No wash, P - Limited  |
| 0.9           | 0.024                                  | 1 wash, P - Limited   | 0.9                   | 3.273                                  | 1 wash, P - Limited   |
| 0.9           | 0.05                                   | 2 washes, P - Limited | 0.9                   | 6.564                                  | 2 washes, P - Limited |
| 0.9           | 0.051                                  | 3 washes, P - Limited | 0.9                   | 6.856                                  | 3 washes, P - Limited |
| 0.9           | 0.046                                  | 1 wash, P - Limited   | 0.9                   | 6.356                                  | 1 wash, P - Limited   |
| 0.9           | 0.059                                  | 3 washes, P - Limited | 0.9                   | 8.036                                  | 3 washes, P - Limited |
| 2.2           | 0.087                                  | 1 wash, P - Limited   | 2.2                   | 15.196                                 | 1 wash, P - Limited   |
| 2.2           | 0.095                                  | 3 washes, P - Limited | 2.2                   | 14.117                                 | 3 washes, P - Limited |
| 4.3           | 0.176                                  | 1 wash, P - Limited   | 4.3                   | 24.324                                 | 1 wash, P - Limited   |
| 4.3           | 0.155                                  | 3 washes, P - Limited | 4.3                   | 25.306                                 | 3 washes, P - Limited |
| 7.2           | 0.054                                  | Control               | 7.2                   | 51.986                                 | Control               |
| 7.2           | 0.020                                  | Field Simulation      | 7.2                   | 10.254                                 | Field Simulation      |
| 7.2           | 0.165                                  | N - Limited           | 7.2                   | 1.862                                  | N - Limited           |
| 7.2           | 0.088                                  | P - Limited           | 7.2                   | 16.102                                 | P - Limited           |

**Fig. 1: Absolute % Ni Removed**  
All conditions



concentrations both algal colonies and carbohydrates (adsorbents) are involved in adsorption process.

Given the complexity of the adsorption system displayed by the cells or colonies of *Dictyosphaerium* and the extracellular polysaccharides in the various treatments, data were sorted (lowest and highest) and standardized for both carbohydrate and number of cells/colonies.

The results in Figure 3a and 3b are categorized in two classes: either stressed (s) or healthy (h) mucilage/cell systems. The data indicate that the Field Simulation treatment has the lowest adsorption performance. With improving the nutrient condition adsorption could be increased by about two times. The Control and the N-limited treatments showed the most effective removal. The effect of nutrient ratio on cell density is evident. Cell density decreases with decreasing N:P ratio, whereas, carbohydrate levels, associated mainly with the mucilaginous sheath increases with decreasing N:P ratio. In fact the ratio of carbohydrate level/ cells for the N-limited case is the greatest of any of the nutrient stress conditions.

The results show that there are two distinct factors involved in nickel adsorption: cell density, and the amount of the mucilaginous sheath (It is assumed that most of the carbohydrate is contributed by the mucilaginous sheath).

Results of the additional nickel adsorption experiments with *Dictyosphaerium pulchellum* subjected to the Control and Field Simulation treatments are presented in Table 5 and plotted in Figure 4 and Figure 5. The Control treatment has a near optimal N:P ratio and produces significantly less carbohydrate per cell as compared with the Field Simulation treatment. The percentages of nickel removed by *Dictyosphaerium pulchellum* at the different concentrations of added nickel are shown in Figures 4 and 5 for the Control and Field Simulation treatments. At very low concentrations of added nickel (up to  $0.2 \text{ mg}\cdot\text{L}^{-1}$ ), removal appears to be efficient in the Field Simulation treatment (with up to 64%). At higher levels of added nickel the removal of nickel decreases considerably (20-35%). The system appears to be saturated. These results show a similar trend as those obtained for the average nickel removed in the previous experiments (Figure 2). Again, the adsorbent



Fig. 3a: Ni removed  
ng Ni/10<sup>6</sup> cells

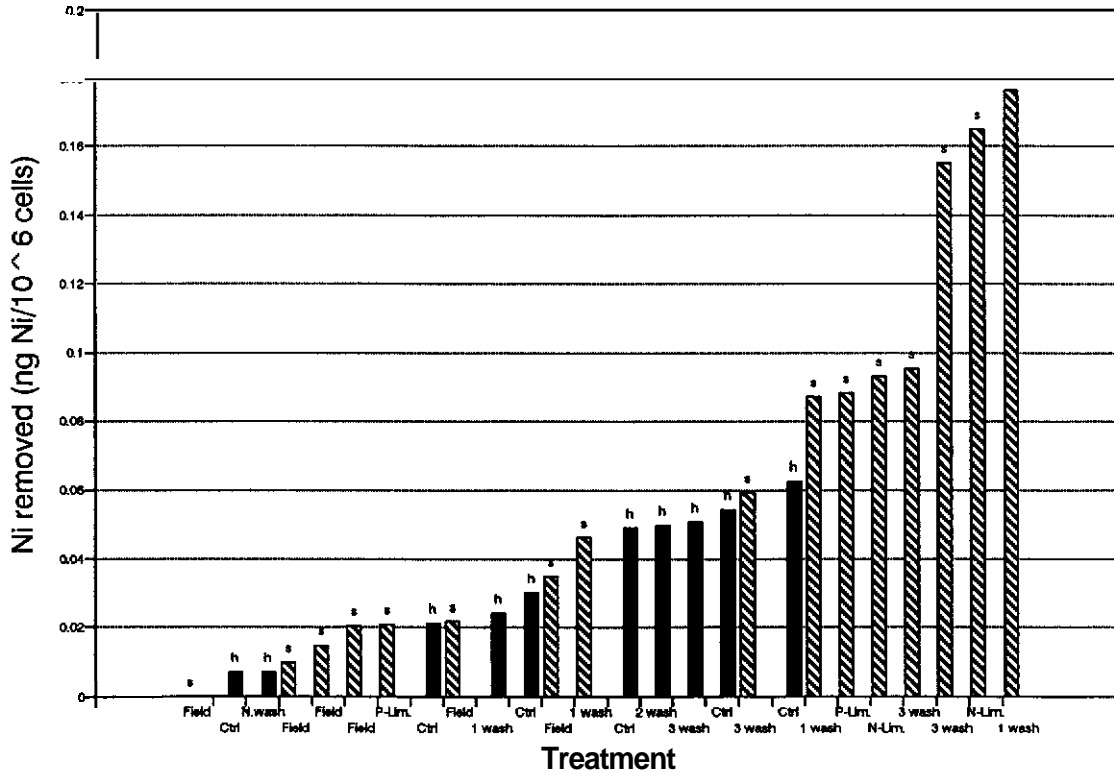


Fig. 3b: Ni removed  
ng Ni/ug Carbohydrate

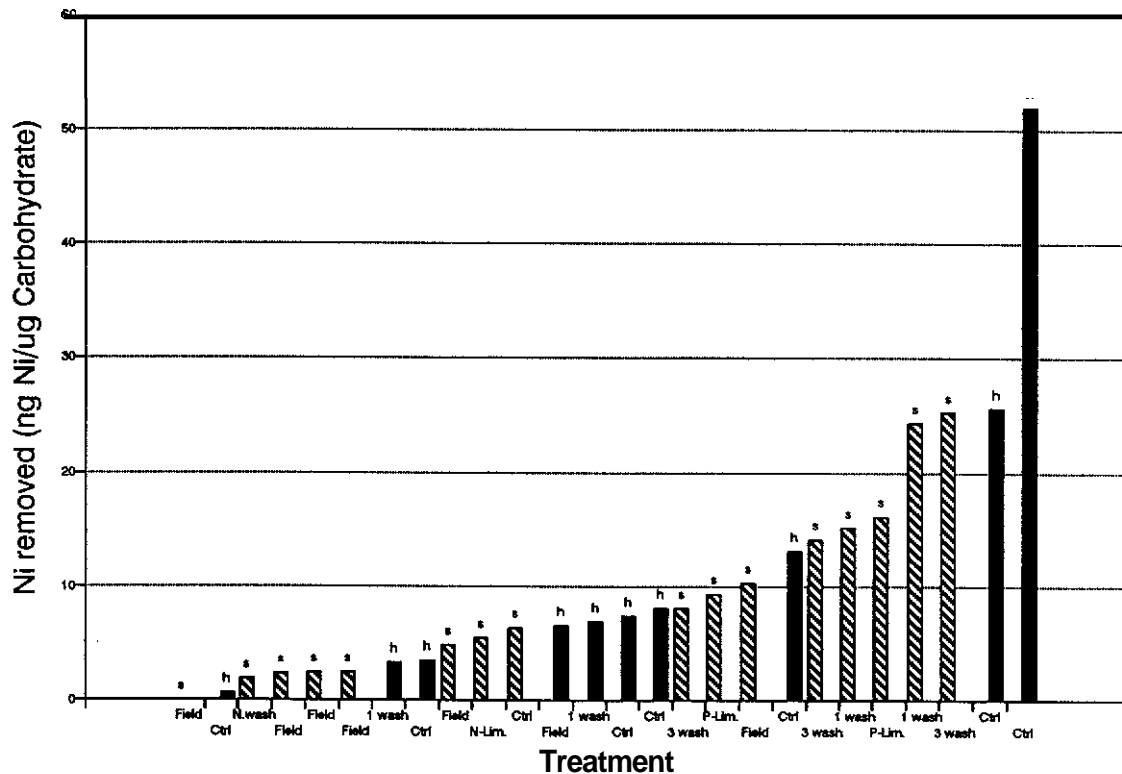


Table 5: The Summary of Nickel Adsorption Experiments

|                | Nutrient Status N:P     | Ni in Solution Before Algae mg/L | Ni in Supernatant After Algae mg/L | Ni Removed by Algae mg/L | Ni Removal | NO Alg. |       |
|----------------|-------------------------|----------------------------------|------------------------------------|--------------------------|------------|---------|-------|
| <b>Control</b> | 10 : 1                  | 0.00                             | 0.00                               | 0.00                     | 0.00       | 0.000   |       |
|                | 10 : 1                  | 0.13                             | 0.10                               | 0.03                     | 21.67      | 0.129   |       |
| <b>Treat-</b>  | 10:1                    | 0.26                             | 0.16                               | 0.10                     | 38.33      | 0.259   |       |
|                | 10 : 1                  | 0.42                             | 0.28                               | 0.14                     | 33.33      | 0.421   |       |
|                | 10 : 1                  | 0.62                             | 0.43                               | 0.20                     | 31.61      | 0.624   |       |
|                | 10 : 1                  | 0.79                             | 0.51                               | 0.28                     | 34.97      | 0.789   |       |
|                | 10 : 1                  | 1.20                             | 0.70                               | 0.50                     | 41.62      | 1.197   |       |
|                | 10 : 1                  | 1.41                             | 0.91                               | 0.50                     | 35.33      | 1.407   |       |
|                | 10 : 1                  | 3.59                             | 2.65                               | 0.94                     | 26.31      | 3.591   |       |
|                | 10:1                    | 5.69                             | 4.53                               | 1.16                     | 20.38      | 5.694   |       |
|                | <b>Field Simulation</b> | 1 : 1                            | 0.00                               | 0.00                     | 0.00       | 0.00    | 0.000 |
|                |                         | 1 : 1                            | 0.12                               | 0.06                     | 0.07       | 54.39   | 0.123 |
| 1 : 1          |                         | 0.29                             | 0.11                               | 0.18                     | 62.69      | 0.289   |       |
| 1 : 1          |                         |                                  |                                    |                          | 53.15      | 0.479   |       |
| 1 : 1          |                         | 0.60                             | 0.24                               | 0.36                     | 60.22      | 0.602   |       |
| 1 : 1          |                         | 0.75                             | 0.37                               | 0.37                     | 50.00      | 0.746   |       |
| 1 : 1          |                         | 1.06                             | 0.65                               | 0.41                     | 38.78      | 1.057   |       |
| 1 : 1          |                         | 1.47                             | 0.97                               | 0.50                     | 34.12      | 1.467   |       |
| 1 : 1          |                         | 3.87                             | 2.40                               | 1.47                     | 38.05      | 3.871   |       |
|                |                         | 5.75                             | 3.67                               | 2.07                     | 36.10      | 5.748   |       |

Fig. 4: % Ni Removal by Dictyosphaerium  
Control Treatment

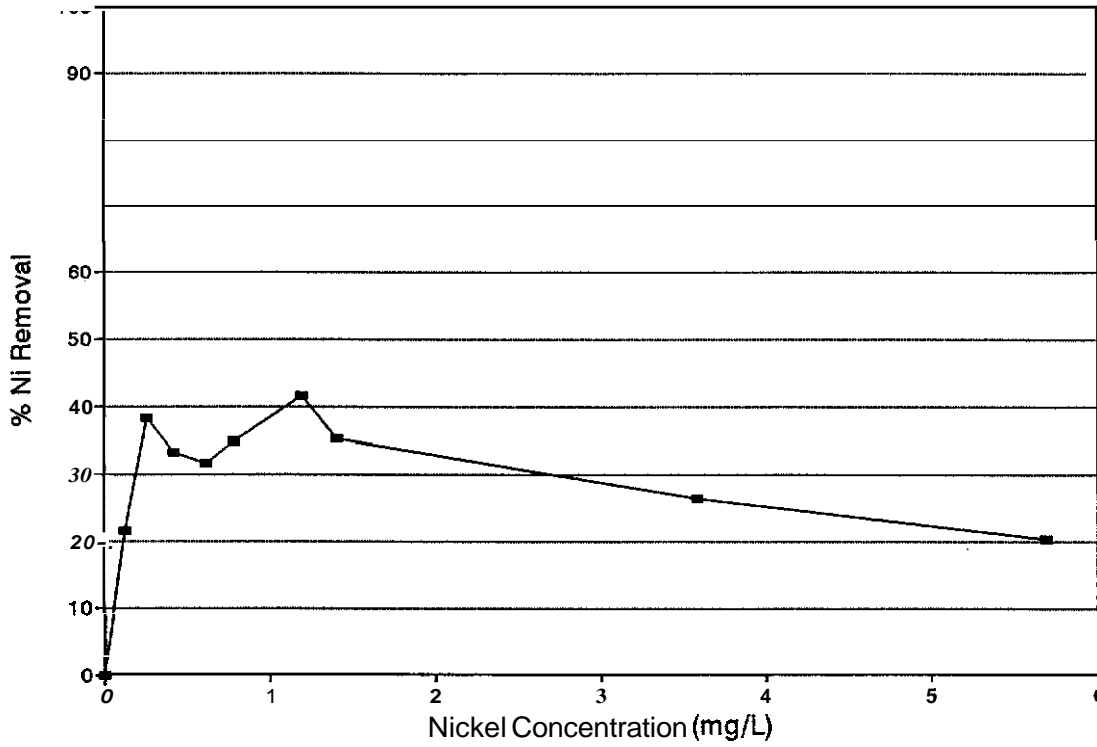
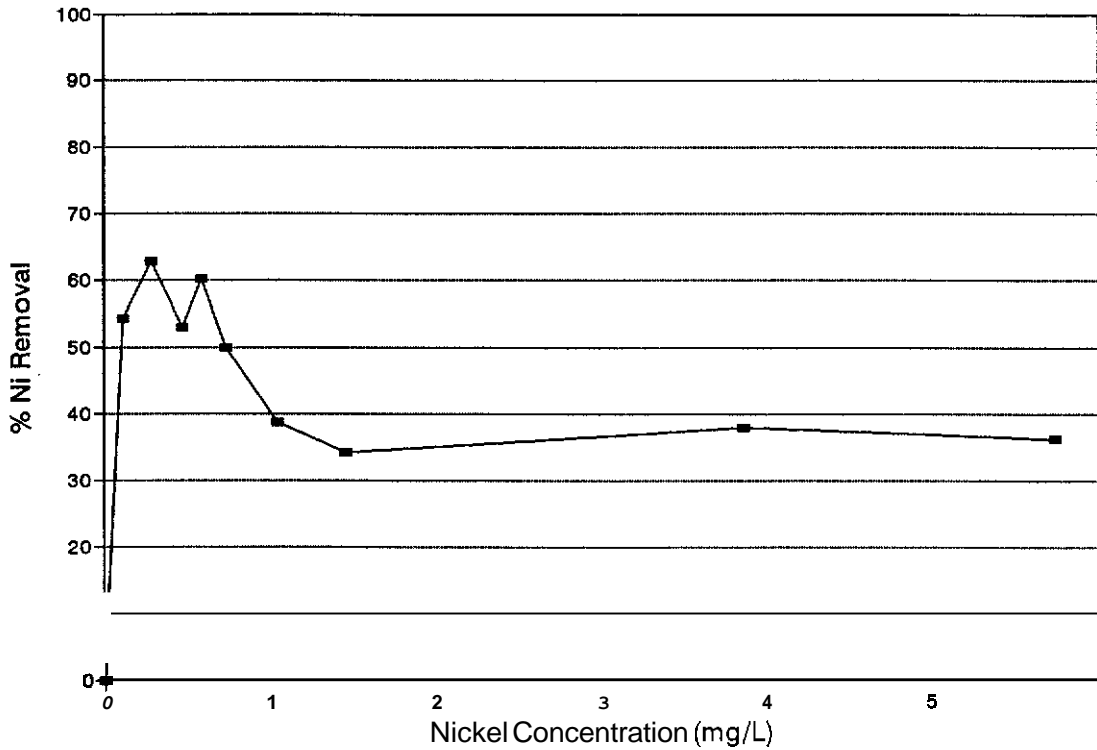


Fig. 5: % Ni Removal by Dictyosphaerium  
Field Simulation



appears to have a higher affinity for the adsorbate at low concentrations of added nickel whereas at higher concentrations of added nickel, affinity decreases rapidly. Good agreement between AAS assays and colorimetric spectrophotometric methods, which were used in the previous work done by Kalin and Olaveson (1996), was observed (Table 6) when the results are compared for nickel removal in ng per  $10^6$  cells (Figure 6) and for nickel removal in  $\mu\text{g}$  per mg carbohydrate (Figure 7). The comparison was carried out with the control cultures.

Table 6: Comparison of Spectrophotometric and AA Results

| Ni in Solution Before Algae mg/L | Ni Kit Ni Removed ng Ni/10 <sup>6</sup> cells | AA Ni Removed ng Ni ■10 <sup>6</sup> cells | Ni Kit Ni Removed µg Ni/mg carbohydrate | AA Ni Removed µg Ni/mg carbohydrate |
|----------------------------------|---|--|---|-------------------------------------|
| 0.020                            |   | 0.0031                                     |   | 0.1386                              |
| 0.170                            |   | 0.0338                                     |   | 1.5250                              |
| 0.130                            | 0.0086  |  | 0.3887                                  |                                     |
| 0.250                            |   | 0.0462                                     |   | 2.0796                              |
| 0.259                            | 0.0305  |  | 1.3754                                  |                                     |
| 0.380                            |   | 0.0554                                     |   | 2.4955                              |
| 0.420                            | 0.0431  |  | 1.9435                                  |                                     |
| 0.490                            |   | 0.0246                                     |   | 1.1091                              |
| 0.520                            |   | 0.0462                                     |   | 2.0796                              |
| 0.624                            | 0.0607  |  | 2.7358                                  |                                     |
| 0.730                            |   | 0.0800                                     |   | 3.6046                              |
| 0.789                            | 0.0849  |  | 3.8272                                  |                                     |
| 1.040                            |   | 0.1292                                     |   | 5.8228                              |
| 1.197                            | 0.1533  |  | 6.9068                                  |                                     |
| 1.407                            | 0.1530  |  | 6.8919                                  |                                     |
| 2.540                            |   | 0.1877                                     |   |                                     |
| 3.591                            | 0.2907  |  |   |                                     |
| 4.010                            |   | 0.2462                                     |   |                                     |
| 5.694                            | 0.3570  |  |   |                                     |

Fig. 6: Nickel Adsorption by cells  
Spectrophotometric and AA Results

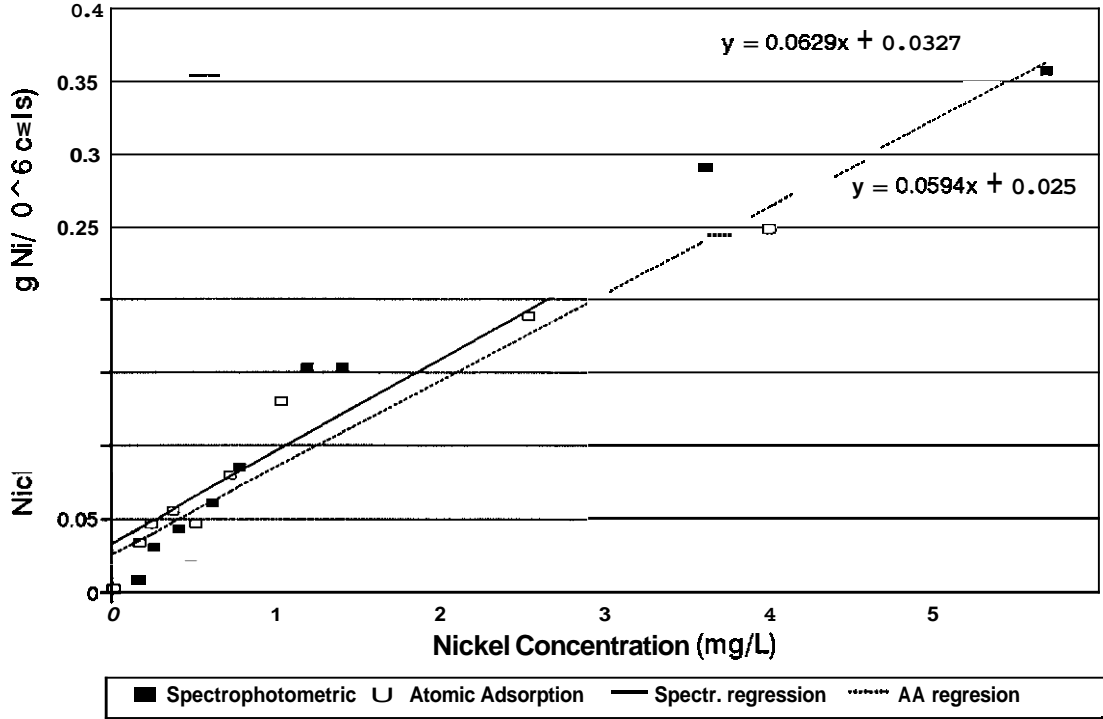
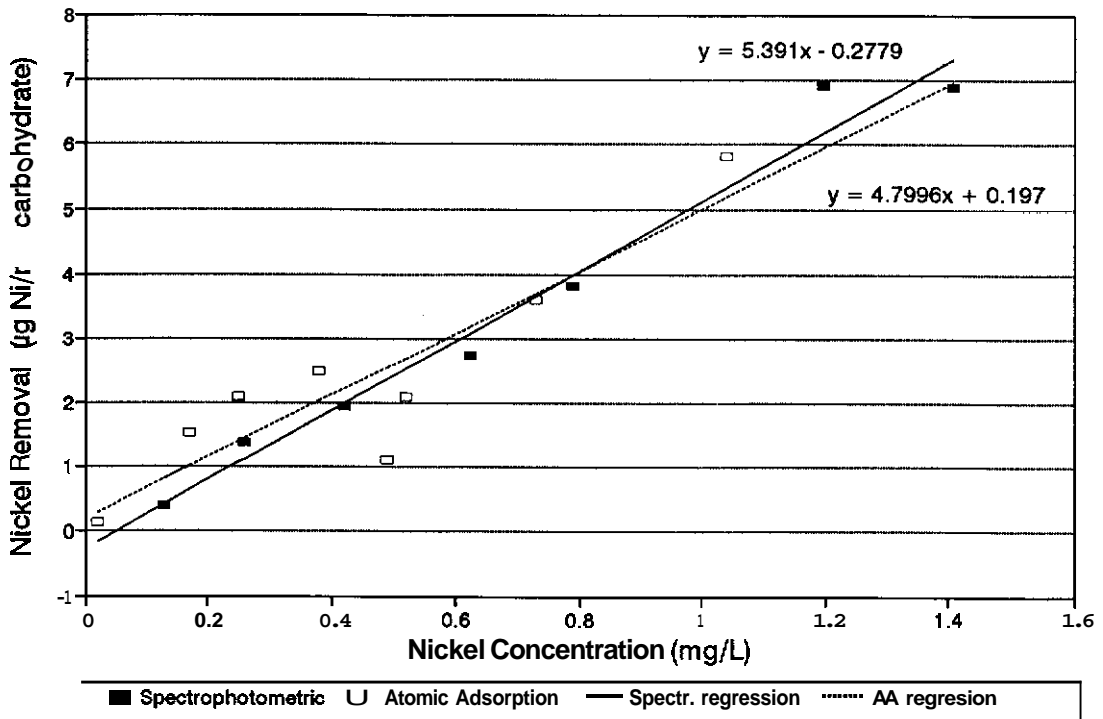


Fig.7: Nickel Adsorption by carbohydrate  
Spectrophotometric and AA Results



#### 4.0 ARSENIC ADSORPTION

The results of the arsenic adsorption experiments are summarized in Table 7 for the Control and Field Simulation treatments. Arsenic is not adsorbed in experiments for the Field Simulation Treatments. In the Control treatment arsenic adsorption does occur but in much lower concentrations than nickel in a similar treatment.

Another striking feature of the arsenic data is the constant amount of arsenic adsorption attained at higher concentrations of arsenic in the test solutions. This suggests that the available sites for arsenic adsorption have become saturated with arsenic and adsorption has reached its maximum. This trend is completely different from that observed in the data from the Ni adsorption experiments. Whereas nickel adsorption even continues at relatively high nickel concentrations in solution, maximum arsenic adsorption is already reached at low arsenic concentrations in solution.

The different adsorption behaviour of the two elements may be closely associated with their different ionic charge and the predominant charge developed on different surface functional groups of various biornolecules at the surface of the cell walls (pH 6.8). Electrostatic interactions between the similarly charged ions (e.g.  $\text{AsO}_4^{2-}$ ) and surface functional groups (e.g.  $\text{S-COO}^-$ ) could greatly affect the movement of arsenic ions towards the surface where surface complexation takes place. Any possible effect of (electrostatic) interactions with carbohydrates (mucilages) on adsorption is difficult to assess as adsorption data for the Field Simulation treatment are lacking for a comparison. If the mucilages have a considerable amount of negatively charged surface functional groups, their effect on arsenic adsorption would be similar to that of other biomolecules attached to the cell walls. Considering their enhancing effect on nickel adsorption ( $\mu\text{g Ni per mg carbohydrate}$ ) in the Control and Field Simulation treatments, they could have a similar but inhibiting effect on the adsorption of arsenic. Without any additional information from arsenic adsorption experiments with only mucilages, their adsorption behaviour can only be inferred from the limited, available data on nickel and arsenic adsorption.

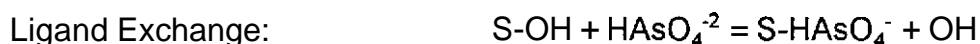
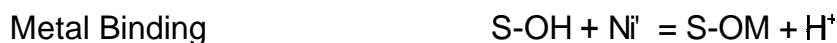
Table 7: The Summary of Arsenic Adsorption Experiments

|                                    | Nutrient Status<br>N:P | [Arsenic] Expected<br>ug/mL | [Arsenic] Measured<br>ug/mL | [Arsenic] Actual<br>ug/mL | Net Change<br>ug/mL | Arsenic Removed<br>% | Cell Density<br>x10 <sup>8</sup> cells/mL | Arsenic Removed<br>ug/10 <sup>8</sup> cells | Carbo-<br>hydrate<br>(ug/mL) | Arsenic<br>Removed<br>ug/ug carbo |
|------------------------------------|------------------------|-----------------------------|-----------------------------|---------------------------|---------------------|----------------------|---|---|------------------------------|-----------------------------------|
| <b>Field<br/>Simula-<br/>tion</b>  | 1:1                    | 0.00                        | 0.002                       | 0.002                     | 0.00                | 0.0                  | 31.0499                                   | 0.0000                                      | 127.720                      | 0.0000                            |
|                                    | 1:1                    | 0.10                        | 0.070                       | 0.114                     | -0.04               | -62.9                | 31.0499                                   | -0.0014                                     | 127.720                      | -0.0003                           |
|                                    | 1:1                    | 0.25                        | 0.185                       | 0.275                     | -0.09               | -48.6                | 31.0499                                   | -0.0029                                     | 127.720                      | -0.0007                           |
|                                    | 1:1                    | 0.50                        | 0.475                       | 0.587                     | -0.11               | -23.6                | 31.0499                                   | -0.0036                                     | 127.720                      | -0.0009                           |
|                                    | 1:1                    | 0.75                        | 0.790                       | 0.862                     | -0.07               | -9.1                 | 31.0499                                   | -0.0023                                     | 127.720                      | -0.0006                           |
|                                    | 1:1                    | 1.00                        | 1.120                       | 1.180                     | -0.06               | -5.4                 | 31.0499                                   | -0.0019                                     | 127.720                      | -0.0005                           |
|                                    | 1:1                    | 1.50                        | 1.740                       | 1.730                     | 0.01                | 0.6                  | 31.0499                                   | 0.0003                                      | 127.720                      | 0.0001                            |
|                                    | 1:1                    | 2.00                        | 2.340                       | 2.280                     | 0.06                | 2.6                  | 31.0499                                   | 0.0019                                      | 127.720                      | 0.0005                            |
|                                    | 1:1                    | 2.50                        | 3.030                       | 3.100                     | -0.07               | -2.3                 | 31.0499                                   | -0.0023                                     | 127.720                      | -0.0005                           |
| <b>Control<br/>Treat-<br/>ment</b> | 10:1                   | 0.00                        | 0.002                       | 0.002                     | 0.00                | 0.0                  | 35.1731                                   | 0.0000                                      | 120.402                      | 0.0000                            |
|                                    | 10:1                   | 0.10                        | 0.070                       | 0.022                     | 0.05                | 68.6                 | 35.1731                                   | 0.0014                                      | 120.402                      | 0.0004                            |
|                                    | 10:1                   | 0.25                        | 0.185                       | 0.059                     | 0.13                | 68.1                 | 35.1731                                   | 0.0036                                      | 120.402                      | 0.0010                            |
|                                    | 10:1                   | 0.50                        | 0.475                       | 0.316                     | 0.16                | 33.5                 | 35.1731                                   | 0.0045                                      | 120.402                      | 0.0013                            |
|                                    | 10:1                   | 0.75                        | 0.790                       | 0.690                     | 0.10                | 12.7                 | 35.1731                                   | 0.0028                                      | 120.402                      | 0.0008                            |
|                                    | 10:1                   | 1.00                        | 1.120                       | 0.933                     | 0.19                | 16.7                 | 35.1731                                   | 0.0053                                      | 120.402                      | 0.0016                            |
|                                    | 10:1                   | 1.50                        | 1.740                       | 1.550                     | 0.19                | 10.9                 | 35.1731                                   | 0.0054                                      | 120.402                      | 0.0016                            |
|                                    | 10:1                   | 2.00                        | 2.340                       | 2.120                     | 0.22                | 9.4                  | 35.1731                                   | 0.0063                                      | 120.402                      | 0.0018                            |
|                                    | 10:1                   | 2.50                        | 3.030                       | 2.970                     | 0.06                | 2.0                  | 35.1731                                   | 0.0017                                      | 120.402                      | 0.0005                            |



## 5.0 DISCUSSION

Adsorption or more precisely surface complexation of nickel and arsenic at surface functional groups on the cell wall (S-OH) takes place through Metal Binding, Ligand Exchange and/or Ternary Surface Complexation:



Both Metal Binding and Ligand Exchange form stronger (covalent) bonds than Ternary Surface Complexes. Before ions can engage in the formation of surface complexes, ions have to travel towards the interface. The ease in doing so depends on electrostatic interactions exerted by diffuse ions in the Diffuse Double Layer and charged surface functional groups at the surface. If the latter have predominantly a negative charge (acquired by (de)protonation or formation of charged surface complexes) the transport of  $Ni^{2+}$  towards the surface will be enhanced but that of  $H_2AsO_4^{-}$  will be impeded. The latter will be more prominent at progressive deprotonation of surface hydroxyls and/or formation of negatively charged surface complexes. This phenomenon can be seen in the shape of adsorption isotherms characterized by an initial steep slope (high affinity at low surface coverage) followed by a gradually declining slope indicative of a decreased affinity. The latter is caused by more repulsive electrostatic interactions when anions are moving towards the interface to become adsorbed.

Both the Langmuir and the Freundlich adsorption isotherms represent the type of curve described above. A Langmuir adsorption isotherm is characterized by a steep initial slope declining rapidly to a constant value whereas a Freundlich isotherm is characterized by a much more gradual decline of the slope. Obviously the Langmuir isotherm is characteristic

of an adsorbent reaching "saturation" of its surface sites whereas the Freundlich isotherm will only show "saturation" of the surface sites at extremely high concentrations in solution. In contrast to the Langmuir isotherm, the Freundlich isotherm applies very well to heterogeneous adsorbents or adsorbents with heterogeneous surface properties.

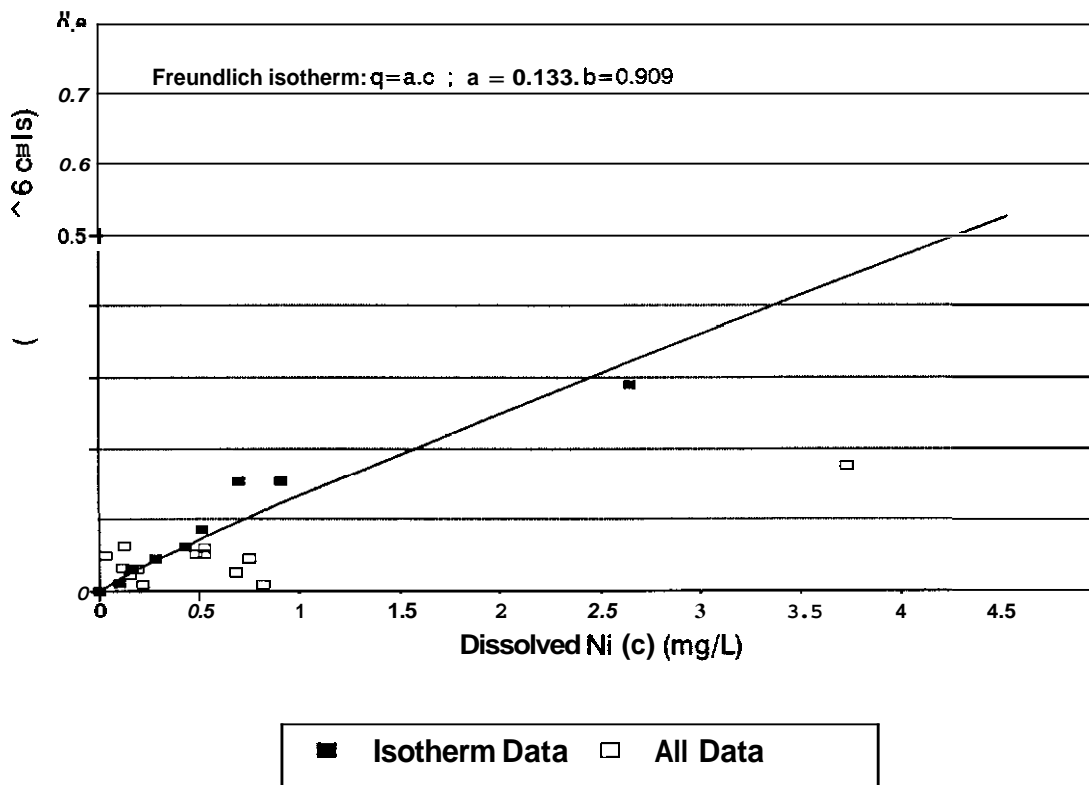
The adsorption data of nickel and arsenic, fitted to either a Langmuir or Freundlich adsorption isotherm are shown in Figures 8 to 13. These figures demonstrate that nickel adsorption is best described by the Freundlich isotherm and arsenic adsorption by the Langmuir isotherm. Considering the discussion on electrostatic interactions earlier, this is not surprising. Only a relative small proportion of the total sites are accessible for arsenic. A much larger proportion of the sites is accessible for nickel.

Although the available data are limited, arsenic adsorption is very well described by the Langmuir isotherm. The contrary applies to the Freundlich isotherm and the nickel adsorption data. Particularly at very high nickel concentrations in solution, the actual amount of adsorbed nickel is sometimes much lower than the amount predicted by the isotherm. An extreme example of this phenomenon is shown in Figure 9. Nickel adsorption, based on the experimental data, is reduced to zero at very high dissolved nickel concentrations contrary to the isotherm prediction. Apparently another "adsorbent" is competing with the cell surface for nickel. This "adsorbent" could be a very strong complexing ligand exuded by the cell as a detoxification mechanism. Alternatively the mucilage could become detached from the cells at high nickel levels resulting in a transfer of nickel from the adsorbed into the dissolved phase. The latter has been observed in other experiments where cells were exposed to extreme stresses resulting in a detachment of biomolecules from the cell wall. These biomolecules cannot be retained on a filter and the collected filtrate will acquire similar "adsorption" characteristics as the cell wall before the biomolecules were detached. Other possible explanations like mineral precipitation or other competing ions for the same surface sites seem unlikely considering the controlled nature of the experiments.

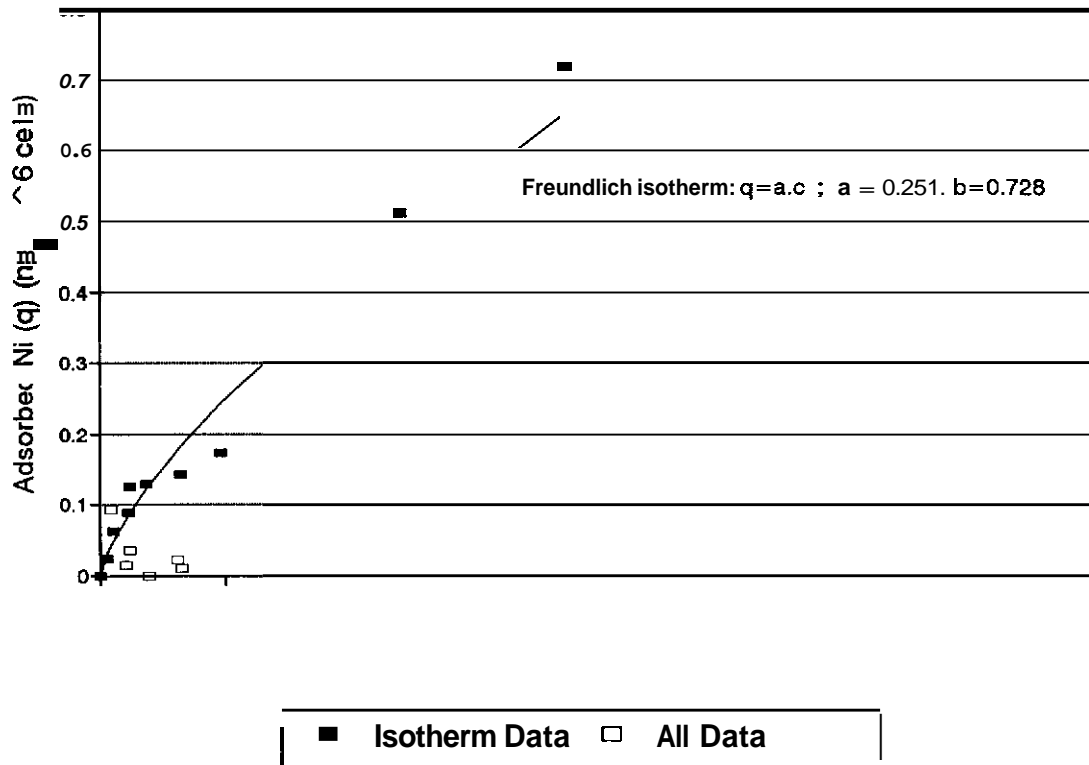
A closer examination of the data in Figures 8 to 13 also reveals differences in the capacity of *Dictyosphaerium pulchellum* to adsorb Ni or As under the Control and Field Simulation treatments. An arsenic adsorption capacity of 0.006  $\mu\text{g}$  per  $10^8$  cells ( $1.8 \mu\text{g}\cdot\text{mg}^{-1}$  carbohydrate) is reached in the Control treatment at dissolved arsenic concentrations of approximately  $0.3 \text{ mg}\cdot\text{L}^{-1}$  As ( $0.5 \text{ mg}\cdot\text{L}^{-1}$ ). Due to the potential inhibiting effect of mucilages in the Field Simulation treatment, arsenic adsorption does not take place.

The nickel adsorption capacity in the Control treatment is approximately 0.4 ng per  $10^6$  cells ( $16 \mu\text{g}\cdot\text{mg}^{-1}$  carbohydrate), reached at  $2.5 \text{ mg}\cdot\text{L}^{-1}$  Ni ( $3.5 \text{ mg}\cdot\text{L}^{-1}$ ). In the Field Simulation treatment the nickel adsorption capacity is more difficult to assess and probably much larger than 0.4 ng per  $10^6$  cells ( $> 16 \mu\text{g}\cdot\text{mg}^{-1}$  carbohydrate) at dissolved nickel concentrations larger than  $3.0 \text{ mg}\cdot\text{L}^{-1}$ . This suggests that *Dictyosphaerium pulchellum* has a higher capacity to adsorb Ni in the Field Simulation treatment due to a higher production of mucilages. These results of adsorption experiments under different treatments confirm the postulated, contrasting effect of mucilage production on nickel and arsenic adsorption.

**Fig. 8: Adsorbed Nickel  
Control Treatment, Freundlich Isotherm**



**Fig. 9: Adsorbed Nickel  
Field Simulation, Freundlich Isotherm**



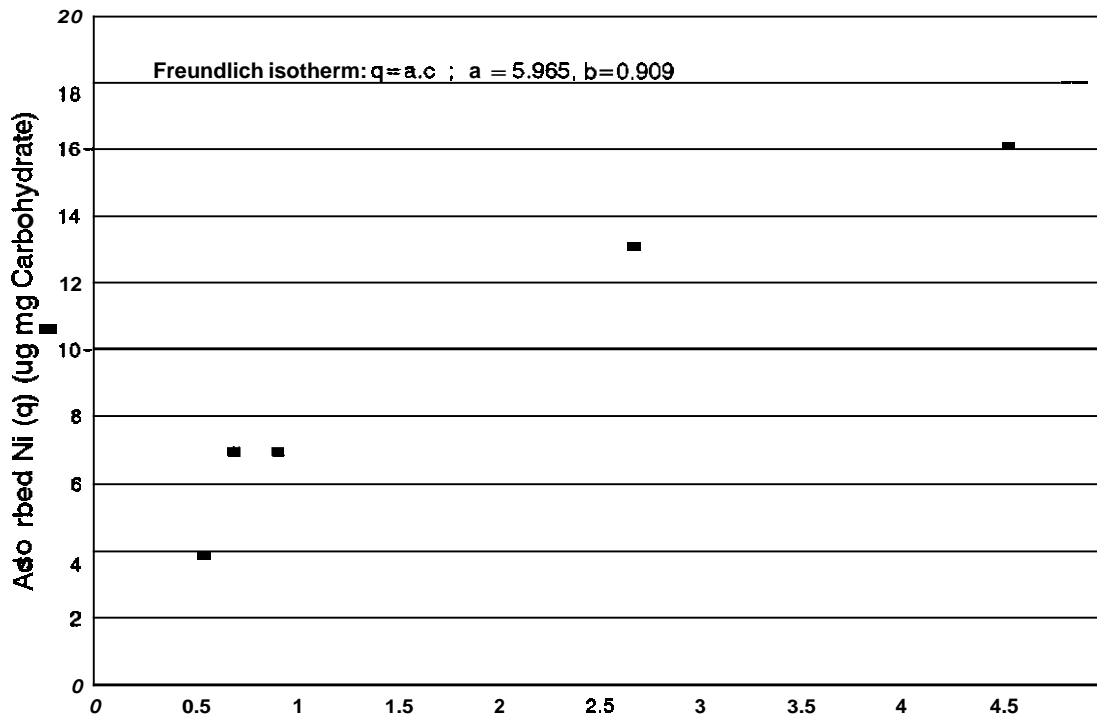


**Fig. 11: Adsorbed Nickel  
Field Simulation, Freundlich Isotherm**

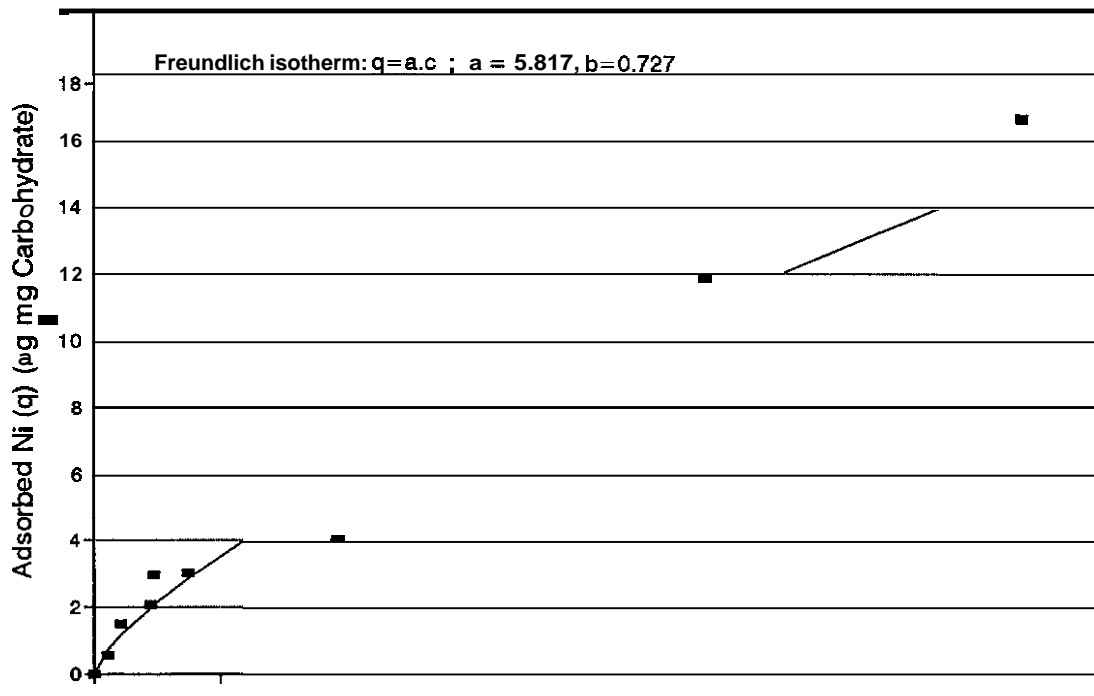
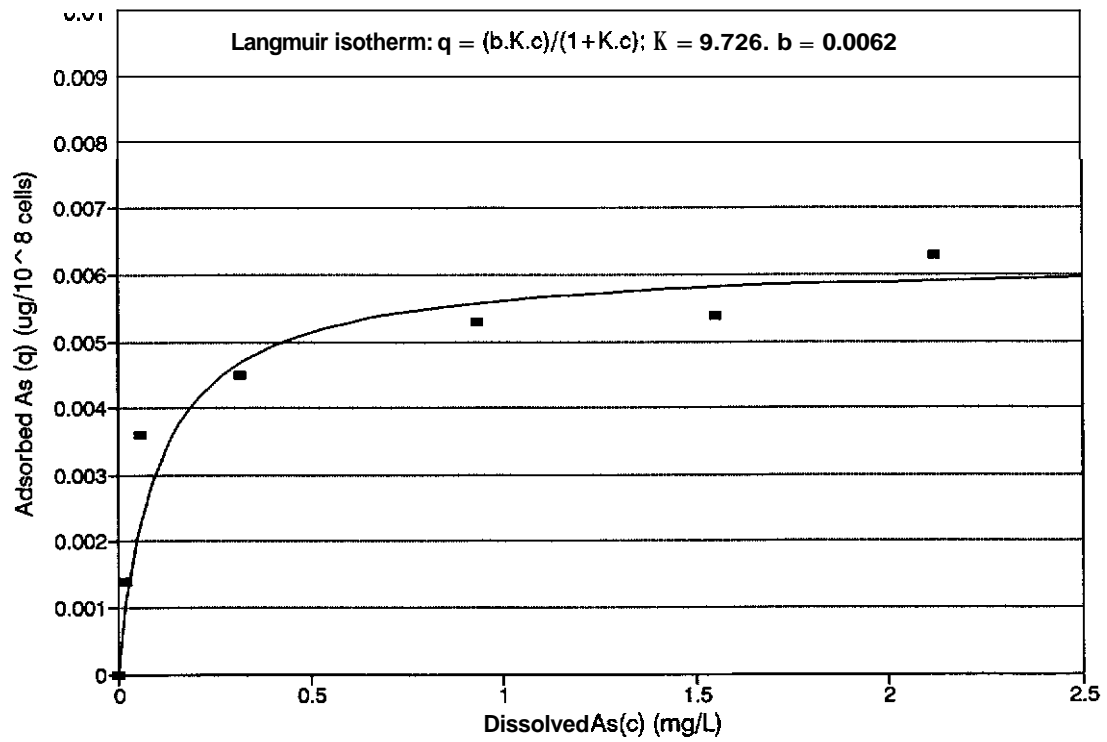


Fig. 12: Adsorbed Arsenic  
Control Treatment, Langmuir Isotherm



## 6.0 CONCLUSIONS

Although results of the adsorption experiments strongly suggest that mucilages are actively involved in adsorption processes, their (quantitative) contribution cannot be isolated from that of other biomolecules on cell walls and in solution. Considering the available information on stress conditions that control the production of mucilages, it is important to determine the adsorption capacity and behaviour of mucilages (e.g. detachment from cell colonies). This information is vital for an assessment of the potential application of both algae and mucilages in bioremediation.

Important issues that should be addressed in future studies are:

1. What are the charge and adsorption capacity of mucilages produced by *Dictyosphaerium pulchellum* and how are they affected by differences in water quality (e.g. pH, salinity, specific adsorption of ions like orthophosphate).
2. What determines the detachment of mucilages from cell surfaces or cell colonies and how does this affect the adsorption characteristics of biomolecules, algal cells or other colloids in the water column.
3. What are the adhesive characteristics of mucilages and how can they be used to affect the stability of other colloids and dissolved substances.

With the available information and experience It should be fairly simple to stimulate the production of mucilages and isolate them from cultures. The charge characteristics and contribution of different surface functional groups (potential surface sites) can be determined in potentiometric acid-base titrations and electrophoresis experiments. Once the charge characteristics and surface functional groups of mucilages are defined, the processes of cell detachment and adhesion can be addressed.

## **APPENDIX I**

**Arsenic analysis -- Graphite Furnace Atomic Absorption**

**Nickel analysis -- Inductively Coupled Plasma Spectrophotometry**



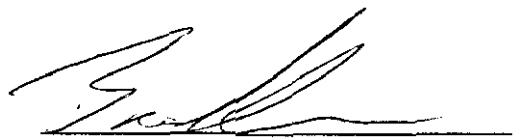
6033-6041

Client: Boojum Research Ltd  
468 Queen St. E. Suite 400  
Box 19  
Toronto, ONT, CANADA  
M5A 1T7  
Fax: 416-861-0634  
Attn: Judita Raskauskas

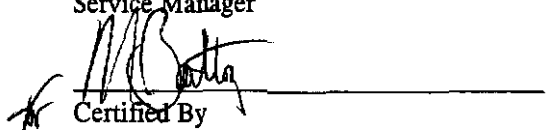
Date Submitted: September 10/96  
Date Reported: September 18/96  
MDS Ref#: 966089  
Client Ref#: BR00792

**Certificate of Analysis**

**Analysis Performed:** Nickel by ICP  
**Methodology:** 1) Analysis of trace nickel in water by Inductively Coupled Plasma Spectrophotometry.  
U.S. EPA Method No. 200.7  
(Ministry of Environment ELSCAN)  
**Instrumentation:** 1) Thermo Jarrell Ash ICAP 61E Plasma Spectrophotometer  
**Sample Description:** Water  
**QA/QC:** Refer to CERTIFICATE OF QUALITY CONTROL report.  
**Results:** Refer to REPORT of ANALYSIS attached.



Certified By  
Brad Newman  
Service Manager



Certified By  
T. Munshaw, M.Sc., C.Chem  
Director, Laboratory Operations

# Certificate of Quality Control

Client : Boojum Research Ltd  
 Contact: Judita Raskauskas

Date Reported: September 18/96  
 MDS Ref # : 966089

Client Ref#: BR00792

Analysis of Water

| Parameter | SAMPLE ID<br>(spike) | LOQ  | Units | Process Blank |             | Accept | Result | Lower Limit | Upper Limit | Accept | Matrix Spike |        |             |             |        | Overall QC<br>Acceptable |
|-----------|----------------------|------|-------|---------------|-------------|--------|--------|-------------|-------------|--------|--------------|--------|-------------|-------------|--------|--------------------------|
|           |                      |      |       | Result        | Upper Limit |        |        |             |             |        | Result       | Target | Lower Limit | Upper Limit | Accept |                          |
| nickel    | Li Ad1)-1 Controls   | 0.01 | mg/L  | nd(b)         | 0.02        | yes    | 105    | 80          | 120         | yes    | *            | *      | *           | *           | *      | yes                      |
| nickel    | Ni Ad6)-0 C          | 0.01 | mg/L  | nd(b)         | 0.02        | yes    | 115    | 80          | 120         | yes    | *            | *      | *           | *           | *      | yes                      |

LOQ = Limit of Quantitation = lowest level of the parameter that can be quantified with confidence  
 \* = Unavailable due to dilution required for analysis  
 na = Not Applicable  
 ns = Insufficient Sample Submitted  
 nd = parameter not detected  
 TR = trace level less than LOQ  
 (b) = Analytic results on REPORT of ANALYSIS have been background corrected for the process blank.

## Report of Analysis

Client : Boojum Research Ltd  
 Contact: Judita Raskauskas

Report Date: September 18/96  
 MDS Ref # : 966089

Analysis of Water

Client Ref#: BR00792

| Parameter | LOQ  | Units | Ni Ad1)-0        | Ni Ad1)-1        | Ni Ad1)-1             | Ni Ad10)-0 | Ni Ad10)-1 |
|-----------|------|-------|------------------|------------------|-----------------------|------------|------------|
|           |      |       | Controls<br>6032 | Controls<br>6022 | Controls<br>Replicate | C<br>6041  | C<br>6031  |
| ickel     | 0.01 | ug/L  | 0.02             | nd               | nd                    | 4.01       | 3.21       |

LOQ = Limit of Quantitation = lowest level of the parameter that can be quantified with confidence.  
 nd = parameter not detected ! = LOQ higher than listed due to dilution ( ) Adjusted LOQ

## Report of Analysis

Client : Boojum Research Ltd  
 Contact: Judita Raskauskas

Report Date: September 18/96  
 MDS Ref # : 966089

Analysis of Water

Client Ref#: BR00792

| Parameter | LOQ  | Units | Ni Ad2)-0<br>Controls<br><b>6033</b> | Ni Ad2)-1<br>Controls<br><b>6023</b> | Ni Ad3)-0<br>Controls<br><b>6034</b> | Ni Ad3)-1<br>Controls<br><b>6024</b> | Ni Ad4)-0<br>C<br><b>6035</b> |
|-----------|------|-------|--------------------------------------|--------------------------------------|--------------------------------------|--------------------------------------|-------------------------------|
| nickel    | 0.01 | µg/L  | 0.17                                 | 0.06                                 | 0.25                                 | 0.10                                 | 0.38                          |

LOQ = Limit of Quantitation = lowest level of the parameter that can be quantified with confidence.

MDS Environmental Services Limited.

Report of Analysis

Client : Boojum Research Ltd  
 Contact: Judita Raskauskas

Report Date: September 18/96  
 MDS Ref # : 966089

Analysis of Water

Client Ref#: BR00792

|      | LOQ  | Units | Ni Ad4)-1<br>C<br>5025 | Ni Ad5)-0<br>C<br>6036 | Ni Ad5)-1<br>C<br>6026 | Ni Ad6)-0<br>C<br>5037 | Ni Ad6)-0<br>C<br>Replicate |
|------|------|-------|------------------------|------------------------|------------------------|------------------------|-----------------------------|
| ckel | 0.01 | g/L   | 0.20                   | 0.49                   | 0.41                   | 0.52                   | 0.52                        |

LOQ = Limit of Quantitation = lowest level of the parameter that can be quantified with confidence.

MDS Environmental Services Limited.

Report of Analysis

Client : **Boojum Research Ltd**  
 Contact: **Judita Raskauskas**

Report Date: **September 18/96**  
 MDS Ref # : **966089**

Analysis of Water

Client Ref#: **BR00792**

| Parameter | LOQ  | Units | Ni Ad9)-0<br>C<br>6040 | Ni Ad9)-1<br>C<br>6030 |  |  |  |
|-----------|------|-------|------------------------|------------------------|--|--|--|
| :kcl      | 0.01 | ug/L  | 2.54                   | 1.93                   |  |  |  |

LOQ = Limit of Quantitation = lowest level of the parameter that can be quantified with confidence.

Client: Boojum Research Ltd  
468 Queen St. E. Suite 400  
Box 19  
Toronto, ONT, CANADA  
M5A 1T7

Fax: 416-861-0634

Attn: Angelo Stamatiou

Date Submitted: July 19/96  
Date Reported: July 24/96  
MDS Ref#: 964535  
MDS Quote#:

Client Ref#: BR00777

### Certificate of Analysis

Analysis Performed: Arsenic, Graphite Furnace

Methodology: 1) Analysis of arsenic in water by Graphite Furnace Atomic Absorption.  
U.S. EPA Method No. 206.2

Instrumentation: 1) Thermo Jarrell Ash Smith-Hieftje 22 AA / CTF 188 Atomizer

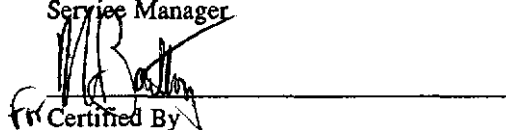
Sample Description: Water

**QA/QC** Refer to CERTIFICATE OF QUALITY CONTROL report.

Results: Refer to REPORT of ANALYSIS attached.



Certified By  
Brad Newman  
Service Manager



Certified By  
T. Munshaw, M.Sc., C. Chem  
Director, Laboratory Operations

MDS Environmental Services Limited.  
**Certificate of Quality Control**

Client : Boojum Research Ltd  
 Contact: Angelo Stamatou

Date Reported: July 24/96  
 MDS Ref # : 964535  
 MDS Quote#:

Client Ref#: BR00777

Analysis of Water

| Parameter | SAMPLE ID<br>(spike) | LOQ   | Units | Pi<br>Result | Process Blank  |        | Process % Recovery |                |                |        | Matrix Spike |        |                |                |        | Overall<br>QC<br>Acceptable |
|-----------|----------------------|-------|-------|--------------|----------------|--------|--------------------|----------------|----------------|--------|--------------|--------|----------------|----------------|--------|-----------------------------|
|           |                      |       |       |              | Upper<br>Limit | Accept | Result             | Lower<br>Limit | Upper<br>Limit | Accept | Result       | Target | Lower<br>Limit | Upper<br>Limit | Accept |                             |
| Arsenic   | 59 54                | 1.002 | mg/L  | nd(b)        | 0.004          | yes    | 98                 | 80             | 120            | yes    | *            | *      | *              | *              | *      | yes                         |
| Arsenic   | na                   | 1.002 | mg/L  | nd(b)        | 0.004          | yes    | 107                | 80             | 120            | yes    | na           | na     | na             | na             | na     | yes                         |

LOQ = Limit of Quantitation = lowest level of the parameter that can be quantified with confidence  
 \* = Unavailable due to dilution required for analysis  
 na = Not Applicable  
 ns = Insufficient Sample Submitted  
 nd = parameter not detected  
 TR = trace level less than LOQ  
 (b) = Analyte results on REPORT of ANALYSIS have been background corrected for the process blank.



## Report of Analysis

Client : Boojum Research Ltd  
 Contact: Angelo Stamatiou

Report Date: July 24/96  
 MDS Ref # : 964535  
 MDS Quote #:

Analysis of Water

Client Ref#: BR00777

| Parameter | LOQ   | u4   | 59<br>39 | 59<br>39<br>Replica | 59<br>40 | 59<br>41 | 59<br>42 | 59<br>43 | 59<br>44 | 59<br>45 |
|-----------|-------|------|----------|---------------------|----------|----------|----------|----------|----------|----------|
| arsenic   | 0.002 | mg/L |          |                     | 0.114    | 0.275    | 0.587    | 0.862    | 1.18     | 1.75     |

LOQ = Limit of Quantitation = lowest level of the parameter that can be quantified with confidence  
 - = Not Requested  
 nd = parameter not detected ! = LOQ higher than listed due to dilution ( ) Adjusted LOQ

## Report of Analysis

Client : Boojum Research Ltd  
 Contact: Angelo Stamatou

Report Date: July 24/96  
 MDS Ref # : 964535  
 MDS Quote #:

Analysis of ~~water~~

Client Ref#: BR00777

| Parameter | LOQ   | Units | 59<br>46 | 59<br>47 | 59<br>48 | 59<br>49 | 59<br>50 | 59<br>51 | 59<br>52 | 59<br>53 |
|-----------|-------|-------|----------|----------|----------|----------|----------|----------|----------|----------|
| Arsenic   | 0.002 | mg/L  | 2.28     | 3.10     | nd       | 0.070    | 0.185    | 0.475    | 0.790    | 1.12     |

LOQ = Limit of Quantitation = lowest level of the parameter that can be quantified with confidence.  
 nd = parameter not detected ! = LOQ higher than listed due to dilution ( ) Adjusted LOQ

# Report of Analysis

Client : Boojum Research Ltd  
 Contact: Angelo Stamatiou

Report Date: July 24/96  
 MDS Ref # : 9645335  
 MDS Quote #:

Analysis of Water

Client Ref#: BR00777

| Parameter | LOQ   | Units | 59   | 54 | 59   | 54 | 59   | 54 | 59 | 54 | 59    | 54 | 59    | 54    |
|-----------|-------|-------|------|----|------|----|------|----|----|----|-------|----|-------|-------|
|           |       |       | 59   | 54 | 59   | 54 | 59   | 54 | 59 | 54 | 59    | 54 | 59    | 54    |
| Chromic   | 0.002 | mg/L  | 1.74 |    | 2.34 |    | 3.03 |    | Ω  |    | 0.022 |    | 0.059 |       |
|           |       |       |      |    |      |    |      |    |    |    |       |    |       | 0.316 |

LOQ = Limit of Quantitation = lowest level of the parameter that can be quantified with confidence.  
 - = Not Requested  
 nd = parameter not detected ! = LOQ higher than listed due to dilution ( ) Adjusted LOQ

## Report of Analysis

Client : Boojum Research Ltd  
 Contact : Angelo Stamatiou

Report Date: July 24/96  
 MDS Ref # : 964535  
 MDS Quote #:

Analysis of Water

Client Ref#: BR00777

| Parameter | LOQ   | Units | 59<br>61 | 59<br>62 | 59<br>63 | 59<br>64 | 59<br>65 |  |  |  |
|-----------|-------|-------|----------|----------|----------|----------|----------|--|--|--|
|           | 0.002 | mg/L  | 0.690    | 0.933    | 1.55     | 2.12     | 2.97     |  |  |  |

LOQ = Limit of Quantitation = lowest level of the parameter that can be quantified with confidence.

**Client:** Boojum Research Ltd  
468 Queen St. E. Suite 400  
Box 19  
Toronto, ONT, CANADA  
M5A 1T7

**Fax:** 416-861-0634

**Attn:** Angelo Stamatiou

**Date Submitted:** July 19/96  
**Date Reported:** July 24/96  
**MDS Ref#:** 964535  
**MDS Quote#:**

**Client Ref#:** BR00777

## Certificate of Analysis

---

**Additional Comments:**

NOTE:

**The results reported were based on the data from two analytical techniques: Graphite Furnace Atomic Absorption Spectrophotometry (GFAAS) and Inductively Coupled Plasma Mass Spectrometry (ICP-MS). The results reported are the average of these two analytical sets of data.**